University of Alberta

BIOTURBATION AND RESOURCE QUALITY: A CASE STUDY FROM THE UPPER CRETACEOUS LYSING AND NISE FORMATIONS, ELLIDA AND MIDNATSOLL FIELDS, NORWEGIAN SEA

By

CAMILO ANDRES POLO CAMACHO

A thesis submitted to the Faculty of Graduate Studies and Research
in partial fulfillment of the requirements for the degree of

MASTER OF SCIENCE

DEPARTMENT OF EARTH AND ATMOSPHERIC SCIENCES

Spring 2013
Edmonton, Alberta

ABSTRACT

Nine cores (approx. 156 m) within the Upper Cretaceous Lysing and Nise formations (Møre Basin, Norwegian continental shelf) are studied in order to assess the relationship between bioturbate fabric and the resulting permeability distribution.

Overall, the Lysing and Nise formations strata comprise unburrowed to completely bioturbated very-fine to fine sandstones and mudstones containing a highly-diverse trace fossil assemblage that represent parts of the proximal through distal *Cruziana* ichnofacies. X-ray microtomography (Micro-CT) imaging, spot-, bulk-permeability measurements and petrographic assessments show that permeability distributions are strongly influenced by the location and nature of bioturbation. Spot permeability data taken from core-plugs indicates that the burrow permeability can be up to two orders of magnitude greater than the matrix. Therefore, it proffers a biogenically influenced dual-permeability flow media. These modifications constitute selective fluid flow networks that occur through the imposition of coarser grained sediment within burrows in otherwise fine-grained strata.

ACKNOWLEDGEMENTS

I would like to acknowledge all the members of the Ichnology Research Group (IRG) at the University of Alberta for their support; they have brought much joy to this journey. They are enthusiastic people who really love what they do. While each of them deserves a chapter herein, I look forward to thanking each of them personally the next time we meet.

My great thanks to George, Murray and JP for introducing to me to the ichnology and its applications. George has been a master, a guide to follow when got off track. I believe I am privileged to have been around you all this time. I gratefully acknowledge you for introducing me to the chaos of ichnology and for keeping me aware of the usefulness of both its light and dark side. My sincere acknowledgment and admiration to Murray who, since the beginning, has been receptive, professional and patient in my learning process. This is a humble statement compare with the great regard I hold for you. Overall, it has been a process of patience, but your step by step guidance has helped me gain confidence and appreciation for the academic journey. Since our first communication you have kept me engaged in my interest for the academy. In hard times you helped me keep my feet on the ground. You had become a role model whose passion and enthusiasm combined with hard work and leadership make your guidance a fantastic process with great results. Thank you for teaching me the methodology and rigourosity the academy requires without forgetting a balance in life. I am very thankful for all your guidance and continuous encouragement.

I would also like to express my thanks to all the staff and personnel from the Department of Earth and Atmospheric Sciences (EAS) at University of Alberta. Special thanks go to Mark Labbe and David Pirie for all their help in the preparation of the samples and for fulfilling my specific requests. To Marsha Boyd for assisting me with my enquiries and helping me with the paperwork anytime I needed to update my status.

As a team member of the IRG, my appreciation is extended to Simon Leary and Beverly Bevs in Statoil and Conoco-Phillips Scandinavia respectively. Their continuous tracking and support allowed the completion of this research project. Also, to the staff of the Weaterford Reservoir Labs® in Stavanger, Norway. Their assistance was important when collecting the data that supports this study.

Many thanks to my landlords, Rod and Sally Griffin, who treated me like a member of their family since I arrived in Edmonton. Their genuine warmth and support gave me a feeling of home, especially during winter when you were always there making sure everything was right for me.

Mom and Dad have been always my inspiration. The humble and hardworking nature my parents showed me through their daily life has been my constant motivation. I imagine them now doing their work as they do every day, a reminder that this achievement comes from those honest roots. My appreciation also goes to those kind and wonderful friends, who from a distance, advised and supported me through my studies and long winters in Edmonton. My support team in Calgary has always been there for me. They never let me forget how valuable I can be and they are the people behind the scenes in every figure, paragraph and conclusion of this thesis.

Lastly, but never less important, thanks to God: for guidance, love and the blessings that made all these beautiful things possible throughout my education and life in Canada. Throughout this experience you have shaped me into a better human being.

TABLE OF CONTENTS

LIST OF TABLES

PAGE

LIST OF FIGURES

LIST OF SYMBOLS AND ABBREVIATIONS

ICHNOFOSSILS

Ar *Arenicolites*
He *Helminthopsis*
As *Asterosoma*
Sh *Schaubcylindrichnus*
Ch *Chondrites*
Op *Ophiomorpha*
Rh *Rhizocorallium*
Rs *Rosselia*
Ne *Nereites*
Co *Cosmorhape*
Sc *Scolicia*
Sk *Skolithos*
Pa *Palaeophycus*
Te *Teichichnus*
Ph *Phycosiphon*
Th *Thalassinoides*
Pl *Planolites*
Zo *Zoophycos*
Di *Diplocraterion*

CHAPTER II - ABBREVIATIONS

BI Bioturbation Index
F1 Facies-*1* Burrowed muddy sandstone
F2 Facies-*2* Burrowed muddy to silty sandstone
F3 Facies-*3* Laminated Mudstone
F4 Facies-*4* Burrowed muddy sandstone

CHAPTER III - ABBREVIATIONS

CT Computed Tomography
Micro-CT micro Computed Tomography
MRI Magnetic Resonance Imaging
K_m Matrix Permeability
K_b Burrow Permeability
K_h Horizontal Permeability
K_v Vertical Permeability
1 Darcy: a flow of 1 cm^3/s of a fluid with viscosity 1 cP (1 mPa*s) under a pressure gradient of 1 atm/cm acting across an area of 1 cm^2. A millidarcy (mD) is equal to 0.001 Darcy.

Permeability “super-K zones”: zones having production rates above 500 barrels of oil per day (bopd) per foot of vertical interval.

NOTE FOR THE READER...

This thesis is written in a paper format. As a consequence of this arrangement, more than one chapter may share large portions of the same document. A brief summary of each chapter is provided below in order to assist the reading process:

CHAPTER I – Provides an introduction to the study presented in this thesis and includes a brief summary of its purpose. This chapter also explains the importance of this thesis by highlighting some relevant case studies and their location.

CHAPTER II – Proposes a facies classification scheme for the Lysing and Nise formations in the Ellida and Midnatsoll field area and develops a depositional model that displays both, affinities and subtle differences from the ones available in the literature.

CHAPTER III – Presents the results of the assessment of the relationship between bioturbation, sediment fabric reorganization, spatial distribution, and the resulting permeability enhancement in the upper Cretaceous Lysing and Nise Formations in the Norwegian Continental Shelf.

CHAPTER IV – Summarizes the major findings developed in Chapters II and III by listing the main conclusions of this thesis and delineates future work for which this study provides a useful basis.

CHAPTER I – INTRODUCTION

Bioturbation alters the resource quality in clastic and carbonate reservoirs. However, the study of biogenically modified strata has a relatively short history in hydrocarbon exploration and development. Applications of ichnology to fluid flow in hydrocarbon reservoirs are still in their early stages. Cumulatively, the existing and expanding evidence shows that biogenic influences on reservoir quality have been overlooked and their economic importance ignored.

In North America, Europe and the Middle East, extensive reserves have been proven in ichnologically altered reservoirs (Table 1; Figure 1). An illustrative example is the Ghawar field in Saudi Arabia. Therein, stratiform "super-K" flow zones are primarily associated with ichnofabrics (Pemberton and Gingras, 2005). The term "super-K zones" have been attributed to these zones, which have extremely high fluid flow. This definition is strictly applied for intervals having production rates above 500 barrels of oil per day (bopd) per foot of vertical interval (Meyer et al., 2000). Commonly, permeability within the "super-K" zones in the Ghawar Arab-D reservoir ranges between 1 to 500 Darcies (Schon and Head, 2007). Consequently, it has been documented that some wells are able to produce up to 40,000 bopd (~$6.4 x 10^6$ litres per day, L/d). Although extreme examples of burrow-permeability enhancement are mostly located in carbonate rocks (Cunningham et al., 2009; Cunningham and Sukop, 2012), the case studies developed in this thesis constitute the type of modifications found in clastic reservoirs and show that burrow fabrics have economic relevance there as well.

Relatively little work has been directed towards the interaction between biogenic modifications of the sediment fabric and fluid storativity and deliverability. Biogenically induced heterogeneities are a common permeability and porosity enhancement mechanism found in the rock record and it has been recognized worldwide (Table 1; Figure 1). More importantly, there are likely to be several hydrocarbon accumulations hosted in biogenically altered reservoirs that have been overlooked, remained undiscovered, or simply have yet to be developed. Current estimates of hydrocarbon-remaining reserves hosted in bioturbated reservoirs are not well known. However, a significant number of cases have been documented from conventional and unconventional reservoirs (Table 1).

Heterogeneity in clastic and carbonate reservoirs is commonly attributable to fractures, diagenesis, stratigraphy, and the development of multiple pore types. Reported as burrows, borings, relict burrows, vugs or merely as bioturbated intervals, ichofabrics constitute, among others, an important cause of reservoir portioning and preferential flow zonation. Biogenically induced reservoir zonation results in preferential fluid flow pathways in highly bioturbated strata. These type of modifications are well documented from hydrocarbons and aquifer reservoirs in the rock record.

Commonly, bioturbation-related reservoir enhancement is critical in the preservation of economic levels of porosity and permeability. This is particularly important in the case of low-permeability gas-charge reservoirs. Therefore, in some oil and gas fields, biogenic-enhancement of permeability could be required to fulfill minimum production rates. Additionally, burrow-permeability enhancement may influence the implementation of any secondary recovery method *(e.g.,* water flooding) (Gingras et al., 2004; Pemberton and Gingras, 2005). This approach can be attributable to the complex textural modifications resulting from sediment-animal interactions. These interactions result in petrophysical modifications (*e.g.,* grain sorting, sediment mixing, differential coarser burrow-infill, and/or selective dolomitization) that mostly occur in early stages of the sediment deposition. Syndepositional modifications are commonly associated to clastic deposits and related to a diversity of depositional environments. The most documented type of

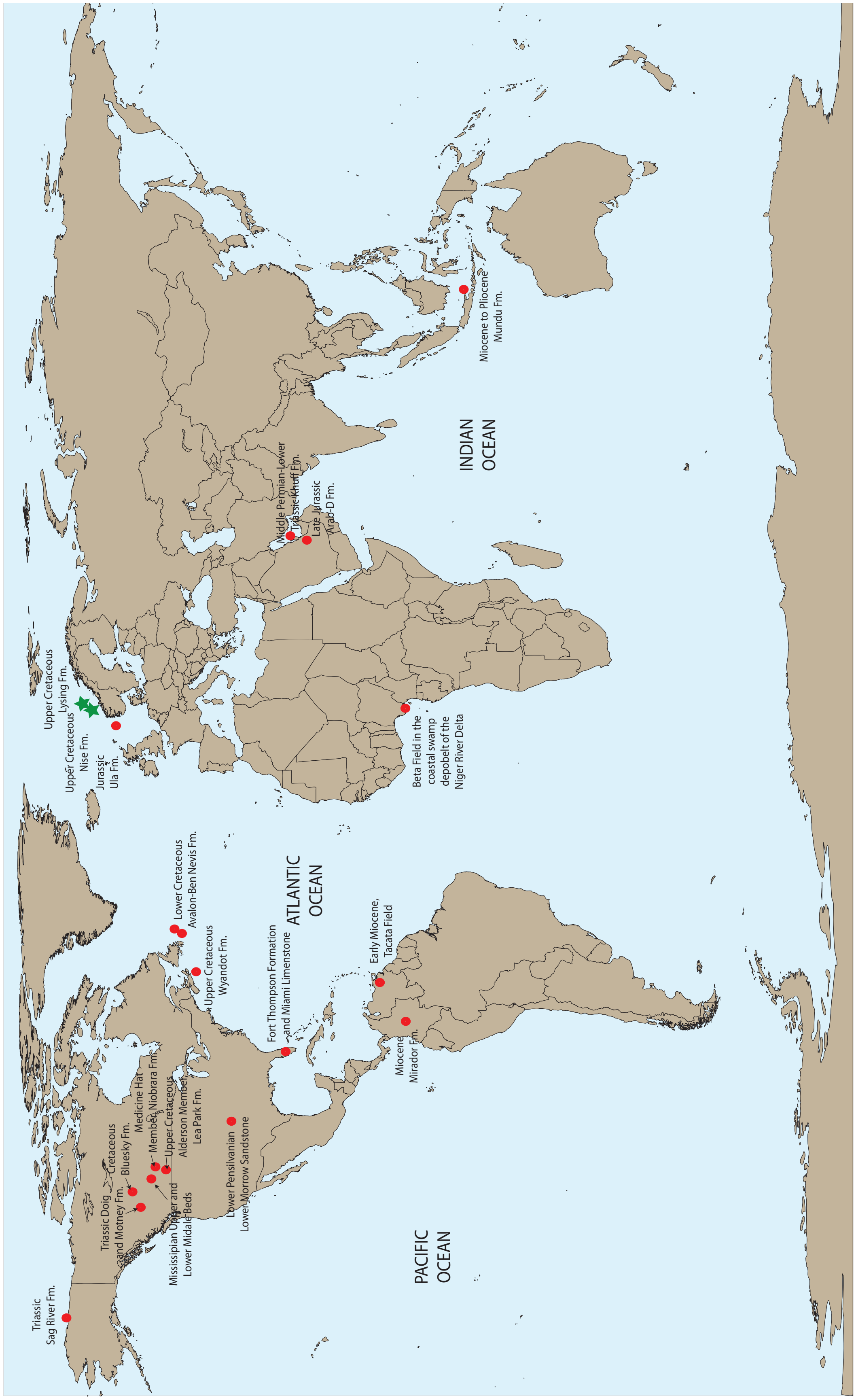
Triassic
Sag River Fm.
Triassic Doig
and Motney Fm.
Cretaceous
Bluesky Fm.
Medicine Hat
Member, Niobrara Fm.
Upper Cretaceous
Alderson Member,
Lea Park Fm.
Mississipian Upper and
Lower Middle Beds
Lower Pensilvanian
Lower Morrow Sandstone
PACIFIC
OCEAN
Fort Thompson Formation
and Miami Limestone
Upper Cretaceous
Wyandot Fm.
Lower Cretaceous
Avalon-Ben Nevis Fm.
ATLANTIC
OCEAN
Early Miocene,
Tacata Field
Miocene
Mirador Fm.
Jurassic
Ula Fm.
Upper Cretaceous
Nise Fm.
Upper Cretaceous
Lysing Fm.
Beta Field in the
coastal swamp
depobelt of the
Niger River Delta
Middle Permian-Lower
Triassic Khuff Fm.
Late Jurassic
Arab-D Fm.
INDIAN
OCEAN
Miocene to Pliocene
Mundu Fm.

Figure 1.1. Worldwide occurrences of bioturbated reservoirs complement to Table-1. Approximated locations of formations and/or fields in which hydrocarbon reservoir petrophysics (*e.g.*, porosity and/or permeability) have been biogenically modified are showed in red dots. Outstanding examples include the world's largest oil field, the Ghawar Field, in Saudi Arabia and the giant oil and gas-condensate Cusiana-Cupiagua field in Colombia. The Lysing and Nise Formations are showed in green stars (see Table-1 for complement of this figure).

biogenically enhanced reservoirs are those related to the broad spectrum of marginal-marine through open-marine depositional environments (Pemberton and Gingras, 2005; Spila et al 2008; Hovikoski et al., 2008; Lemiski et al., 2008; Lacroix et al., 2012; Gingras et al., 2012). This has led to the recognition of the role that biogenically induced heterogeneities play in clastic and carbonate reservoirs. A recent body of research, has documented the influences of bioturbation in resource quality (Zonneveld and Moslow, 2001; Gingras et al., 2004; Pemberton and Gingras, 2005; Spila et al., 2005; Keswani and Pemberton, 2006; Gingras et al., 2005; Hovikoski et al., 2008; Cunningham et al., 2009; Knaust, 2009a; Gordon et al., 2010; Tonkin et al., 2010; Lemiski et al., 2011; Lacroix et al., 2012). The literature also recognizes that the utility of trace fossils is not limited to paleobathymetry or paleoenvironmental interpretation. Burrow-associated petrophysical modifications (*e.g.,* enhanced permeability and porosity) constitute a growing field among sedimentary workers in both academe and industry. Commonly, the literature describes biogenic fabrics just as bioturbated media or digenetic mottling in siliciclastic and carbonate sedimentary deposits respectively. Since some of these features are difficult to identify at core scale, this approach results in confusing interpretations and a poor understanding of the bioturbated reservoir units (Pemberton and Gingras, 2005). For instance, the role of bioturbated fabrics in oil production, development and reserve calculation lack understanding (Spila et al., 2005; Pemberton and Gingras, 2005). With the necessity for producing the remaining reserves in already discovered fields, research in bioturbated media and its implication on fluid flow deserve more experimental

Field or aquifer and Location	Oil	Gas	Reservoir/Age	Cv	Ucv	Reservoir Characteristics	Reference
• Cusiana-Cupiagua Field. • Llanos Foothills, Eastern Cordillera, Colombia.	✓	✓	• Mirador Formation, Eocene; • Barco Formation, Paleocene; • Guadalupe Group, Upper Cretaceous.	✓		• Quartz arenites (Mirador and Barco formations) • Phosphatic litharenites (Guadalupe Group).	• Pemberton and Gingras, 2005; • Fajardo and Ramon 2009.
• Red River Formation and its subsurface equivalent • Yeoman Formation. Williston Basin, Canada.	✓		• Selkirk Member, Red River Formation (Tyndall stone). • Yeoman Formation. Ordovician.	✓		• Dolomite-mottled limestone and • Burrow-mottled epicontinental carbonate platform deposits.	• Pemberton and Gingras 2005; • Kendall, 1977.
• Sirasun-Terang Field. • Offshore Bali.		✓	• Mundu Formation. • Miocene to Pliocene.	✓		• Lower and upper Paciran Sandstone Member and the • Paciran Limestone Member.	• Pemberton and Gingras 2005.
• Midnattsol Field, • Møre Basin, Norwegian Sea.	✓		• Nise Formation. • Upper Cretaceous.	✓		• Shallow, inner- to outer shelf marine sand and mud deposits.	• Polo et al., 2010; 2012.
• Hibernia Field. • Offshore Newfoundland Atlantic Canada.	✓		• Avalon/Ben Nevis Formation. • Lower Cretaceous.	✓		• Shallow marine clean and muddy to silty sandstones.	• Spila et al 2005; • Pemberton et al 2001.
• Biscayne aquifer, • Southeastern Florida, USA.	Aquifer		• Fort Thompson Formation and • Miami Limestone.	Aquifer		• Shallow subtropical-to tropical-marine shelf or continental-marine transitional carbonates.	• Cunningham et al., 2009; 2011; (in press).
• Ellida Field, • Møre Basin. Norwegian continental shelf.		✓	• Lysing Formation. • Upper Cretaceous.	✓		• Shallow, mid- to outer shelf marine sand and mud deposits.	• Gingras et al., 2012.
• Hatton Field. • Western Canada Sedimentary Basin.		✓	• Alderson Member, Lea Park Fm. • Upper Cretaceous.		✓	• Shallow marine • Mudstone deposits.	• Hovikoski et al., 2008; • Lemisky et al., 2011.
• Weyburn Field. • Northgate Field. • Southeastern Sastkatchewan Williston Basin.	✓		• Upper and Lower Midale Beds. • Missisipian.	✓		• Bioturbated Dolomudstones.	• Keswani A. D., 1999; • Keswani and Pemberton, 1993; 2006; 2007; 2010a; 2010b.
• Ghawar Field. • Saudi Arabia.	✓		• Arab-D Formation. • Late Jurassic (Tithonian).	✓		• Skeletal grainstones and packstones, with ooid grainstones.	• Pemberton and Gingras 2005.
• Southwestern Kansas, USA	✓		• Lower Pennsylvanian, • Lower Morrow Sandstone.	✓		• Deposits of the estuarine facies-assemblage.	• Buatois et al., 2002.
• Ghawar Field, Saudi Arabia. • North Field, Qatar; South Pars field, Iran.		✓	• Khuff Formation • Middle Permian-Lower Triassic.	✓		• Shallow-marine carbonate platform deposits	• Knaust, 2009a.

Field or aquifer and Location	Oil	Gas	Reservoir/Age	Cv	Ucv	Reservoir Characteristics	Reference
• Karst-carbonate, Edward-Trinity aquifer system, Texas.	Aquifer		• Kainer Formation. • Cretaceous.	Aquifer		• Megaporous and highly permeable *Thalassinoides*-dominated ichnofabric.	• Cunningham and Sukop, 2012.
• British Columbia, Western Canada Sedimentary Basin.		✓	• Doig Formation, Motney Formation • Triassic.		✓	• Shale/Tight gas reservoir. • Thick deposits of fine-grained (shale/ siltstone).	• Zonneveld and Moslow, 2001; • Egbobawaye et al., 2010.
• 6407-10-1Nyk well, • Vøring Basin. Norwegian Sea	✓		• Nise Formation, Upper Cretaceous.	✓		• Deep-sea fan system deposits.	• Knaust, 2009b.
• Medicine Hat Field. Western Canada Sedimentary Basin		✓	• Medicine Hat Member. Niobrara Formation		✓	• Shallow marine, mudstone deposits.	• Lacroix, 2010.
• Guando Field, • Cordillera Basin, Colombia.	✓		• Guadalupe Group, • Upper Cretaceous.	✓		• Transgressive and regressive shallow-marine deposits.	• Leckie et al., 2003.
• Eagle D-21, Primrose A-41, and Subenacadie H-100 wells. Offshore Nova Scotia.			• Wyandot Formation, • Upper Cretaceous			• Pure chalk and an interbedded kaolinite-bearing, argillaceous and calcareous claystone.	• Phillips and McIlroy, 2010.
• Early Miocene, Tacata Field, • Eastern Venezuela.	✓		• SM1 Section of the Tacata fields, • Early Miocene.	✓		• Wave-dominated delta and wave-dominated strandplain deposits.	• Buatois et al., 2008.
• Beta Field in the Coastal Swamp Depobelt of the Niger Delta.	✓		• Reservoirs of the Coastal Swamp Depobelt of the Niger Delta.	✓		• Foreshores, upper shoreface, proximal and distal middle shoreface, and offshore deposits.	• Egbu et al., 2008.
• Jurassic Ula Formation, • Norwegian North Sea.	✓		• Highly (cryptically) bioturbated shales, siltstones, and sandstones	✓		• Bioturbated shelf to storm-influenced shoreface deposits.	• Baniak et al., 2011.
• Prudhoe Bay field, • Beaufort shelf, Alaska.	✓		• Sag River Formation, • Triassic.	✓		• Marine shelf deposits with erosional diastems, demarcated by the *Glossifungites* ichnofacies.	• Pemberton and Gingras, 2005.
• Cretaceous Bluesky Formation, • La Glace area, Alberta, Canada.		✓	• Bluesky Formation, • Cretaceous.	✓		• Upper shoreface sediments. Fine- to medium-grained chert-rich. Litharenite intensely bioturbated with *Macaronichnus segregatus*.	• Gordon et al., 2010.
• Hebron-Ben Nevis field, • Offshore Newfoundland	✓		• Lower Cretaceous Ben Nevis Formation, Jeanne d'Arc Basin. Atlantic Canada.	✓		• Fluviodeltaic, tidal flat, salt marsh, barrier Island to lagoon, and shoreface to offshore deposits characterized by *Ophiomorpha*-dominated ichnofabrics.	• Tonkin et al., 2010.

Table 1. Formations or fields where aquifer or hydrocarbon reservoir petrophysics have been biogenically modified. Age of these bioturbated units range from the Paleozoic through the Tertiary, showing that biogenic-modification of reservoirs is a recurrent process in the rock record. Similar fabrics have been documented worldwide in conventional (Cv) and unconventional (Uv) oil and gas, silisiclastic and carbonate reservoirs (see Figure-1 for complement of this table).

efforts. Animal-sediment interactions are complex processes that revolve around bioturbating infauna. Behavioural patterns are directed for complex adaptations of animals to the surrounding media and variety of conditions. The interplay between these conditions results in contrasting grain size, composition and distribution that may have variable impact on reservoir petrophysics. Bioturbated units may also enhance hydrocarbon migration on a basin scale by allowing better fluid pathways acting as "carrier beds." This is related to discontinuity surfaces at a large scale characterized by elements of the *Glossifungites* ichnofacies. The capability of bioturbated fabrics to act as a better fluid host and improve deliverability has to do with their intrinsic chaotic nature. Thus, allowing burrow interconnectivity along discontinuity surfaces that have the potential to constitute stratiform high-permeability zones. Despite the fact that many oil and gas fields worldwide have been documented as bioturbated reservoirs (Table 1); their economic significance is typically underestimated. The understanding of the role that bioturbation plays in oil exploration and exploitation is not yet fully understood. This is the result of earlier approaches that dislike the heterogeneous nature of most ichnofabrics in oil production.

Purpose of this Study

This study focuses on assessing the relationship between bioturbation, sediment fabric reorganization, and the resulting petrophysical enhancement (*i.e.,* permeability) in the Lysing and Nise formations. As a result of this approach, the reservoir facies within these formations in the Ellida and Midnatsoll fields are presented as a case study on the impact of bioturbation in reservoir petrophysics. Ichnological paired with sedimentological characteristics allowed the identification of three facies within the core interval studied for the Nise Formation. Throughout the Lysing Formation analized samples, only one facies was recognized. The facies-association scheme built improves the understanding of the paleoenvironmental interpretation of these formations in the study area. This also contributes to the understanding of the sedimentology and ichnology of similar deposits regionally. Spot permeability, X-ray computer tomography (micro-CT) and thin sections petrography were conducted for each facies of the Lysing and Nise reservoirs. These analyses were carried out to: 1) illustrate that these modifications constitute selective fluid flow networks; 2) visualize the spatial distribution and interconnectivity of fluid flow pathways; 3) show the affectivity of these bioturbated flow pathways; and, 4) highlight the textural heterogeneities of selected samples and their role on resource quality. Biogenic permeability enhancement within the studied dataset is classified as a case of *non-constrained textural heterogeneities* category (*sensu* Pemberton and Gingras, 2005). The role of bioturbation on reservoir quality presented herein may be useful in the optimization of secondary recovery methods and the delineation of future exploratory campaigns in the Norwegian Sea basins.

REFERENCES

BANIAK, G., GINGRAS, M.K., PEMBERTON, S.G., AND BURNS, B., 2011, Facies Characteristics and Depositional Models for Highly Bioturbated Siliclastic Strata: an example from the Upper Jurassic Ula Formation, Norwegian North Sea. American Association of Petroleum Geologist (AAPG) Annual Convention and Exhibition (ACE) Poster sessions Abstracts, Houston, Texas.

BUATOIS, L.A., MANGANO, M. G., ALISSA A. AND CARR, T.R., 2002, Sequence stratigraphic and sedimentologic significance of biogenic structures from a late Paleozoic marginal- to open-marine reservoir, Morrow Sandstone, subsurface of southwest Kansas, Sedimentary Geology, v 152, p. 99 – 132.

BUATOIS, L,A., SANTIAGO, N., PARRA, K., AND STEEL, R., 2008, Animal-substrate interactions in early interactions in an Early Miocene Wave-dominated tropical delta: Delineating environmental stresses and depositional dynamics (Tacata field, eastern Venezuela). Journal of Sedimentary Research, v. 78, p. 458 – 479.

CUNNINGHAM, K. J., SUKOP, M. C., HUANG, H., ALVAREZ, P. F., CURRAN, H. A., RENKEN, R. A., DIXON, J. F., 2009, Prominence of ichnologically influenced macroporosity in the karst Biscayne aquifer: Stratiform “super-K” zones: Geological society of America, Bulletin, v. 121, p. 164 – 180.

CUNNINGHAM, K.J., AND SUKOP, M.C., 2011, Multiple technologies applied to characterization of porosity and permeability of the Biscayne aquifer, Florida: U.S. Geological Survey Open-File Report 2011-1037, 8 p.

CUNNINGHAM, K.J., AND SUKOP, M.C., 2012, Megaporosity and permeability of *Thalassinoides*-dominated ichnofabrics in the Cretaceous karst-carbonate Edwards-Trinity aquifer system, Texas: United States Geological Survey Open-File Report 2012–1021, 4 p.

CUNNINGHAM, K.J., SUKOP, M.C., AND CURRAN, H.A., (in press), Carbonate aquifers; in Knaust, D. and Bromley, R.G., (eds.), Trace Fossils as Indicators of Sedimentary Environments: Amsterdam, Elsevier.

EGBU, O. C., OBI, G. C., OKOGBUE, C. O., AND MODE, A. W., 2008, Ichnofacies and Reservoir Properties of Shoreline Deposit in the Coastal Swamp Depobelt of the Niger Delta. American Association of Petroleum Geologist (AAPG) International Conference and Exhibition (ICE), Cape Town, South Africa, October 26 – 29.

EGBOBAWAYE, E. I., ZONNEVELD, J. P., AND GINGRAS, M. K., 2010, Tight Gas Reservoir Evaluation in Montney Formation and Lower Doig Formation, Northeastern British Columbia, Western Canada, American Association of Petroleum Geologist (AAPG) Annual Convention and Exhibition (ACE) Poster sessions Abstracts, New Orleans, Louisiana.

FAJARDO, A., AND RAMON, J. C., 2009, Sedimentology, Sequence Stratigraphy, and Reservoir Architecture of the Eocene Mirador Formation, Cupiagua Field, Llanos Foothills, Colombia, in P. M. Harris and L. J. Weber, eds., Giant hydrocarbon reservoirs of the world: From rocks to reservoir characterization and modeling: American Association of Petroleum Geologist (AAPG) Memoir 88/Society of Economic Paleontologist and Mineralogist Special Publication, p. 433 – 469.

GINGRAS, M.K., PEMBERTON, S.G., AND MENDOZA, C., 2004, fossilized worm-burrows influence the resource quality of porous media: American Association of Petroleum Geologist (AAPG) Bulletin, v. 88, p. 875 – 883.

GINGRAS, M.K., PEMBERTON, S.G., HENK F. B., MACEACHERN, J. A., MENDOZA, C A., ROSTRON, B., O'HARE, R., SPILA, M., AND KONHAUSER K., 2005, Applications of ichnology to fluid and gas production in hydrocarbon reservoirs: in Applied Ichnology. Society of Economic Paleontologist and Mineralogist short courses notes, p. 128 – 143.

GINGRAS, M.K., BANIAK, G.M., GORDON, J., HOVIKOSKI, J., KONHAUSER, K.O., LA CROIX, A.D., LEMISKI, R.T., MENDOZA, C., PEMBERTON, S.G., POLO, C. AND ZONNEVELD, J.P., 2012, Permeability and porosity in bioturbated media. In: D. Knaust and R.G. Bromley (eds). Trace Fossils as Indicators of Sedimentary Environments: Developments in Sedimentology. Elsevier, Amsterdam, v. 63.

GORDON, J.B., PEMBERTON, S.G., GINGRAS, M.K., AND KONHAUSER, K.O., 2010, Biogenically enhanced permeability; a petrographic analysis of *Macaronichnus segregatus* in the Lower Cretaceous Bluesky Formation, Alberta, Canada. American Association of Petroleum Geologist (AAPG) Bulletin 94, 1779 – 1795.

HOVIKOVSKI, J., LEMISKI, R., GINGRAS, M., PEMBERTON, S.G., AND J. MACEACHERN, 2008, Ichnology and sedimentology of a mud-dominated deltaic coast: Upper Cretaceous Alderson Member (Lea Park Fm.), Western Canada: Journal of Sedimentary Research, v. 78, p. 803 – 824.

KENDALL, A.C., 1977, Origin of dolomite mottling in Ordovician limestones from Saskatchewan and Manitoba: Bulletin of Canadian Petroleum Geology, v. 25, p. 480 – 503.

KESWANI, A.D., AND PEMBERTON, S. G., 1993, Sedimentology, Ichnology, and Paleoecology of the Mississipian Midale Carbonates in the Williston Basin, Radville Area, Saskatchewan: Preliminary Interpretations: in Karvonen, J. Den Haan, K Jang, D. Robinson, G. Smith, T. Webb, J. Wittenberg, eds., Carboniferous to Jurassic Pangea, Core Workshop Guidebook, Canadian Society of Petroleum Geologist, Calgary, p. 206 – 228.

KESWANI, A.D., 1999, An Integrated Ichnological Perspective for Carbonate Diagenesis. [Unpublished M.Sc. thesis] Earth and Atmospheric Sciences Department, University of Alberta. Edmonton, Alberta, Canada.

KESWANI, A.D., AND PEMBERTON, S. G., 2006, Paleobiological controls on dolomitization and reservoir development in the Mississippian Midale Beds, Weyburn oilfield, Southeastern Saskatchewan, Canadian Society of Petroleum Geologist Reservoir, September Issue p. 20.

KESWANI, A.D., AND PEMBERTON, S. G., 2007, Applications of ichnology in exploration and exploitation of Mississippian carbonate reservoirs, Midale Beds, Weyburn oilfield, Saskatchewan; Calgary, Alberta, Canada, Canadian Society of Petroleum Geologist and Society of Exploration Geologist Joint Conference, 14 – 17 May 2007, Extended Abstract, 28 p.

KESWANI, A.D., AND PEMBERTON, S. G., 2010, Why Are Mudstones Dolomitized in Mississippian Midale Beds, Weyburn Oilfield, Saskatchewan?. American Association of Petroleum Geologist (AAPG) Annual Convention and Exhibition Abstracts, New Orleans, Louisiana.

KESWANI, A.D., AND PEMBERTON, S. G., 2010a, Hydrocarbon Reservoir in Deeper-Water Carbonates: Paleobiological Breakdown of Permeability Barriers in Mississippian Dolomudstones, Midale Beds, Weyburn Oilfield. American Association of Petroleum Geologist (AAPG) International Conference and Exhibition (ICE) Convention Abstracts. Calgary, Alberta.

KESWANI, A. D., AND PEMBERTON, S. G., 2010b, Why Are Mudstones Dolomitized in Mississippian Midale Beds, Weyburn Oilfield, Saskatchewan?. American Association of Petroleum Geologist (AAPG) Annual Convention and Exhibition Abstracts, New Orleans, Louisiana.

KNAUST, D., 2009a, Characterisation of a Campanian deep-sea fan system in the Norwegian Sea by means of ichnofabrics. Marine and Petroleum Geology, v. 26, p. 1199 – 1211.

KNAUST, D. 2009b. Ichnology as a tool in carbonate reservoir characterization: A case study from the Permian-Triassic Khuff Formation in the Middle East. GeoArabia, v. 14, 3, p. 17 – 38 Gulf Petro Link, Bahrain.

LEMISKI, R., HOVIKOVSKI, J., GINGRAS, M., AND PEMBERTON, S.G., 2008, Sedimentological, ichnological and resource characteristics of the low-permeability, gas-charged Alderson member (Hatton gas pool, Southwest Saskatchewan): Implications on resource development, Canadian Bulletin of Petroleum Geology.

LACROIX, A., 2010, Ichnology, sedimentology, stratigraphy and trace fossil-permeability relationships in the Upper Cretaceous Medicine Hat Member, Medicine Hat gas field, southeast Alberta, Canada. [Unpublished M.Sc. thesis] Earth and Atmospheric Sciences Department, University of Alberta, Edmonton, Alberta, Canada.

LA CROIX, A., D., GINGRAS, M. K., DASHTGARD, S. E., AND PEMBERTON, S. G., 2012. Computer modeling bioturbation: the creation of porous and permeable fluid flow pathways. American Association of Petroleum Geologist (AAPG) Bulletin v. 96, p. 545 – 556.

LECKIE, D. A., DE ARMAS, M. J., GLAZEBROOK, K., GOMEZ, E., KROSHKO. P., NORRIS B., PARSONS, A., PENA, R., AND GREENE S., 2003, Depositional setting of the Cretaceous Guadalupe Formation, Colombia – Nexen's partnership in the Guando Oil Field. Canadian Society of Petroleum Geologist/Society of Exploration Geologist Joint Convention Abstracts. Calgary, Alberta, Canada.

LEMISKI, R. 2010, Sedimentology, Ichnology and Resource Characteristics of the low-permeability Alderson member, Hatton gas pool, Southwest Saskatchewan, Canada. Unpublished M.Sc. thesis, Earth and Atmospheric Sciences Department, University of Alberta. Edmonton, Alberta, Canada.

LEMISKI, R.T., HOVIKOSKI, J., GINGRAS, M.K., AND PEMBERTON, S.G., 2011, Sedimentological, ichnological, and resource characteristics of the low-permeability, gas-charged Alderson Member (Hatton Gas Pool, southwest Saskatchewan): Implications on resource development, Canadian Bulletin of Petroleum Geology.

MEYER, F.O., PRICE, R.C., AND AL-RAINI, S.M., 2000, Stratigraphic and petrophysical characteristics of cored Arab-D Super-k intervals, Hawiyah Area, Ghawar field, Saudi Arabia: GeoArabia, v. 5, p. 355 – 384.

PEMBERTON, S. G., FREY, R.W., RANGER, M.J. AND MACEACHERN, J. A., 1992a, The conceptual Framework of Ichnology. In S.G. Pemberton, ed., Applications of Ichnology to Petroleum Exploration, a Core Workshop, SEPM Core Workshop No. 17 Society of Economic Paleontologist and Mineralogist, p. 132.

PEMBERTON, S.G., SPILA, M.V., PULHAM, A.J. SAUNDERS, T.D.A., MACEACHERN, J. A., ROBBINS, D. AND SINCLAIR, I.K., 2001, Ichnology and Sedimentology of Marginal Marine Systems: Ben Nevis and Avalon Reservoirs, Jeanne d'Arc Basin, Geological Association of Canada, Short Course Notes, v. 15, 343 p.

PEMBERTON, S.G., AND GINGRAS, M. K., 2005, Classification and characterization of biogenically enhanced permeability: American Association of Petroleum Geologist (AAPG) Bulletin, v. 89, p. 1493 – 1517.

PHILLIPS, C., AND MCILROY, D., 2010. Ichnofabrics and biologically mediated changes in clay mineral assemblages from a deep-water, fine-grained, calcareous sedimentary succession: an example from the Upper Cretaceous Wyandot Formation, offshore Nova Scotia. Bulletin of Canadian Petroleum Geology v. 58, n. 3., p. 203 – 218.

POLO, C., BANIAK, G.M., AND GINGRAS, M.K., 2010, Biogenic Influences on Resource Quality Within the Upper Cretaceous Nise Formation, Møre Basin, Norwegian Sea. American Association of Petroleum Geologist Annual Convention and Exhibition Abstracts, New Orleans, Louisiana.

POLO, C., BANIAK, G.M., GINGRAS, M.K., AND PEMBERTON, S.G., 2012, Using X-ray microtomography (micro-CT) in characterizing biogenically-enhanced, low-permeability reservoirs: a case study from the Upper Cretaceous Nise Formation, Møre Basin, Norwegian Sea: American Association of Petroleum Geologists (AAPG), Annual Convention and Exhibition (ACE), Long Beach, Technical Program.

SCHON, S.C., AND HEAD, J.W., 2007, Super-permeability zone and the formation of outflow channels on Mars: League City, Texas, 38th Lunar and Planetary Science Conference: http://www.lpi.usra.edu/meetings/lpsc2007/pdf/

SPILA, M.V., PEMBERTON, S. G., ROSTRON, B., AND GINGRAS M. K., 2005, Biogenic textural heterogeneity, fluid flow and hydrocarbon production: bioturbated facies Ben Nevis Formation, Hibernia Field, offshore Newfoundland. in Applied Ichnology. Society of Economic Paleontologist and Mineralogist short courses notes.

TONKIN, N.S., MCILROY, D., MEYER, R., AND MOORE-TURPIN, A., 2010. Bioturbation influence on reservoir quality; a case study from the Cretaceous Ben Nevis Formation, Jeanne d'Arc Basin, offshore Newfoundland, Canada. American Association of Petroleum Geologist (AAPG) Bulletin 94, 1059 – 1078.

ZONNEVELD, J-P., AND MOSLOW, T.F., 2001, Reservoir architecture of fine-grained turbidite system from outcrop exposures of the Triassic Montney Formation, Western Canada Sedimentary Basin: American Association of Petroleum Geologist (AAPG) Annual Meeting, Abstracts with Programs, Denver, p. A225.

CHAPTER II – FACIES DESCRIPTION AND INTERPRETATION OF THE UPPER CRETACEOUS LYSING AND NISE FORMATIONS, ELLIDA AND MIDNATSOLL FIELDS AREA, NORWEGIAN SEA

INTRODUCTION

The Norwegian continental shelf is divided in three areas: the North Sea, the Norwegian Sea and the Barents Sea. Within the Norwegian Sea, the Møre and Vøring basins have proven hydrocarbon potential hosted in Cretaceous and Tertiary deep-water reservoirs (Figure 2.1). In the past decades, the shallow eastern areas (*e.g.,* Halten Terrace, Møre Margin and Trøndelag Platform; Figure 2.1), have concentrated the majority of the drilling activity, targeting Jurassic-age reservoirs. These deposits are profoundly buried westwards in deep-water areas off the Norwegian continental shelf in the Møre Basin (Brekke et. al., 1999; Vergara et al., 2001). Thus investing them with challenges when exploring and developing potential and already discovered hydrocarbons accumulations respectively. As a result of this approach, current exploratory efforts are focusing on Cretaceous and Tertiary deep-water reservoirs, albeit suffer from a lack of understanding of their distribution and quality.

Within the Norwegian Sea basins, Upper Cretaceous strata have traditionally been interpreted as the result of deep-sea turbidite depositional processes (*e.g.*, Kittilsen et al., 1999; Brekke et al., 1999; Brekke et al., 2001; Vergara et al., 2001; Fjellanger et al., 2005; Kjennerud and Vergara, 2005; Martinsen et al., 2005; Fugelli and Olsen, 2005a, Fugelli and Olsen, 2005b; Fugelli and Olsen, 2007; Knaust, 2009a). The Upper Cretaceous (Coniacian) Lysing and (Campanian) Nise formations have also been ascribed to a turbidite-related depositional system. This approach stems mainly from regional models built from the integration of seismic with low

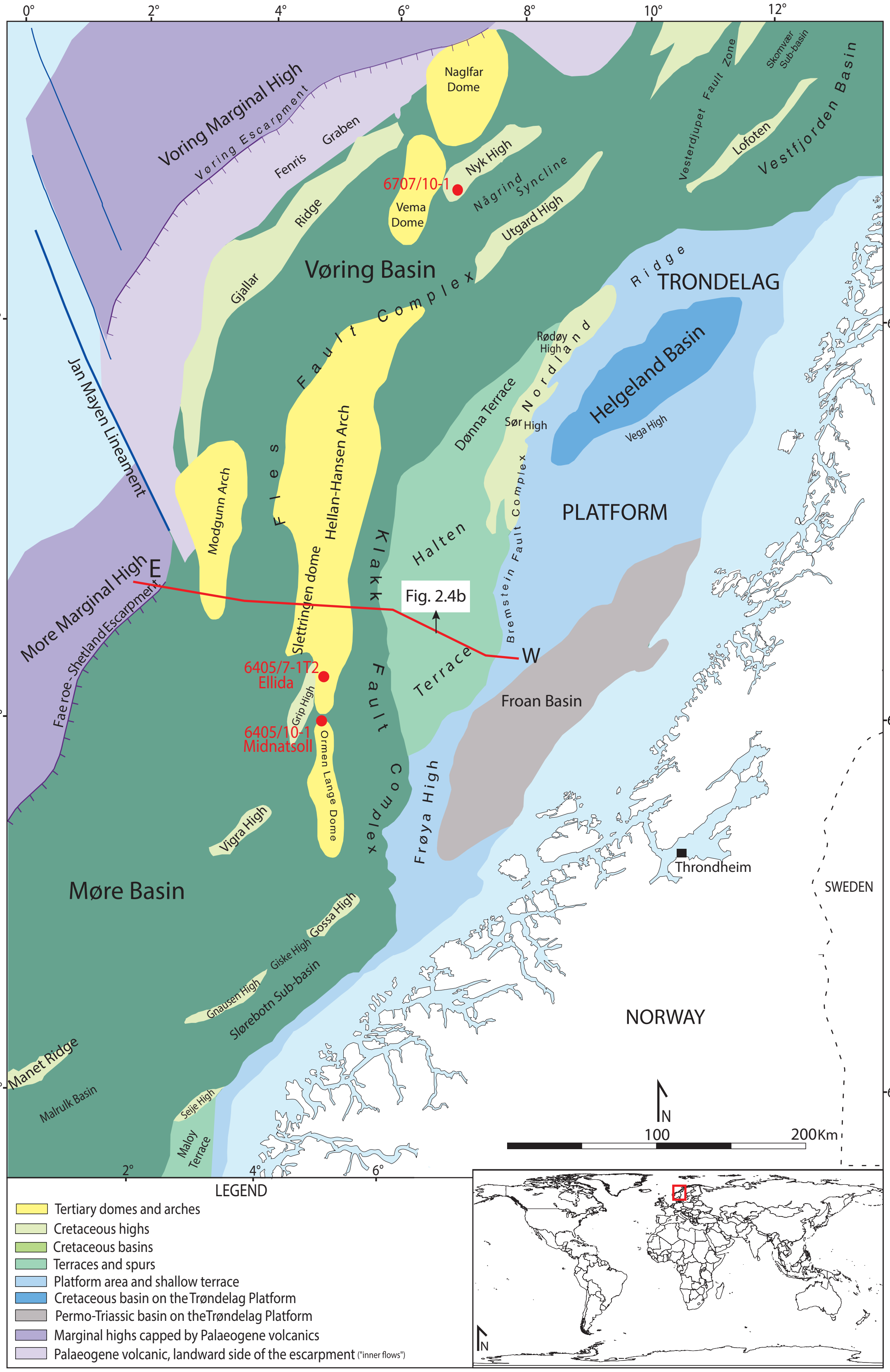

Figure 2.1. Main tectonic elements of the Norwegian Sea basins, offshore mid-Norway (modified from Blystad et al., 1995). Wells involved in this study (*i.e.*, 6405/7-1 T2 and 6405/10-1) or mentioned in the text (*i.e.*, 6707/10-1) are highlighted in red.

density of well data in largely unexplored areas. More recently, Knaust (2009) using ichnofabrics and sedimentological data from well 6707/10-1 (Figure 2.1) identified different sub-environments of a deep-sea fan in sediments pertaining to the Nise Formation. These results support the proposed depositional setting previously documented in the literature by introducing ichnological data analysis.

Ichnology provides valuable data for identifying depositional environments including siliciclastic marginal marine settings (MacEachern and Pemberton, 1992; MacEachern and Pemberton, 1994; Pemberton et al., 1992b; Pemberton and Frey, 1985; MacEachern et al., 1999b; Bann et al., 2004; MacEachern et al., 2005; Gingras et al., 1999; Knaust, 2009; MacEachern et al., 2010). A significant research body has demonstrated the importance of the integration of ichnological and sedimentological datasets as paleoenvironmental indicators (Frey and Haward 1978; Pemberton et al., 1982; Ekdale et al., 1984; Bromley 1996; Pemberton and MacEachern, 1997; Buatois and Mangano, 1998; Hasiotis and Honey, 2000; Gingras et al., 2001; MacEachern et al., 2007a). Paleoecological factors such as water oxygenation (Bromley and Ekdale, 1984; Savrda and Bottjer 1986, 1989; Sageman et al., 1991; Boyer and Droser, 2011) and salinity (Pemberton et al., 1982; Beynon and Pemberton 1992; Ranger and Pemberton 1997; Gingras et al., 1999) can be also discerned from ichnological observations. Ichnofossil assemblages also have genetic stratigraphic significance and reflect changes of relative sea level (Pemberton et al., 1992; Pemberton and MacEachern 1995; Savrda et al., 2001; Gingras et al., 2002). Trace fossils analysis also provides an insight in sedimentary processes such as sedimentation rates and depositional events at both local and regional scale (Bromley 1996; Pemberton and MacEachern 1997; Gingras et al., 1999).

The principal contribution of the work outlined in this chapter is to provide an ichnological synthesis paired with sedimentological analyses of the Lysing and Nise Formation in the Ellida and Midnatsoll fields area (Figure 2.1). Herein, an alternative depositional model is proposed for these formations. The ichnological and sedimentological analysis also allowed the reconstruction of a local paleogeographical model with shallow-water affinities in some lithofacies, thereby complementing the interpreted deep-water settings available in the literature.

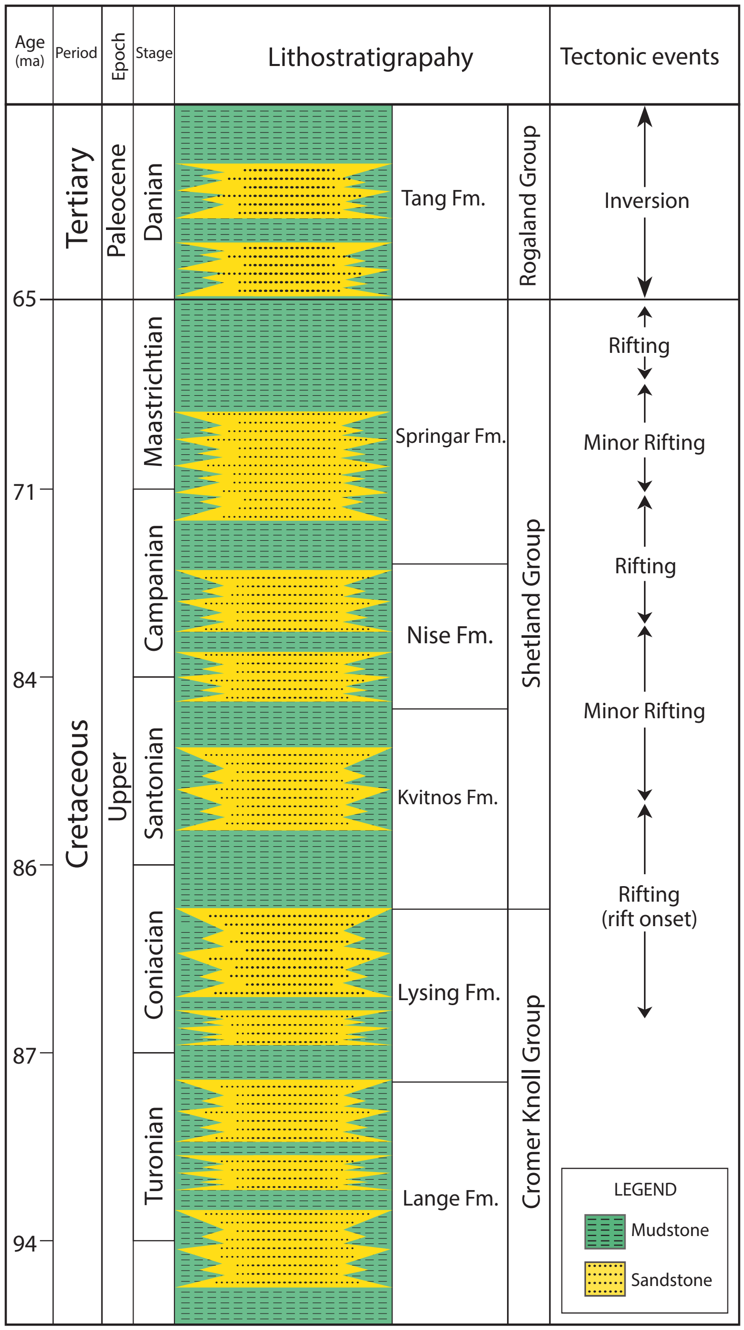

Figure 2.2. Stratigraphy and major tectonic events of the upper Cretaceous within the Møre Basin, Norwegian continental shelf. Adapted from Knaust, (2009). Stratigraphic framework based in Dalland et al., (1998), and on the section penetrated by well 6405/7-1 Ellida, reported in the Norwegian Petroleum Directorate NPD, (2011). Major tectonic events based on Blystad et al., (1995).

GEOLOGICAL SETTING

The Cretaceous Møre basin is located offshore mid-Norway between 62°N to 65°N and 0°E to 6°30'E and is an elongated, wedge-shaped sediment accumulation which strikes NE-SW sub-parallel to the Norwegian coastline (Figure 2.1). The Møre Basin has a complex tectonic history with multiple rift events since Carboniferous times (Ziegler, 1990; Brekke et al., 1999). Different authors have studied the tectonic evolution of the Norwegian Sea basins, resulting in a variety of models and interpretations of its evolution (*e.g.,* Brekke and Riis, 1987; Ziegler, 1990; Blystad et al., 1995; Grunnaleite and Gabrielsen, 1995; Bjørnseth et al., 1997; Lundin and Dore, 1997; Brekke et al., 1999; Doré et al., 1999; Brekke 2000; Skogseid et al., 2000; Gabrielsen et al., 2001; Farseth and Lien, 2002; Lundin and Dore, 2002; Fjeldskaar et al., 2003; Fonneland et al., 2004).

Overall crustal extension in the Late Jurassic followed by thermal subsidence throughout the Cretaceous and Tertiary are thought to be responsible for the modern architecture of the Møre Basin (Blystad et al., 1995; Dore et al., 1996). However, according to Grunnaleite and Gabrielsen (1995), the main structure of the Møre Basin started in the Late Triassic, which was followed by accelerating subsidence in the Early Cretaceous (timing differs among different authors). A subsequent phase of compression in the latest Cretaceous caused tectonic inversion prior to a significantly more intense phase of inversion in the Eocene-Miocene (Grunnaleite and Gabrielsen, 1995). These Tertiary compressional events can be seen as elongated domal structures and reverse faults disturbing the Cretaceous-Tertiary sediment infill (Figure 2.4b)

Within the Møre Basin, several sub basins coexisted due to the presence of intra-basinal structural highs (henceforth called paleo-highs) during the Upper Cretaceous. These paleo-highs were oriented sub parallel and parallel to the NE-SW Møre-Trondelag and Klakk Fault Complexes respectively (Figure 2.1). This

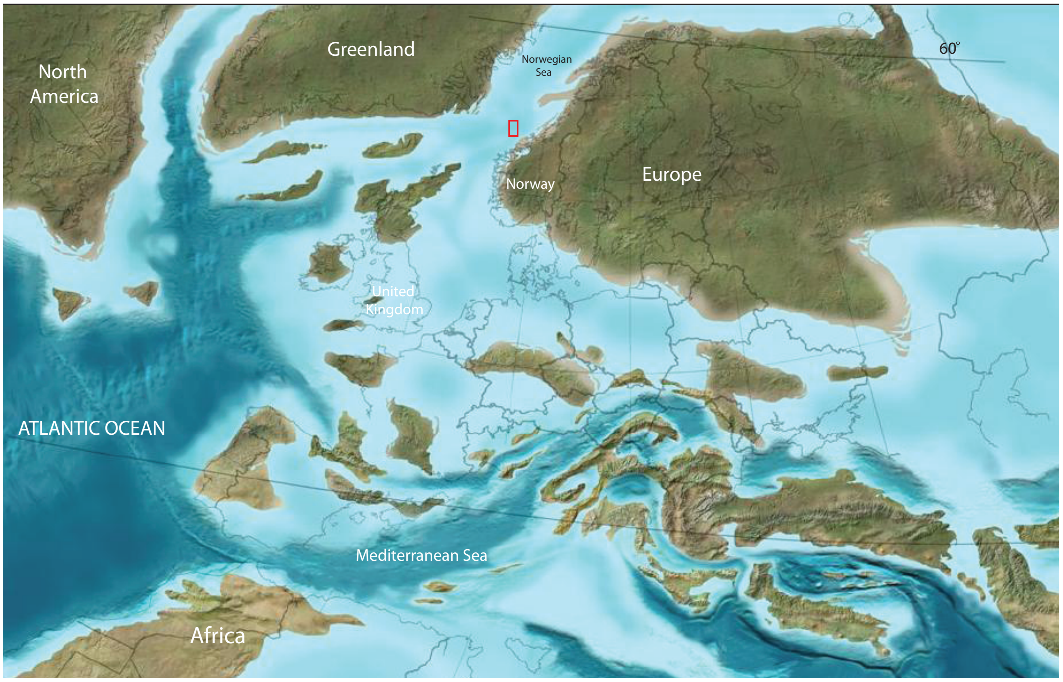

Figure 2.3. Upper Cretaceous (75 ma) paleogeographic map of Europe. The study area is located within the red square (modified from Blakey, 2011).

configuration was developed in response to Late Jurassic to Early Cretaceous extension. Some of these highs were further affected by extensional and/or contractional deformation (Blystad et al., 1995; Grunnaleite and Gabrielsen, 1995; Doré et al., 1999). Therefore, local basin geometry, sediment supply and deposition vary considerably due to the presence of separate source-depocentres systems. The Hellan-Hansen Arch as well as the Vigra, Ona and Gossa highs are most of the prominent positives tectonic features within the Møre Basin (Figure 2.1). North of the study area, in the Vøring basin, there is evidence that some paleo-highs (*e.g.,* the Utgard High) have undergone late Cretaceous uplift and erosion. These events have been identified in seismic sections across the Norwegina Sea basins (Vergara et al., 2001). Consequently, fault-driven syntectonic sedimentary accumulations developed along the main paleo-highs axes.

The Møre Basin can be subdivided into two areas: a shallow-water area to the east and deep-water area to the west (Figure 2.1). A thick Cretaceous succession that locally exceeds 7 km is found throughout the Møre Basin in the deep-water area (Figure 2.4b). Sediment source areas for the Upper Cretaceous reservoirs within the

Møre Basin remain a matter of some dissent. However, it is generally accepted that the Scandinavian landmass was the main sediment source for the east whereas Greenland was likely the sediment source area for the western Møre Basin (Figure 2.2). Additionally, multiple rift events might have created areas emergent by pre-Cretaceous times supplying sediment to the Møre Basin (Brekke et al., 1999).

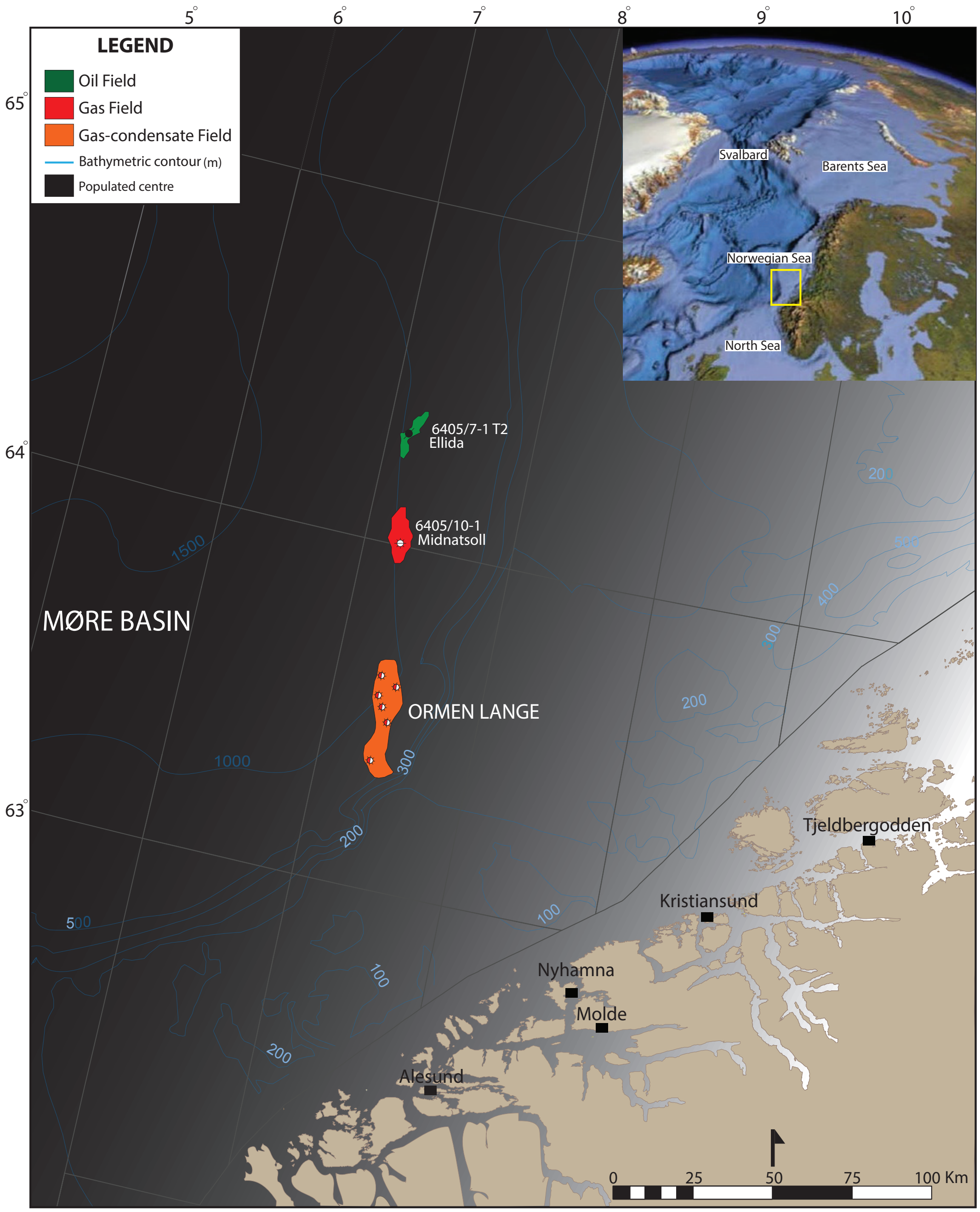

Figure 2.4. Detailed location map showing the wells involved in this study. Pool boundaries are defined by the Norwegian Petroleum Directorate NPD as of November 2011. Top right corner shows the location of the enlarged area within the Norwegian continental shelf. Well 6405/10-1 Midnatsoll is located about 40 kilometers north of the giant Ormen Lange field.

The western Møre Basin is still considered a deep-water frontier basin with vast areas yet underexplored. Recently, hydrocarbon potential has been discovered in deep-water Upper Cretaceous and Tertiary reservoirs (Figure 2.3). The Ellida and Midnatsoll Fields (in this thesis) are examples of recent hydrocarbon discoveries in the Norwegian continental shelf. In the Ellida Field, hydrocarbons are hosted within the Lysing and Nise Formations, whereas the Nise Formation constitutes the main reservoir in the Midnatsoll field. Throughout these two reservoir units a pre-existing sedimentary fabric has been strongly modified and overprinted due to bioturbation. Therefore, reservoir quality accounts as one of the major factors when evaluating prospects in this area and future development plans.

Within this study, the stratigraphic framework adapted is that of Dalland et al., (1988). All reference depths and tops within the studied core interval are based on information published in the Norwegian Petroleum Directorate website NPD (2011).

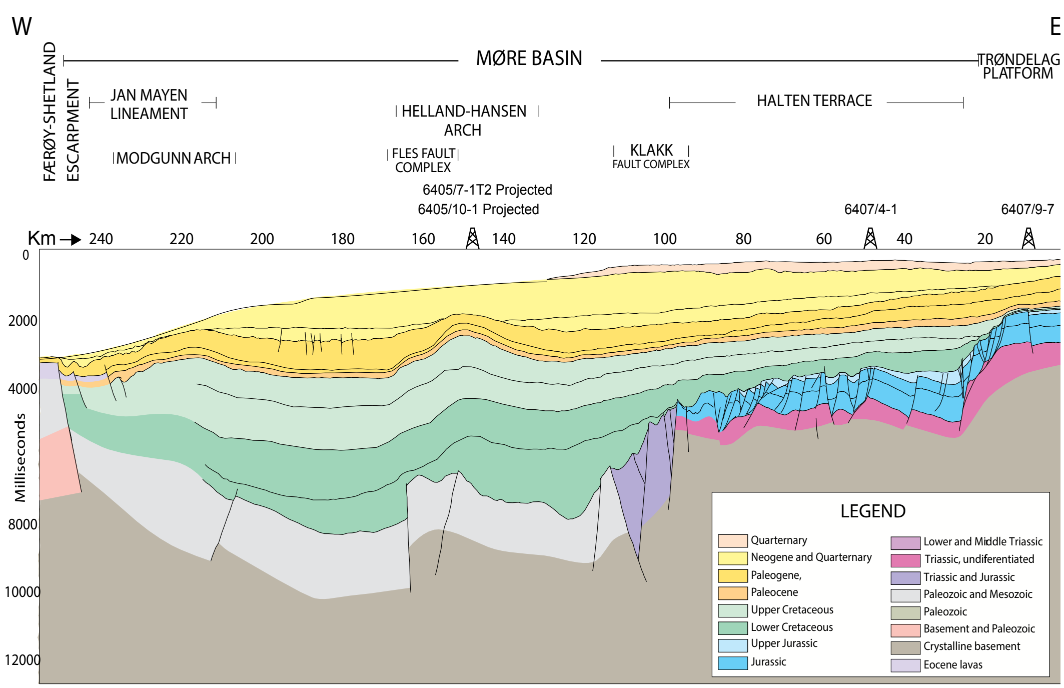

Figure 2.4b. Squematic recostruction of the sediment fill of the Møre Basin. Modified from Dalland et al., (1998). Wells 6405/10-1 Midnatsoll and 6405/7-1T2 are located (Projected) for reference. For location of the cross-section within the Norwegian continental shelf see Figure-2.1.

METHODS

Core analysis

Nine cores (approximately 156 m) were logged to assess the sedimentological and ichnological character of their lithofacies (Table 2.1). Sedimentological analysis concentrated on characteristics such as lithology, grain-size variations, and accessory minerals, bedding contacts, bed-thickness variations and primary physical sedimentary structures. Ichnological determinations included trace-fossil identification, size, relative abundance, diversity, distribution and intensity of bioturbation (Bioturbation Index - BI, Reineck, 1963; Droser and Bottjer 1986; Taylor and Goldring, 1993).

Well Name	Core No.	Core Depth (m)	Length (m)	Formation
6405/7-1 T2 Ellida Discovery	1	2754.00 – 2764.00	10	Nise
	2	2781.00 – 2806.60	25.6	Nise
	3	2808.00 – 2831.60	23.6	Nise
	4	2835.00 – 2861.50	26.5	Nise
	5	2862.00 – 2869.40	7.4	Nise
	6	3751.00 – 3756.00	5	Lysing
	7	3757.00 – 3783.10	26.1	Lysing
6405/10-1 Midnatsoll Discovery	1	3004.00 – 3013.97	9.97	Nise
	2	3014.00 – 3035.18	21.18	Nise

Table 2.1. Summary of the core intervals studied in this thesis.

Trace fossil determination in this study is restricted to the ichnogenus level. In most of the studied cores, a high degree of bioturbation made it difficult to identify primary sedimentary structures. Due to the paucity of physical sedimentary structures, mineralogical accessories (*e.g.,* coal detritus and glaucony) also constitute important criteria in the facies classification and interpretation. Additionally, ichnological characteristics assisted in paleoenvironmental interpretations and provided insight into the sedimentary processes and environmental conditions at the time of deposition of the Lysing and the Nise formations.

RESULTS AND INTERPRETATION

SEDIMENTARY FACIES

This thesis examines core pertaining to two different formations from the Upper Cretaceous in the Norwegian Sea. These are the Coniacian Lysing Formation and the Campanian Nise Formation. Facies description in this study is carried out pairing sedimentological and ichnological assessments. From this analysis, four sedimentary facies are described from the studied core interval including both the Lysing and Nise formations. The most prominent lithological, sedimentological and ichnological characteristics of each facies are presented in (Table 2.2). Nise Formation strata is made up of three facies grouped into one Facies Association termed the *Offshore-structural basin Facies Association* (Osbfa). Three recurrent facies made up Osbfa: 1) Burrowed muddy sandstone (F1); 2) Burrowed muddy to silty sandstone (F2); and 3) Laminated mudstone (F3). Within the Lysing Formation studied core interval, only one facies was identified: 4) Burrowed sandy mudstone (F4). Bioturbation in each facies is reported in a descriptive manner and using the bioturbation index (BI) (Appendix 1 in this thesis). Particular interpretations will be considered within a facies associations framework, which is presented below.

FACIES ASSOCIATIONS

Offshore-structural basin Facies Association (*Osbfa*)

Sediments of the Offshore-structural basin Facies Association (Table 2.2) characterize the Nise Formation (Figure 2.6 and 2.7). Overall, these deposits comprise unburrowed to completely bioturbated (BI = 0 – 6), fine- to very-fine sandstones and mudstones containing a high-diversity trace-fossil assemblage that comprises parts of the proximal through distal *Cruziana* ichnofacies, implying deposition in an offshore fully marine setting mostly below storm wave base (Pemberton et al., 1992; Pemberton and MacEachern, 1995; MacEachern et al., 1999b; MacEachern et al., 2010). Preservation of sedimentary structures is rare to absent. The contacts between facies pertaining to Osbfa are commonly gradational and abrupt. Locally, erosive contacts are identified by the presence *Glossifungites*-demarcated discontinuity surfaces.

Facies 1(F1): Burrowed muddy sandstone

<u>Description:</u>

Facies 1 consist of fine-to very fine-grained sandstone and may grade upwards and downwards into finer sediments of Facies 2 (F2) and Facies 3 (F3). The mud content within Facies 1 ranges from 10% to 20%. Beds are typically 50 cm to 2 m thick and bioturbation is very common. Facies 1 commonly shares gradational and abrupt contacts with F2 and F3 (Figure 2.8 and 2.9). However, erosive basal contacts can be found and are interpreted by the presence of *Glossifigungites*-demarcated discontinuity surfaces (Pemberton and Frey, 1985; Pemberton and MacEachern, 1995; Gingras et al., 2001) (Figure 2.7G). Due to intense bioturbation, any primary physical sedimentary structures are difficult to discern. Parallel and wavy-parallel lamination are common (Figure 2.5F), whereas low angle cross lamination occurs rarelly (Figure 2.5J). Locally, due to the intense burrowing and recurrent overprinting, individual trace fossils and primary bed architecture are difficult to identify. Coal detritus constitutes the most important accessory mineral as well as glaucony. Carbonaceous debris is abundant throughout this facies. Glaucony is disseminated and is commonly concentrated within burrow infill (Figure 2.5K). The highest concentrations were found within burrow fills of *Thalassinoides* and *Planolites* (Figure 2.5 D). Typically, this facies is structureless, and no vestige of the original bedding can be identified. However, an interbedded mud and sand primary fabric can be inferred from the sporadic preservation of the original bedding (Figure

Facies Association 1 (Osbfa): *Offshore-tructural basin Facies Association* – Nise Formation					
FACIES	**LITHOLOGY/ACCESORIES**	**SEDIMENTARY STRUCTURES**	**ICHNOLOGY**	**CONTACTS**	**ENVIRONMENTAL INTERPRETATION**
Facies 1: (F1) Burrowed muddy sandstone	• Fine-grained sandstone. • Abundant, glaucony disseminated and as part of the burrow-fill. • Abundant carbonaceous detritus. • Locally, siderite nodules and sideritic cement.	• Rarely, planar and wavy-parallel lamination. • Locally, convolute lamination, and soft sediment deformation. • Very rare low-angle cross lamination.	• High to complete bioturbation (BI = 4-6). • Very common *Th, Pl, Ne* and *Zo.* • Common *Pa, Sc, Ar, Ch, He, Co* and *Sk.* • Sparse *Rh, Op, Di, Ph, Rs* and *Te.* • Rare *As,* and *Sh.*	• Typically gradational. • Occasionally abrupt. • Locally, erosive lower contacts with F3 at the base of *Glossifungites*-demarcated discontinuity surfaces.	• Fine-grained sedimentation possibly indicative of an overall moderate energy setting. • Carbonaceous detritus suggest a proximity to the shore/sediment source, likely a fluvial input in a steep depositional environment. • High to complete bioturbation suggest that burrowing organisms developed under favorable peleoecological conditions and slow sedimentation rates. • The source of the sand is unknown, but probable erosion of older rocks and/or episodic high-energy/turbiditic events may be responsible for the sand supply. • Sand distribution as clean burrow fills suggests an initially interbedded origin. • Possible transport mechanism includes deltaic deposition and turbidity currents. However, sedimentological evidences of turbidity processes are absent. • Conclusion: Archetypical *Cruziana* ichnofacies, in an epipelagic, tectonically active setting.
Facies 2: (F2) Burrowed muddy to silty sandstone	• Very fine-grained sandstone. • Sparse glaucony. • Rare carbonaceous detritus. • Locally, siderite cement occurs as burrow-fill in some traces (*e.g., Scolicia* and *Planolites*).	• Rarely, planar and wavy-parallel lamination. • Occasionally, soft-sediment deformation.	• Moderate to complete bioturbation (BI = 3-6). • Very common *Ne, Th, Pl* and *Zo.* • Common *He*, *Pa*, *Ph* and *Te*. • Sparse *Ch, Sc*, *As*, *Sh* and *Rs.* • Rare *Ar*, *Sk* and *Ph.*	• Typically gradational. • Occasionally abrupt.	• Very fine-grained sedimentation possibly indicative of an overall low to moderate energy setting. • The origin of the sand is unknown, but probable erosion of older rocks and/or episodic high/energy turbiditic events may be responsible for the sand supply. • Remaining lamination may imply an originally interbedded fabric. • Possible transport mechanism includes deltaic deposition and turbidity currents. However, sedimentological evidences of turbidity processes are absent. • The sporadic occurrence of carbonaceous detritus indicate some relation to the shoreline, but likely more seaward/deeper than F1. • Conclusion: distal *Cruziana* ichnofacies, in a mesopelagic depositional setting, likely as a response of fault-block subsidence.

FACIES	LITHOLOGY/ACCESORIES	SEDIMENTARY STRUCTURES	ICHNOLOGY	CONTACTS	ENVIRONMENTAL INTERPRETATION
Facies 3: (F3) Laminated Mudstone	• Mudstone, with very fine sand/ silt pinstripe laminae. • Sparse siderite nodules.	• Common planar and wavy-parallel lamination. • Locally, structureless with a black-massive appearance. • Occasionally, graded laminae.	• Absent to localized bioturbation (BI = 0-2). • Where present, bioturbation is associated with the very-fine sand/silt laminae. • Rare *Pl.* • Local *Th* associated with *Glossifungites*-demarcated discontinuity surfaces. • Very rare *Zo* and *Ch.*	• Typically gradational. • Occasionally abrupt. • Locally, erosive upper contacts with F1 at the base of *Glossifungites*-demarcated discontinuity surfaces.	• Mud accumulation may correspond to an overall low-energy depositional setting. Deposition primarily occurs from suspension after energetic events. • Generally absent to rare bioturbation suggest lowered oxygen conditions or, due to the homogenous nature of the sediment, burrowing is not evident. Alternatively, sedimentation rates may have been generally high. • The source of the sand is unknown. However, very-fine grained sand/silt pinstripe laminae suggest variable energy events in an overall low energy environment. • Possible transport mechanisms of fine sediments include low density sediment gravity flows caused by 1) tempestites or 2) deltaic sedimentation in shallow waters. • Conclusion: impoverished *Cruziana* ichnofacies, in a bathy-pelagic depositional setting.
Facies 4 (F4): *Bioturbated muddy sandstone* – Lysing Formation					
FACIES	**LITHOLOGY/ACCESORIES**	**SEDIMENTARY STRUCTURES**	**ICHNOLOGY**	**CONTACTS**	**ENVIRONMENTAL INTERPRETATION**
Facies 4:(F4) Burrowed sandy mudstone *(restricted to the Lysing Formation)*	• Very fine-grained sandstone within a muddy matrix. • Abundant glaucony as burrow-fill. • Rare carbonaceous detritus.	• Rare planar and wavy-parallel lamination. • The original fabric appears to be horizontally laminated sand with thin mudstone laminae (?).	• Intense to complete bioturbation • (BI = 4-6). • Abundant *Th*, *Pl* and *Ne.* • Common *Ar, Sk*, *Ch, Zo, Op* and *Rh.* • Sparse *Sc, Pa* and *He*.	• Not referenced as this is the only facies identified in the Lysing Formation.	• Fine-grained sediment possibly indicative of a generally quiescent sediment accumulation. Delta shifting may be responsible of high mud content and carbonaceous detritus in a steep depositional environment. • Abundant and intense bioturbation may indicate that burrowing organisms flourished under favorable conditions like water oxygenation, food resources under more likely low sedimentation rates. • Episodic high-energy events may be responsible for the sand supply. • Sand distribution as clean burrow infill suggests an originally interbedded fabric. • Possible transport mechanism includes sediment-gravity flows and tempestites. However, sedimentological evidence of either process is absent. • Conclusion: distal with proximal elements of the *Cruziana* ichnofacies in a meso- to bathy-pelagic, depositional setting.

Table 2.2 (continued): Interpreted lithofacies of the Lysing and Nise Formation (Ellida and Midnatsoll Fields area, Norwegian continental shelf). Interpretations are expanded upon in the main body of the text. The 4 facies are grouped into 1 Facies Association–Offshore-structural basin Facies Association for the Nise Formation deposits; and Facies 4 for the Lysing Formation strata. Trace fossil abbreviations: *Arenicolites* (Ar), *Asterosoma* (As), *Chondrites* (Ch), *Cosmorhaphe* (Co) *Diplocraterion* (Di), *Helminthopsis* (He), *Nereites* (Ne), *Ophiomorpha* (Op), *Palaeophycus* (Pa), *Planolites* (Pl), *Phycosiphon* (Ph), *Rhizocorallium* (Rh), *Rosselia* (Rs), *Scolicia* (Sc), *Schaubcylindrichnus* (Sh), *Skolithos* (Sk), *Teichichnus* (Te), *Thalassinoides* (Th), and *Zoophycos* (Zo).

2.5F). Examples of F1 commonly exhibit oil-staining making it difficult to differentiate between burrows and the surrounding matrix (Figure 2.5H).

Ichnology:

Facies 1 is distinctive for its abundant and diverse trace fossil assemblage. The ichnofossil suite within this facies exhibits large-diameter burrows, and locally intense bioturbation. The degree of bioturbation in Facies 1 varies from moderately burrowed to completely bioturbated (BI = 4 – 6). Consequently, occurrences of F1 commonly display a totally disrupted primary sedimentary fabric (Figure 2.5).

Trace fossils present within this facies include *Planolites*, *Thalassinoides*, *Rhizocorallium*, *Helminthopsis*, *Nereites*, *Cosmorhaphe*, *Zoophycus*, *Teichichnus*, *Paleophycus*, *Ophiomorpha*, *Schaubcylindrichnus, Arenicolites, Phycosiphon, Asterosoma, Scolicia, Rosselia, Skolithos, Diplocraterion* and *Chondrites* (Figure 2.5H). This bioturbate texture is dominantly composed of very well defined horizontal to inclined burrows. Inclined to vertical traces are also common but less abundant (Figure 2.5C and 2.5H). Horizontal to inclined burrows are attributable mostly to *Thalassinoides* and *Planolites* whereas the inclined to vertical burrows are interpreted as *Skolithos* and *Arenicolites.* The fill of *Thalassionoides* and *Planolites* comprises a significant portion of the sand material within F1. *Thalassinoides* occurs as very well defined-large diameter burrows filled with slightly coarser sand. Carbonaceous debris and glaucony are also present as part of the burrow-infill (Figure 2.5D). Commonly, *Thalassinoides* occurs preferentially re-burrowed and overprinted by mixed ichnofauna such as *Planolites, Palaeophycus* and deep tier *Zoophycus* and *Chondrites* (Figure 2.5I). *Planolites* is abundant and can be found in high densities. The burrow-fill of *Planolites* exhibit coarser material than the surrounding matrix. Horizontal to low angle inclined *Zoophycus* occurs bigger than 10 cm long and 1.5 cm wide and are common in the uppermost portion of the Nise Formation (Figure 2.5I). *Zoophycos* is also commonly seen to cross-cut *Thalassinoides.*

Interpretation:

This facies is characterized by a robust an abundant trace-fossil suite, the presence of glaucony and abundant coal detritus. Glaucony associated with trace-fossils is interpreted to form in fully marine environments with low sedimentation rates, some organic matter content and some degree of turbulence (Miller et al., 2006). The presence of coal detritus disseminated throughout all the occurrences of F1 suggests proximity to the sediment source reflecting more likely a mixed offshore and deltaic-influenced deposition (*e.g.,* Dafoe et al., 2010). Mud deposition and intense burrowing took place between sedimentation events. Interbedded mudstone reflects most likely hypopycnal-flows implying riverine discharge (Figure 2.5F). The presence of low-angle cross-stratified sandstone suggests exposure to increased nearshore wave activity, more likely with moderate to high energy levels (Figure 2.5J). Alternatively, subtle bioturbation present in the foresets may represent slow migration of barforms in a steeply dipping delta front within a steep depositional slope basin margin (Figure 2.5J).

Erosive contacts are interpreted by the presence of *Glossifigungites*-demarcated discontinuity surfaces (Figure 2.8 and 2.9). In a broader scale, *Glossifungites*-demarcated discontinuity surfaces have been interpreted as sequence boundaries

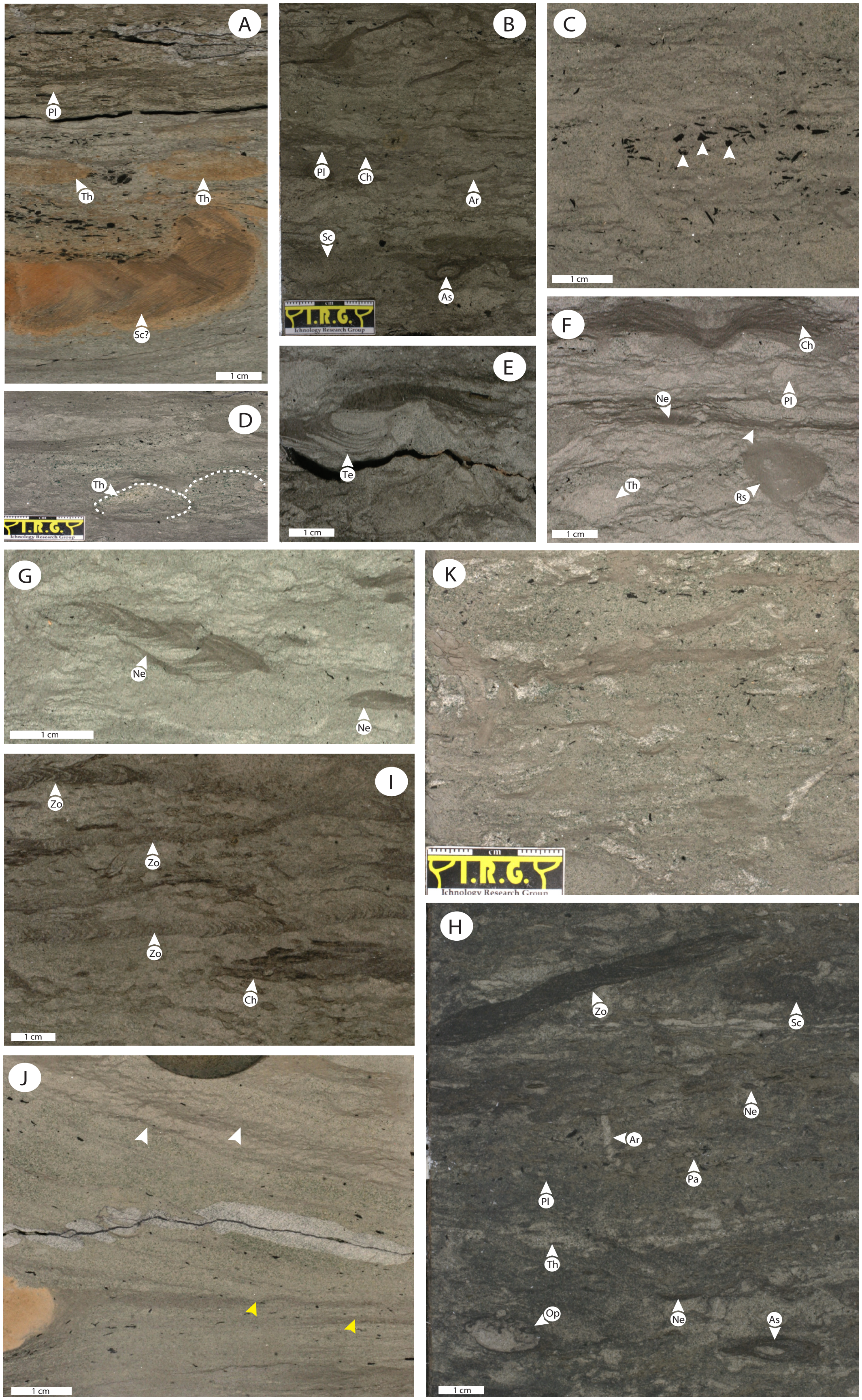
A
Pl
Th
Th
Sc?
1 cm
B
Pl
Ch
Ar
Sc
As
I.R.G.
Ichnology Research Group
C
1 cm
D
Th
I.R.G.
E
Te
1 cm
F
Ch
Ne
Pl
Th
Rs
1 cm
G
Ne
Ne
1 cm
K
I.R.G.
Ichnology Research Group
I
Zo
Zo
Zo
Ch
1 cm
H
Zo
Sc
Ne
Ar
Pa
Pl
Th
Op
Ne
As
1 cm
J
1 cm

Figure 2.5. Facies 1-Burrowed muddy sandstone. **A)** Siderite cement developed as burrow-fill in *Scolicia* (Sc). 2849.48 m, well 6405/7-1 T2, Ellida Field. **B)** Mixing and overprinting of inclined *Arenicolites* (Ar) and horizontal *Planolites* (Pl) burrows. 2829.49 m, well 6405/7-1 T2, Ellida Field. **C)** Inclined *Arenicolites* (Ar) surrounded by abundant coal detritus (white arrows) in a sandy matrix with indistict burrow mottling. 2849.22 m, well 6405/7-1 T2, Ellida Field. **D)** *Thalassinoides* (Th) burrow-fill is commonly made up of glaucony and coal detritus within F1. 3033.67 m, Midnatsoll Field, well 6405/10-1. **E)** Cross-sectional view of *Teichichnus* occurrence (Te) overprinting the original interstratified fine sandstone and mudstone fabric. 2866.79 m, well 6405/7-1 T2, Ellida Field. **F)** Sporadic occurrence of *Rosselia* (Ro) within F1 deposits. Also, low-angle planar-parallel to subparallel lamination (White arrows) suggesting an original sand and mud interbedded fabric. 3025.91 m, Midnatsoll Field, well 6405/10-1. **G)** Well developed *Zoophycos* within a surrounding indistinctly burrow mottled sandy matrix. 3021.47 m, Midnatsoll Field, well 6405/10-1. **H)** Overall highly diverse trace-fossil suite characteristic of F1 displaying *Ophiomorpha* (Op), *Scolicia* (Sc), *Arenicolites* (Ar) and *Scolicia* (Sc), *Ophiomorpha* (Op) and *Asterosoma* (As). Note the low contrast between trace-fossils and matrix due to oil staining characteristic of this facies. 2811.5 m, well 6405/7-1 T2, Ellida Field. **I)** Deep tier *Chondrites* (Ch)-*Zoophycos* (Zo) dominated ichnofabric overprinting a previous *Planolites* (Pl)-*Thalassinoides* (Th) rich ichnofabric. 2809.72 m, well 6405/7-1 T2, Ellida Field. **J)** Low-angle cross lamination (white arrows) and planar-parallel lamination (yellow arrows) more likely denoting a reactivation surface. 2857.16m, well 6405/7-1 T2, Ellida Field. **K)** Glaucony is disseminated throughout the studied core interval giving a greenish colour to some intervals of F1. 3036.67m. Midnatsoll Field, well 6405/10-1.

by exhumation and erosion of previous deposits (Gingras et. al., 2001; Gingras et. al., 2002). However these features are not restricted to be formed after subaerial exposure (Pemberton and Frey, 1985).

The trace fossil-suite of F1 is dominated by infaunal dwelling and grazing structures of ichnogenera interpreted to reflect predominantly deposit-feeding (*i.e., Thalassinoides, Planolites, Teichichnus, Cosmorhape*, *Asterosoma, Chondrites, Palaeophycus, Ophiomorpha* and *Rhizocorallium*) and grazing behaviours (*i.e., Helminthopsis, Phycosiphon* and *Zoophycos*). Rare dwellings of interpreted suspension-feeders (*i.e., Arenicolites, Rosselia, Schaubcylindrichnus, Skolithos,* and *Diplocraterion*) are also present within this suite. This diverse assemblage delineates an archetypical expression of the *Cruziana* Ichnofacies and is representative of a proximal lower offshore setting (Pemberton and MacEachern, 1995; Pemberton et al., 2001; MacEachern et al., 2007).

The occurrence of *Zoophycus* and glaucony indicates a fully marine-offshore shelf environment. The ichnofossil *Rosselia* occurs sparsely (Figure 2.5F), and is often prevalent in the lower shoreface in Mesozoic strata (Pemberton et al., 2001).

Tiering analysis reveals that *Thalassinoides* and *Paleophycus* trace-makers were the first to colonize whereas deep tier *Zoophycos* and *Chondrites* were the last traces to be emplaced in the Facies 1 ichnofabric (Figure 2.5I). Trace-fossil assamblages with abundant *Chondrites, Planolites,* and *Zoophycos* have been interpreted to be the result of stressful conditions such as low levels of oxygen in the water column (Bromley and Ekdale 1984; Savrda and Bottjer 1989; Sageman et al., 1991, Gingras et al., 2002) and low energy depositional conditions. Because of the overall larger size of the trace fossils and intense churning of the sediment, dysaerobic conditions are not interpreted in Facies 1. Rather, the continuous overprinting and diverse trace-fossil suite (*e.g., Thalassinoides, Teichichnus, Arenicolites, Ophiomorpha, Rhizocorallium, Planolites, Skolithos* and *Asterosoma)* suggest favorable long-term conditions for multiple generations of bioturbating infauna to develop (Figure 2.5). This is also interpreted as stable, well-oxygenated paleoenvironmental conditions with low sedimentation rates over extended periods of time. Favourable conditions such as constant food availability may be reflected in the occurrences of suspension-feeder such as U-shaped *Arenicolites* and *Skolithos* (Figure 2.5B and 2.5H). These traces are interpreted to be originated most likely in high energy settings rich in nutrients suspended in the water column (Pemberton and Frey, 1984). Horizontally inclined *Ophiomorpha* is sparsely found throughout the Facies 1 (Figure 2.5H) and is interpreted to reflect deposition in the more distal, below fair weather wavebase but above the storm weather wavebase zone (shoreface-offshore transition zone) (MacEachern et al., 2007a; Cummings and Hodgson 2011).

From the integration of the aforementioned sedimentological and ichnological characteristics, F1 strata reflects near wave base long periods of deposition alternating with short periods of sedimentation above storm wave base

(Pemberton and MacEachern, 1995; MacEachern et al., 2007; MacEachern et al., 2010). This occurred most likely in an epipelagic depositional setting (Figure 2.12).

Facies 2 (F2): Burrowed muddy to silty sandstone

Description:

This facies is composed of very fine-grained sandstone and grades upwards and downwards into coarser and finer sediments of F1 and F3 respectively. Recurrent beds of Burrowed muddy to silty sandstone represent a significant portion of the Nise Formation reservoir (Figure 2.8 and 2.9). This facies displays gradational and abrupt contacts with F2 and F3 (Figure 2.6A and 2.6J). An overall robust and highly diverse trace fossil suite characterizes this facies. Within F2, burrow morphologies are easier to identify due to its slightly higher mud content (20-40%) than F1. Therefore, sediment contrast provides a better differentiation between burrow-fill and surrounding matrix. Unlike F1, glaucony and carbonaceous detritus are rarely present within F2 strata. Beds are typically 1m to 2m thick and a biogenic fabric makes it difficult to discern the original bedding architecture. Horizontal to wavy lamination occurs locally and is the sole remaining primary sedimentary structure within F2 deposits (Figure 2.6E).

Ichnology:

A highly diverse and abundant ichnofossil assemblage characterizes F2. The majority of F2 occurrences exhibit very highs levels of bioturbation (BI = 4 – 6). Therefore, primary physical sedimentary structures are difficult to identify. The ichnological assemblage in this facies includes *Thalassinoides*, *Planolites*, *Nereites*, *Teichichnus, Asterosoma*, *Palaeophycus*, *Rhizocorallium*, *Phycosiphon, Zoophycos, Arenicolites*, *Scolicia, Rosselia, Schaubcylindrichnus*, *Skolithos, Helminthopsis* and *Chondrites* (Figure 2.6). Overall, the trace fossil suite in this

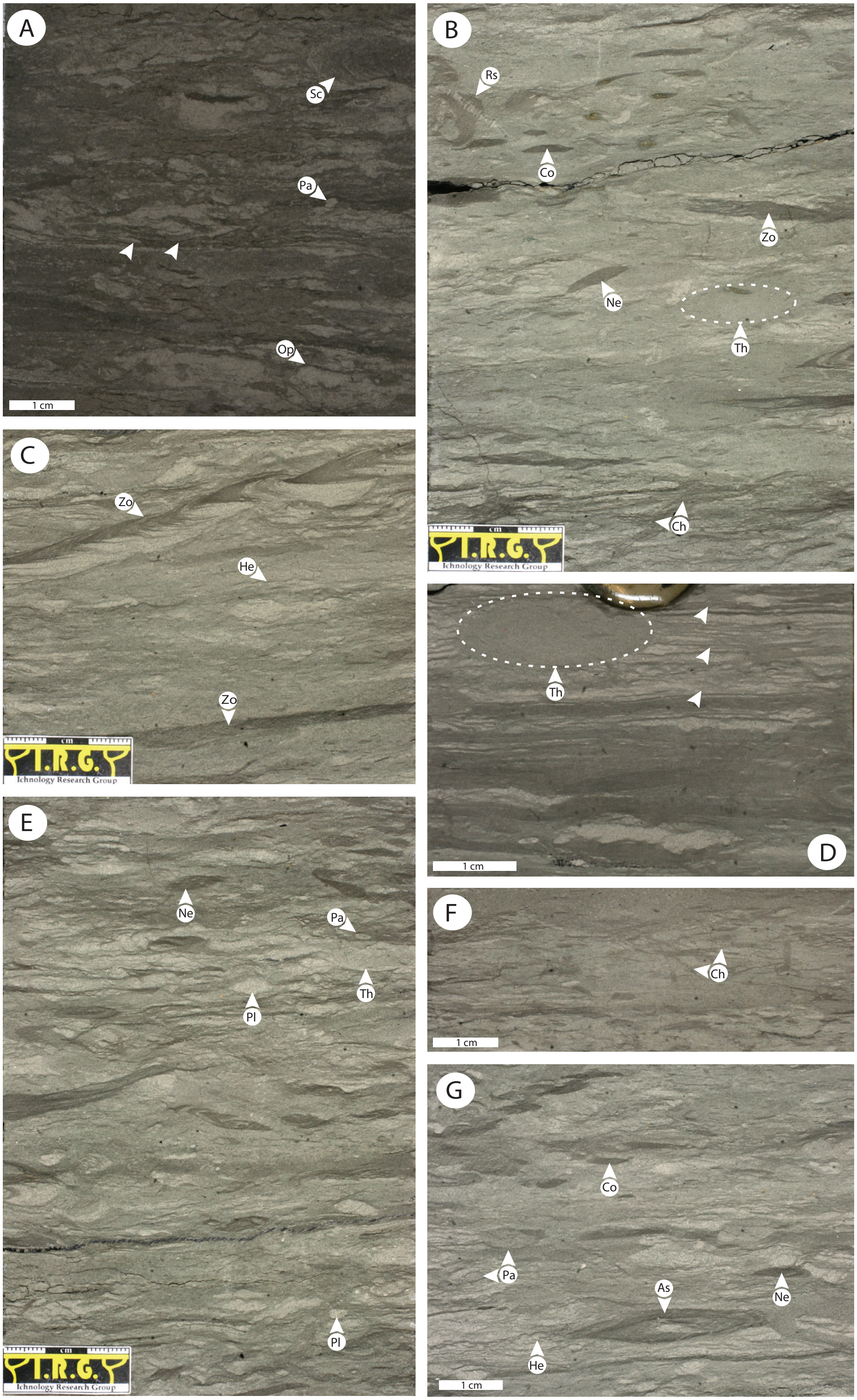
A
Sc
Pa
Op
1 cm
B
Rs
Co
Zo
Ne
Th
Ch
cm
I.R.G.
Ichnology Research Group
C
Zo
He
Zo
cm
I.R.G.
Ichnology Research Group
D
Th
1 cm
E
Ne
Pa
Th
Pl
Pl
cm
I.R.G.
Ichnology Research Group
F
Ch
1 cm
G
Co
Pa
As
Ne
He
1 cm

Figure 2.6. Facies 2-Burrowed muddy to silty sandstone. **A)** Discernable *Scolicia* (Sc), *Paleophycus* (Pa) and *Ophiomorpha* (Op) in an oil stained portion with remaining planar-parallel lamination (white arrows). 2827.48m, well 6405/7-1 T2, Ellida Field. **B)** *Thalassionoides* (Th), *Rosselia* (Ro), *Nereites* (Ne) and *Chondrites* (Ch), *Zoophycos* (Zo) and *Cosmorhaphe* (Co) within a massive appearance silty sandstone fabric. 3029.90m, Midnatsoll Field, well 6405/ 10-1. **C)** *Zoophycus* (*Zo*) is abundant as well as *Helminthopsis* (He) throughout the occurrences of F2. 3023.90m, Midnatsoll Field, well 6405/ 10-1. **D)** *Thalassionoides* (Th) disturbing the remaining wavy-parallel lamination. 2853.41m, well 6405/7-1 T2, Ellida Field. **E)** Diverse ichnofossil assemblage includes *Planolites* (Pl), *Nereites* (Ne), *Chondrites* (Ch), *Cosmorhaphe* (Co) and *Phycosiphon* (Ph). 3030.50m, Midnatsoll Field, well 6405/ 10-1. **F)** *Chondrites* (Ch) is common as clusters in some occurrences of F2 2858.51m, well 6405/7-1 T2, Ellida Field. **G)** *Asterosoma* (As), *Paleophycus* (Pa), *Helminthopsis* (He) and *Cosmorhaphe* (Co) within a *Nereites* (Ne) dominated segment. 3029.50m, Midnatsoll Field, well 6405/ 10-1.

facies is predominantly made up of horizontal burrows. Unlike F1, vertical trace fossils are rarely found in the occurrences of F2. Throughout this facies *Nereites* and *Zoophycus* are the most common trace fossils. *Nereites* is easily identified from the surrounding matrix and locally can be found in high amounts (Figure 2.6H and 2.6K). Well defined *Zoophycus* display large diameter burrows some of them up to 1,5 cm diameter and 8 cm length (Figure 2.6B). Recurrent sand-filled horizontal burrows mostly attributable to *Thalassinoides* and *Planolites* are present throughout F2. Like Facies 1, slightly coarser sand is present as the infill of *Thalassinoides* and *Planolites* in Facies 2. However, unlike F1, Facies 2 burrow-fills display very low to rare coal detritus and glaucony (Figure 2.6L and 2.6G). Despite burrow overprinting in F2 is common, it is not as abundant as the one in the F1 (Figure 2.6B). Sparse *Paleophycus, Scolicia* and *Chondrites* are seen overprinting and cross-cutting the previously established biogenic fabric (Figure 2.6A and 2.6K).

Interpretation:

The principal differences between F1 and F2 are the decrease in abundance of vertical to inclined trace-fossils (*e.g., Skolithos*, *Arenicolites)*, the sporadic appearances of glaucony and coal detritus, and higher mud content.

The abundant and robust trace fossil suite of F2 is dominated by deposit-feeding and dwelling structures (*i.e., Thalassinoides*, *Planolites*, *Nereites*, *Teichichnus, Asterosoma*, *Palaeophycus*, *Rhizocorallium*, *and Chondrites*) with common occurrences of grazing traces (*i.e., Phycosiphon, Zoophycos and Helminthopsis*), and rare burrows of inferred suspension-feeding animals (*i.e., Arenicolites*, *Schaubcylindrichnus*, and *Skolithos*). This assemblage reflects an expression of the distal *Cruziana* Ichnofacies (Pemberton and MacEachern, 1995; MacEachern et al., 2007; MacEachern et al., 2010).

The diverse trace-fossil suite suggests that there was little to no significant change in paleoenvironmental conditions compared to F1. The diversity of ichnogenera and intense burrow overprinting of F2 point towards stable, and abundant nutrients, favourable for the endobenthic fauna as seen in F1. High degrees of burrowing within F2 suggest that bioturbating infauna had sufficient time to colonize and bioturbate between sedimentation events. Also, the burrow diameter and well-developed uniform distribution show no sign of environmental stresses (*e.g.,* water oxygenation and salinity fluctuation) (Figure 2.6B, 2.6K and 2.6I). Fewer dwellings of inferred suspension-feeding organisms and increased proportions of grazing traces, is interpreted to represent a seaward shifting of the depositional environment to a more distal setting than F1. The upward and downward transition of F2 into the bioturbated strata of F1 or F3 was mostly gradual (Figure 2.6A and 2.6J) and no primary lamination is preserved within F2 intervals.

The aforementioned sedimentological and ichnological characteristics discussed for F2 are interpreted to reflect deposition in a more distal setting than F1, most likely below storm wave base (Pemberton and MacEachern, 1995; MacEachern et al., 2007; MacEachern et al., 2010), in a mesopelagic depositional setting (Figure 2.12).

Facies 3 (F3): Laminated Mudstone

Description:

Facies 3 comprises the muddy portion of the studied strata and is the less recurrent segment within Osbfa. Overall, F3 is characterized by its very low intensities of bioturbation and pinstripe lamination. Locally, some segments appear typically dark and dark-gray, massive without any visible burrowing (Figure 2.7B). Nodules of pyrite up to 4 cm are present within a surrounding massive-appearing muddy matrix (Figure 2.7 D).

The trace fossil assemblage is less diverse and abundant of the facies within Osbfa (Figure 2.8 and 2.9). Excluding the pinstripe laminae that contain *Planolites* and some sporadic segments, this facies is generally unburrowed. Primary sedimentary structures are composed of wavy-parallel lamination and low angle parallel lamination (Figure 2.7 C and 2.7 H). The segments of F3 commonly exhibit gradational and sharp contacts with F1 and F2 (Figure 2.7 A and 2.7 J). Occasionally, F3 shares erosional upper contacts with F1 interpreted by *Glossifungites*-demarcated discontinuity surfaces (Figure 2.7 G).

Ichnology:

This facies association is characterized by an overall impoverished trace fossil suite. The degree of bioturbation within this facies varies from absent to rare (BI 1 - 2), but typically could be described as sparse. Unlike F1 and F2, very low levels of ichnologic diversity characterize F3 deposits. Where bioturbation is present, a diminutive, monospecific assemblage of *Planolites* is persistent.

Throughout this interval, burrowing appears to be restricted to the sand/silt pinstripe laminae horizons (Figure 2.7A). Where present, the ichnofauna is majority composed of diminutive *Planolites* and some isolated occurrences of *Zoophycus* and *Chondrites* (Figure 2.7A). Locally, large sand-filled *Thalassinoides* are found

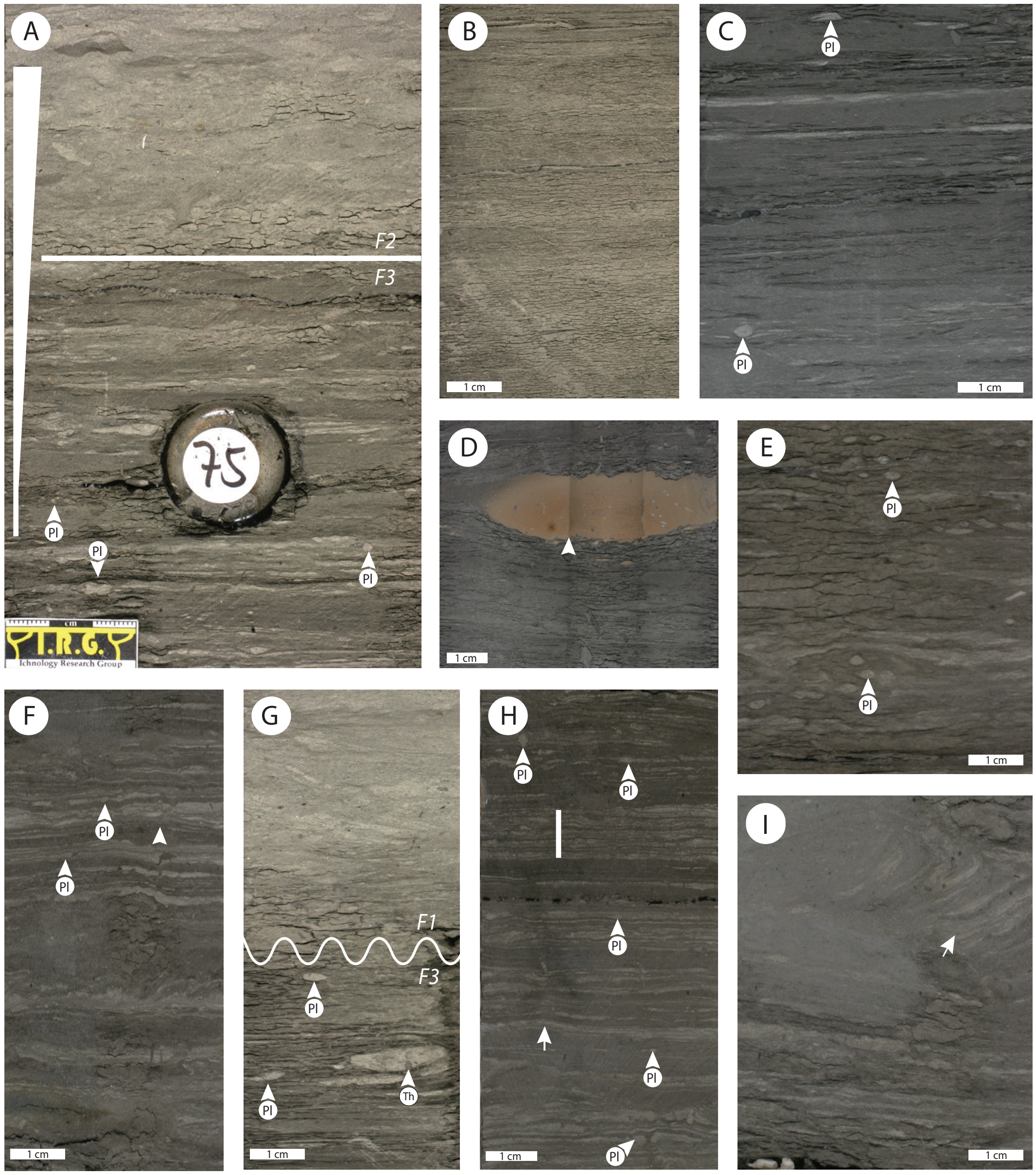

Figure 2.7. Facies 3-Laminated Mudstone**. A)** Abrupt contact between F3 and F1. Note that *Planolites* is associated preferentially to the very-fine sand/silt pinstripe lamination. 3022.54 m, well 6405/10-1, Midnatsoll Field. **B)** Unburrowed massive-appereance dark to light grey mudstone layer common in F3. 3016.61 m, well 6405/10-1, Midnatsoll Field. **C)** Parallel low-angle lamination sparce throughout F3. 3016.19 m, well 6405/10-1, Midnatsoll Field. **D)** Massive siderite nodules surrounded by dark mudstone. 3022.54 m, well 6405/10-1, Midnatsoll Field. **E)** Relatively highly burrowed interval containing *Planolites* (Pl) and *Helminthopsis*? (He). 2816.42 m, well 6405/7-1 T2, Ellida Field. **F)** Low angle parallel to wavy lamination (white arrow) displaying *Planolites* (Pl). 2813.03 m, well 6405/7-1 T2, Ellida Field. **G)** Erosive facies contact between F3 and F1. A *Glossifungites*-demarcated discontinuity surface developed when *Thalassinoides* (Th) descended into the previously buried and later exhumated muddy substrate of F3. 3015.19 m, well 6405/10-1, Midnatsoll Field. **H)** Recurrent lamination (white bar) may be indicative of some tidal influence at the time of deposition of F3. *Planolites* (Pl) monospecific assemblages developed along the coarser sediment segments F3. 2821.48 m, well 6405/7-1 T2, Ellida Field. **I)** *Teichichnus*-like burrow feature (white arrow) is locally present. 2817.55 m, well 6405/7-1 T2, Ellida Field.

on the upper contacts of F3 and are interpreted as *Glossifungites*-demarcated discontinuity surfaces.

Burrows are remarkably smaller (*e.g., Planolites*), than those observed in F1 and F2. *Planolites* occurs as monospecific assemblages linked to pinstripe very-fine sand/silt laminae (fig. 2.7F and 2.7H). The average burrow diameter in F3 ranges from 1 mm (*e.g., Planolites*) up to 2 cm (*e.g., Thalassinoides*), (Figure 2.7G).

<u>Interpretation:</u>

The overall higher amount of mud deposition suggests nearly continuous fair-weather conditions. The interbedding of pinstripe very-fine sand/silt laminae within F3 indicates fluctuating energy conditions within an overall low hydraulic energy setting. Sand laminae are interpreted as being the product of distal sporadic storm events, or turbiditic flows. Infaunal feeding burrows (*e.g., Planolites*) are interpreted to develop after these episodic events. These conditions persisted for short periods of time, but were enough for the *Planolites* monospecific assemblage to colonize. However, overall rare to absence burrowing persists throughout the occurrences of F3.

The trace fossil suite of F3 is dominantly composed by burrows reflecting deposit-feeding and dwelling structures (*Planolites* and *Thalassinoides*) with subordinate occurrences of grazing traces (*Zoophycos*). The ichnological suite reflects elements of an impoverished *Cruziana* ichnofacies (Ekdale et al., 1984; MacEachern et al., 2007a). This ichnofacies typically represents open marine, mid-shelf to outer-shelf marine environments.

The paucity of trace fossils probably reflects that bioturbating infauna lived under some stressful conditions (*e.g.,* fluctuating salinity and oxygenation). Impoverished ichnogeneric diversity and abundance, either reflects dysaerobic conditions (Bromley and Ekdale, 1984; Savrda and Bottjer 1986; Boyer and Droser, 2007, Boyer and Droser, 2009, Boyer and Droser, 2011) or can be explained more likely as the result of lack of lithological contrast (MacEachern et al., 1999). Alternatively, sedimentation rates may have been high, so no colonization took place. The simple morphology, small size and poorly-developed ichnofossil assemblage of F3 may reflect variations in the bottom-water oxygen levels (Figure 2.7). Siderite nodules also suggest an upward migration of the redox boundary due to low water oxygenation (Figure 2.7D). Similar responses of endobenthic infauna to anoxic events and variations in the bottom-water oxygen levels are recorded in Mesozoic and Cenozoic strata (Bromley and Ekdale, 1984; Savrda and Bottjer 1986, Savrda and Bottjer 1989). This interpretation is based in the impoverished, low diversity and small size of the trace fossil suite within F3. Significant variations in the energy of the environments allowed the deposition of very-fine sand/silt laminae. These intervals were subsequently colonized by a restricted fauna able to tolerate stressful conditions (Figure 2.7A, 2.7F and 2.7E).

The aforementioned sedimentological and ichnological characteristics discussed for F3 are interpreted to reflect deposition below storm-weather wave base (Pemberton and MacEachern, 1995; MacEachern et al., 1999; MacEachern et al., 2010), with sporadic energetic events. This most likely took place in a bathypelagic, tectonically active depositional setting (Figure 2.12).

Offshore-structural basin Facies Association (Osbfa) – Nise Formation interpretation

The robust and diverse trace-fossil suite in sandy intervals of *Offshore-structural basin Facies Association* (Osbfa) suggests that abundant nutrient supply and negligible ecological stresses (*e.g.,* water salinity and oxygenation) persisted at the time of deposition of F1 and F2 (Figure 2.5 and 2.6). These paleonvironmental conditions suitable for benthic life to colonize and flourish persisted between stressful ecological intervals evidenced by the diminutive impoverished trace-fossil suite of F3 (Figure 2.7). Much of the ichnofauna diversity of Osbfa resides in ichnogenera interpreted to have been produced by deposit feeding behaviours. Among others, *Thalassinoides* and *Planolites* are the most abundant ichnogenus within Osbfa strata. Infaunal dwelling burrows also constitute a significant component of the trace-fossil suite of this facies association. Overall, the ichnofossil assemblage that typifies Osbfa is characteristic of the proximal through distal *Cruziana* ichnofacies (Pemberton and MacEachern, 1995; MacEachern et al., 2007; MacEachern et al., 2010). Typically, this ichnofacies develops and is representative of open marine, inner to outer-shelf equivalent environments. High degrees of bioturbation (BI 3 – 6) resulted in total disruption of the primary sedimentary fabric (Figure 2.5 and 2.6). However, parallel and wavy-parallel lamination persisted locally, pointing towards an original interbedded fabric. Stable, long term conditions are evidenced by the highly diverse and abundant trace-fossil suite present in the sandy beds (*i.e,* F1 and F2) of Osbfa deposits. In contrast, F3 deposits display a poorly-developed monospecific *Planolites* trace-fossil suite. This is interpreted to reflect bottom-water dysaerobic conditions for benthic ichnofauna to develop diminishing the abundance and size of individuals (Bromley and Ekdale, 1984; Savrda and Bottjer 1986, 1989; Boyer and Droser, 2011). This diminutive trace fossil suite developed

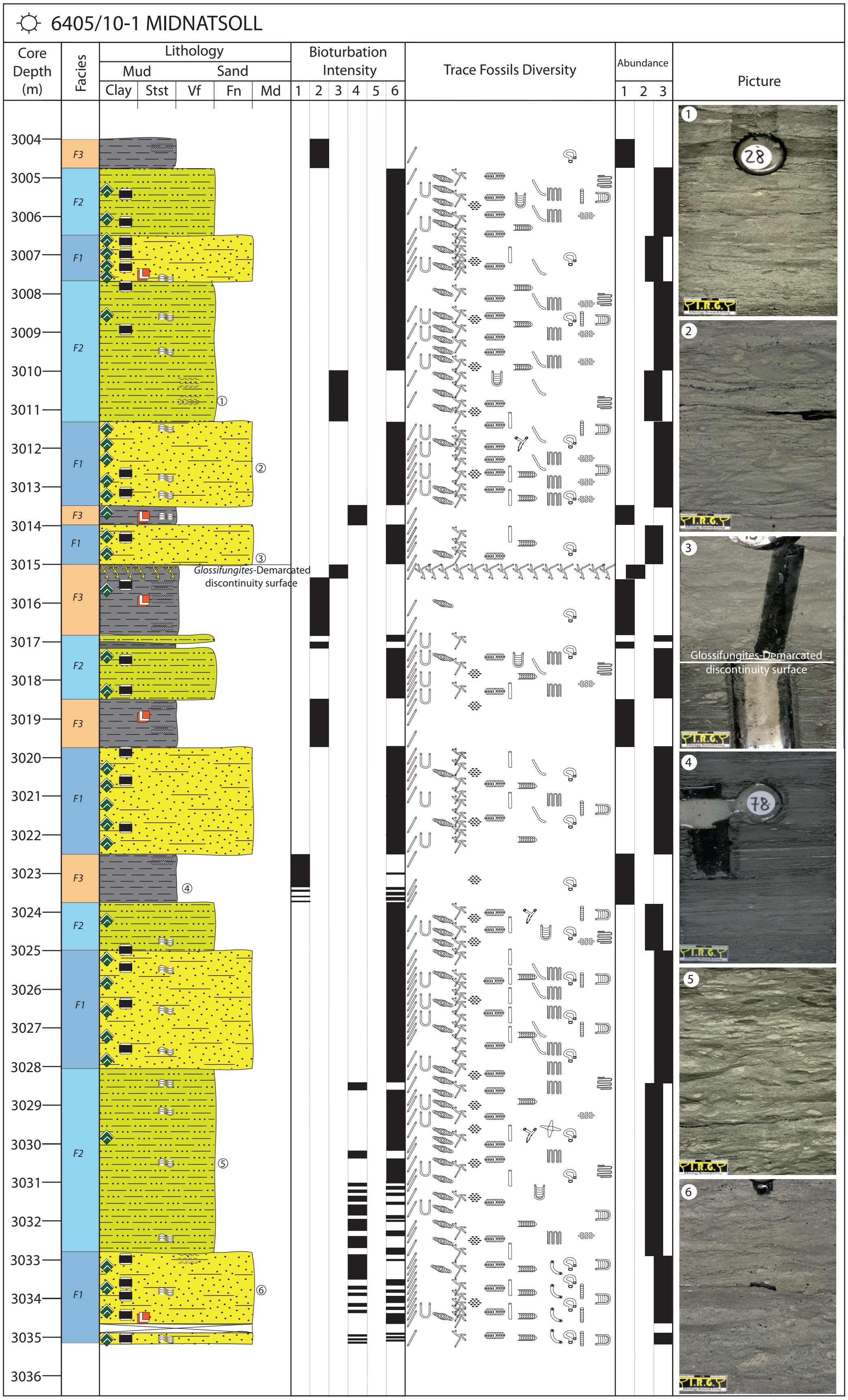
6405/10-1 MIDNATSOLL
Core Depth (m)
Facies
Lithology
Mud
Sand
Clay
Stst
Vf
Fn
Md
Bioturbation Intensity
1 2 3 4 5 6
Trace Fossils Diversity
Abundance
1 2 3
Picture
3004
3005
3006
3007
3008
3009
3010
3011
3012
3013
3014
3015
3016
3017
3018
3019
3020
3021
3022
3023
3024
3025
3026
3027
3028
3029
3030
3031
3032
3033
3034
3035
3036
F3
F2
F1
Glossifungites-Demarcated discontinuity surface
Glossifungites-Demarcated discontinuity surface

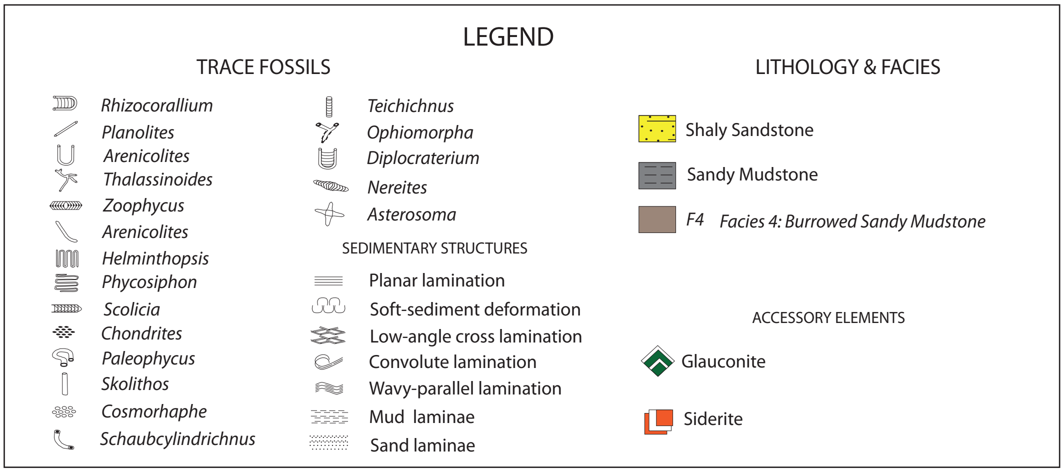

Figure 2.8. Composite plot showing the resulting sedimentological and ichnological characteristics of the interpreted lithofacies for the Nise Formation in well 6405/10, Midnatsoll.

only when conditions were favourable (*e.g.,* emplacement of very-fine sand/silt laminae) evidenced by a decrease in depth of feeding and residence of bioturbating infauna.

Between the Osbfa beds, erosive events are identified by the presence of *Glossifungites*-demarcated discontinuity surfaces. The recurrent interbedding of sandstone and mudstone records variations in the sea level in response to cycles of rifting in the Late Cretaceous within the Møre Basin. Evidence of this recurrent shifting in the energy of the sedimentary environment may be found in the development of *Glossifungites*-demarcated discontinuity surfaces (MacEachern et al., 1999; Gingras et al., 2001; Gingras et al., 2002). This implies burrow architectures and sedimentological relationships that demonstrate burrowing into a firm substrate. Although, this type of surfaces are not restricted to colonization of semiconsolidated substrates in which subaerial exposure took place (Pemberton and Frey, 2005). The widespread exposure of compacted sediment requires erosion of previously buried sediment, due to changes in local base level. Such changes are most commonly attributed to fluctuations in sediment supply, subsidence/uplift, autocyclic avulsion (such as delta-lobe or channel abandonment), or eustatic adjustment (Gingras et al., 2002). Where *Glossifungites*-demarcated surfaces are widespread, mappable, and recurrent in the stratigraphic succession, their presence is generally attributed to changes of relative sea level. Several researchers have demonstrated the importance of identifying *Glossifungites* Ichnofacies assemblages in the rock record, particularly as they are commonly associated with transgressive surfaces of erosion (TSE) (Pemberton and Frey 1985; Pemberton and MacEachern 1995; Gingras et al., 2001; 2002).

Depositional environments and sediment supply were significantly influenced by an active tectonic setting during Upper Cretaceous times within the Møre Basin. Tectonic changes may have driven shifts in sediment source and were responsible for sand accumaltions along paleo-high margins and axis. This tectonic configuration created different sub-basins with different erosion-deposition systems ranging from shallow marine presented in F1, to traditionally interpreted deep-water settings like the one interpreted for F3 in a tectonically influenced, steep paleo-high depositional setting (*e.g.,* Kittilsen et al., 1999; Brekke et al., 1999; Brekke et al., 2001; Vergara et al., 2001; Fjellanger et al., 2005; Kjennerud and Vergara, 2005; Martinsen et al., 2005; Fugelli and Olsen, 2005a, 2005b; Knaust; 2009a). Herein, *Glossifungites*-demarcated discontinuity surfaces are interpreted to record the uplift and down lift of the positive features (*e.g.,* Paleo-highs) that may imply subaerial exposure, erosion and deposition along the paleo-highs margins and axis. Within this framework, it is possible that coal abundant in F1 and rare in F2 appears as the result of erosion of pre-existing Jurassic sediments located on top of paleo-highs. Grunnaleite and Gabrielsen (1995), have documented erosion of coal seems hosted within Jurassic-age deposits in the Møre Basin. This coal deposits were exposed, later re-deposited and available throughout the sediments pertaining to F1 and in minor proportion F2 beds (Figure 2.5 and 2.6 respectively). Palaeogeographic reconstructions and integration of 2D/3D seismic and well data have revealed a series of paleo-highs that have undergone different tectonic phases

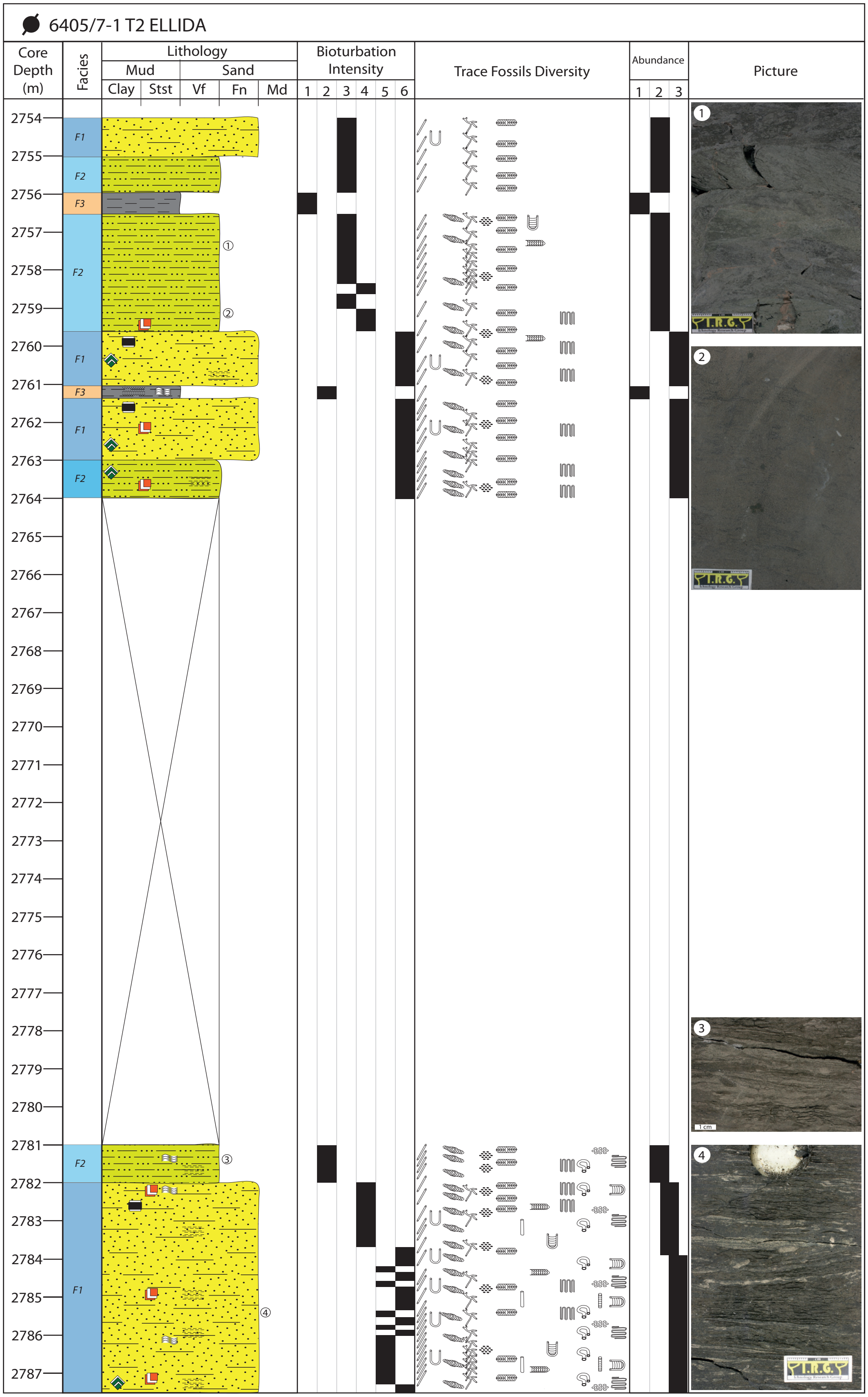

Figure 2.9. Continued.

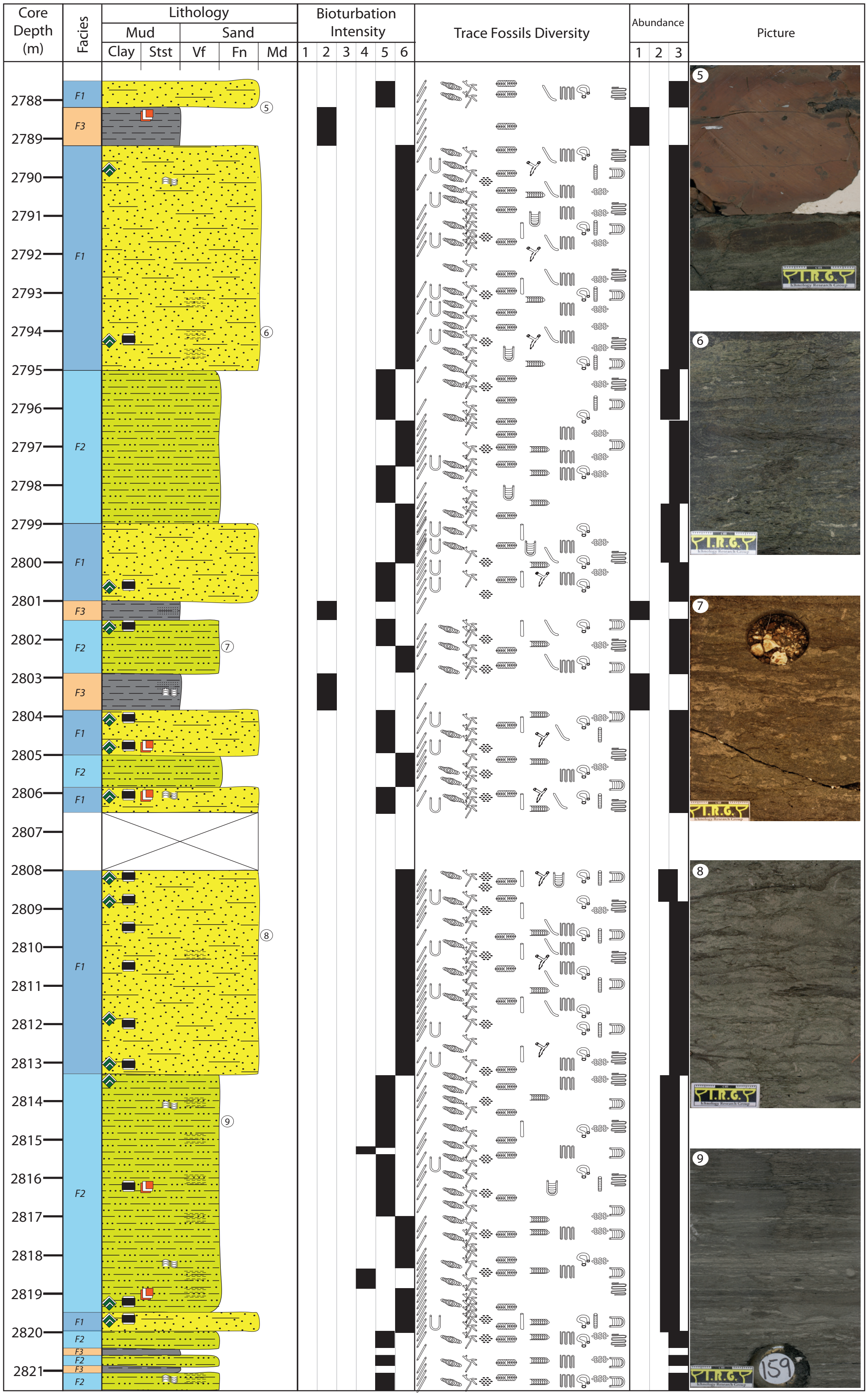

Figure 2.9. Continued.

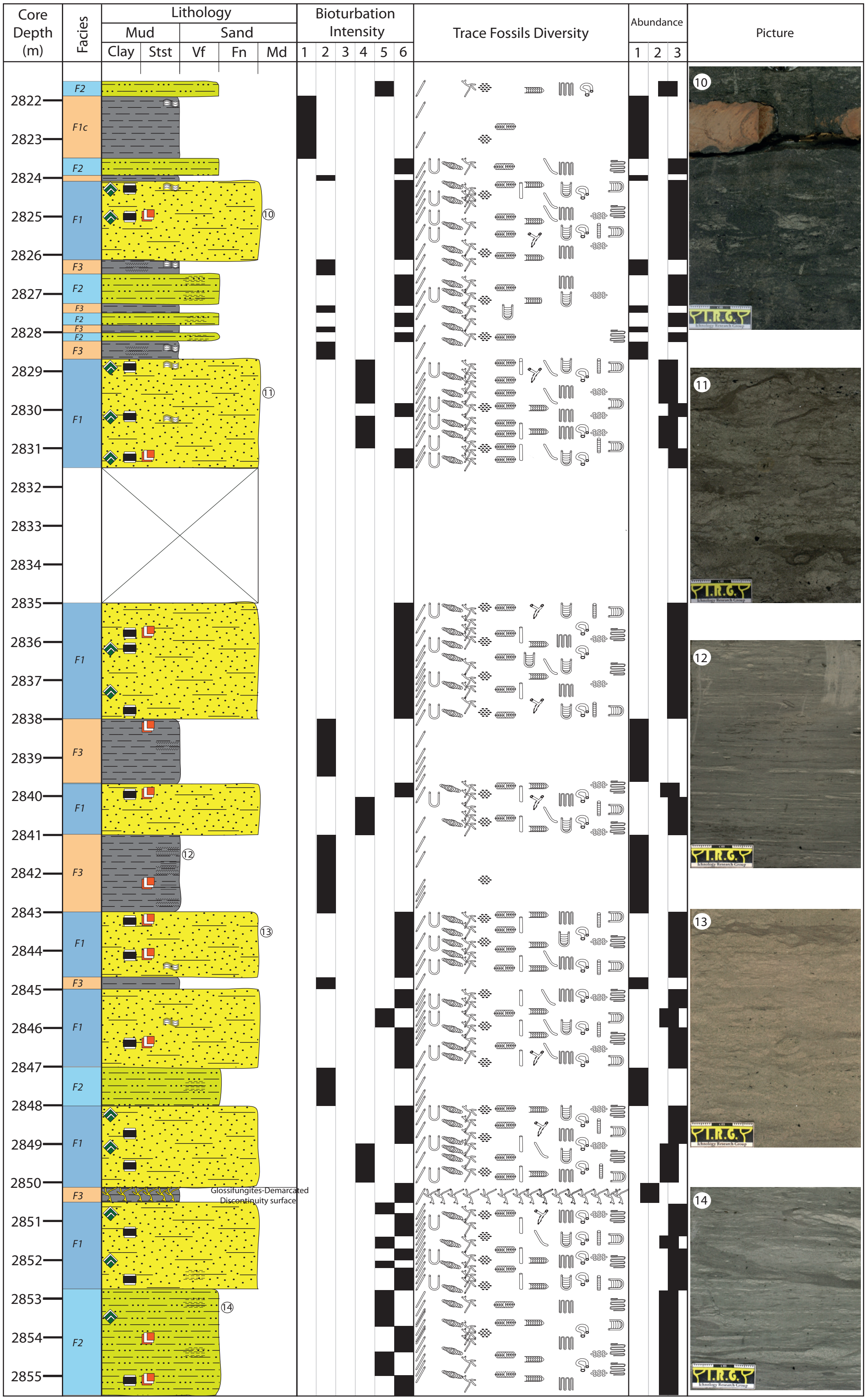

Figure 2.9. Continued.

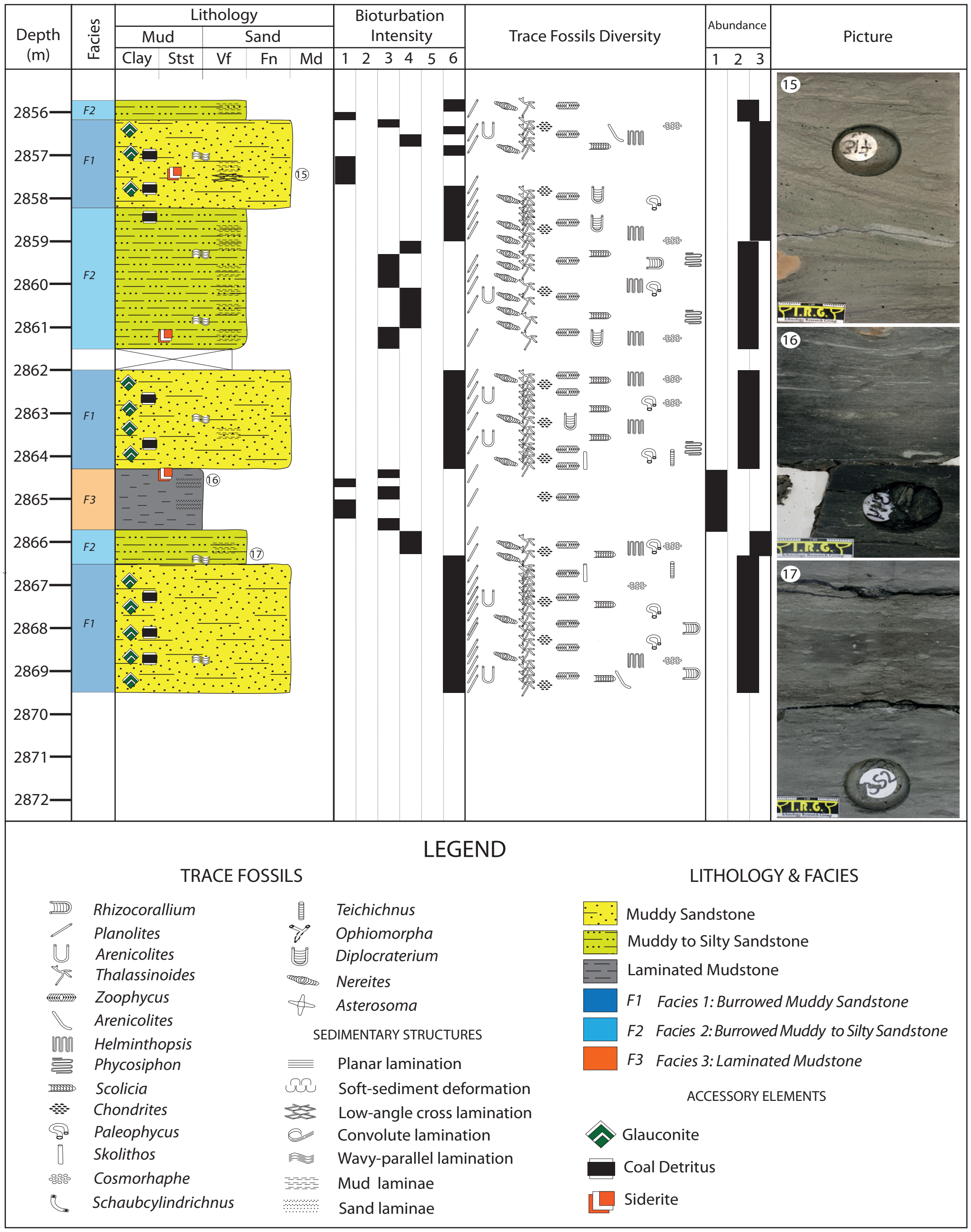

Figure 2.9. Composite plot showing the resulting sedimentological and ichnological characteristics of the interpreted lithofacies for the Nise Formation in well 6407/10-1, Ellida.

and sedimentation cycles (Vergara et al., 2001, Kjennerud and Vergara, 2005; Fugelli and Olsen; 2005a, Fugelli and Olsen 2005b, Fugelli and Olsen 2007). Consequently, these prominent features may display a different sedimentary record than the traditional deep-water depositional approach in the Norwegian Sea basins.

Facies 4 (F4): Burrowed sandy mudstone

<u>Description:</u>

This facies is restricted to the Lysing Formation strata, thus the only one proposed for the entire core interval studied for this Formation in the well 6405/7-1T2, Ellida Field. Burrowed sandy mudstone is made up of interbedded very-fine sandstone and mudstone, with common fine-grained sand as burrow-fills. Intense to high bioturbation (BI = 4 – 6) levels typifies Facies 4. Horizontal to low-angle and wavy-parallel lamination constitute the primary physical sedimentary structures preserved in Facies 4 (Figure 2.10C). Where present, these remaining sedimentary structures suggest an original interbedded fabric. Facies 4 is distinctive for its significantly high mud content (Figure 2.10). Some intervals display a dark, massive appearance in which any discrete burrowing is difficult to discern. Sandier portions allow lithological contrast and better differentiation between the burrow-fill and surrounding matrix (Figure 2.10E and 2.10G). Trace fossils within this facies are very large and a significant proportion of traces occur on a centimeter scale (*e.g., Thalassinoides, Arenicolites*).

Abundant glaucony and siderite are the accessory minerals present in the F4 deposits. Glaucony occurs throughout the entire interval and is concentrated as burrow-fills (Figure 2.10G) whereas, siderite occurs locally as massive nodules with a distinctive dark to light brown colour (Figure 2.10H). Unlike F1 and F2 of the aforementioned Offshore-structural basin Facies Association, coal detritus are rare in F4. Locally, the mud beds appear massive and rarely displaying horizontal and wavy-parallel lamination (Figure 2.10C). Upper and lower contacts of Facies 4 are not discussed herein as F4 is the only facies identified within the studied cores of the Lysing Formation.

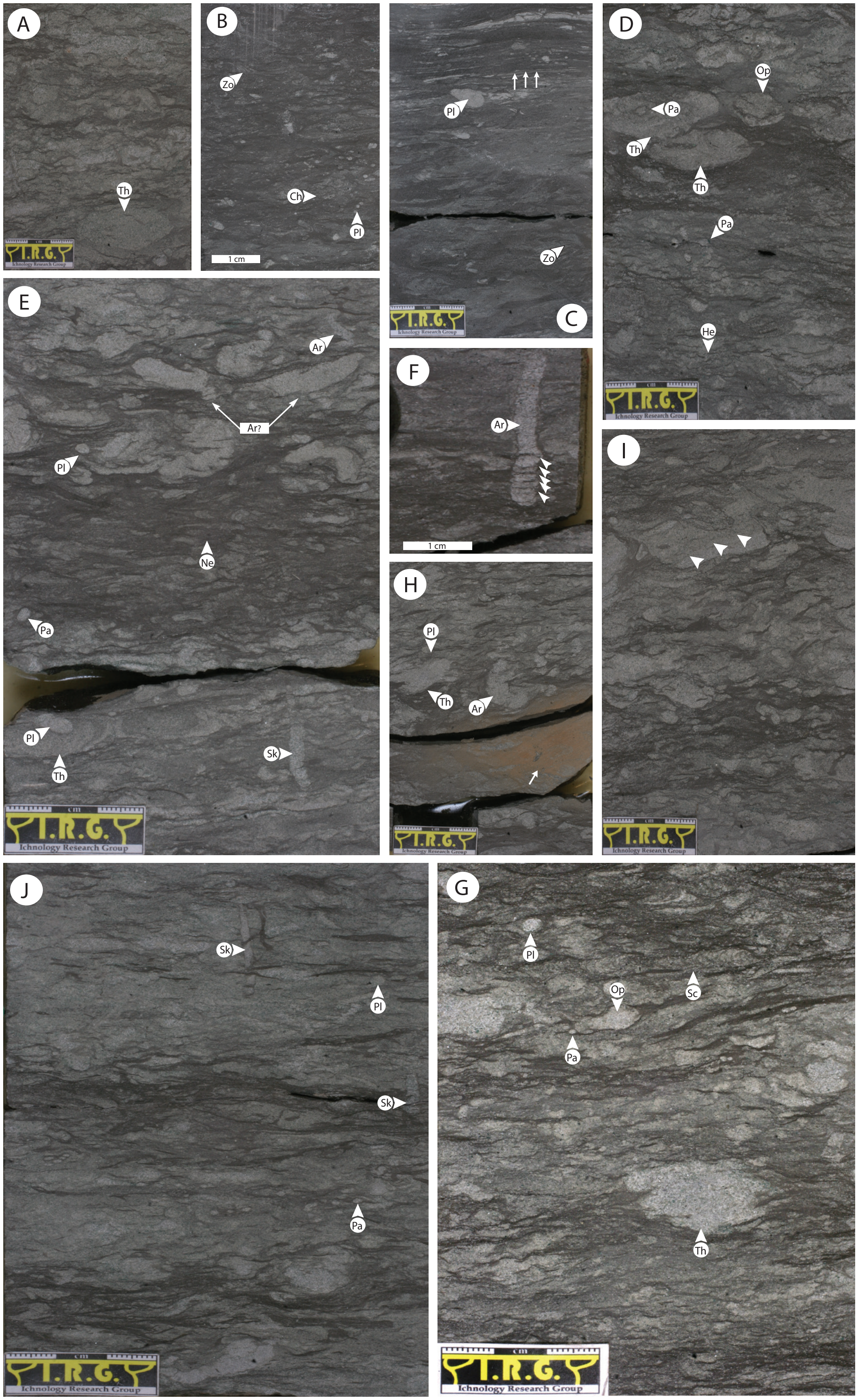
A
Th
I.R.G.
Ichnology Research Group
B
Zo
Ch
Pl
1 cm
Pl
Zo
C
D
Op
Pa
Th
Th
Pa
He
E
Ar
Ar?
Pl
Ne
Pa
Pl
Th
Sk
F
Ar
1 cm
H
Pl
Th
Ar
I
J
Sk
Pl
Sk
Pa
G
Pl
Op
Sc
Pa
Th

Figure 2.10. Facies 4–Burrowed sandy mudstone. **A)** *Thalassinoides* (Th) up to 3 cm in diameter with burrow-fill rich in glaucony are sparse throughout the F4 deposits. 3780.76 m, well 6405/7-1 T2, Ellida Field. **B)** Massive-appearance dark grey mudstone interval with small *Chondrites* (Ch), *Zoophycos* (Zo) within a *Planolites* (Pl). 3755.73 m, well 6405/7-1 T2, Ellida Field. **C)** Low angle parallel to wavy lamination (white arrow) with sparce diminutive *Planolites* (Pl). The lack of contrasting lithology does not allow indentify discrete trace fossils. 3776.88 m, well 6405/7-1 T2, Ellida Field. **D)** *Paleophycus* (Pa) reburrowed *Thalassinoides* (Th). Recurrent overprinting of trace-fossils is common throughout the entire studied interval. 3754.73 m, well 6405/7-1 T2, Ellida Field. **E)** Intensely burrowed sand-rich interval containing *Arenicolites* (Ar) and *Planolites* (Pl). 3782.94 m, well 6405/7-1 T2, Ellida Field. **F)** Tabular Tidalites (?)/ Skolithos with lamination (white arrows) being part of the burrow-fill may be indicative of some tidal influence at the time of deposition of F4. 3753.90 m, well 6405/7-1 T2, Ellida Field. **G)** Archetypical biogenic fabric of the F4 showing a highly diverse and abundant trace-fossil suite including *Thalassinoides* (Th), *Planolites* (Pl), *Ophiomorpha* (Op) and *Scolicia* (Sc). 3752.73 m, well 6405/7-1 T2, Ellida Field. **H)** Siderite nodule surrounded by well-developed burrows including *Arenicolites* (Ar), *Thalassinoides* (Th) and *Planolites* (Pl). 3779.46 m, well 6405/7-1 T2, Ellida Field. **I)** Glaucony (white arrows) is common throughout F4 deposits as burrow-fill. 3774.23 m, well 6405/7-1 T2, Ellida Field. **J)** Intensely burrowed and trace-fossil overprinting of mixed horizontal and vertical burrows including *Planolite*s (Pl), *Paleophycus* (Pa) and *Skolithos* (Sk) respectively.

Ichnology:

A robust and abundant trace-fossil assemblage characterizes the entire segment of F4. Commonly, burrow-fill is made up of slightly coarser material that allows well differentiation from the surrounding matrix (Figure 2.10C and 2.10G). The degree of sediment reworking results in an intense to complete bioturbated fabric (BI = 4 – 6) throughout the entire studied interval.

Large *Thalassinoides* up to 3 cm (Figure 2.10A and 2.10D), *Planolites* and *Nereites* are the most abundant trace fossils within F4 strata. As well as the aforementioned, *Zoophycos*, *Chondrites*, *Scolicia*, *Paleophycus* and *Helminthopsis* are commonly present (Figure 2.10B). This ichnofabric is dominantly composed of discernible horizontal to inclined burrows. Inclined to vertical burrows are also common but less abundant (Figure 2.10E and 2.10J). Horizontal to inclined burrows are attributable to *Thalassinoides, Planolites, Paleophycus, Rhizocorallium*, *Helminthopsis* and *Ophiomorpha* and are interpreted to represent mostly dwelling and deposit-feeding behavior. Inclined to vertical burrows identified within F4 deposits are interpreted most likely to record suspension-feeding behavior (*e.g., Skolithos* and *Arenicolites)* (Figure 2.10E).

Glaucony is mostly present within the *Thalassionoides* and *Planolites* burrow-fill (Figure 2.10G). Cross cutting relationship reveals that *Thalassionoides* and *Planolites* are commonly re-burrowed and overprinted by mixed ichnofauna such as *Palaeophycus*, deep tier *Zoophycos* and *Chondrites* (Figure 2.10I). *Planolites* is abundant and can be found in high densities locally. As seen in *Thalassinoides*, the *Planolites* burrow-fills are slightly coarser than the surrounding material, within an overall muddy matrix (Figure 2.10D and 2.10G).

<u>Interpretation:</u>

The high presence of mud that typifies F4 suggests fair-weather conditions within an overall low hydraulic energy setting. Sand beds are the result of alternating fine- and coarse-grained sedimentation within a sedimentary environment with fluctuating energy. The presence of sand may be indicative that coarser sediments were deposited by sporadic higher-energy turbiditic events. Alternatively, the trace-fossil suite in this facies most likely comprises opportunistic assemblages that colonized and exploited either distal sandy tempestites or turbiditic deposits (MacEachern et al., 2007). The vertical stacking of sand and mud intervals supports this observation (Figure 2.11). The presence of tabular tidalites (Figure 2.10F) suggest some degree of tidal influence in the F4 deposits. However, additional evidence suggesting tidal processes within Facies 4 is absent. Within F4 the ichnofossil suite consists mainly of deposit-feeding or dwelling traces (*i.e., Thalassinoides, Planolites, Scolicia, Chondrites, Ophiomorpha, Paleophycus, Zoophycos, Helminthopsis* and *Phycosiphon*), and less common burrows of suspension-feeders (*i.e., Arenicolites*, *Skolithos* and *Schaubcylindrichnus*). This ichnofossil suite exhibits a mixing distal with proximal elements of the *Cruziana* Ichnofacies (Pemberton and MacEachern, 1995; MacEachern et al., 2007; MacEachern et al., 2010). This ichnofacies typically represents open marine, mid- to outer-shelf or equivalent marine

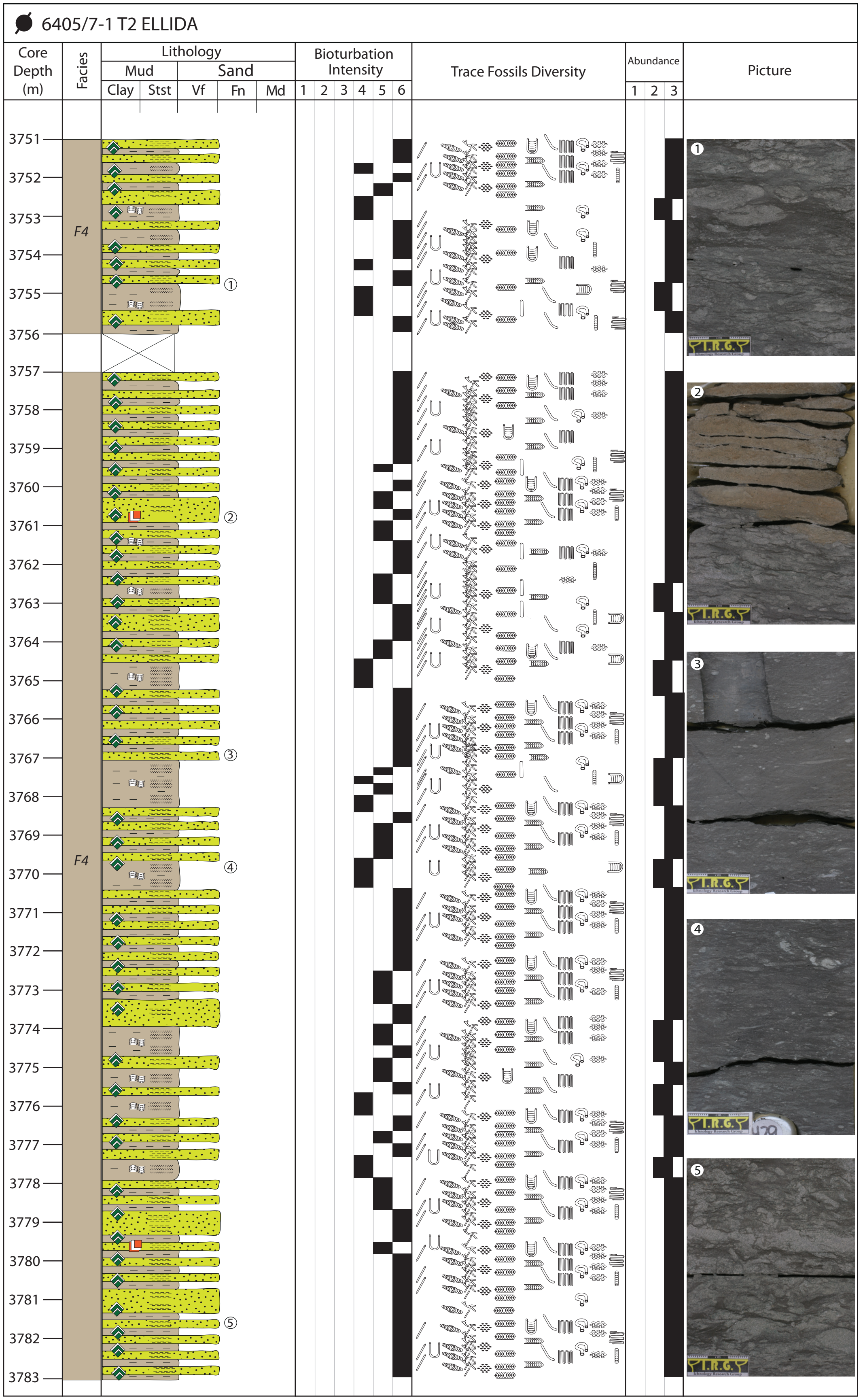

6405/7-1 T2 ELLIDA
Core Depth (m)
Facies
Lithology
Mud
Sand
Clay
Stst
Vf
Fn
Md
Bioturbation Intensity
1
2
3
4
5
6
Trace Fossils Diversity
Abundance
1
2
3
Picture
3751
3752
3753
3754
3755
3756
3757
3758
3759
3760
3761
3762
3763
3764
3765
3766
3767
3768
3769
3770
3771
3772
3773
3774
3775
3776
3777
3778
3779
3780
3781
3782
3783
F4
F4
①
②
③
④
⑤

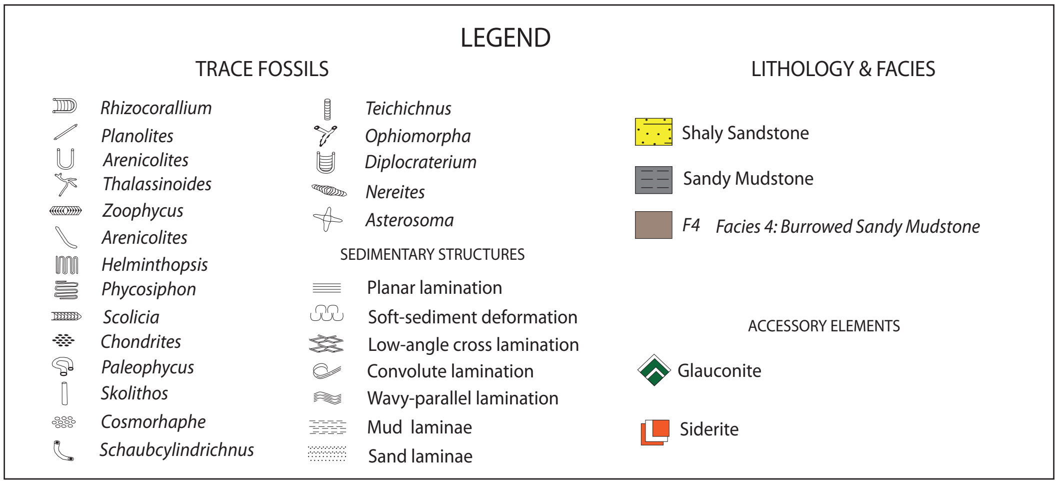

Figure 2.11. Composite plot showing the resulting sedimentological and ichnological characteristics of the interpreted lithofacies for the Lysing Formation in well 6407/10-1, Ellida

environments. Overprinting and cross-cut relationships between trace-fossils suggest that *Zoophycos* trace-makers represent a last stage of burrowing (Figure 2.10I). *Zoophycos* have been classified as being most likely the grazing burrow of a vermiform organism (Wetzel and Werner, 1981) an its presence within the F4 strata suggests an open marine offshore-shelf environment.

The aforementioned sedimentological and ichnological characteristics reflect deposition in an environment below storm wave base, with episodic high-energy events (Pemberton and MacEachern, 1995; MacEachern et al., 2007; MacEachern et al., 2010). This occurred most likely in a well-oxygenated mesopelagic to bathypelagic depositional setting (Figure 2.12).

DISCUSSION

Traditionally, strata pertaining to the Upper Cretaceous Lysing and Nise formations have been presented as being deposited in a deep-sea setting by turbiditic flows (*e.g.,* Kittilsen et al., 1999; Brekke et al., 1999; Brekke et al., 2001; Vergara et al., 2001; Fjellanger et al., 2005; Kjennerud and Vergara, 2005; Martinsen et al., 2005; Fugelli and Olsen, 2005a, Fugelli and Olsen 2005b; Fugelli and Olsen, 2007; Knaust, 2009a). This study provides evidence of deposition in a tectonically active offshore setting, more likely along paleo-high margins and axis that arises from sedimentological data in concert with ichnological analysis. Tempestites and deltaic sedimentation may have also been present in different settings throughout Upper Cretaceous times. Coal detritus as burrow-fill throughout F1 and F4 beds suggest the proximity to a terrigenous source. The overall diverse and abundant trace-fossil suite of F1, F2 and F4 suggests relatively stable paleoecological conditions (*e.g.,* water oxygenation, salinity) and low sedimentation rates that favoured productivity of bioturbating infauna with shorts periods of fluctuating conditions most likely related to episodic, highly energetic depositional events. These conditions can be found along marginal marine settings with nearshore proximity and/or along paleo-high margin axis in active tectonic settings (Figure 2.12). The impoverished trace-fossil suite of F3 is interpreted to record less suitable dysaerobic conditions, more likely in a seaward/deeper depositional setting than F1 and F2.

The different facies that compose the studied core interval of the Lysing and Nise formations presented herein reveal that sedimentation and bioturbation processes were strongly influence by the tectonic framework. The studied dataset suggest that sand accumulation took place along the paleo-high margins more likely due to changes in local base level as a response of an active tectonic setting. Erosion cycles due to tectono-eustatic sea level variation are interpreted by the presence of *Glossifungites*-demarcated discontinuity surfaces within the Nise Formation. However, colonization and development of elements that reflect the *Glossifungites* ichnofacies can also be formed after episodic emplacements of contrasting lithologies in deep sea settings. Additionally, the stratigraphic architecture and bioturbation patterns reveal alternating fine- and coarse-grained sedimentation cycles as a result of an active tectonics.

Within the Møre Basin, depositional environments and sediment supply were significantly influenced by an active tectonic setting in the Upper Cretaceous. Different cycles of tectonic compression and rifting created emerged zones (*i.e.,* paleo-highs), that controlled sediment transport, geometry and depocentres. Consequently, some stratigraphic units may display major lithological variability along interbasinal highs and the basin margins (Dalland et al., 1988). Vergara et al., (2001) interpreted differences of thicknesses in deposits equivalent to Nise Formation as the result of uplifting and erosion events in some paleo-highs in Late Cretaceous times. In both wells (6405/7-1 T2, Ellida and 6405/10-1, Midnatsoll), erosional events are interpreted by the presence of *Glossifungites*-demarcated discontinuity surfaces within the Nise Formation (Figure 2.9 and 2.7G). These are here inferred to be probably the result of sub-aerial exposure and later colonization of bioturbating infauna. In the rock record and modern settings these burrows have been interpreted as the work of the thalassinid shrimp (Shinn 1968; Rice and Chapman 1971; Frey and Howard 1975; Dworshak 1983; Griffis and Chavez, 1988; Gingras et al., 2001; Gingras et al., 2002). The resulting colonization of firmgrounds indicates depositional hiatuses associated with lowstand cycles and exposure of paleo-highs. *Glossifungites*-demarcated discontinuity surfaces are interpreted herein to be likely the record of the tectonic activity that may have driven tectono-eustatic sea-level changes that significantly affected sediment deposition within the study area. Also, they may constitute an indicator of the erosional unconformity associated with a compressional event by the end of the Campanian. This discordance records an important regional event recognized at a basin scale. In the northwestern part of the study area, (*e.g.,* the Slettringen dome) (Figure 2.1) this unconformity constitutes an important sequence boundary (Vergara et al., 2001). In the north part of the Vøring Basin this event is located at the top of sandstone deposits equivalent to the Nise Formation in well 6710/10-1 (Vergara et al., 2001). This indicates that periodic adjustments of interior platforms and changes in relative base level may have driven shifts in sediment source and may be responsible for sand accumaltions along paleo-high margins. This may explain the origin of the sand within a shelf-equivalent depositional setting (*e.g,* F1 and F2). Later transgression and sediment deposition of these paleo-highs were responsible for the smoothing of the overall paleotopography and modern basin architecture.

Extensive basin-floor fan deposits are interpreted to be widespread across the Norwegian Sea basins with better development to the north in the Vøring Basin during Campanian time (Vergara et al., 2001; Knaust, 2009a). Morphological and architectural elements of the Upper Cretaceous deep-marine systems within the Møre basin have been documented by integration of 2D/3D seismic and well data (*e.g.*, Fugelli and Olsen; 2005a, Fugelli and Olsen, 2005b; Fugelli and Olsen 2007). The sandy intervals within the Lysing and Nise Formation and in general the Upper Cretaceous sequence have been interpreted as sand-rich basin-floor-fan systems within a mud-rich amalgamated fan-complexes system. (Kittilsen et al., 1999; Vergara et al., 2001; Fjellanger et al., 2005; Knaust, 2009a). This interpretation also arises from the fact that within the Møre and the Vøring basins the thick Cretaceous sequence is composed primarily of mudstone (Peltonen et al., 2008). Consequently, sand accumulation is thought to be the result of deep-water turbidites or/and slump-derived deposits sourced from local highs and areas located to the west and east of Scandinavia and Greenland respectively (Hastings,

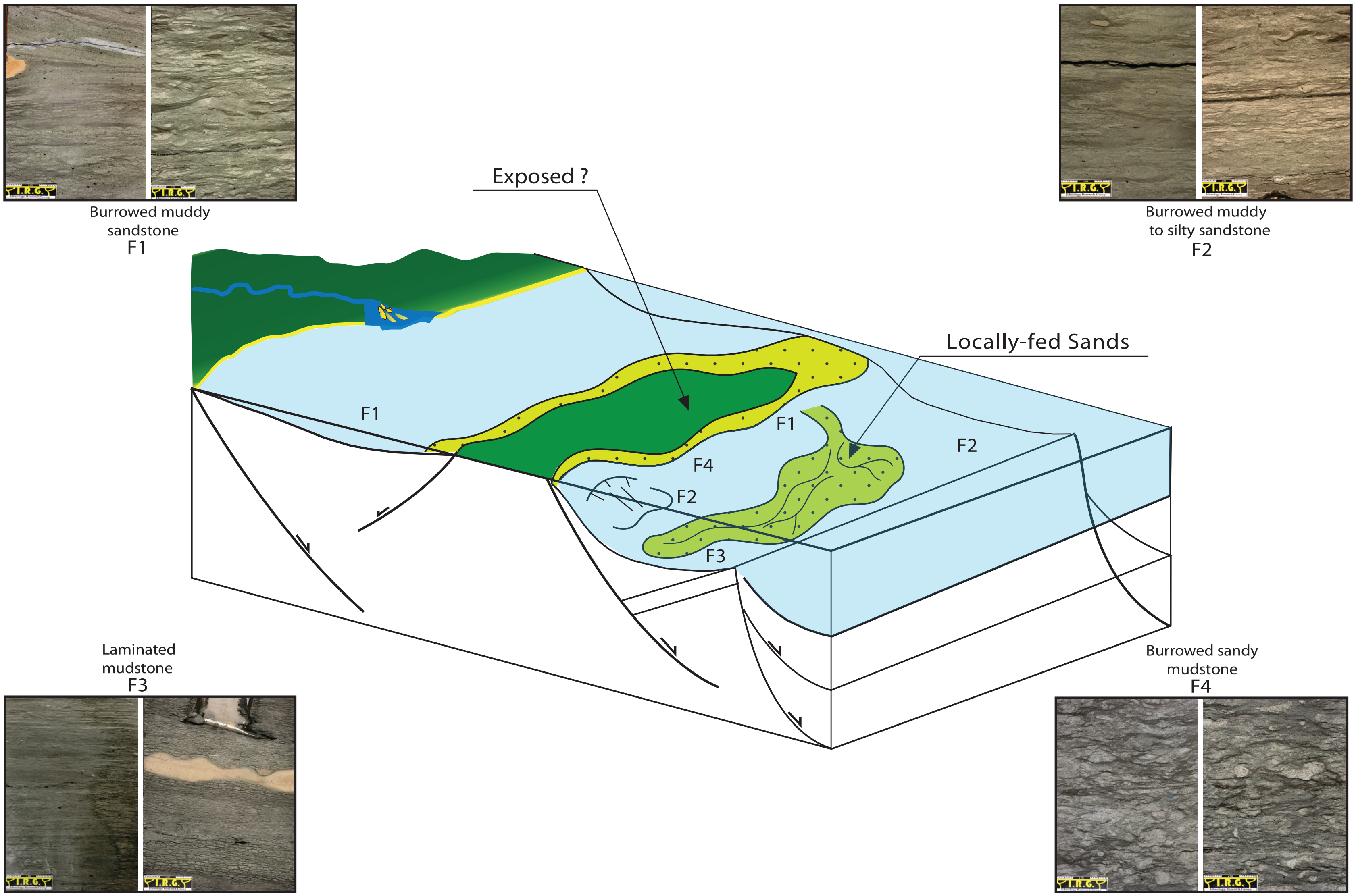
Burrowed muddy
sandstone
F1
Exposed ?
Burrowed muddy
to silty sandstone
F2
Locally-fed Sands
F1
F1
F4
F2
F2
F3
Laminated
mudstone
F3
Burrowed sandy
mudstone
F4

Figure 2.12. Schematic depositional model showing the facies distribution for the Lysing and Nise formations in the Ellida and Midnatsoll fields (Norwegian continental shelf). Adapted after Martinsen et al., 2005.

1987; Brekke et al., 1999; Sanchez-Ferrer et al., 1999; Vergara et al., 2001; Lien, 2005; Fugelli and Olsen; 2005a, Fugelli and Olsen 2005b).

Within this thesis, ichnological in concert with sedimentological analysis suggests that sediment pertaining to the Lysing and Nise formations were deposited in tectonically active, steep paleo-high depositional setting, with some affinities to traditional interpretations (Figure 2.12). However, sediments exhibiting shallow-water depositional affinities (*e.g.,* F1) can be identified within the studied interval. Given that recent exploratory campaigns within the Norwegian Sea basins revealed a significant hydrocarbon potential hosted in deep-water Upper Cretaceous reservoirs, their distribution and expected quality are among the most valuable elements to be discerned for future exploration and development plans.

RECONCILIATION WITH PREVIOUS MODELS

It is generally accepted that tectonism and rifting in the late Jurassic- earliest Cretaceous are responsible for an overall change from shallow-marine sedimentation to deep-water sedimentation in offshore mid-Norway (Brekke *et al*., 2001). It is also thought that these conditions prevailed at the time of deposition of the Lysing and Nise Formations. The Nise Formation studied core interval, exhibits affinities with sedimentary environments in which turbidity processes may have taken place (*e.g.,* Kittilsen et., al 1999; Brekke et., al 1999; Brekke et., al 2001; Vergara et al., 2001; Fjellanger et al., 2005; Kjennerud and Vergara, 2005; Martinsen et al.*,* 2005; Fugelli and Olsen; 2005a, Fugelli and Olsen 2005b, Fugelli and Olsen 2007; Knaust, 2009a). Despite that fact, no conclusive evidence was found ponting towards turbiditic-flows in the Nise Formation. The presence of *Glossifungites*-demarcated discontinuity surfaces, abundant coal detritus and elements of the proximal *Cruziana* ichnofacies within this unit may suggest shallower water depths at the time of its deposition (Figure 2.12), likely as a response of tectonic uplift. This argument is consistant with the findings of Knejjerud and Vergara, (2005) that reconstructed the Vøring basin Palaeobathymetry (Figure 2.13). Therein, Palaeobathymetry is estimated among other relevant data by combining seismic sequence and facies geometries, sedimentological/seismostratigraphic indicators of shallow or zero water depth and micropalaeontological data. Their study shows water depths for the study area presented in this thesis that supports the findings within this study (Figure 2.13). Previous interpretations of the Nise Formation in the well 6707/10-1 thought to be part of a Campanian basin-floor system (*e.g.,* Knaust, 2009a; Fjellanger et al., 2005), is explained by an increase in accommodation space caused by subsidence in the Nagrind Syncline area (Figure 2.13). This zone was later filled by sediments equivalent to the Nise sandstones and penetrated by well 6707/10-1(Figure 2.1) that may display a different trace fossil-suite (*e.g.,* Knaust, 2009a) than the one discussed within this study.

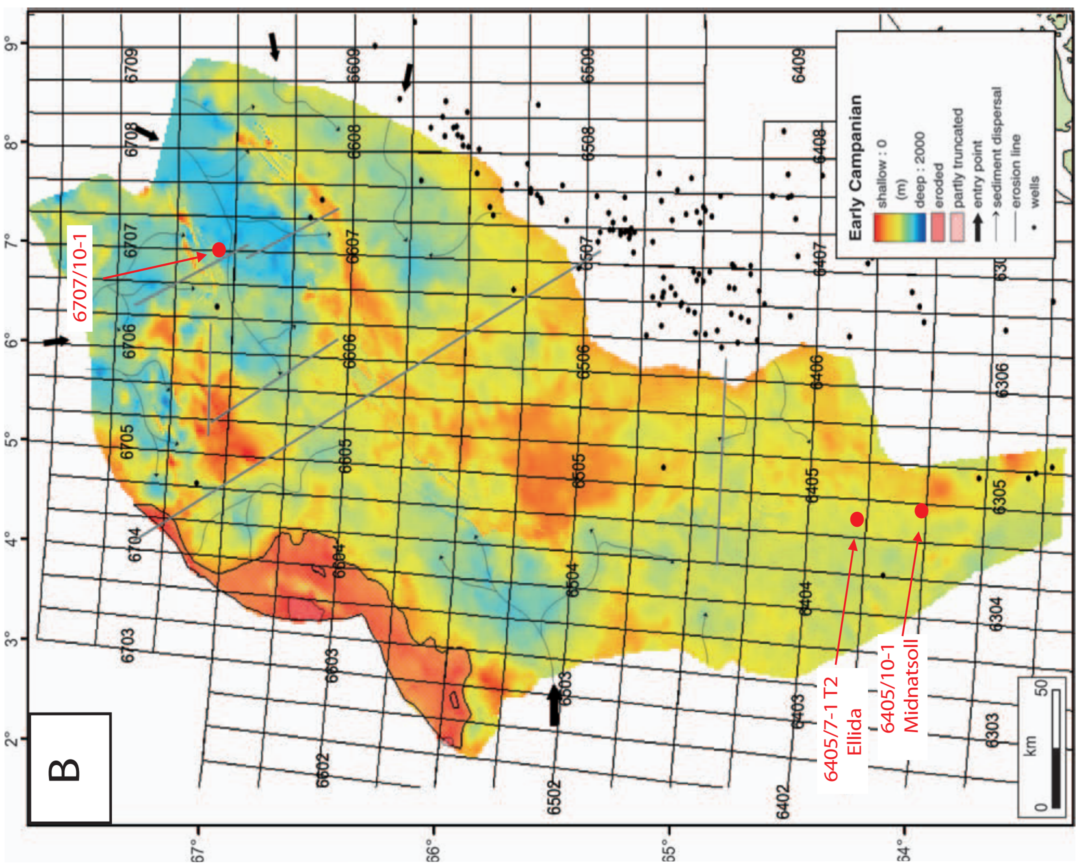
B
6707/10-1
6405/7-1 T2
Ellida
6405/10-1
Midnatsoll
Early Campanian
shallow : 0
(m)
deep : 2000
eroded
partly truncated
entry point
sediment dispersal
erosion line
wells
km

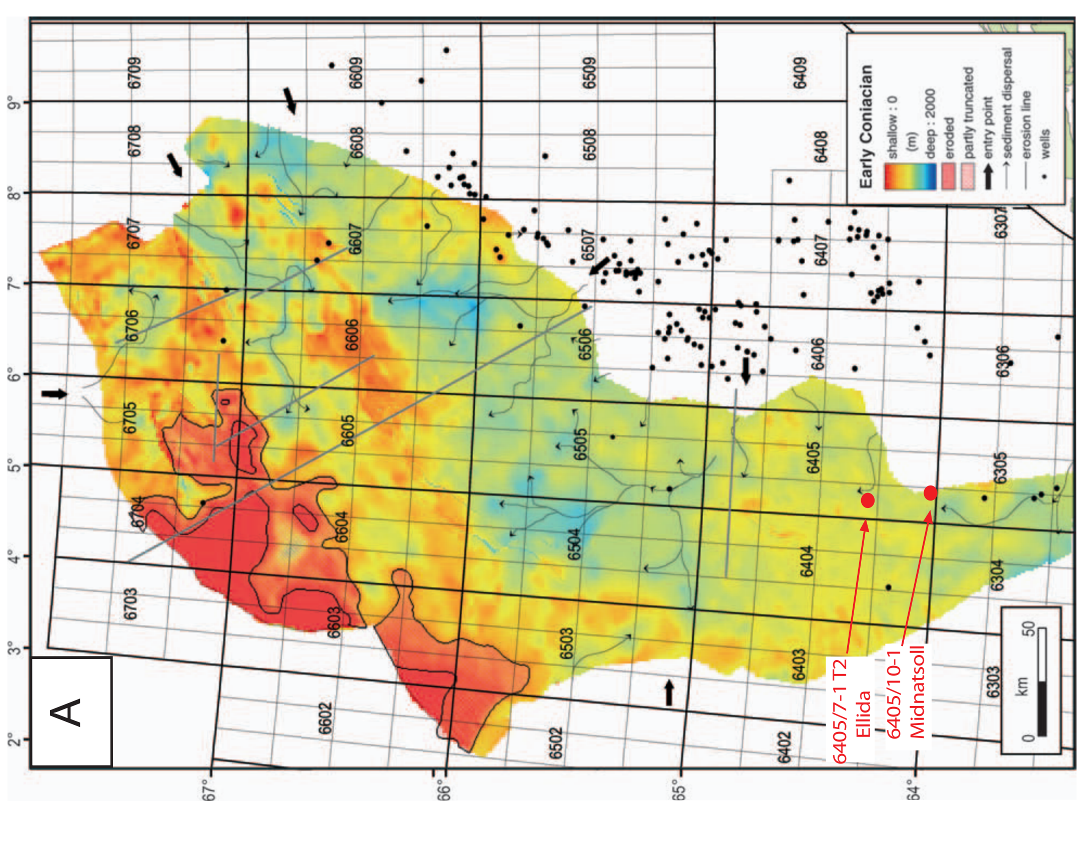
A
6405/7-1 T2
Ellida
6405/10-1
Midnatsoll
Early Coniacian
shallow : 0
(m)
deep : 2000
eroded
partly truncated
entry point
sediment dispersal
erosion line
wells
km

Figure 2.13. Upper Cretaceous paleobathymetric map of the Vøring Basin and the northernmost part of the Møre basin. **A**) Early Coniacian reconstruction reflecting the morphology of the study area at the time of deposition of the Lysing Formation. **B**) Early Campanian configuration, showing the basinal water depths at the time of deposition of the Nise Formation. Well 6707/10-1 is located in the map for reference, Modified from (Kjennerud and Vergara, 2005).

SUMMARY

Throughout the studied core interval of the Lysing and Nise formations a dynamic ichnofossil suite is commonly present. Overall, the trace fossil assamblage present contains elements of the proximal through distal *Cruziana* ichnofacies.

Within the Møre Basin, depositional environments and sediment supply were significantly influenced by an active tectonic setting in the Upper Cretaceous. This can be seen as alternating fine- and coarse-grained sedimentation within a depositional environment with relatively stable hydraulic energy and paleoecological conditions. Tectonic changes may have driven shifts in sediment source and were responsible for sand accumaltions along paleo-high margins. This tectonic configuration created different sub basins with different erosion-deposition systems ranging from shallow marine (presented in this thesis *e.g.*, Facies 1) to traditionally interpreted deep-sea settings (*e.g.,* Kittilsen et., al 1999; Brekke et., al 1999; Brekke et., al 2001; Vergara et al., 2001; Fjellanger et al., 2005; Kjennerud and Vergara, 2005; Martinsen et al*.,* 2005; Fugelli and Olsen; 2005a, Fugelli and Olsen 2005b, Fugelli and Olsen 2007; Knaust, 2009a).

Uplift and down lift of the positive tectonic features shaped the sedimentation and erosion cycles in the Møre Basin. At a local scale, these positive features controlled sediment supply, depocentres and bioturbation patterns (*e.g.,* intensity and distribution). Erosional events are interpreted by the presence of *Glossifungites*-demarcated discontinuity surfaces within the Nise Formation and may be interpreted as evidence of an intense tectonic setting at the time of deposition of Lysing and Nise Formations.

The Nise Formation exhibits an intense bioturbation in the sandy intervals (BI = 4 – 6), whereas the mudstone intervals display very low levels of bioturbation (BI = 1 – 2) throughout the examined core interval. Recurrent overprinting of trace-fossils reveals low sedimentation rates with favourable conditions for bioturbation infauna to develop. A diverse and abundant trace fossil-suite (*i.e.,* F1 and F2) reveals that endobenthic organisms flourished under low physico-chemical environmental stresses. This is probably the result of stable, favourable ecological-conditions such as oxygenation, food availability, salinity and temperature. Therefore, suspension- and deposit-feeding endobenthic fauna flourished and were responsible for the total disruption of the primary sedimentary fabric. The lithological contrast allowed the differentiation of tiering and recurrent overprinting of burrows. The Nise Formation deposits in the Ellida and Midnatsoll Fields area are interpreted to record deposition on a siliciclastic, tectonically active setting, mostly above- alternating with periods below-storm wave-base.

The Lysing Formation shows an intense bioturbation (BI = 4 – 6) throughout the entire examined core interval. These robust and abundant trace-fossil suite suggest favourable conditions at the time bioturbation took place. Small changes in trace fossil diversity and abundance are related to continuous favourable environmental conditions with minimal fluctuations allowing colonization and continuous overprinting of trace fossils. The Lysing Formation in the Ellida Field area is interpreted to record deposition in tectonically active paleodepositional setting, mostly below storm wave-base with episodic, high-energy events in which sand deposits were emplaced most likely as a response of turbiditic flows.

REFERENCES

BANN, K. L., FIELDING, C. R., MAcEACHERN, J.A., AND TYE, S. C., 2004, Differentiation of estuarine and offshore marine deposits using integrated ichnology and sedimentology: Permian Pebbly Beach Formation, Sydney Basin, Australia, *in* McIlroy, eds., The application of ichnology to Palaeoenvironmental and Stratigraphic Analysis. Geological Society, London, Special Publications, 228, p. 179 – 211.

BEYNON, B.M., AND PEMBERTON, S.G., 1992, Ichnological signature of a brackish water deposit: an example from the Lower Cretaceous Grand Rapids Formation, Cold Lake oil sands area, Alberta, *in* Pemberton, S.G., eds., Applications of Ichnology to Petroleum Exploration: SEPM, Core Workshop Notes 17, p. 199 – 221.

BLAKEY, R., 2011, Upper Cretaceous , *in* Paleogeography and Geologic Evolution of Europe. Retrieved from CD purchased through http://cpgeosystems.com/paleomaps.html

BJØRNSETH, H.M., GRANT, S.M., HANSEN, E.K., HOSSACK, J.R., ROBERTS, D.G. AND THOMPSON, M., 1997, Structural evolution of the Vøring Basin, Norway, during the Late Cretaceous and Palaeogene. Journal of the Geological Society, London 154, p. 559 – 563.

BLYSTAD, P., BREKKE, H., FAERSETH, R. B., LANSEN, B. T., SKOGSEID, J. AND TØRUDBAKKEN, B., 1995, Structural elements of the Norwegian continental shelf. Part II: The Norwegian Sea Region. Norwegian Petroleum Directorate Bulletin, 8, p. 1 – 45.

BOYER, D.L., AND DROSER, M.L., 2007, Devonian monospecific assemblages: New insights into the ecology of reduced-oxygen depositional settings: Lethaia, v. 40, p. 321 – 333.

BOYER, D.L., AND DROSER, M.L., 2009, Palaeoecological patterns within the dysaerobic biofacies: Examples from Devonian black shales of New York: Palaeogeography, Palaeoclimatology, Palaeoecology, v. 276, p. 206 – 216.

BOYER, D.L., AND DROSER, M.L., 2011, A combined trace-and body-fossil approach reveals high-resolution record of oxygen in Devonian seas. Palaios, v. 26, p. 500 – 508.

BREKKE, H., AND F. RIIS, 1987, Tectonics and basin evolution of the Norwegian Shelf between 62ºN and 72ºN, *in* A. G. Koestler and S. Olaussen, eds., Tectonics and deposition in sedimentary basins: Norsk Geologisk Tidsskrift, v. 67, p. 295 – 322

BREKKE, H., DALHGREN, S., NYLAND, B. AND MAGNUS, C., 1999, The prospectivity of the Vøring and Møre Basins on the Norwegian Sea continental margin. *in* Fleet. A. J. & Boldy, S. A. R., eds., Petroleum Geology of Northwest Europe: Proceedings of the 5th Conference. Geological Society, London, p. 261 – 274.

BREKKE, H, 2000, The tectonic evolution of the Norwegian Sea continental margin with emphasis on the Vøring and Møre basins. *in* Nøttvedt, A. & Larsen, B.T., eds., Dynamics of the Norwegian Margin. Geological Society, London, Special Publications, 167, p. 327 – 378.

BREKKE, H., H. I. SJULSTAD, C. MAGNUS, AND R. W. WILLIAMS, 2001, Sedimentary environments offshore Norway– An overview, *in* O. J. Martinsen and T. Dreyer, eds., Sedimentary environments offshore Norway– Palaeozoic to Recent: Norwegian Petroleum Society (NPF) Special Publication 10, p. 7–37.

BROMLEY, R.G., AND EKDALE, A.A., 1984, *Chondrites*: a trace fossil indicator of anoxia in sediments: Science, v. 224, p. 872 – 874.

BROMLEY, R.G., 1996, Trace Fossils, 2nd Edition: Suffolk, U.K., Chapman & Hall, 361 p.

BUATOIS, L.A., AND MANGANO, M.G., 1998, Trace fossil analysis of lacustrine facies and basins: Palaeogeography, Palaeoclimatology, Palaeoecology, v. 140, p. 367 – 382.

BUGGE, T., KNARUD, R., AND MØRK, A., 1984, Bedrock geology on the mid-

Norwegian continental shelf. *in* Spencer, A.M., eds., Petroleum Geology of the North European Margin. Graham and Trotman, London, p. 271 – 283.

CUMMINGS J., P., AND HODGSON D., M., 2012, An agrichnial feeding strategy for deep-marine Paleogene Ophiomorpha group trace fossils. PALAIOS, 2011, v. 26, p. 212 – 224.

DAFOE, L. T., GINGRAS, M. K., PEMBERTON, S. G., 2010, Wave-influenced deltaic sandstone bodies and offshore deposits in the Viking Formation, Hamilton Lake area, south-central Alberta, Canada. Bulletin of Canadian Petroleum Geology. v. 58–2, p. 173 – 201.

DALLAND, A., WORSELY, D. AND OFSTAD, K., 1988, A lithostratigraphic scheme for the Mesozoic and Cenozoic succession, offshore Mid- and Northern Norway. Norwegian Petroleum Directorate Bulletin, 4, p. 1 – 65.

DORÉ, A. G., AND E. R. LUNDIN, 1996, Cenozoic compressional structures on the NE Atlantic margin: Nature, origin and potential significance for hydrocarbon exploration: Petroleum Geoscience, v. 3, p. 117 – 131.

DORÉ, A. G., E. R. LUNDIN, L. N. JENSSEN, Ø. BIRKELAND, P. E. ELIASSEN, AND C. FICHLER, 1999, Principal tectonic events in the evolution of the northwest European Atlantic margin, *in* A. J. Fleet and S. A. R. Boldy, eds., Petroleum geology of northwest Europe: Proceedings of the 5th Conference, Geological Society (London), p. 41 – 61.

DROSER, M.L., AND D.J., BOTTJER, 1986, A semiquantitive field classification of Ichnofabrics: Journal of Sedimentary Petrology, v. 56, p. 558 – 559.

DWORSCHAK, P.C., 1983, The biology of *Upogebia pusilla* (Petagna) (Decopoda, Thalassinidae): Marine Ecology, v. 4, p. 19 – 43.

EKDALE, A.A., BROMLEY, R.G., AND PEMBERTON, S.G., 1984, Ichnology; Trace Fossils in Sedimentology and Stratigraphy: SEPM, Short Course 15, 317 p.

FARSETH, R., B. AND LIEN, T., 2002, Cretaceous evolution in the Norwegian

Sea–a period characterized by tectonic quiescence. Marine and Petroleum Geology. 19, p. 1005 – 1027.

FJELDSKAAR, W., JOHANSEN, H., DODD, T.A. AND THOMPSON, M., 2003, Temperature and maturity effects of magmatic underplating in the Gjallar Ridge, Norwegian Sea. *in* Duppenbecker, S. & Marzi, R., eds., Multidimensional basin modeling. American Association of Petroleum Geologists AAPG; Datapages Discovery Series, p. 71 – 85.

FJELLANGER, E., SURLYK, F., WAMSTEEKER, L, C., AND MIDTUN, T., 2005, Upper cretaceous basin-floor fans in the Vøring Basin, Mid Norway shelf. Norwegian Petroleum Society Special Publications v. 12, p. 135 – 164.

FONNELAND, H.C., LIEN, T., MARTINSEN, O.J., PEDERSEN, R.B., AND KOSLER, J., 2004, Detrital zircon ages; a key to understanding the deposition of deep marine sandstones in the Norwegian Sea. Sedimentary Geology, 164 (1–2), p. 147 – 159.

FREY, R.W., AND HOWARD, J.D., 1975, Endobenthic adaptations of juvenile thalassinid shrimp: Geological Society of Denmark, Bulletin, v. 24, p. 283 – 297.

FREY, R.W., HOWARD, J.D., AND PRYOR, W.A., 1978, *Ophiomorpha*; Its morphologic, taxonomic, and environmental significance: Palaeogeography, Paleoclimatology, Palaeoecology, v. 23, p. 199 – 229.

FUGELLI, E. M. G., AND T. R. OLSEN, 2005a, Screening for deep-marine reservoirs in frontier basins: Part 1–Examples from offshore mid-Norway: AAPG Bulletin, v. 89, p. 853 – 882.

FUGELLI, E. M. G., AND T. R. OLSEN, 2005b, Risk assessment and play fairway analysis in frontier basins: Part 2–Examples from offshore mid-Norway: AAPG Bulletin, v. 89, p. 883 – 896.

FUGELLI, E. M. G., AND T. R. OLSEN, 2007, Delineating confined slope turbidite systems offshore mid-Norway: The Cretaceous deep-marine Lysing Formation. AAPG Bulletin, v. 91, p. 1577 – 1601.

GABRIELSEN, R. H., KYRKJEBØ, R., FALEIDE, J. I., FJELDSKAR, W. AND KJENNERUD, T., 2001, The Cretaceous post-rift basin configuration of the northern North Sea. Petroleum Geoscience, 7, p. 137 – 154.

GINGRAS, M.K., MACEACHERN, J.A., AND PEMBERTON, S.G., 1998, A comparative analysis of the ichnology of wave- and river-dominated allomembers of the Upper Cretaceous Dunvegan Formation. Bulletin of Canadian Petroleum Geology, v. 46, p. 51 – 73.

GINGRAS, M.K., PEMBERTON, S.G., SAUNDERS, T.D.A., AND CLIFTON, H.E., 1999, The ichnology of modern and Pleistocene brackish-water deposits at Willapa Bay, Washington: variability in estuarine settings: Palaios, v. 14, p. 352 – 374.

GINGRAS, M.K., HUBBARD, S.M., PEMBERTON, S.G., AND SAUNDERS, T.D.A., 2000, The significance of Pleistocene *Psilonichnus* at Willapa Bay, Washington: Palaios, v. 15, p. 142 – 151.

GINGRAS, M.K., PEMBERTON, S.G., AND SAUNDERS, T.D.A., 2001, Bathymetry, sediment texture, and substrate cohesiveness; their impact on modern *Glossifungites* trace assemblages at Willapa Bay, Washington: Palaeogeography, Palaeoclimatology, Palaeoecology, v. 169, p. 1 – 21.

GINGRAS, M.K., RÄSÄNEN, M., AND M. RANZI, A., 2002, The significance of bioturbated inclined heterolithic stratification in the southern part of the Miocene Solimoes Formation, Rio Acre, Amazonia Brazil: Palaios, v. 17, n. 6, v. 17, p. 591 – 601.

GRIFFIS, R.B., AND CHAVEZ, F.L., 1988, Effects of sediment type on burrows of *Callianassa californiensis* Dana and *C. gigas* Dana: Experimental Marine Biology and Ecology, v. 117, p. 239 – 253.

GRUNNALEITE, I., AND GABRIELSEN, R.H., 1995, Structure of the Møre Basin, mid-Norway continental margin. Tectonophysics, v. 252, p. 221 – 251.

HASIOTIS, S.T., AND HONEY, J.G., 2000, Paleohydrologic and stratigraphic significance of crayfish burrow in continental deposits: examples from several Paleocene Laramide basins in the Rocky Mountains: Journal of Sedimentary Research, v. 70, p. 127 – 139.

HASTINGS, D. S., 1987, Sand-prone facies in the Cretaceous of mid- Norway, in J. Brooks and K. Glennie, eds., Petroleum geology of north west Europe: London, Grahamand Trotman, p. 1065 – 1078

KITTILSEN, J. E., OLSEN, R. R., MARTEN, R. F., HANSEN, E. K. AND HOLLINGSWORTH, R. R., 1999, The first deepwater well in Norway and its implications for the Upper Cretaceous Play, Vøring Basin. *in* Fleet, A. J. and Boldy, S. A. R., eds., Petroleum Geology of North–west Europe: Proceedings of the 5th Conference. Geological Society, London, p. 275 – 280.

KJENNERUD, T. AND VERGARA, L., 2005, Cretaceous to Palaeogene 3D palaeobathymetry and sedimentation in the Vøring Basin, Norwegian Sea. *in* Dore, A. G. and Vining, B. A., eds., Petroleum Geology: North-West Europe and Global Perspectives–Proceedings of the 6th Petroleum Geology Conference, p. 815 – 831.

KNAUST, D., 2009a, Characterisation of a Campanian deep-sea fan system in the Norwegian Sea by means of ichnofabrics. Marine and Petroleum Geology, v. 26, p. 1199 – 1211.

LIEN, T., 2005, From rifting to drifting: Effects on the development of deep-water hydrocarbon reservoirs in a passive margin setting, Norwegian Sea: Norwegian Journal of Geology, v. 85, p. 319 – 332.

LUNDIN, E. R. AND DORÉ, A. G., 1997, A tectonic model for the Norwegian passive margin with implications for the NE Atlantic: Early Cretaceous to breakup. Journal of the Geological Society, 154, p. 545 – 550.

LUNDIN, E. R. AND DORÉ, A. G., 2002, Mid-Cenozoic post-breakup deformation in the “passive” margins bordering the Norwegian–Greenland Sea. Marine and Petroleum Geology, 19, p. 79 – 93.

MACEACHERN, J.A., AND PEMBERTON, S.G., 1992, Ichnologic aspects of Cretaceous bay margin successions and bay margin variability in the Western

Interior Seaway of North America, *in*: Pemberton, S.G., (eds), Applications of Ichnology to Petroleum Exploration: SEPM, Core Workshop, Notes 17, p. 57 – 84.

MACEACHERN, J.A., AND PEMBERTON, S.G., 1994, Ichnological aspects of incised-valley fill systems from the Viking Formation of the Western Canada sedimentary basin, Alberta, Canada, *in*: Dalrymple, R.W., Boyd, R., and Zaitlin, B.A., eds., Incised-Valley Systems; Origin and Sedimentary Sequences: SEPM, Special Publication 51, p. 129 – 157.

MACEACHERN, J.A., STELCK, C.R., AND PEMBERTON, S.G., 1999, Marine and marginal marine mudstone deposition: paleoenvironmental interpretations based on the integration of ichnology, palynology and foraminiferal paleoecology, *in*: Bergman, K.M., and Snedden, J.W., eds., Isolated Shallow Marine Sand Bodies; Sequence Stratigraphic Analysis and SedimentologicInterpretation: SEPM, Special Publication 64, p. 205 – 225.

MACEACHERN, J.A., ZAITLIN, B.A. AND PEMBERTON, S.G.,1999b, A sharp-based sandstone of the Viking Formation, Joffre Field, Alberta, Canada: criteria for recognition of transgressively incised shoreface complexes. Journal of Sedimentary Research, v. 69, p. 876 – 892.

MACEACHERN, J.A., BANN, K.L., BHATTACHARYA, J.P., AND C.D. HOWELL, 2005, Ichnology of deltas: organism responses to the dynamic interplay of rivers, waves, storms and tides, *in* Bhattacharya, B.P., and Giosan, L., eds., River Deltas: Concepts, Models and Examples: SEPM, Special Publication 83, p. 49 – 85.

MACEACHERN, J.A., PEMBERTON, S.G., BANN, K.L., AND M.K. GINGRAS, 2007a, Departures from the archetypal ichnofacies: effective recognition of environmental stress in the rock record, *in* MacEachern, J.A., Bann, K.L., Gingras, M.K., and Pemberton, S.G., eds., Applied Ichnology: Tulsa, Oklahoma, SEPM (Society for Sedimentary Geology) Short Course Notes 11.

MACEACHERN, J.A., PEMBERTON, S.G., M.K. GINGRAS, AND BANN, K.L., 2010. Ichnology and facies models, *in* Facies Models 4, eds., by James, N. P., and Dalrympe, R. W., Geological Association of Canada IV, Series: GEOtext 6, p. 19 – 58.

MARTINSEN, O. J., LIEN, T., AND JACKSON, C., 2005, Cretaceous and Palaeogene turbidite systems in the North Sea and Norwegian Sea Basins: source, staging area and basin physiography controls on reservoir development. Geological Society, London, Petroleum Geology Conference series 2005, v. 6, p. 1147–1164.

MILLER S, B., PEMBERTON, S. G., AND WEHR, 2006, Upper Cretaceous Bahariya Formation, Western Desert, Egypt: A Unique Occurrence of Glaucony in Bioturbated, Marginal Marine Deposits.

NORWEGIAN PETROLEUM DIRECTORATE (NPD), 2011, TheNorwegian Petroleum Directorate's fact-pages: http://www.npd.no/engelsk/cwi/pbl / en/ index.htm (accessed August, 2011).

NORWEGIAN PETROLEUM DIRECTORATE (NPD), 2011, Well data summary sheets:http://www.npd.no/engelsk/cwi/pbl/en/wdss_index.htm (accessed November 2011).

PELTONEN, C., MARCUSSEN, Ø., BJØRLYKKE, K., AND JAHREN, J., 2008, Clay mineral diagenesis and quartz cementation in mudstones: The effects of smectite to illite reaction on rock properties. Marine and Petroleum Geology. v. 26, p. 887 – 898.

PEMBERTON, S.G., FLACH, P.D., AND MOSSOP, G.D., 1982, Trace fossils from the Athabasca oilsands, Alberta, Canada: Science, v. 217, p. 825 – 827.

PEMBERTON, S.G., AND FREY, R.W., 1984, Ichnology of storm-influenced shallow-marine sequence: Cardium Formation (Upper Cretaceous) at Seebe Alberta. *in* Stoot, D. F. and Glass, D. J., eds., The Mesozoic of Middle North America. Canadian Petroleum Society of Petroleum Geologist Memoirs, Calgary, Alberta, 9, p. 281 – 304.

PEMBERTON, S.G., AND FREY, R.W., 1985, The *Glossifungites* Ichnofacies: Modern examples from the Georgia coast, U.S.A., *in* Curran, H.A., ed., Biogenic Structures: Their Use in Interpreting Depositional Environments: SEPM, Special Publications 35, p. 237 – 259.

PEMBERTON, S.G., MACEACHERN, J.A., AND FREY, R.W., 1992, Trace fossil facies models: environmental and allostratigraphic significance, *in* Walker, R.G., and James, N.P., eds., Facies Models: Response to Sea Level Change: Geological Association of Canada, p. 47 – 72.

PEMBERTON, S.G., MACEACHERN, J.A., AND RANGER, M. J., 1992b Ichnology and event stratigraphy: the use of trace fossils in recognizing tempestites. *in* Pemberton, S. G., eds., Applications of Ichnology to Petroleum Exploration: A Core Workshop. Society of Economic Paleontologist and Mineralogist, Core Workshops, Tulsa, Oklahoma, 17, p. 85 – 118

PEMBERTON, S.G., AND MACEACHERN, J.A., 1995, The sequence stratigraphic significance of trace fossils: Examples from the Cretaceous foreland basin of Alberta, Canada, *in* Van Wagoner, J.C., and Bertram, G.T., eds., Sequence Stratigraphy of Foreland Basin Deposits: American Association of Petroleum Geologists, Memoir 64, p. 429 – 475.

PEMBERTON, S.G., AND MACEACHERN, J.A., 1997, The ichnological signature of storm deposits: the use of trace fossils in event stratigraphy, *in* Brett, C.E., and Baird, G.C., eds. Paleontological Events: New York, Columbia University Press, p. 73 – 109.

PEMBERTON, S.G., SPILA, M., PULHAM, A.J., SAUNDERS, T., MACEACHERN, J.A., ROBBINS, D., AND I.K. SINCLAIR, 2001, Ichnology and sedimentology of shallow to marginal marine systems: Ben Nevis and Avalon reservoirs, Jeanne d'Arc Basin: Geological Association of Canada, Short Course Notes Volume 15

RANGER, M.J., AND PEMBERTON, S.G., 1997, Elements of a stratigraphic framework for the Mc- Murray Formation in South Athabasca area, Alberta, *in* Pemberton, S.G., and James, D.P., eds., Petroleum Geology of the Cretaceous Mannville Group, Western Canada: Canadian Society of Petroleum Geologists, Memoir 18, p. 263 – 291.

REINECK, H.E., 1963, Sedimentgefüge im Bereich der südlichen Nordsee. *Abhandlungen der senckenbergische naturforschende Gesellschaft*, v. 505, p. 1 – 138.

RICE, A.L., AND CHAPMAN, C.J., 1971, Observations on the burrows and burrowing behavior of two mud-dwelling decapod crustaceans, *Nephrops norvegicus* and *Goneplax rhomboides*: Marine Biology, v. 10, p. 330 – 342.

SAGEMAN, B.B., WIGNALL, P.B., AND KAUFFMAN, E.G., 1991, Biofacies models for oxygen-deficient facies in epicontinental seas: tool for paleoenvironmental analysis, *in* Einsele, G., Ricken, W., and Seilacher, A., eds., Cycles and Events in Stratigraphy: Berlin, Springer-Verlag, p. 542 – 564.

SANCHEZ-FERRER, S., S. D. JAMES, B. LAK, AND A. M. EVANS, 1999, Techniques used in the exploration of turbidite reservoirs in a frontier setting– Helland Hansen license, Vøring Basin, offshore mid-Norway, *in* A. J. Fleet and S. A. R. Boldy, eds., Petroleum geology of northwest Europe: Proceedings of the 5th Conference: Geological Society, London, p. 281 – 292.

SAVRDA, C.E., AND BOTTJER, D.J., 1986, Trace fossil model for reconstruction of paleo-oxygenation in bottom waters: Geology, v. 14, p. 3 – 6.

SAVRDA, C.E., AND BOTTJER, D.J., 1989, Trace fossil models for reconstructing oxygenation histories of ancient marine bottom waters: application to Upper Cretaceous Niobrara Formation, Colorado: Palaeogeography, Paleoclimatology, Palaeoecology, v. 74, p. 49 – 57.

SAVRDA, C.E., KRAWINKEL, H., MCCARTHY, F.M.G., AND MCHUGH, C.M.G., 2001, Ichnofabrics of a Pleistocene slope succession, New Jersey margin: relations to climate and sea-level dynamics: Palaeogeography, Palaeoclimatology, Palaeoecology, v. 171, p. 41 – 61.

SHINN, E.A., 1968, Burrowing in recent lime sediments of Florida and the Bahamas: Journal of Paleontology, v. 42, p. 879 – 894.

SKOGSEID, J., PLANKE, S., FALEIDE, J.I., PEDERSEN, T., ELDHOLM, O. AND NEVERDAL, F., 2000, NE Atlantic continental rifting and volcanic margin formation. *in*: Nøttvedt, A. and Larsen, B.T., eds., Dynamics of the Norwegian Margin.Geological Society, London, Special Publications, 167, p. 295 – 326.

TAYLOR, A.M., AND R. GOLDRING, 1993, Description and analysis of bioturbation and ichnofabric: Journal of the Geological Survey, London, vol. 150, p. 141 – 148.

VERGARA, L., I.WREGLESWORTH, M. TRAYFOOT, AND RICHARDSSEN, G., 2001, The distribution of Cretaceous and Paleocene deep-water reservoirs in the Norwegian Sea basins: Petroleum Geoscience, v. 7, p. 395 – 408.

WETZEL, A. AND WERNER, F., 1981, Morphology and ecological significance of *Zoophycos* in deep-sea sediments off NW Africa. Palaeogeography, Palaeoclimatology, Palaeoecology, v. 32, p. 185 – 212.

ZIEGLER, P. A., 1990, Geological Atlas of Western and Central Europe. Shell Internationale Petroleum Maatschappij B.V., The Geological Society, London.

CHAPTER III – RELATIONSHIP BETWEEN BIOTURBATION, SEDIMENT FABRIC MODIFICATIONS, SPATIAL VISUALIZATION AND THE RESULTING PERMEABILITY DISTRIBUTION

INTRODUCTION

Burrow networks can influence reservoir quality. Bioturbated strata is common in the sedimentary record and contributes to resource quality. Biogenic enhancement of reservoir petrophysics (*i.e.,* permeability) influences oil production, reservoir development and reserve calculation (Gingras et al., 2004b; Pemberton and Gingras, 2005; Gingras et al., 2012). However, the impact of bioturbation is often overlooked leading to inaccurate assessment of the fluid flow characteristics in sedimentary media. Parameters controlling fluid flow and storage such as porosity and permeability can be partially or fully modified as a result of bioturbation (Dawson, 1978; Gunatilaka et al., 1987; Meadows and Tait, 1989; Martin et al., 1994; Gingras et al., 1999; Gingras et al., 2004a, 2004b; Mehrtens and Selleck, 2002; McKinley et al., 2004; Sutton et al., 2004; Cunningham et al. 2009; Gordon et al., 2010; Keswani and Pemberton, 2010; Polo et al., 2010; Tonkin et al., 2010; Baniak et al., 2011; Lemiski et al., 2011). These changes range from biogenic modification of the primary sedimentary fabric to diagenetic alteration of the sedimentary matrix (Pemberton and Gingras, 2005). Factors such as burrow abundance and interconnectivity influence the potential volume of hydrocarbons hosted and able to be delivered from bioturbated reservoirs. Pemberton and Gingras (2005) demonstrated that biogenically-enhanced permeability fabrics can be classified into five interrelated scenarios: 1) surface-constrained textural heterogeneities; 2) non-constrained textural heterogeneities; 3) weakly defined textural heterogeneities; 4) diagenetic textural heterogeneities; and, 5) cryptic bioturbation. Also, bioturbation may be present as two types of flow media. Highly contrasting permeability fields, which are known as dual- permeability flow media; or lowly contrasting permeability fields, which are referred to as dual-porosity flow media. Dual-porosity media results in reduction of the resource quality of the bioturbated units. Dual-permeability flow media results even in poorer resource quality of the affected strata. Important factors influencing the characteristics of the bioturbated flow media includes: 1) burrow density/bioturbation intensity; 2) burrow connectivity; and 3) the degree of permeability contrast between matrix and burrows (Gingras et al., 2004b; Pemberton and Gingras, 2005). This chapter focuses on assessing the relationship between bioturbation and the resulting permeability enhancement in the Upper Cretaceous Lysing and Nise Formations in the Norwegian Continental Shelf.

Biogenic Enhancement	Thickness	Areal extent	Proportion of media affected
Surface-constrained Textural Heterogeneities.	Zones up to 3m in thickness but generally less than 1m; multiple zones can be formed.	100m to Km scale.	10-50% volume occupied by burrows is common with *Glossifungites* ichnofacies.
Nonconstrained Textural Heterogeneities.	Zones can be up to 10m in thickness, but extreme examples can be greater than 100m.	1-10 Km scale.	20-90% volume occupied by burrows is common with nonconstrained bioturbation.
Weakly Defined Textural Heterogeneities.	Zones can be up to 10m in thickness.	100m to Km scale.	10-50% volume occupied by burrows.
Diagenetic Textural Heterogeneities.	Zones can be up to 10m in thickness; extreme examples can be greater than 100m.	1 to 100 Km.	30-80% volume occupied by burrows.
Cryptic Bioturbation.	Zones can be up to 10m in thickness; extreme examples can be greater than 100m.	100m to Km scale.	100% volume occupied by burrows.

Table 3.1. Scale of the burrow affected zone for each category of the biogenic permeability enhancement classification. Modified from Pemberton and Gingras (2005).

BACKGROUND

Permeability enhancement in clastic and carbonate reservoirs has traditionally been related mostly to diagenetic effects on porosity. The common assumption is based on the relation between porosity and permeability. Therefore, permeability trends are directly influenced by the bulk porosity in clastic reservoirs. Diagenesis more likely reduces porosity via compaction, cementation and biogenically influenced geochemical modifications (Keswani, 1999; Pak and Pemberton, 2003; Gingras et al., 2004a, 2004b; Pemberton and Gingras, 2005; Knaust, 2009a; Phillips and McIlroy, 2010; Corlett and Jones, 2012; Petrash et al., 2011). However, diagenetic processes may also increase porosity and permeability (Cunningham et al., 2009; Cunningham and Sukop, 2012; Gingras et al., 2012).

Recent research aims to assess the impact of bioturbation on reservoir quality, including petrophysical properties such as porosity and permeability in clastic and carbonate reservoirs (Gingras et al., 1999; Gingras et al., 2004b; Pemberton and Gingras, 2005; Spila et al., 2005; Keswani and Pemberton, 2006, 2010; Cunningham et al., 2009; Knaust, 2009a, 2009b; Lacroix et al., 2012; Lemiski et al. 2011; Cunningham and Sukop, 2012; Polo et al., 2012; Gingras et al., 2012). It has been long known that in modern sediments bioturbation infauna (*e.g.,* earthworms, decapod crustaceans, amphipods, polychaetes) can enhance porosity and permeability by creating macropores (Pemberton and Gingras 2005; Tonkin et al., 2010). Specific examples of permeability enhancement and its classification are presented by Pemberton and Gingras (2005). Their work emphasizes the importance of recognizing biogenically-modified reservoirs. The case studies and the impact on resource quality presented therein are drawn from the Ordovician Yeoman Formation in Saskatchewan; the Devonian Wabamun Formation in Alberta; the Triassic Sag River Formation in Alaska; the Jurassic Arab-D in Saudi Arabia; the Cretaceous Toro Formation in Papua New Guinea; the Cretaceous Ferron Sandstone Member in Utah, United States; the Miocene Mirador Formation in Colombia; the Miocene to Pliocene Mundu Formation in Indonesia; and the Pleistocene to Holocene deposits at Willapa Bay, Washington, United States. Their study demonstrated that biogenic structures alter fluid flow and enhance reservoir quality. From this departing point sedimentary workers are able to characterize biogenically enhanced reservoirs taking into account the occurrence, nature, thickness and areal distribution of bioturbation (Table 3.1). The proposed classification serves as foundation for future research in assessing biogenically associated heterogeneities. More recently, Gingras et al., (2012), rewiewed the general history and paradigm of ichnological permeability, aiming to establish a framework within which future research can progress.

Classification of biogenic porosity enhancement in karstic systems

Burrow-related porosity modification in carbonates was recently revisited by Cunningham et al., (2009). As result of their discussion, they have proposed a classification related to macroporosity in karst due to trace fossils. The proposed classification scheme for carbonate rocks of the Biscayne aquifer (southeastern Florida) is based on a modification of the rock-fabric petrophysical classification of carbonate pore space presented by Lucia (1995). The classification is useful in defining stratiform "Super K" zones related to biogenically enhanced permeability in carbonate systems. By studying the Biscayne aquifer they found that biogenic macroporosity is largely manifested as: (1) ichnogenic macroporosity and (2) biomoldic macroporosity (Table 3.2).

Type of biogenically induced enhancement/modification	Characteristics
Ichnogenic macroporosity	• Related to post-depositional burrowing activity. • Bioturbating infauna primarily associated by *Callianassid* shrimp and fossilization of their complex burrow systems (*Ophiomorpha*). • Takes into account intra- and inter-burrow macroporosity. • Less commonly, intra-or inter-root macroporosity.
Biomoldic macroporosity	• Formed by the dissolution of skeletal material. • Burrowing infauna associated principally to mollusks. • Takes into account intra- and inter-burrow macroporosity.

Table 3.2. Macroporosity classification in karst due to biogenically-induced fabric heterogeneities proposed by Cunningham et al., (2009). Ichnogenic and Biomoldic macroporosity takes into account intra-and inter-burrow macroporosity and is based on a modification of Lucia's (1995) rock-fabric–petrophysical classification of carbonate pore space.

Ichnology and dual-porosity vs. dual-permeability systems

Permeability and porosity enhancement associated with burrows fabrics in sedimentary flow media occurs as dual permeability or dual porosity networks (Gingras et al., 2005; Gingras et al., 2012). Dual porosity systems occur wherein the matrix permeability and the burrow permeability are similar. Dual porosity results in reducing the resource quality of the sedimentary media. On the other hand, dual permeability flow media occurs when the matrix permeability and the burrow permeability differ by more than two orders of magnitude. Dual permeability flow media is even more detrimental to the resource quality of the sedimentary media by imposing barriers and baffles for fluid flow.

Case studies

Using computer simulations, laboratory and field measurements Gingras et al., (1999) showed that petrophysical parameters can be biogenically modified. For example, permeability can be enhanced by burrows emplaced into sedimentary firmgrounds. Their study showed that the presence of sand-filled burrows of the *Glossifungites* Ichnofacies increase the potential reservoir volume and serve as permeable conduits at the base of a reservoir. The *Glossifungites* Ichnofacies can even interconnect different reservoir packages by providing fluid-flow pathways between otherwise isolated reservoirs. The results of these studies indicate that three variables determine the flow characteristics of a burrowed matrix: 1) the degree of permeability contrast between matrix and the burrows; 2) the degree to which burrows are interconnected; and, 3) the burrow density. By assessing the above mentioned parameters and using computer modeling, (Gingras et al., 1999) showed that effective permeability can be approximated using analytical formulae that can be applied in any bioturbated geological medium as a first run approximation.

Gingras et al., (2002) integrated petrographic data with magnetic resonance images (MRI) to analyze *Macaronichnus*-burrowed sandstone. In their study they mapped the distribution of the porosity and textural characteristics were mapped in a sample where *Macaronichnus* is the dominant trace-fossil. The study suggested that the complex distribution of porosity and its relationship with the matrix represents a dual porosity-permeability system and may affect similarly altered reservoirs.

Using core analysis, petrography, plug/probe permeability analyses and numerical modeling for the upper Ben Nevis Formation, Hibernia Field, offshore Newfoundland, Spila et al., (2005) suggested that mud-filled burrows represent a rather intricate, low-permeability three-dimensional network of obstacles that baffle fluid flow. The study demonstrated that the resulting flow pathways are highly sinuous and tortuous and thereby induce dispersion. Additionally, Spila et al., (2005) warn that bioturbation influences reservoir volumetric calculations and as a result of the high reservoir volume modified by bioturbation (Table 3.1).

Cunningham et al., (2009) suggested that the stratiform ichnogenic groundwater flow zones of the Pleistocene of the Biscayne aquifer (in southeastern Florida) proffer superpermeability flow zones. Their study integrated data from cyclostratigraphic, ichnologic, borehole-fluid flow measurements, tracer studies and permeabilities derived from lattice Boltzmann methods (LBMs). The "super-K" zones are approximately 2–5 orders of magnitude higher than the Arab-D carbonate reservoir within the Upper Jurassic Arab and Jubaila Formations of the Ghawar field in Saudi Arabia (Pemberton and Gingras, 2005). Cunningham et al., (2009) suggested that ichnogenic macroporosity represents a pathway for concentrated groundwater flow. This concept differs considerably from standard karst flow-systems, which consists of groundwater movement through fractures and dissolution features.

SPATIAL VISUALIZATION OF BIOTURBATED MEDIA

Destructive (*e.g.,* thin sections) and nondestructive methods (*e.g.,* X-ray Computed Tomography (CT), Microtomography (Micro-CT) and Magnetic Resonance Imaging (MRI)) can be applied to resolve primary sedimentary and biogenic structures. The application of these methods contributes in identifying and quantifying textural heterogeneities. Various case-studies from the literature highlight the application of these methods (Gingras et al., 1999 and Gingras et al., 2002 and Gingras et al., 2005; Polo et al., 2010; Baniak et al., 2011; Polo et al., 2012). Alternatively, the most common techniques for assessing the petrophysical properties of bioturbate texture are destructive methods (*i.e.,* thin sections and coring). However, Gingras et al., (2005) suggest that CT, Micro-CT and MRI techniques have the most potential in three-dimensional rock analyses.

Magnetic resonance imaging (MRI)

Magnetic resonance imaging (MRI) provides a non-destructive, three-dimensional imaging method applicable to bioturbated media. This method maps the contrast in density and (magnetic) relaxation properties of protons; these features are unique for each sediment type and pore-fluid. Few MRI studies have been conducted in sedimentary geology (Gingras et al., 2002). Nevertheless, MRI has been successfully employed for a variety of petrophysical applications (see Gingras et al., 2002, for reviews). Also, this technique has been applied to map the structure, porosity and permeability of rocks (Marten et al., 2008). Examples of these applications include imaging irreducible water in cored reservoir samples (Attard et al., 1998) and characterizing fluid movement through solids (Bencsik and Ramanathan, 2001).

Magnetic Resonance Imaging does not measure the density of a rock directly; rather it is sensitive to fluids imbibed into the pore space of a rock (Gingras et al., 2002). Furthermore pore-filling fluids, such as salt- and fresh water, can be differentiated by MRI in porous rocks (Marteen et al., 2008). Therefore, MRI allows for the three-dimensional mapping of a magnetic resonance signal, and constitutes a tool useful in assessing and map the pore-space distribution in bioturbated rocks. A major limitation of MRI is the image quality. This limitation results in limited work focused on resolving physical or biogenic sedimentary structures (Gingras et al., 2002).

X-ray computed tomography (CT) & (Micro-CT)

Spatial three-dimensional (3D) visualization of bioturbated media, was in the past gained mostly from serial sectioning and polishing of biogenic structures (*e.g.,* Uchman 1995; Gatesy et al., 1999; Wetzel and Uchman 2001; Hasiotis 2002, 2004; Milan et al., 2004). Lately, computer tomography (CT) (*e.g.,* Fu et al., 1994; Ekdale et al. 2006; Polo et al., 2010; Baniak et al., 2011; Lacroix, 2012), and magnetic resonance imaging (MRI) (Gingras et al., 2002) have been incorporated allowing 3D views of tracks, burrows and trails in bioturbated strata. Perez et al., (1999), applied CT scan to study estuarine benthic species. Alternatively, Naruse and Nifuku (2008) combined serial polishing and computer graphics to obtain 3D images of *Phycosiphon incertum* providing other examples of spatial visualization of ichnofossils. More recently, Platt et al., (2010) have suggested another nondestructive tool for 3D visualization of trace fossils. This consists of multistripe laser triangulation (MLT) scanner and three-dimensional (3D) software for semi quantitative and quantitative analyses of ichnofossils and modern traces. This technique also can be used for surface analysis in bioturbated media.

Conventional reservoir characterization is often restricted to porosity and permeability assessments. Commonly, visualization of the reservoir properties is limited to two dimensional analyses by using destructive methods (*e.g.,* thin sections coring, core-plug drilling, lacquer profiles, photomicrographs or wax sampling).

The majority of these methods are destructive and the spatial distribution of the grains and sedimentary structures is lost. Due to intricate textural heterogeneities, assessing spatial variability in three dimensions (3D) is often overlooked. X-ray Microtomography (Micro-CT) is a non-destructive technique that allows visualization of density-associated petrophysical properties. In bioturbated, low-permeability reservoirs three dimensional visualization contributes to the understanding of burrow spatial distributions (*e.g.,* burrow density and interconnectivity) and more accurate reservoir characterization. Gingras et al., (1999) demonstrated that changes in burrow density have a significant effect on the horizontal permeability (k_h) and vertical permeability (k_v). Therefore spatial visualization plays an important role when modeling fluid flow in bioturbated media.

X-rays provide ‘‘flattened’’ three-dimensional data onto a plane. Computed Tomography provides a three-dimensional image computed from a series of X-ray images. CT-scans can provide three-dimensional views, but they are not particularly sensitive to the slight variations in density that characterize most rocks (Gingras et al., 2002).

Another important tool in imaging bioturbated reservoirs is microfocus X-ray computed tomography (Micro-CT). Like the above mentioned method, Micro-CT constitutes a non-destructive, three dimensional method to image bioturbated reservoirs. Micro-CT is based on recording X-ray projections of the studied object in different angles (Van Geet et al., 2003). The projections are gathered then as a set of 2D cross-sections than can be processed to construct rendered 3D models of the studied object. This allows three dimensional visualization of the internal microstructure of the sample. Therefore, Micro-CT provides higher resolution than conventional CT scans. Micro-CT has enormous potential for quantifying and visualizing internal structures in sedimentary rocks at a very detailed scale. More importantly, Micro-CT allows three-dimensional imaging without the presence of a vacuum and does not require special coating (Gingras et al., 2005). This allows the observation of the original characteristics of the specimen such as the pore space and burrow shape. Moreover, Micro-CT can link petrography and petrophysics in sedimentary media (Van Geet et al., 2003).

Petrographic analysis

The most common destructive method used in assessing bioturbated textures is petrographic analysis. This consists of hand-sample, core sample and thin sections descriptions. In particular, thin sections have been used for this purpose. An example of the use of thin-section analysis paired with magnetic resonance images (MRI) is given in (Gingras et al., 2002). The study applied these techniques to map the biogenic-heterogeneities and porosity distribution in a sample of *Macaronichnus*-burrowed sandstone. Spila et al., (2005) used thin sections analysis and core description to determine the ichnogenera and petrophysical properties of bioturbated reservoirs. More recently, Gordon et al., 2010 conducted a detailed petrographic analysis on core samples from the Cretaceous Bluesky Formation. The study showed that zones highly bioturbated with *Macaronichnus segregatus* exhibit enhanced petrophysical properties (*i.e.,* porosity and permeability), thus improving reservoir quality.

METHODS

The core plugs in this thesis were collected by StatoilHydro as part of the on-going production license PL282 covered by block 6405 located in the Norwegian continental shelf (Figure 2.1; Chapter II within this thesis). Selected plug samples from the Ellida and Midnatsoll fields, wells 6405/7-1 T2 and 6405/10-1 respectively, provided the data set for this study. A total of 6 cores, approx. 156 m, were analyzed for this study (Table 2.1, Chapter II within this thesis). Overall, the main portion of the core-logging and plug selection for spot permeability test and CT-scan imaging was conducted at the Weatherford Reservoir Laboratories located in Stavanger, Norway. Representative samples were scanned and 3D models were constructed. Sample selection was based on production zone, facies, fluid-storability and fluid-deliverability potential of the lithofacies defined for the Lysing and Nise formations.

Spot permeability tests

Core-plug samples from the facies classification scheme proposed in Table 2.1, (Chapter II within this thesis) were chosen for spot-minipermeametry testing with special emphasis on the productive zones. The spot-minipermeametry tests were carried out on plug samples of Facies 1 and Facies 2, and Facies 4 for the Nise and Lysing formations respectively. The plug samples for analyses were collected from slabbed core with a one inch bore and were drilled parallel to the bedding planes. The resulting cylindrical core plugs are 1 inch in diameter and 1 inch height and are listed in Table 3.3.

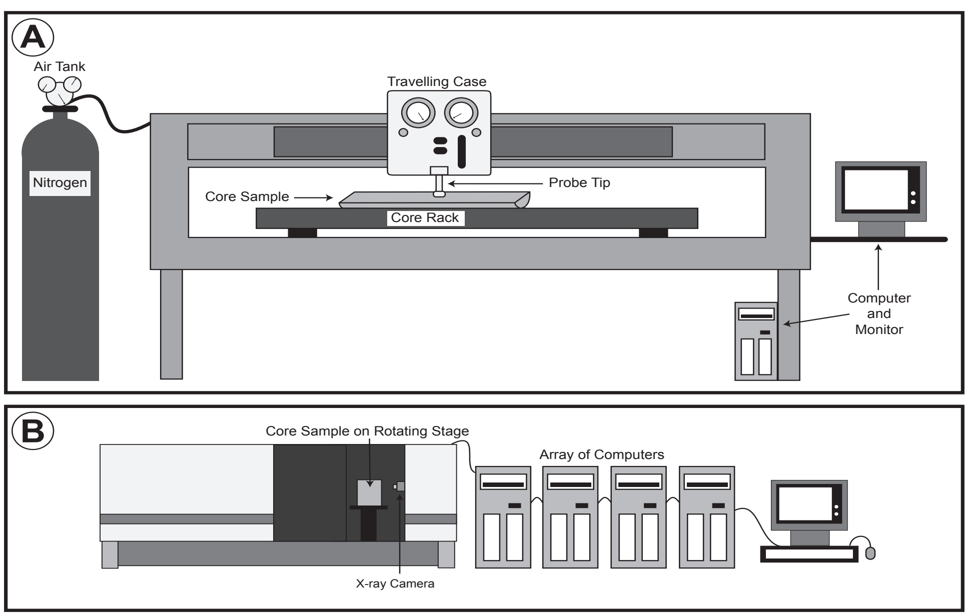

Figure 3.1. **A**) Core Laboratories PDPK – 400 Pressure-Decay Profile Permeameter and main components of the system (modified from Core Laboratories instrument manual, (1996), and Lemiski, 2010. **B**) SkyScan 1172 Desktop X-ray microtomograph and main components of the system (modified from SkyScan, 2005 and Lacroix, 2010).

Since spot-permeability analysis requires a flat surface for measurements; the locations for spot measurements were conducted on a fabric-selective basis on flat surfaces of the plugs (Figure 3.2 to 3.5 and 3.8 to 3.12). Spot permeability assessments were done using the Core Laboratories PDPK – 400 Pressure-Decay Profile Permeameter (Figure 3.1). A total of 5 measurements from each point were taken, then the maximum and minimum values for each spot were discarded, and the remaining three values averaged (*e.g.,* Lemiski et al., 2011; La Croix et al. 2010). Finally, the averaged permeability values were plotted for each sample and graphs of the statistical relationships between layered heterogeneity and anisotropy were constructed for each plug-sample (Figure 3.2 to 3.5 and 3.8 to 3.12).

Thin sections

For a more accurate microscopic ichnofabric analysis and its relation to the reservoir petrophysics, thin sections were prepared for each facies. These sections were done preferentially in the same flat surfaces of the plugs where spot-permeability test were performed. The thin sections, were impregnated with blue-epoxy resin in order to estimate the porosity of the selected samples. Porosity determination was done by the estimation of the void space not filled by matrix or grains by using point counts. Petrographic observations were conducted in order to assess the biogenically-induced local variations in the mineral content as well as the original detrital grains and cement/replacive minerals.

X-Ray microtomography CT-Scan

Due to intricate textural variations in bioturbated media, Spatial heterogeneity is often overlooked or difficult to discern. X-ray computed tomography (Micro-CT/ uCT) is used in this study for the visualization of biogenically-induced density contrast. Also, this type of non-destructive technique contributes to the understanding of burrow interactions in 3D that influence the reservoir quality such as burrow density and interconnectivity (Gingras et al., 1999). From each reservoir facies a selected sample was taken for microfocus X-ray computed tomography (Micro-CT/ uCT). Micro-CT imaging is based on recording 2D X-ray projections of the samples in different angles. The instrument used for the study presented in this thesis is a SkyScan 1172 Desktop X-ray microtomograph. Images were made at 100 kV and 30 uA and the scanning time was approximately 5 hours for each sample.

ELLIDA FIELD - WELL 6405/7-1 T2					
Formation	**Facies**	**Plug Sample**	**Depth**	**Spot Permeametry**	**CT-Scan imaging**
Nise	*F1*	103	2799.5		x
	F2	279	2847.5	x	
Lysing	*F4*	452	3775.5	x	
	F4	425	3768.7	x	x
	F4	417	3766.7	x	
	F4	413	3765.7	x	
	F4	385	3758.5	x	
MIDNATTSOL FIELD - WELL 6405/10-1					
Formation	**Facies**	**Plug Sample**	**Depth**	**Spot Permeametry**	**CT-Scan imaging**
Nise	*F1*	122	3034.2	x	
	F1	42	3014.2	x	
	F2	28	3010.7	x	x
	F3	48	3015.7		x

Table 3.3. List of plugs selected for spot permeametry and CT-Scan imaging. When selected the samples special emphasis was given to the sandy reservoir intervals: Facies 1-*(F1)* Burrowed muddy sandstone, Facies 2-*(F2)* Burrowed muddy to silty sandstone for the Nise Formation and Facies 4-*(F4)* Burrowed sandy mudstone for the Lysing Formation.

Graphs and statistical relationships between textural heterogeneity and resulting permeability anisotropy

The search for a better understanding of the resulting porosity and permeability distribution has led to the application of statistical methods in bioturbated media (*e.g.,* Gingras et al., 1999; La Croix et al., 2012; Gingras et al., 2012). Among the different measures of central tendency for a random variable (*e.g.,* median, mode) the harmonic, geometric, and arithmetic means have numerous applications including characterization of effective permeability in layered porous media (Limbrunner et al., 2000). As an example, Gomez-Hernandez and Gorelick (1989) have demonstrated that the harmonic mean can be applied to assess the lower limit to the effective hydraulic conductivity of an aquifer system.When applied to bioturbated media, each of these central tendency measurements is appropriate for different situations. However, determination of which scenario may be suitable for the application of any central tendency measurement depends on multiple factors. To properly asses the problem, Gingras et al. (1999) explored the application of the arithmetic and harmonic means to estimate the bulk permeability of biogenically modified media. The study showed that bulk permeability could be best characterized using the harmonic mean when low burrow connectivity is preponderant. Also, a modified arithmetic mean could be used as interconnectivity increases, particularly for the estimation of vertical permeability (k_v) (Gingras et al., 2012). Finally, they demonstrated that in transitional situations, the geometric mean broadly applied where the permeable burrow structures were connected just locally.

Fluid flow in layered sedimentary media occurs preferentially parallel to the beds. For a homogeneous layer, the entire system can be characterized as a single homogeneous and anisotropic layer (Freeze and Cherry, 1979). Therefore, a simple volume weighted arithmetic mean of the permeability of each layer, can be applied to obtain an estimation of the overall bulk permeability occurring parallel to stratification. This relationship can be described as:

$$k_{arithmetic} = \sum_{i=1}^{n} \frac{k_i d_i}{d} \qquad \text{(Equation 3.1)}$$

Where: ki = permeability of each layer
d_i = individual layer thickness

d = total thickness.

When fluid flow occurs perpendicular to layered media, an estimation of the bulk vertical permeability could be obtained by applying a volume-weighted harmonic mean, the calculation then is based in the following equation.

$$k_{harmonic} = \frac{1}{\sum_{i=1}^{n} \frac{d_i}{k_i d}} \qquad \text{(Equation 3.2)}$$

Finally, homogeneous, isotropic systems where fluid flow occurs in all dimension scan be best represented by the volume-weighted geometric mean of the permeability of multiple layers (Warren and Price, 1961), this relation can be expressed as:

$$\ln(k_{geometric}) = \sum_{i=1}^{n} \frac{\ln(k_i) d_i}{d} \qquad \text{(Equation 3.3)}$$

Within the aforementioned equations (3.1 to 3.3) the weighted volume (*i.e.,* d_i/d) represents the burrow intensity. Which reflects the volume occupied by burrows (bioturbation intensity).

RESULTS AND INTERPRETATION

Spot-permeametry

Overall, the results of the minipermeametry data suggest that the permeability in burrowed intervals is more likely to be preserved within trace fossils. In general, as the proportion of traces increase, so too does the average permeability (*e.g.*, Lacroix, 2010). Commonly, permeability values in trace-fossils are greater compare to the matrix (by up to two orders of magnitude) in all the studied samples for both, the Lysing and Nise formations. Thus it constitutes a dual-permeability flow medium (Baniak et al., 2011; Lemiski, 2010; Lacroix et al., 2012; Gingras et al., 2012). Horizontal permeability (K_h) differs from the vertical permeability (K_v) up to two orders of magnitude and is thereby anisotropic (Figure 3.13).

Lysing Formation

Measured spot permeability values range between 2×10^{-2} and 2.29 mD in the tested plug samples of the Lysing Formation (Figure 3.8 and 3.12). Burrow-associated permeabilities range from 1.4×10^{-1} to 2.29 mD, while matrix permeability ranges from 2×10^{-2} to 4.3×10^{-1} mD (Figure 3.8 and 3.12 respectively).

Nise Formation

Within the Nise Formation, burrow-associated permeabilities range from 1.01 to 1.06 mD, while matrix permeability ranges from 8×10^{-2} to 7.6×10^{-1} mD in Facies 1. For Facies F2, burrow-associated permeabilities range from 7.6×10^{-1} to 2.12 mD, whereas matrix permeability ranges from 5×10^{-2} to 1.37 mD.

Well	Formation	Facies	Plug Sample	Approx. Depth, Measured Depth-MD (m)	Spot permeametry Air Permeability (mD)		Local Bioturbation Intensity- BI (%)	Statoil Internal Report	
					Highest value	Lowest value		Horizontal Permeability K_h (mD)	Vertical Permeability K_v (mD)
6405/7-1 T2, Ellida	Lysing	F4	452	3775.53	0.97	0.08	95	0.26	0.07
6405/7-1 T2, Ellida		F4	425	3768.7	2.29	0.04	95	0.48	0.04
6405/7-1 T2, Ellida		F4	417	3766.7	2.1	0.02	90	0.53	0.15
6405/7-1 T2, Ellida		F4	413	3765.7	0.74	0.09	95	0.37	0.05
6405/7-1 T2, Ellida		F4	385	3758.5	0.43	0.06	95	0.25	0.07
6405/10-1, Ellida	Nise	F1	122	3034.2	1.01	0.21	85	Not reported	2.96
6405/10-1, Midnatsoll		F1	42	3014.2	1.06	0.13	90	7.50	0.33
6405/10-1, Midnatsoll		F2	28	3010.7	1.61	0.07	75	0.11	0.03
6405/7-1 T2, Ellida		F2	279	2847.5	2.12	0.05	85	0.2	Not reported

Table 3.4. Data applied to build burrowing intensity versus permeability graphs. The permeability measurements were taken from the spot-minipermeametry dataset obtained using a Core Laboratories PDPK – 400 Pressure-Decay Profile Permeameter (PDPK – 400) and used to infer the permeability of 0% bioturbated media (the lowest values), and 100% bioturbated media (the highest values), respectively**.** Data provided by Statoil (conducted at the Weatherford reservoir labs in Stavanger, Norway) used to plot on the graphs of burrowing intensity versus permeability is also shown. The data is useful for comparison between two different permeametry methods and overall assessment of the nature of fluid flow in bioturbated strata of the Lysing and Nise formations.

Graphs and statistical relationships between textural heterogeneity and resulting permeability anisotropy

The graphs showing the relationship between the intensity of bioturbation and measured permeability are shown in figures 3.2 to 3.5 and figures 3.6 to 3.9 for the Lysing and Nise formations respectively. The harmonic, geometric, and arithmetic means are plotted in green, blue, and red. These three curves more likely characterize the behaviour of permeability resulting from burrow-associated heterogeneity in the Lysing and Nise formations strata. Superimposed upon the graphs are also displayed the bulk permeability values from the Statoil internal permeability report marking data points for the k_h and k_v. The values used to construct the graphs are listed in Table 3.4.

Lysing Formation

Graphs and statistical relationships between layered heterogeneity and anisotropy indicate that permeability in the plug samples for the Lysing Formation (Facies -4) follows approximately the harmonic mean. This relationship suggest that fluid flow dominantly occurs across the low permeability matrix, in the high permeability portion of the strata (throughout the burrow system) (Figures 3.8 to 3.12).

Nise Formation

Within the Nise Formation, the arithmetic mean of trace fossils and matrix permeabilities better represent the bulk permeability in Facies 1 intervals (Figure 3.2 and 3.3). This relationship supports the interpretation that the burrows form a well-connected, horizontal flow network for delivery of fluid (Figure 3.14). In contrast, the harmonic mean provides the most accurate estimate of bulk permeability in Facies- 2 (Figure 3.4 and 3.5), suggesting rather a less connected flow network (Figure 3.16) in spite of the high levels of bioturbation (BI = 4 – 6). Thus, pointing towards some flow complexities within these intervals.

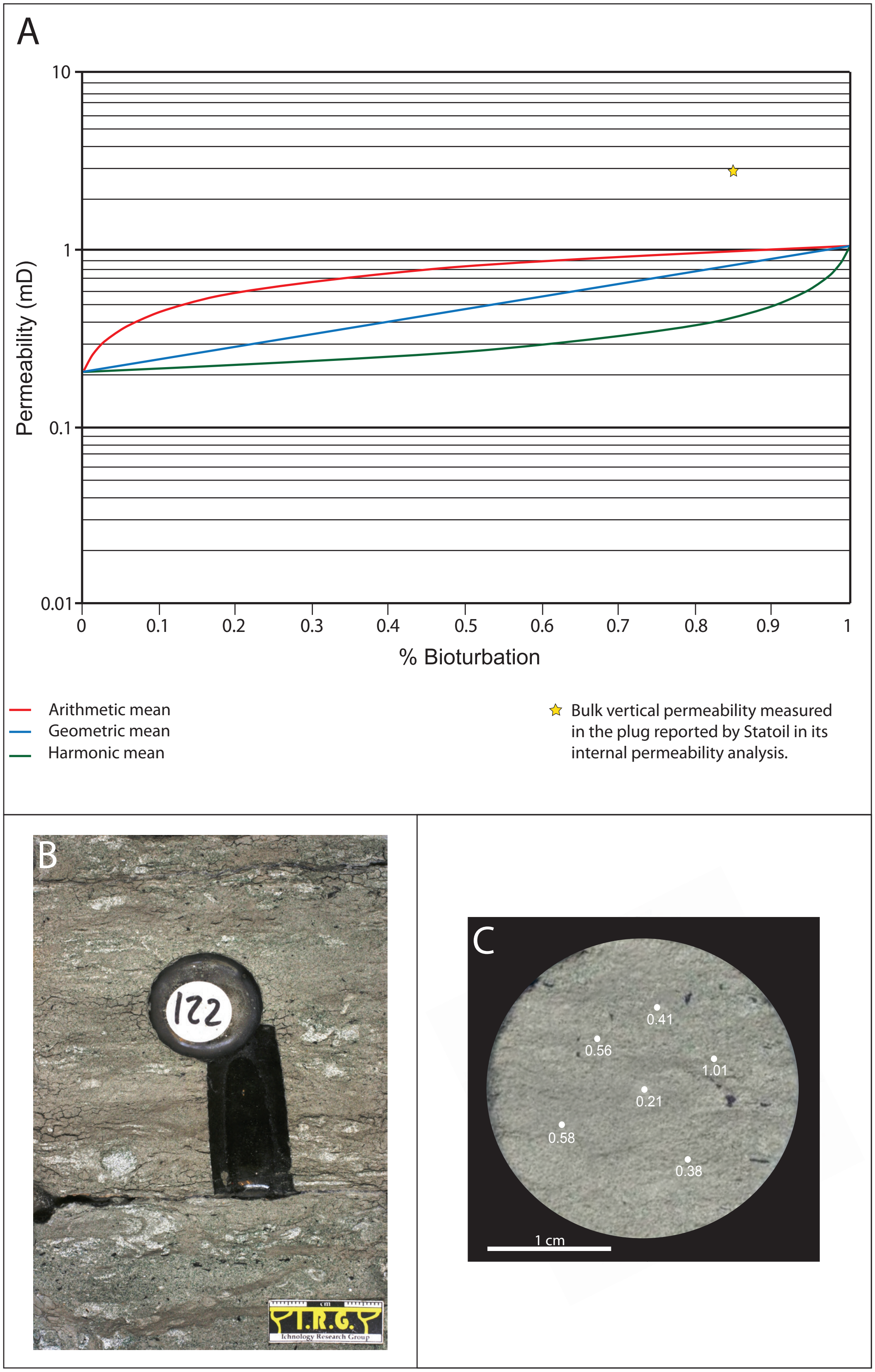

Figure 3.2. Facies F1-Plug 122 graph of the statistical relationship between textural heterogeneity and resulting permeability anisotropy, core appearance and location of the spot permeatry values, 2804.25 m, well 6405/7-1 T2, Ellida.

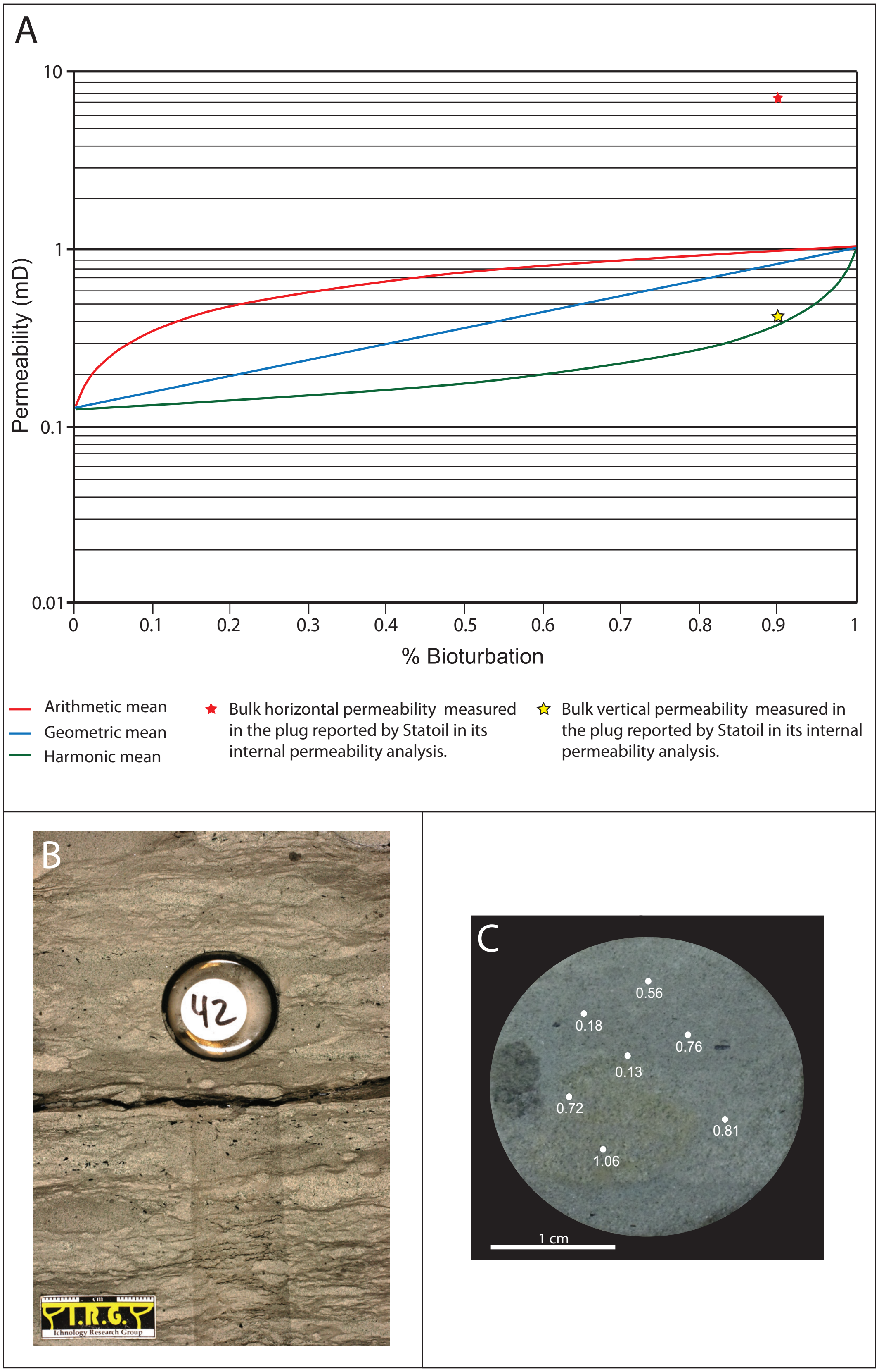

Figure 3.3. Facies F1-Plug 42 graph of the statistical relationship between textural heterogeneity and resulting permeability anisotropy, core appearance and location of the spot permeatry values, 3014.25 m, well 6405/10-1, Midnatsoll.

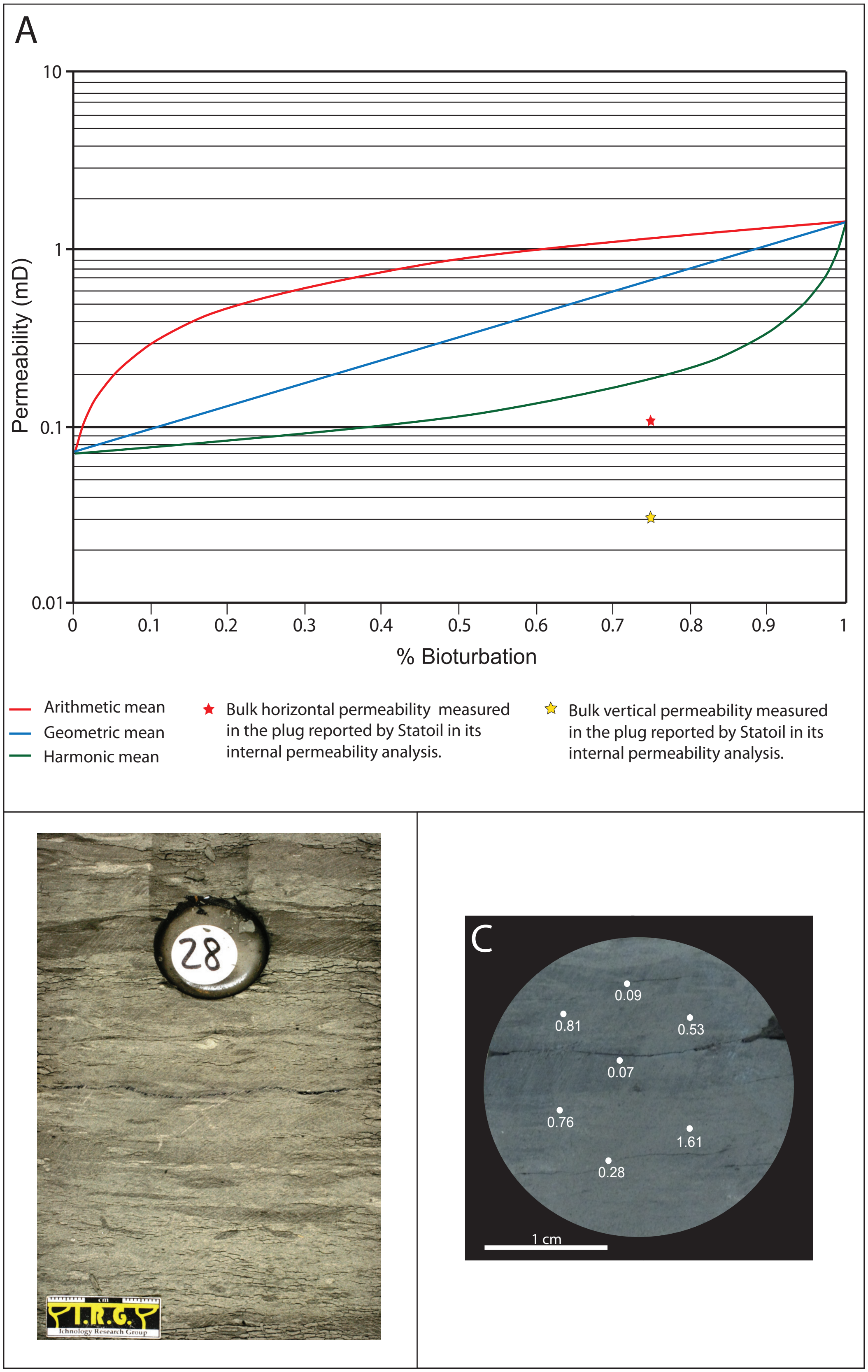

Figure 3.4. Facies F2-Plug 28 graph of the statistical relationship between textural heterogeneity and resulting permeability anisotropy, core appearance and location of the spot permeatry values, 3010.75 m, well 6405/10-1, Midnatsoll.

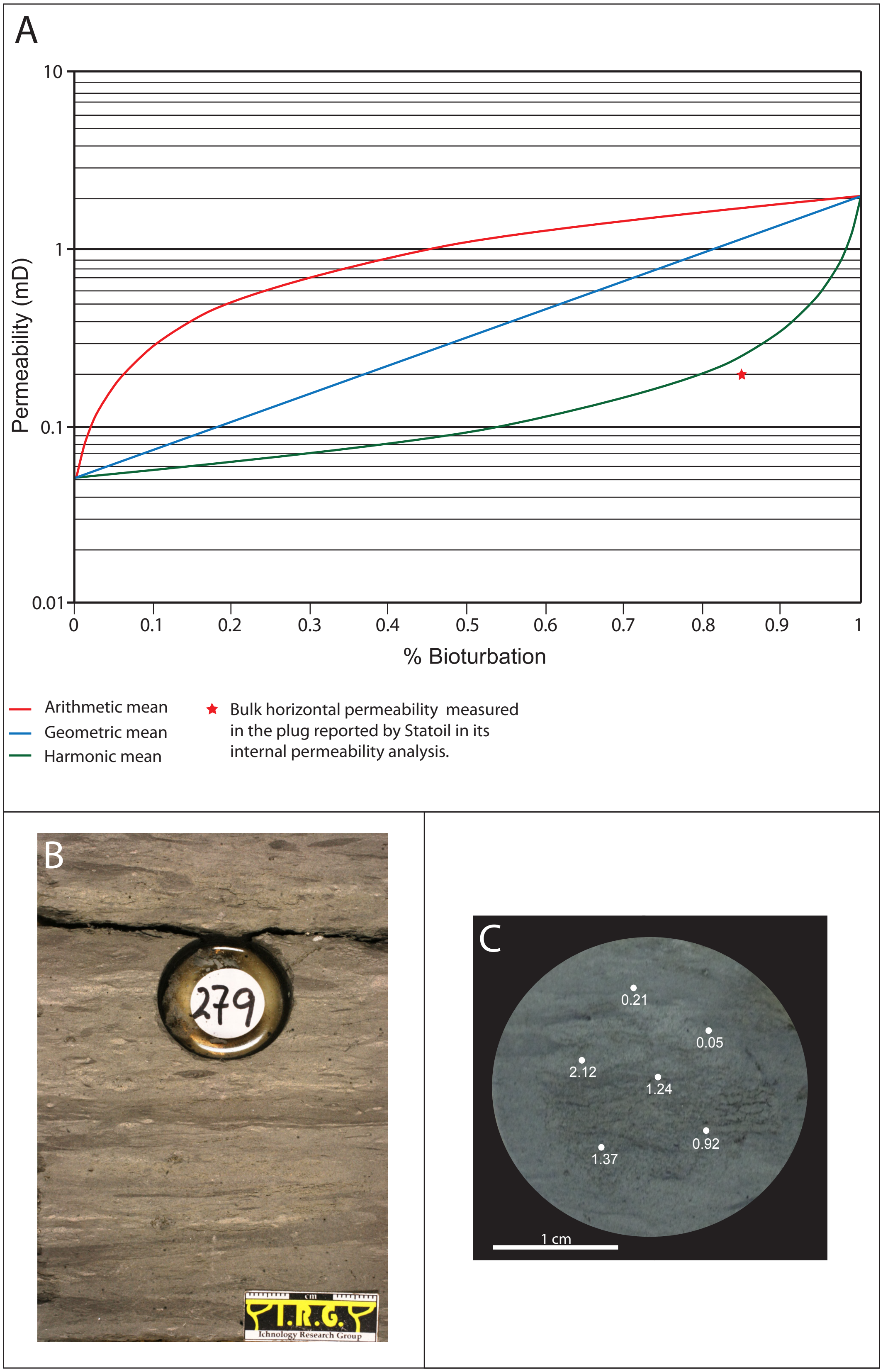

Figure 3.5. Facies F2-Plug 279 graph of the statistical relationship between textural heterogeneity and resulting permeability anisotropy, core appearance and location of the spot permeatry values, 2847.50 m, well 6405/7-1 T2, Ellida.

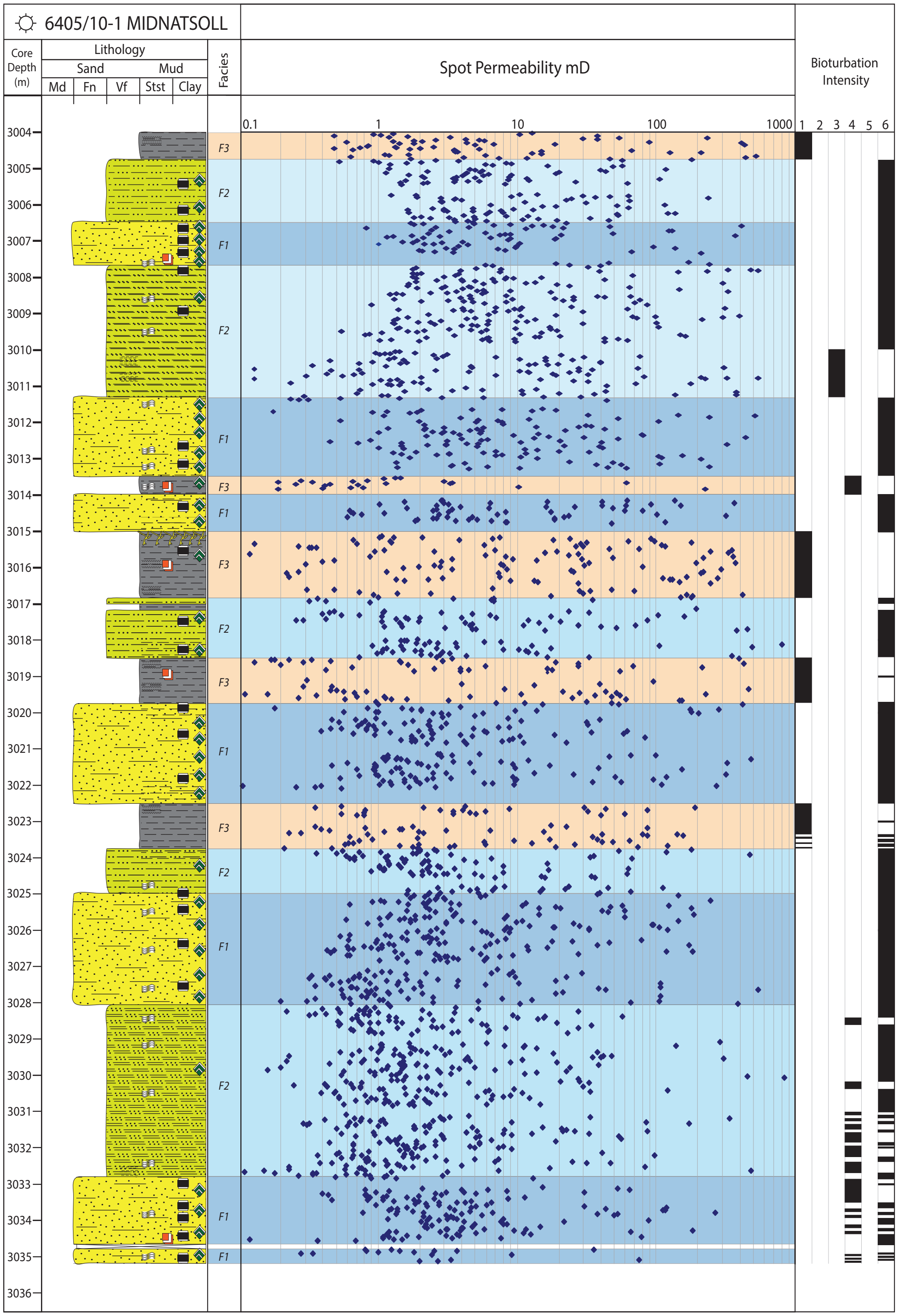

Figure 3.6. Vertical variation of the spot permeability and Bioturbation Index (BI) for each facies in well 6405/10-1, Midnatsoll field. Spot permeametry values taken every 1 cm on slabbed core reported by Statoil on its internal permeability report allowed the comparison between the spot permeability measured in core plugs (presented in this chapter) obtained in a fabric selective manner (*i.e.*, Kburrow vs. K matrix) and Statoil's reported values for the same intervals.

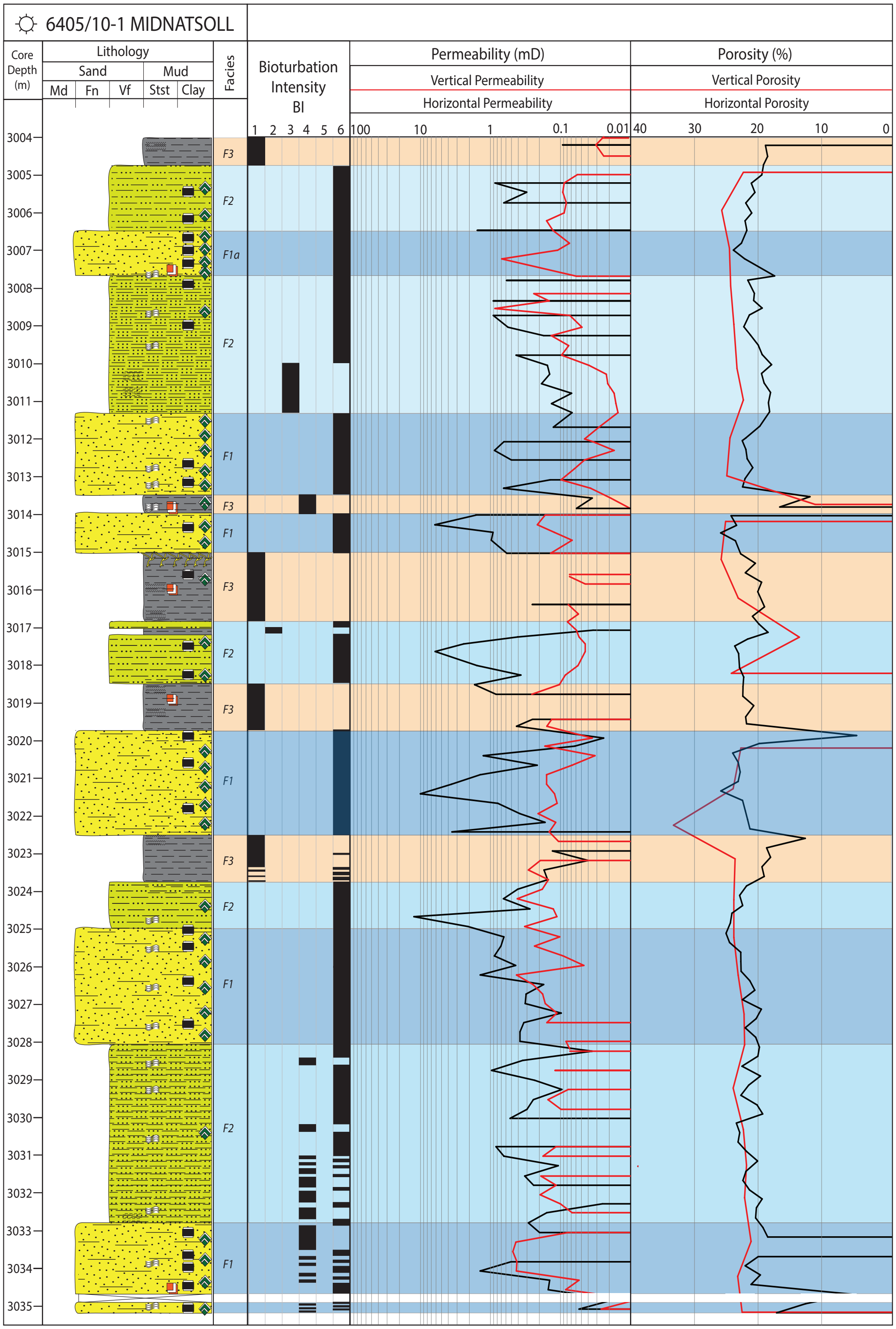

Figure 3.7. Core description showing the interpreted lithofacies, Bioturbation Index (BI) and the vertical variation of both the bulk horizontal k_h and vertical k_v permeability in well 6405/10-1, Midnatsoll field. Bulk horizontal and vertical permeability measurements carried out on core plugs reported by Statoil on its internal permeability report. This also allowed the comparison between the spot permeability measured in core plugs (presented in this chapter) obtained in a fabric selective manner (*i.e.*, Kburrow vs. Kmatrix) and Statoil's reported values for the same intervals.

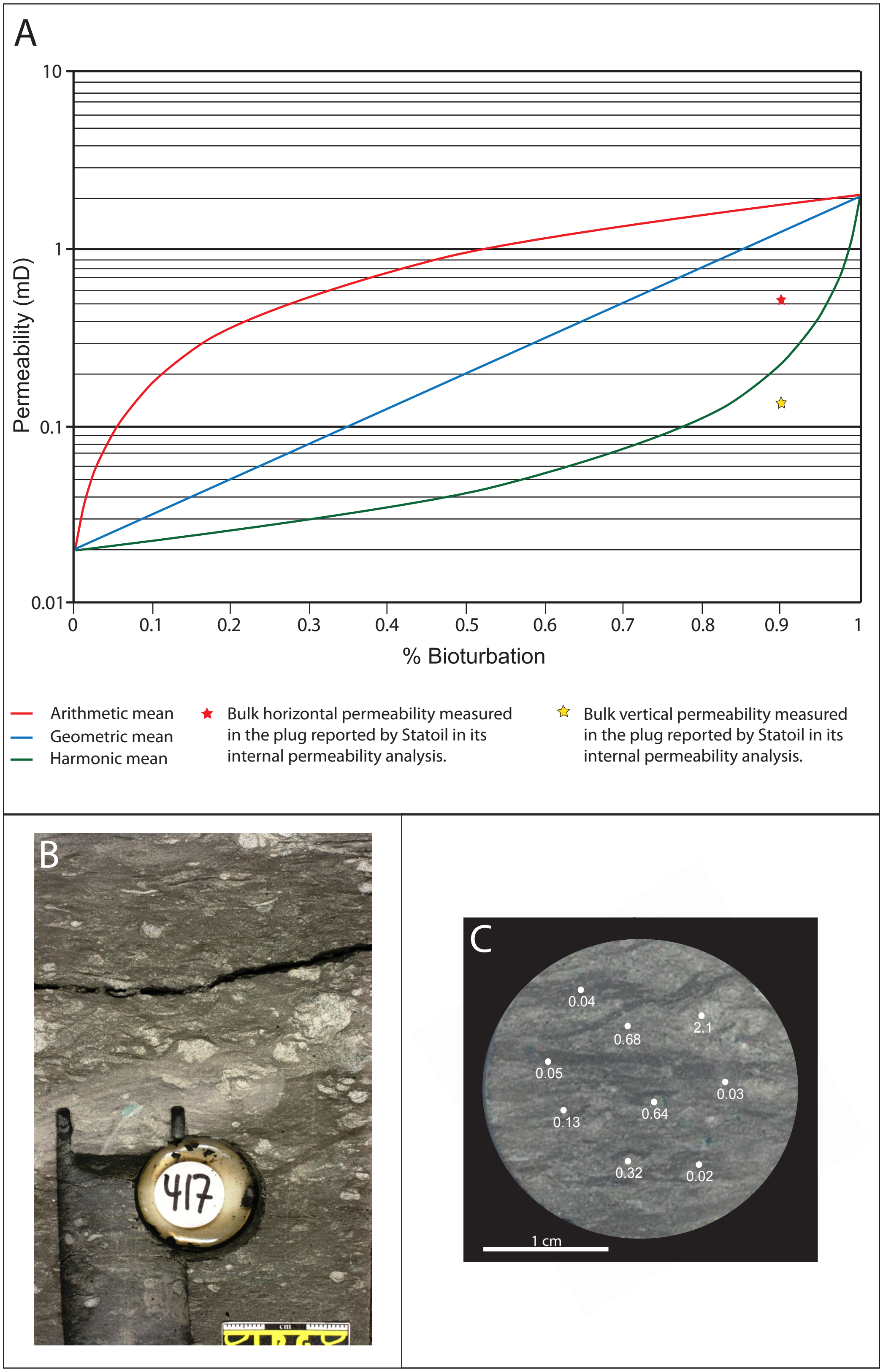

Figure 3.8. Facies F4-Plug 417 graph of the statistical relationship textural heterogeneity and resulting permeability anisotropy, core appearance and location of the spot permeatry values, 3766.75 m, well 6405/7-1 T2, Ellida.

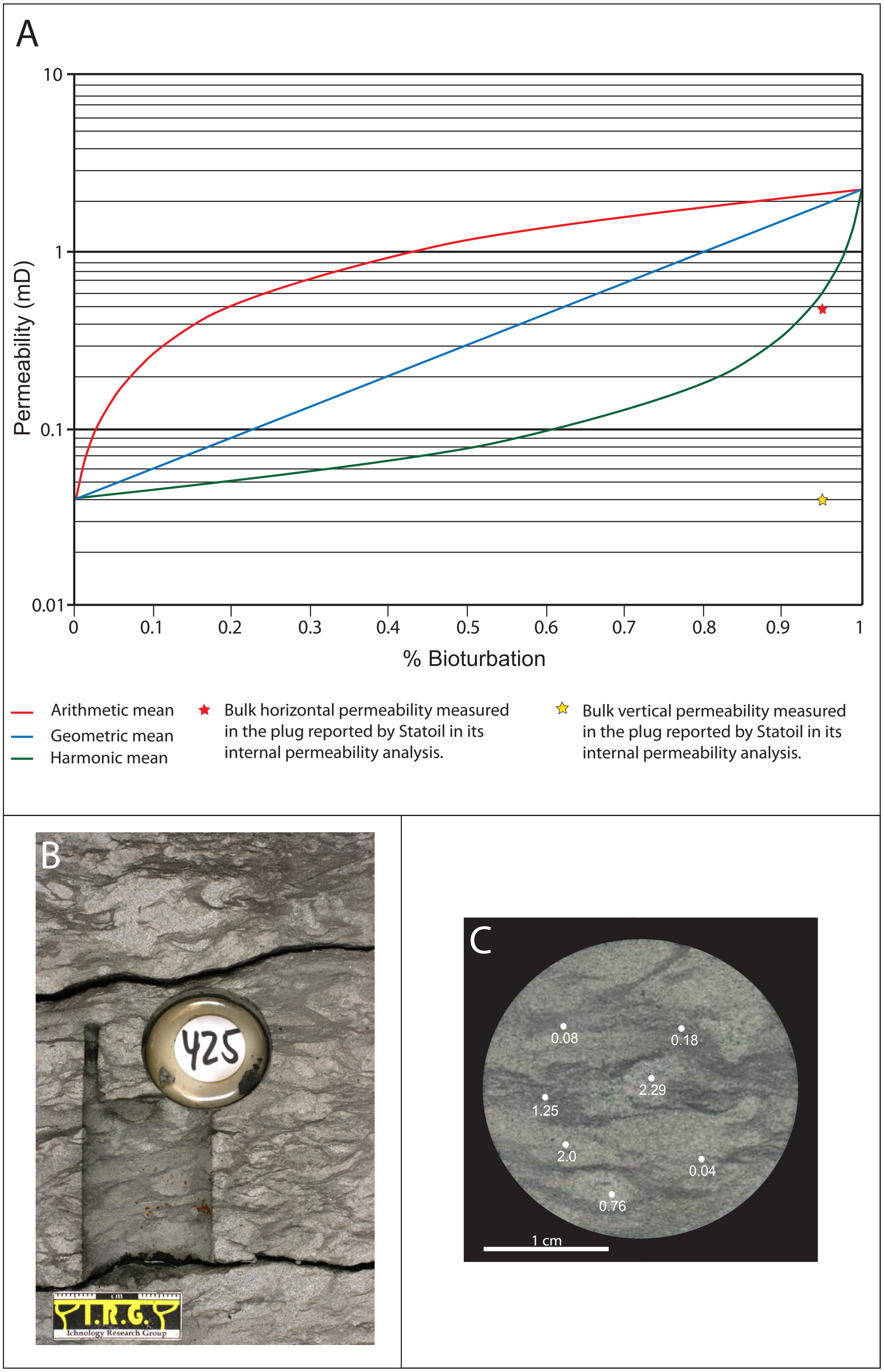

Figure 3.9. Facies F4-Plug 425 graph of the statistical relationship between textural heterogeneity and resulting permeability anisotropy, core appearance and location of the spot permeatry values, 3768.75 m, well 6405/7-1 T2, Ellida.

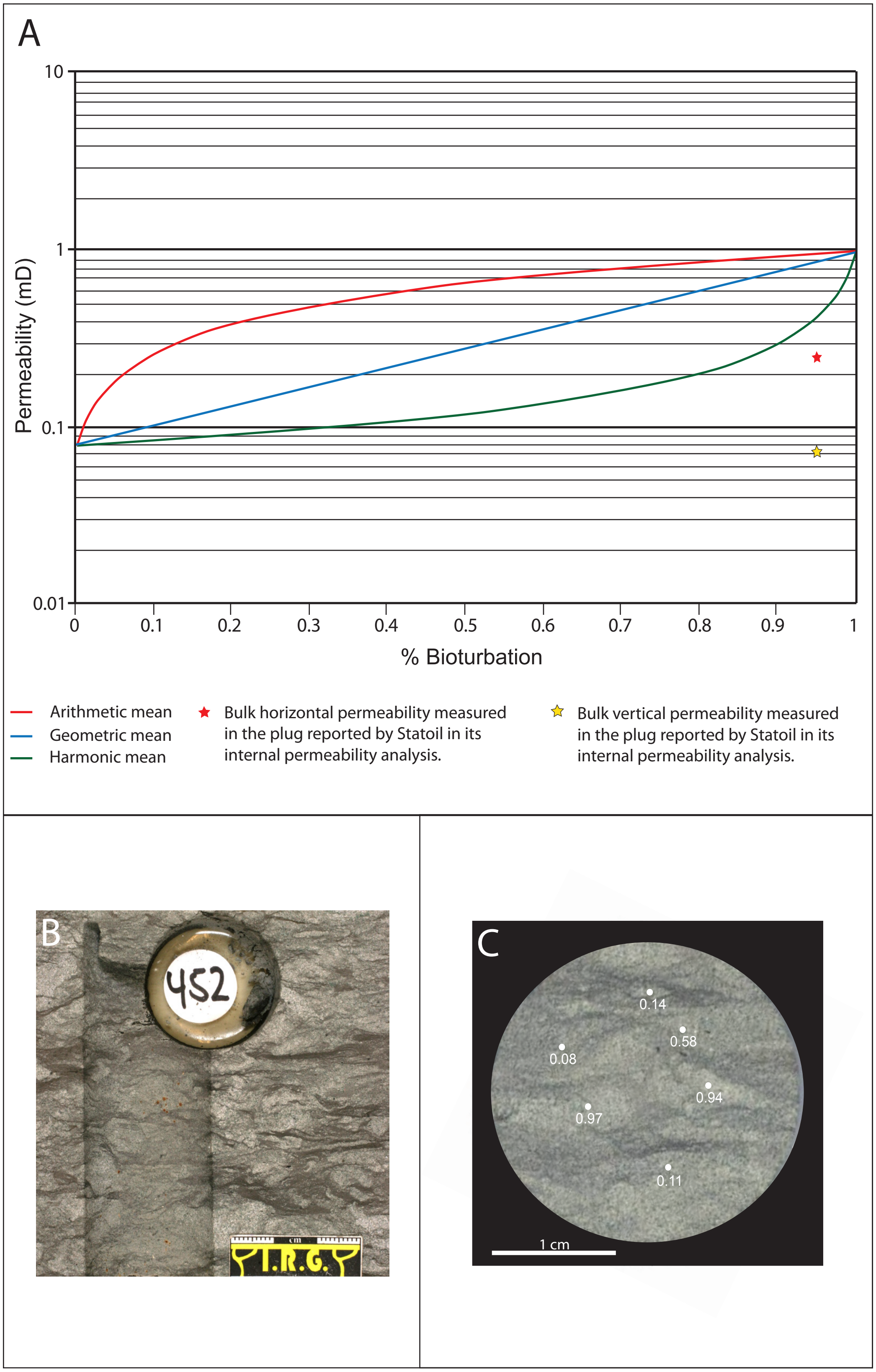

Figure 3.10. Facies F4-Plug 452 graph of the statistical relationship between textural heterogeneity and resulting permeability anisotropy, core appearance and location of the spot permeatry values, 3775.50 m, well 6405/7-1 T2, Ellida.

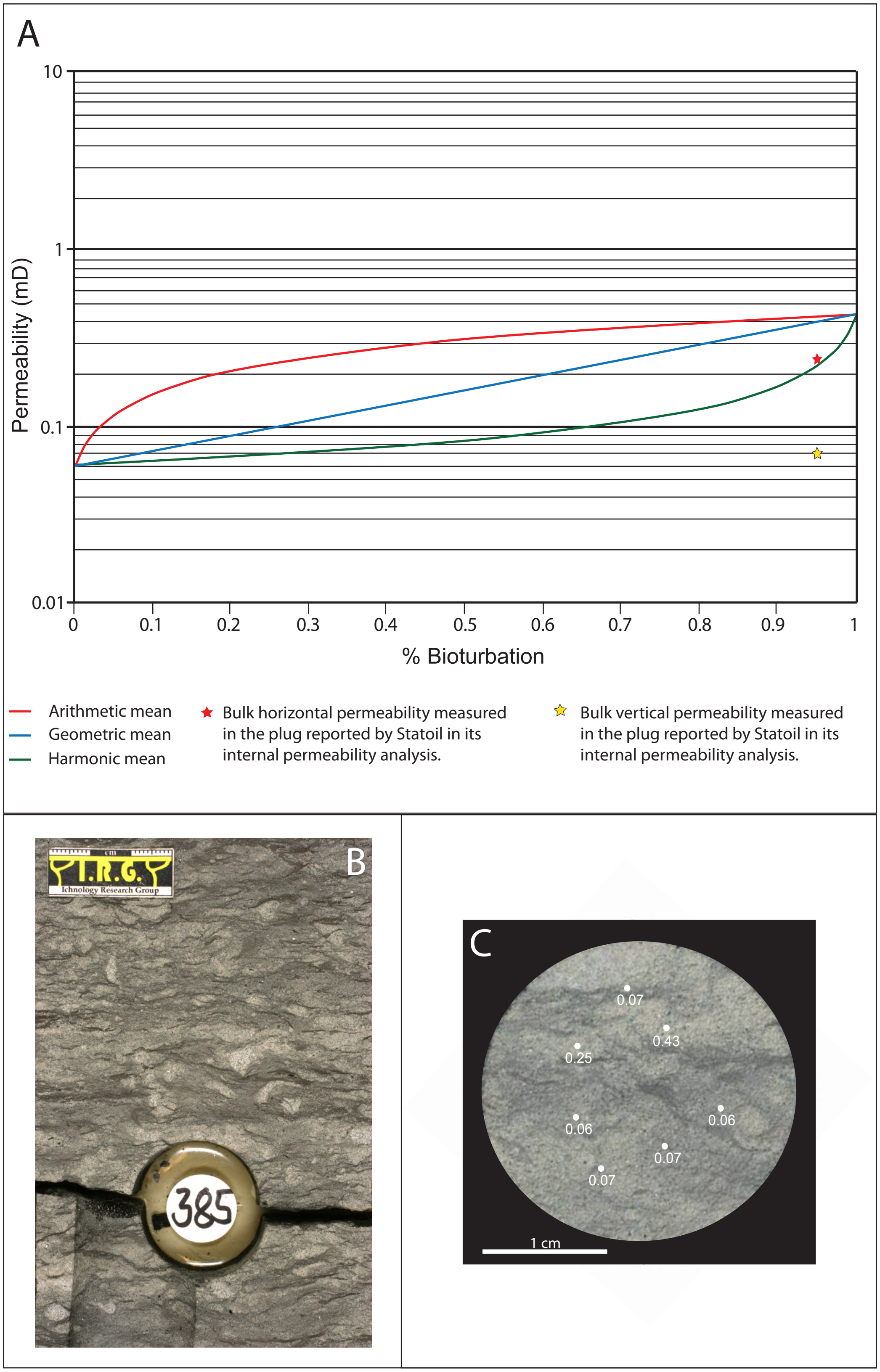

Figure 3.11. Facies F4-Plug 385 graph of the statistical relationship between textural heterogeneity and resulting permeability anisotropy, core appearance and location of the spot permeatry values, 3758.50 m, well 6405/7-1 T2, Ellida.

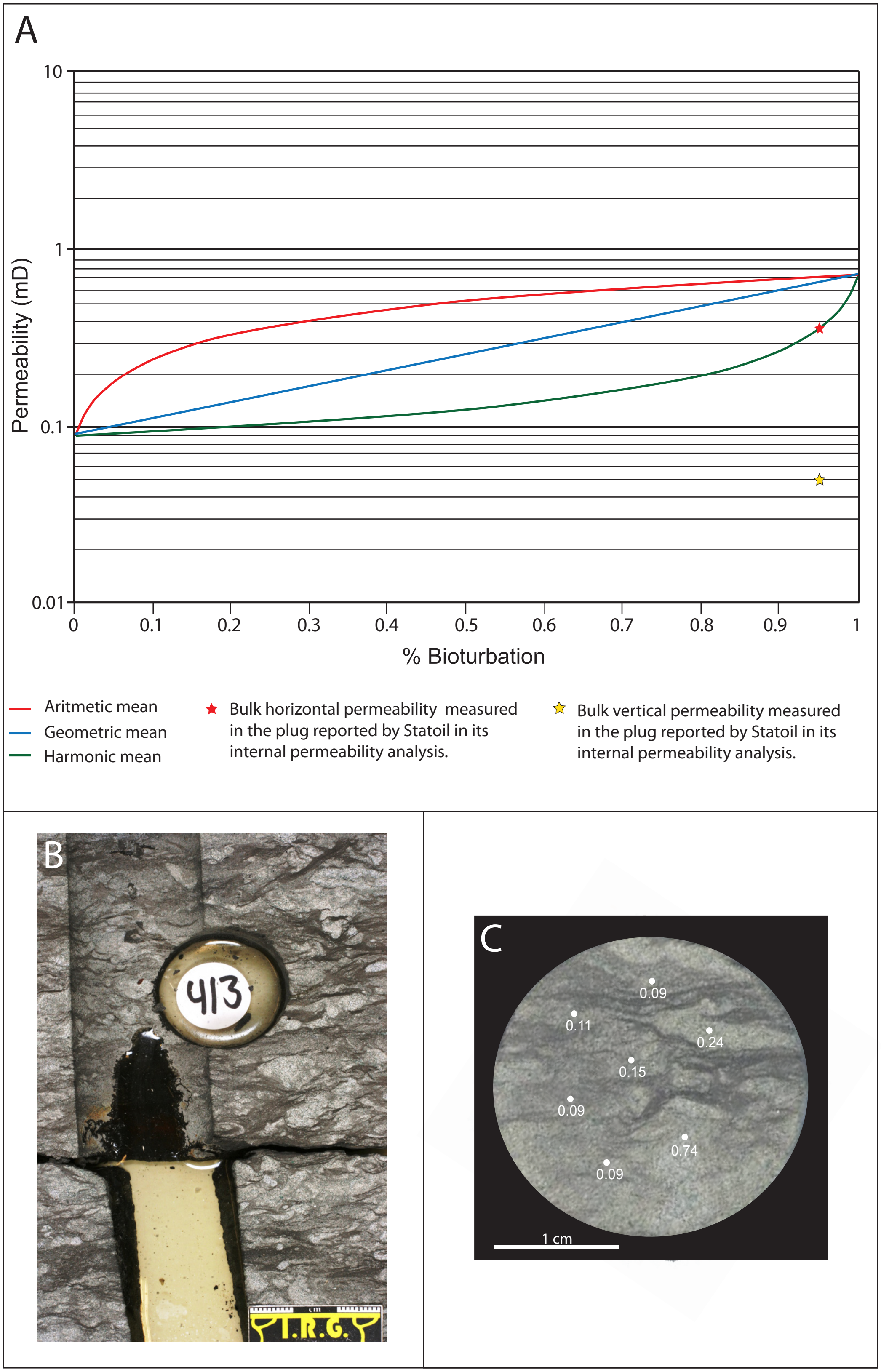

Figure 3.12. Facies F4-Plug 413 graph of the statistical relationship between textural heterogeneity and resulting permeability anisotropy, core appearance and location of the spot permeatry values, 3765.75 m, well 6405/7-1 T2, Ellida.

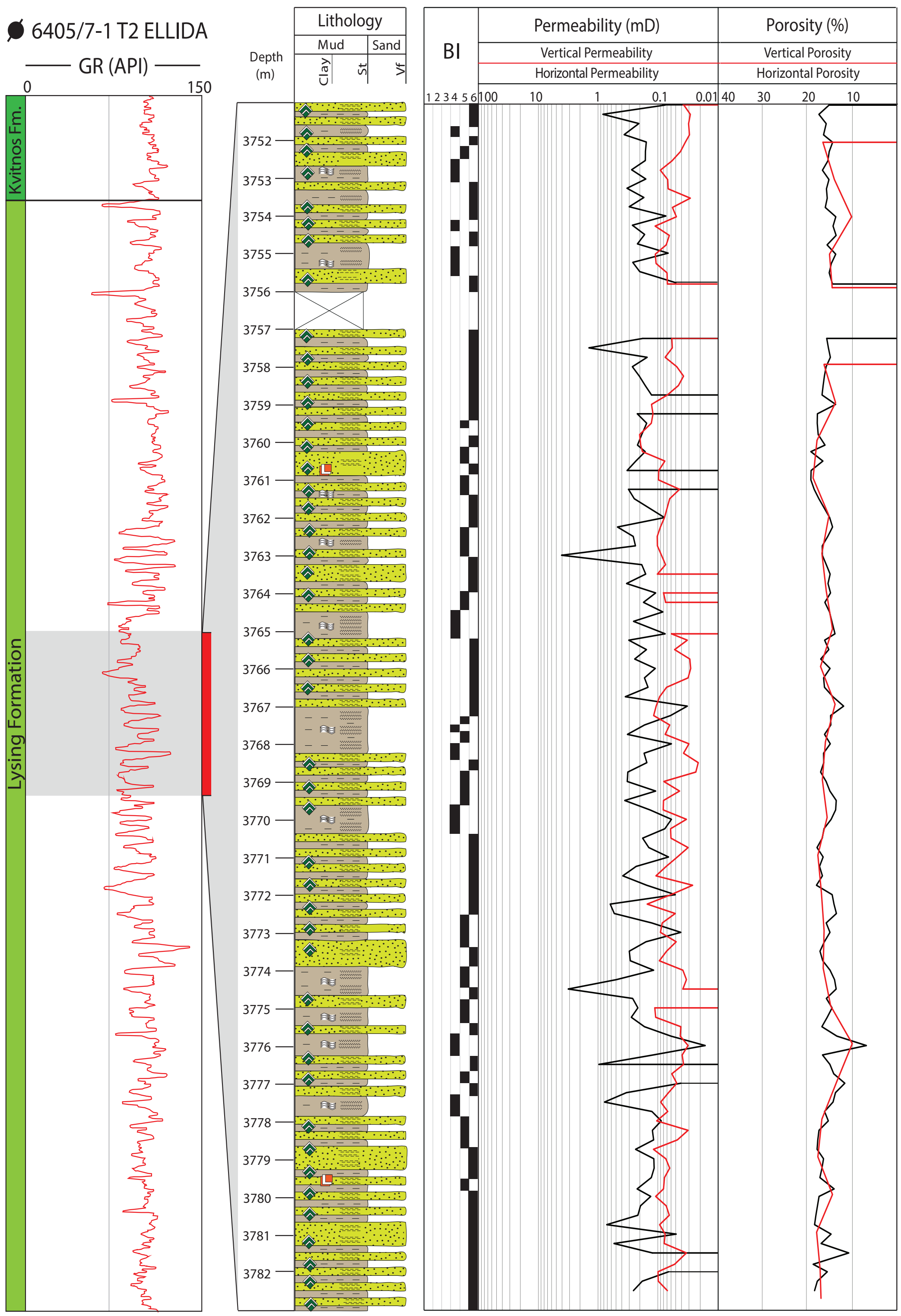

Figure 3.13. Core description showing the interpreted lithofacies, Bioturbation Index (BI) and the vertical variation of both the bulk horizontal k_h and vertical k_v permeability in well 6405/7-1 T2, Ellida field. Bulk horizontal and vertical permeability measurements carried out on core plugs reported by Statoil on its internal permeability report. This also allowed the comparison between the spot permeability measured in core plugs (presented in this chapter) obtained in a fabric selective manner (*i.e.*, Kburrow vs. Kmatrix) and Statoil's reported values for the same intervals.

X-Ray microtomography CT-scan and thin sections

The samples imaged for both the Lysing and Nise Formations exhibit similar characteristics and will be described without any particular subdivision. The three-dimensional 3D rendered volumes of X-ray micro-computed tomography data and X-ray micro-computed tomography images are presented in figures 3.14; 3.16 and 3.20. Each figure shows the micro-CT 3D volume next to the corresponding core photograph where the plug sample was extracted allowing better interpretation of any region of interest visualized in the model. The 3D volumes and rendered models are useful to illustrate, delineate, compare, and contrast X-ray attenuation (density) heterogeneities associated with burrowing and other porous and/or mineral features (Polo et al., 2010; Baniak et al., 2011; Lacroix et al., 2012; Gingras et al., 2012; Polo et al., 2012). Herein, X-ray micro-computed tomography is paired with petrography with the aim to visualize textural differences between burrows and matrix that induce density variations.

In the micro-CT analysis presented herein, low density was the proxy for higher porosity, which in turn was inferred to represent higher permeability (*e.g.*, Lacroix et al., 2010). This is consistent with the observations in the thin sections which show significant textural differences between burrow-fill and the surrounding matrix (Figure 3.15, 3.17 and 3.21). Petrographically, Facies-1 is a well-sorted, subangular to subrounded, mid- to upper fine-grained sandstone with textural selective burrowing (Figure 3.15). Whereas, Facies-2 is moderately well-sorted, locally poorly sorted, dominantly very fine-grained sandstone in which burrow-fill induce even more density contrast (Figure 3.17). The micro-CT rendered 3D volumes sections and high-resolution X-ray computed tomography scan images showed in figures 14, 16 and 20 illustrate some of the most important morphological features of the burrows.

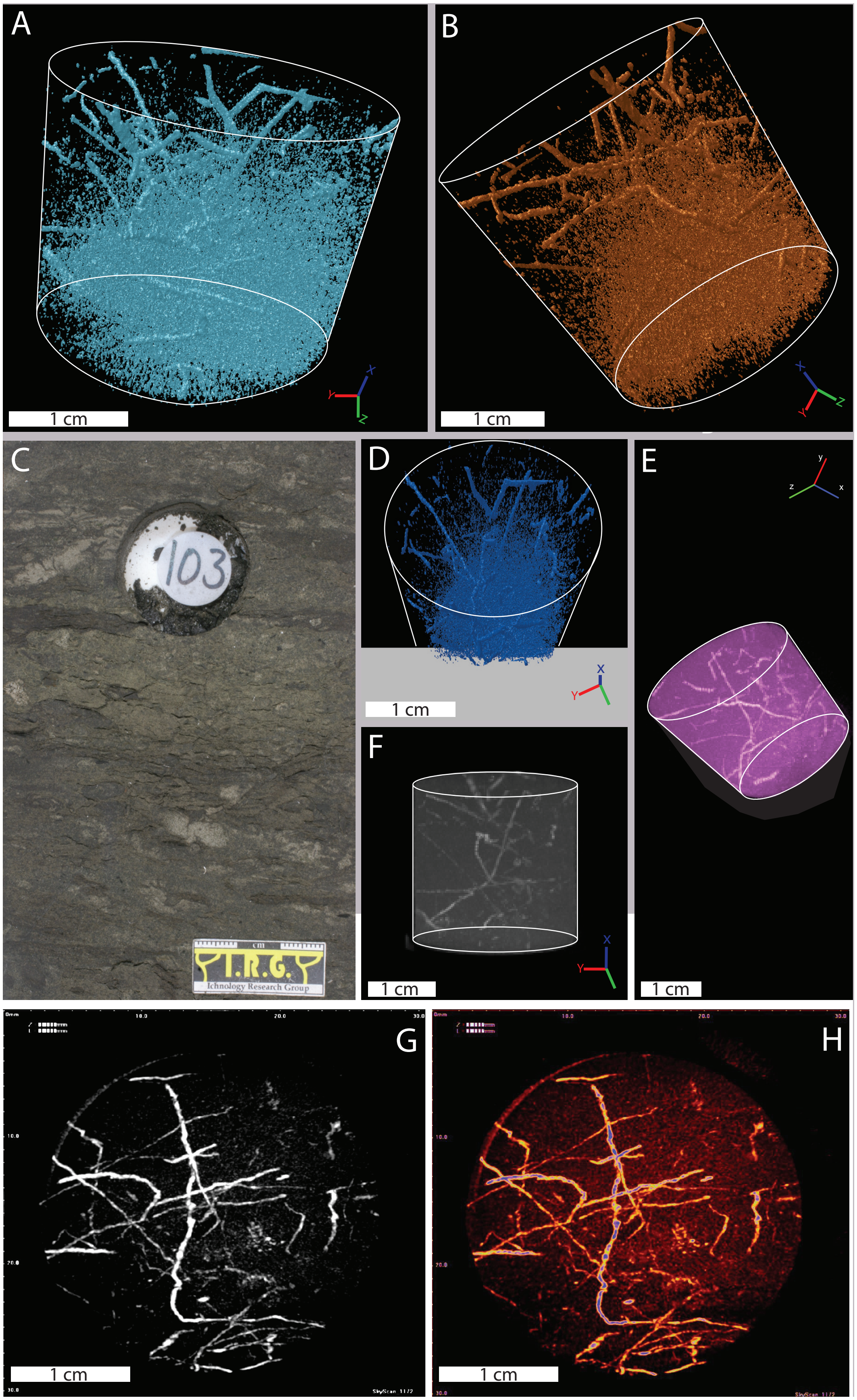
A
B
C
D
E
F
G
H
1 cm
103
I.R.G.
Ichnology Research Group

Figure 3.14. X-ray computed tomography scan images, micro-CT rendered 3D volumes and models and core picture of the Nise Formation, Facies F1-Burrowed muddy sandstone, Plug 103, 2799.5 m, well 6405/7-1 T2, Ellida Field. (**A**, **B**) False colour rendered 3D models of the plug that allows the identification of a highly contrasting density field interpreted as burrows an low constrasting density fileds interpreted as surrounding matrix. **C**) Core plug location on the suface of the slabbed core. Note the high bioturbation (BI = 6) in the interval that surrounds the location of the plug 103. Also, oil stain is a recurrent characteristic within intervals of F1. **D**) Oblique view of the plug 3D model cut by a plane allows identification of different levels of low and highly contrasting density zones. (**E**, **F**) False and greyscale colour rendered 3D models contructed by processing images of individual high-resolution X-Ray images. (**G**, **H**) High-resolution X-ray computed tomography scan images of greyscale and false colour of the top view of plug 103. The white and blue colours were assigned to the areas indicated as burrows and black was assigned to the rock matrix in G and H respectively.

Burrowing patterns throughout the samples can be seen as dominantly horizontally oriented traces (Figure 3.14G and 3.14H). The majority of the morphologies display sinuous and unbranched patters. However, some burrows exhibit branching features (figures 3.14A, 3.14H, 3.16A and 3.16D). The burrows are generally parallel to the bedding planes and commonly tilt upwards and downwards in complex and locally dense interpenetrations (Figure 3.14 and 3.16). Due to the complex nature of the burrow distributions (Häntzschel, 1975), assessments of burrow quantity and interconnectivity are difficult to establish. However, 3D volumes and models allowed the identification of highly contrasting density fields interpreted as burrow fills (*e.g., Thalassinoides, Planolites, Skolithos*) or burrow-linings (*e.g., Ophiomorpha, Paleophycos*). Due to intense bioturbation throughout the Lysing and Nise formations, biogenically-induced textural heterogeneities likely represent a highly interconnected burrow system with complex interactions. The majority of the imaged trace-fossils are straight to curved, and circular to elliptical in cross-section (Figure 3.14D). Diameter of burrows is constant along the burrow axis and ranges from less than 1 mm up to 4 mm. Smooth to irregularly shaped traces are common in the all the models and images. Discernable trace fossils are essencially cylindrical, predominantly horizontal and of variable diameter(Figure 3.14 and 3.16). Especific morphological features or external ornamentation were not identified.

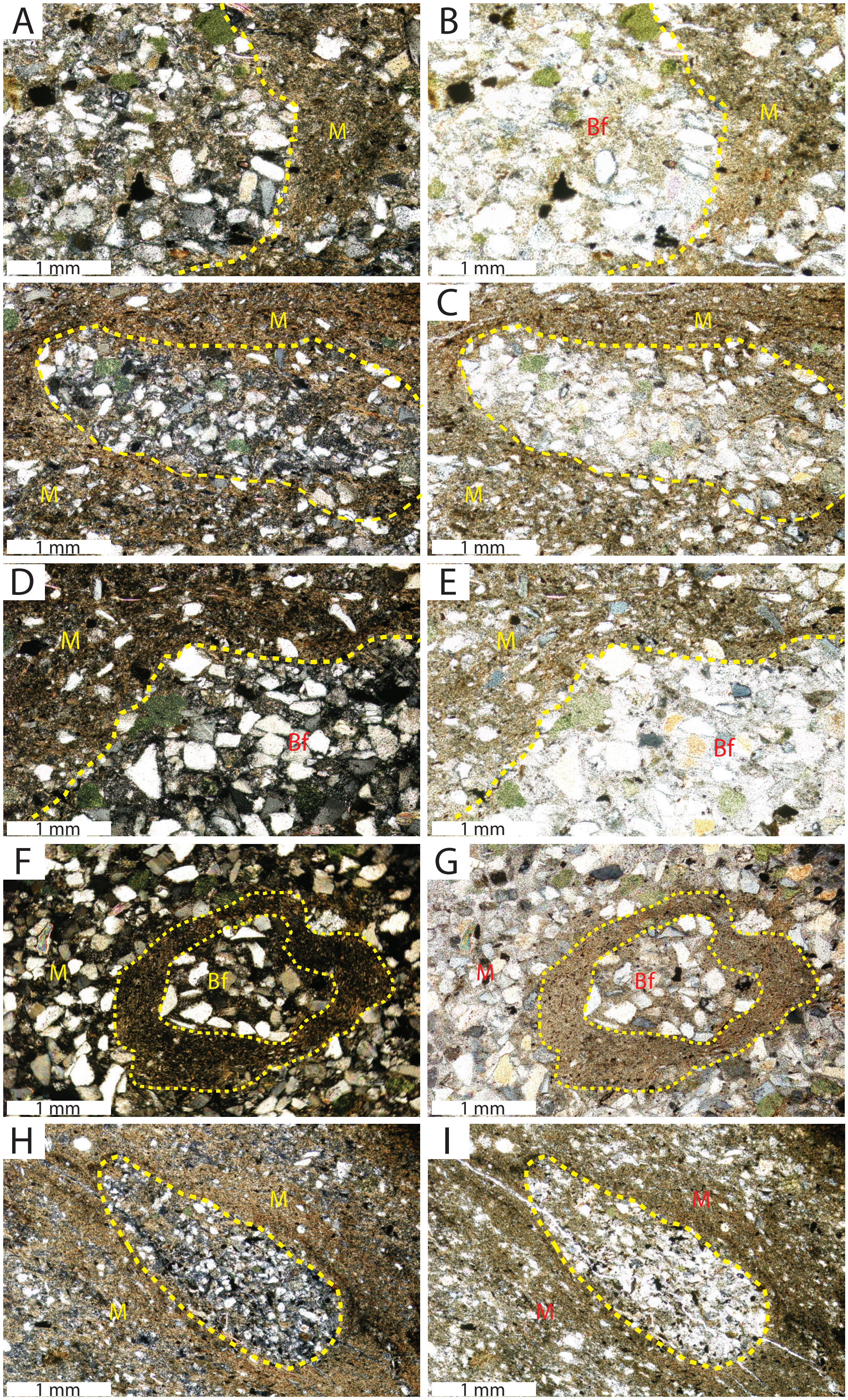

A
M
1 mm
B
Bf
M
1 mm
M
M
1 mm
C
M
M
1 mm
D
M
Bf
1 mm
E
M
Bf
1 mm
F
M
Bf
1 mm
G
M
Bf
1 mm
H
M
M
1 mm
I
M
M
1 mm

Figure 3.15. Thin sections photomicrographs of the Nise Formation Facies F1-Bioturbated shaly sandstone. Cross-polarized light (XPL) photos are displayed on the left column with its correspondent Plane-polarized light (PPL) on the right. (**A**, **B**) Well-sorted, subangular to subrounded, mid- to upper fine-grained sandstone that typifies F1. Yellow dashed line separates a burrow from the matrix (M). Glaucony (Green spots) and carbonaceous detritus (Black spots) characteristic of this facies are also seen in this photo. Plug 103, 2799.5 m, well 6405/7-1 T2, Ellida. (**C**, **D**) Highly-contrasting textural characteristics between burrow-fill and matrix (M) in a burrow most likely attributable to *Planolites*. Plug CB-119, 3033.5 m, well 6405/7-1 T2, Ellida. (**E**, **F**) Irregularly outlined burrow (Dashed yellow line) separated from the matrix with a characteristically textural different lining. The burrow is mostly filled with sediments essentially identical to surrounding sediments Plug CB-119, 3033.5 m, well 6405/7-1 T2, Ellida. (**G**, **H**) Lined burrow most likely attributable to *Paleophycos*. Within the photomicrograph the muddy lining can be distinguished from the burrow-fill and the matrix (M). This induces density contrasting fields as a result of the textural differences. Plug CB-119, 3033.5 m, well 6405/7-1 T2, Ellida. (**I**, **J**) Subrounded burrow with a clean-contrasting infill from the matrix (M). Plug 103, 2799.5 m, well 6405/7-1 T2, Ellida.

Burrow geometry and morphology does not allow for the identification of specific ichnogenera. Therefore, no taxonomical application is described in this study by using the high-resolution X-ray images and rendered 3D volumes presented in figures 3.14, 3.16 and 3.20, despite its potential. Alternatively, thin sections helped in identifying ichnogenera particularly those able to produce a strong density contrast that allowed better imaging (Figure 3.15; 3.17 and 3.21).

Despite the moderate bioturbation (BI = 3) that characterizes plug 28, Facies F2 and the surrounding zone, a contrasting burrow network can be discerned from the surrounding matrix, primary as a result of the differential burrow-fill (Figure 3.16). The images of plug 48 pertaining to Facies F3 display horizontal contrasting density features mostly associated to the pinstripe lamination of silt/very fine sandstone (Figure 3.17 and 3.19). In general, the micro-CT rendered volumes illustrate that the bulk of density-associated heterogeneity is mostly horizontal (roughly parallel to bedding) dominated by traces interpreted more likely as *Thalassinoides, Planolites, Ophiomorpha* and *Paleophycus*. Less commonly inclined to vertical burrows (*e.g.*, *Skolithos, Arenicolites*) are also common throughout the studied core interval (Facies 1 and Facies 2).

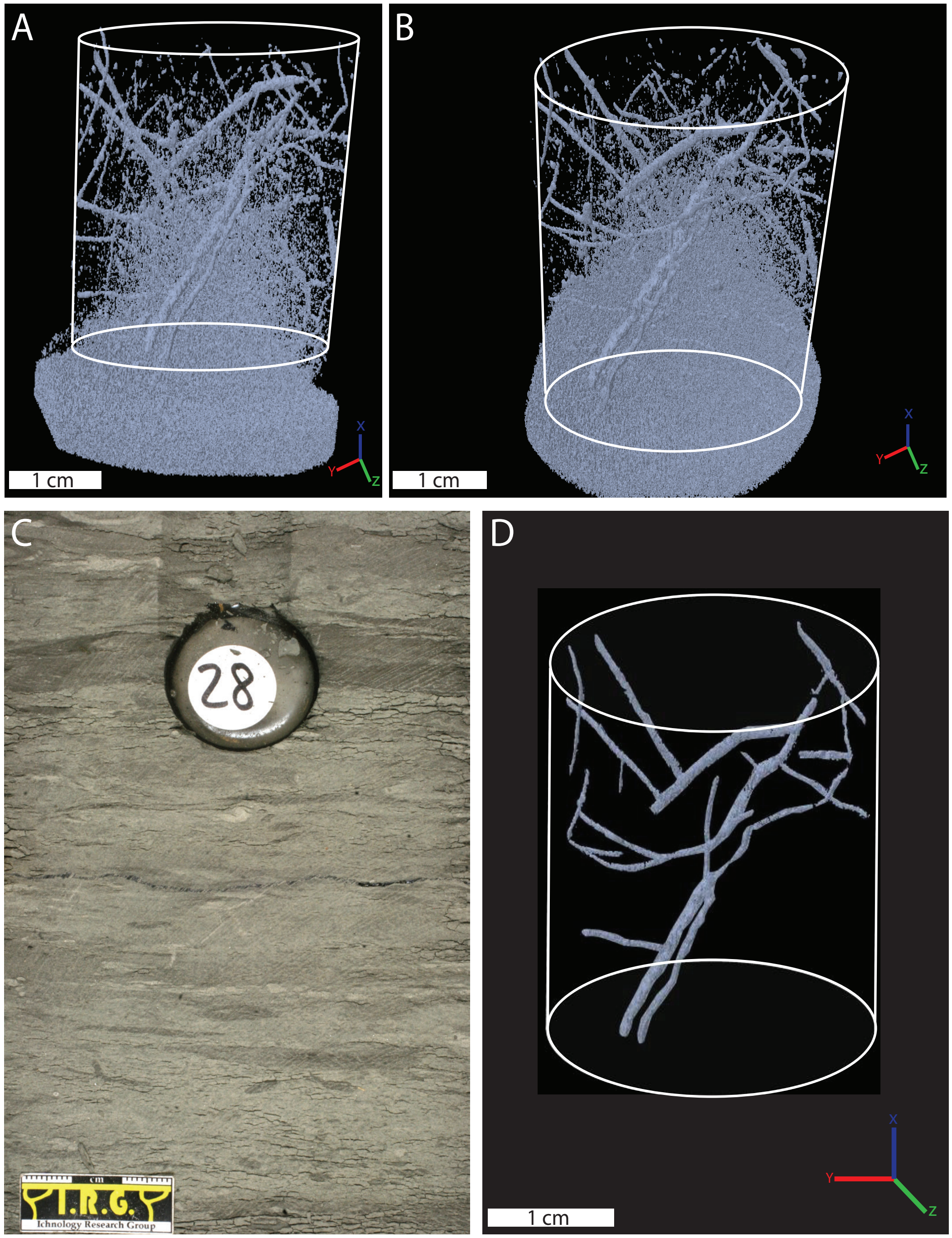

Figure 3.16. Micro-CT rendered 3D volumes and models of the Nise Formation, Facies-2 Burrowed muddy to silty sandstone, plug 28, 3010.7 m, Midnatsoll Field, well 6405/ 10-1. **A**) Lateral and (**B**) oblique false colour 3D models of the plug allow differentiation between high contrast density fields interpreted as burrows and low contrasting density fields interpreted as surrounding matrix. **C**) location of plug 28 and its corresponding photo of the slabbed core surface. Note the moderate bioturbation (BI = 3) in the zone that surrounds the location of plug 103. Like seen in F2-Burrowed muddy sandstone segments, oil stain is a recurrent characteristic within intervals of F2. **D**) Oblique view of plug 28 3D model modified in Adobe Illustrator® to clean out the surrounding particles interpreted as high density spots within the matrix and outside the burrows. Thus allowing a better display of the density and interconnectivity of the burrow network.

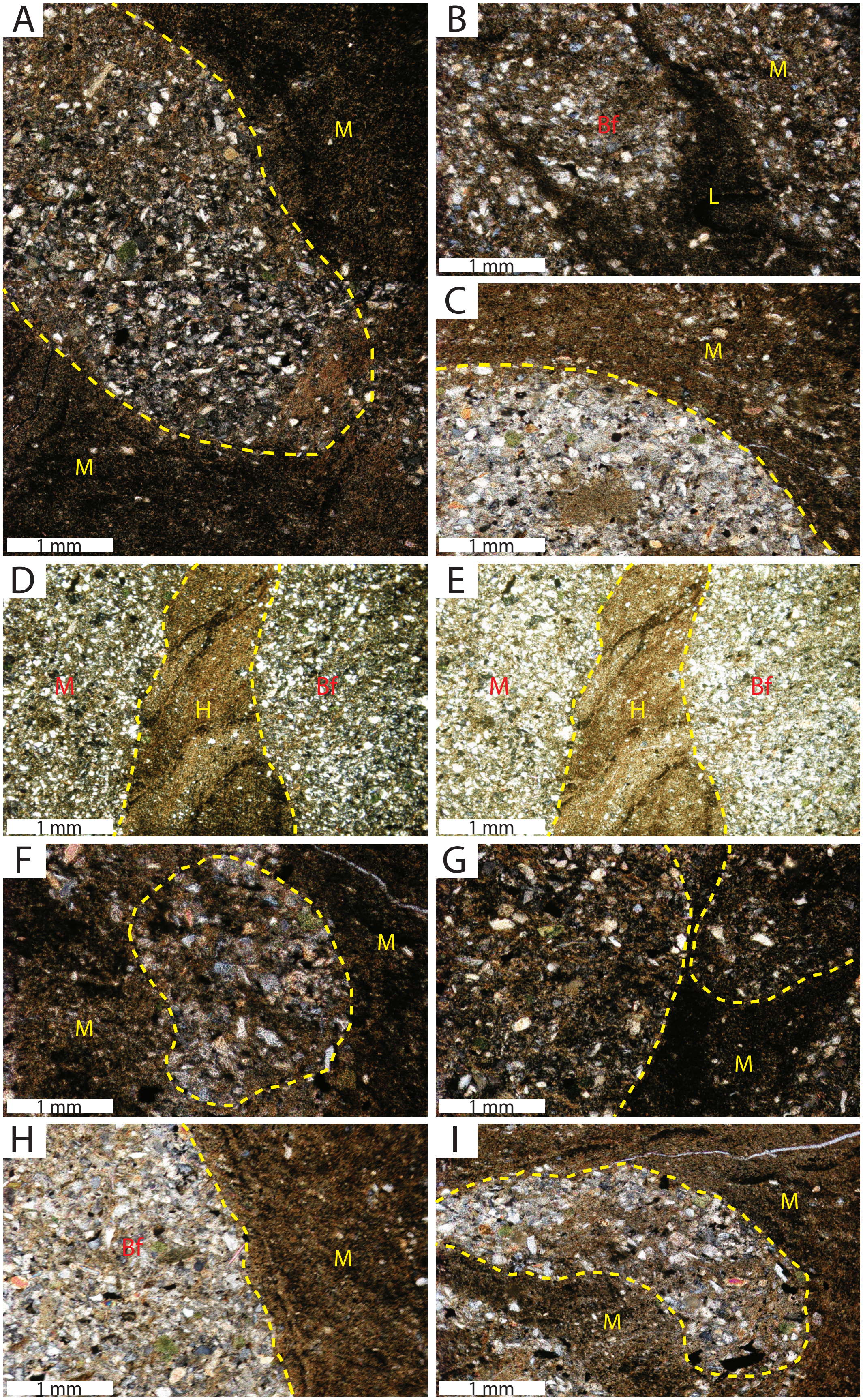
A
M
M
1 mm
B
M
Bf
L
1 mm
C
M
1 mm
D
M
H
Bf
1 mm
E
M
H
Bf
1 mm
F
M
M
1 mm
G
M
1 mm
H
Bf
M
1 mm
I
M
M
1 mm

Figure 3.17. Thin sections photomicrographs of the Nise Formation Facies F2-Bioturbated muddy to silty sandstone. All the photos are taken under cross-polarized light (XPL) with the exception of E. **A**) Cross-polarized light (XPL) photomicromosaic showing a well differentiated burrow attributable to *Planolites* within a muddy matrix. Note the textural difference between burrow-fill and surrounding matrix, plug L-78, 2793.1 m, well 6405/7-1 T2, Ellida. **B**) Cross-polarized light (XPL) distinctive mud lining of *Palaeophycos* (L) that allows differentiation between matrix (M) and burrow-fill (Bf), plug L-78, 2793.1 m, well 6405/7-1 T2, Ellida. **C**) Highly contrasting textural characteristics between burrow-fill and matrix (M) in a burrow most likely attributable to *Planolites* with overprinting of a smaller burrow in the center, plug L-78, 2793.1 m, well 6405/7-1 T2, Ellida. (**D**, **E**) Cross-polarized light and its correspondent plane polarized light photomicrograph of *Ophiomorpha* lining (H). Burrow-fill (Bf) and matrix (M) can be very well differentiated as a sharp boundary separated by the lining in the center plug L-240, 2837.8 m, well 6405/7-1 T2, Ellida, plug L-240, 2793.1 m, well 6405/7-1 T2, Ellida. **F**) Dashed yellow lines differentiate clean sand *Planolites* from the surrounding matrix (M). Dashed red line denotes interactions between two burrows more likely as the result of deep-tiering, plug L-78, 2793.1 m, well 6405/7-1 T2, Ellida. **G**) Close up view of burrows most likely attributable to *Planolites* and *Thalassinoides* burrow-fills. The size of the burrows are roughly the same as those found in the X-ray computed tomography scan images and micro-CT rendered 3D volumes displayed in figure 3.16, plug L-78, 2793.1 m, well 6405/7-1 T2, Ellida. **H**) Sharp contact between burrow-fill (Bf) and matrix (M) that typifies deposits that behave as a dual permeability media, plug L-240, 2793.1 m, well 6405/7-1 T2, Ellida. **I**) Subrounded burrow with a contrasting infill from the matrix (M), plug L-78, 2793.1 m, well 6405/7-1 T2, Ellida.

Within the models, true branching of burrows can easily be confused with the crosscutting and interpenetrations. Consequently, evidence to truly distinguish branching from crosscutting of burrows and its complex interpenetrations may be enigmatic, and in some cases may not be discernible (*e.g.*, Keighley and Pickerill, 1995). Three-dimensional (3D) rendered volumes of X-ray micro-computed tomography data and X-ray micro-computed tomography serial images presented in Figures 3.14, 3.16 and 3.20 support these observations. This shows that in three-dimensional space, most traces (or other density heterogeneity) occur as a mix of planar, inclined and vertical entities (Figure 3.14, 3.16 and 3.20).

The X-ray computed tomography scan images and micro-CT rendered 3D volumes of the Lysing Formation show affinities with the ones obtained for the Nise Formation Facies 1 and Facies 2. The exposed inchnofabric displays preferentially horizontal complex spatial distributions resulting in an intricate, interconnected burrow-system (Figure 3.18).

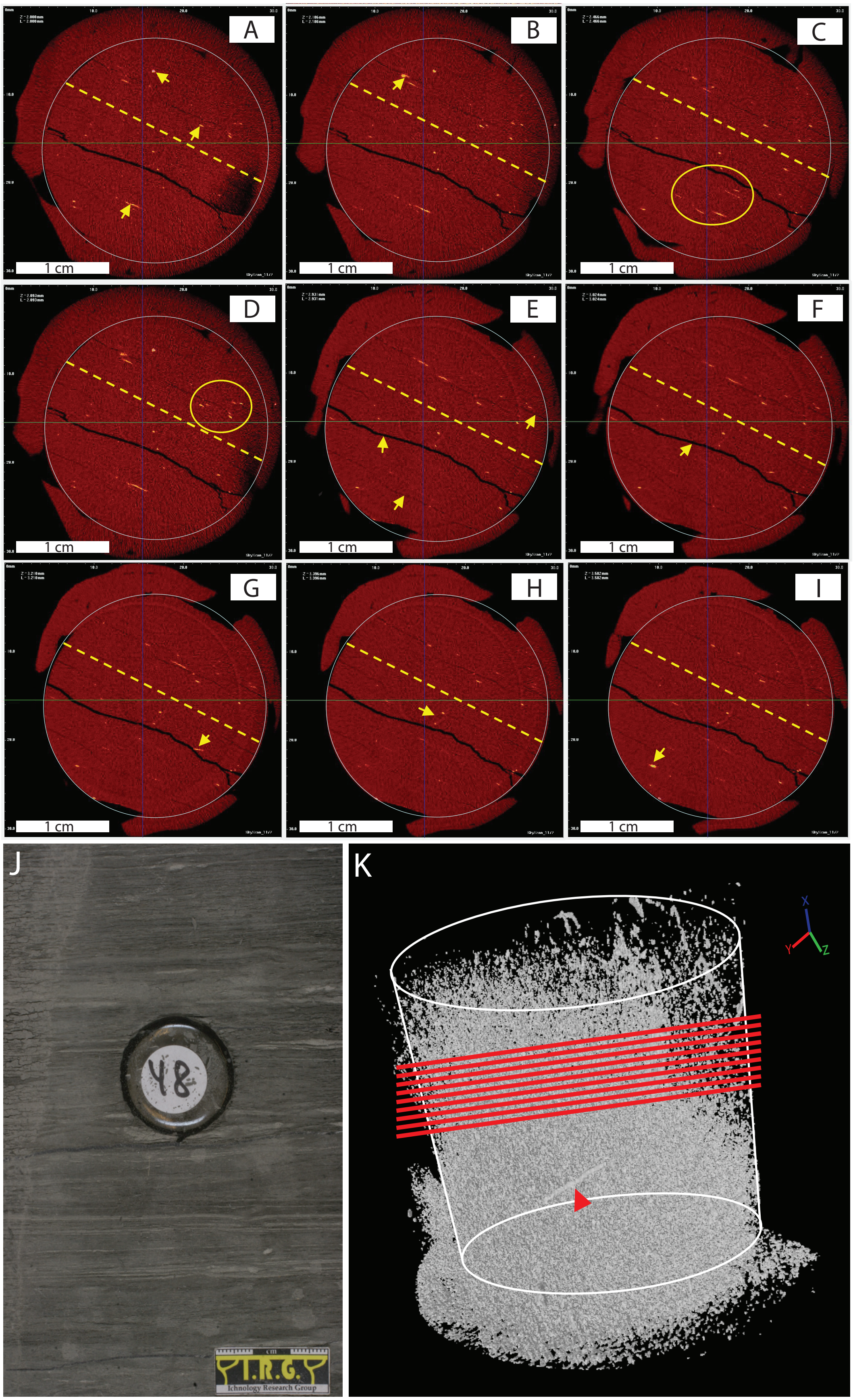
A
B
C
D
E
F
G
H
I
1 cm
J
K
48
I.R.G.
Ichnology Research Group
X
Y
Z

Figure 3.18. High-resolution X-ray computed tomography scan images through plug and Micro-CT rendered 3D volume of the Nise Formation, Facies-3 with the corresponding core photo and vertical X-ray image for comparison, plug 48, 3015.7, well 6405/ 10-1, Midnatsoll Field. Frames **A** to **I** are arranged from the top to the bottom of the sample. Red-brownish colours represent the lower densities, whereas yellow is used to show the higher end of the density values. Overall, the equally-spaced sections show the pinstripe lamination of silt/very fine sandstone (Figures **D**, **E** and **G**) and most likely the associated Planolites burrows (Figures **A** and **B**). **J**) Core plug location on the suface of the slabbed core. Note the low to localized bioturbation (BI = 1) that characterizes the segments of Facies-3. **K**) micro-CT rendered 3D volume of plug 48 showing an overall very low contrasting density fields. However, the red arrow shows a horizontal feature that could be interpreted as either a burrow or a segment of the pinstripe lamination of silt/very fine sandstone.

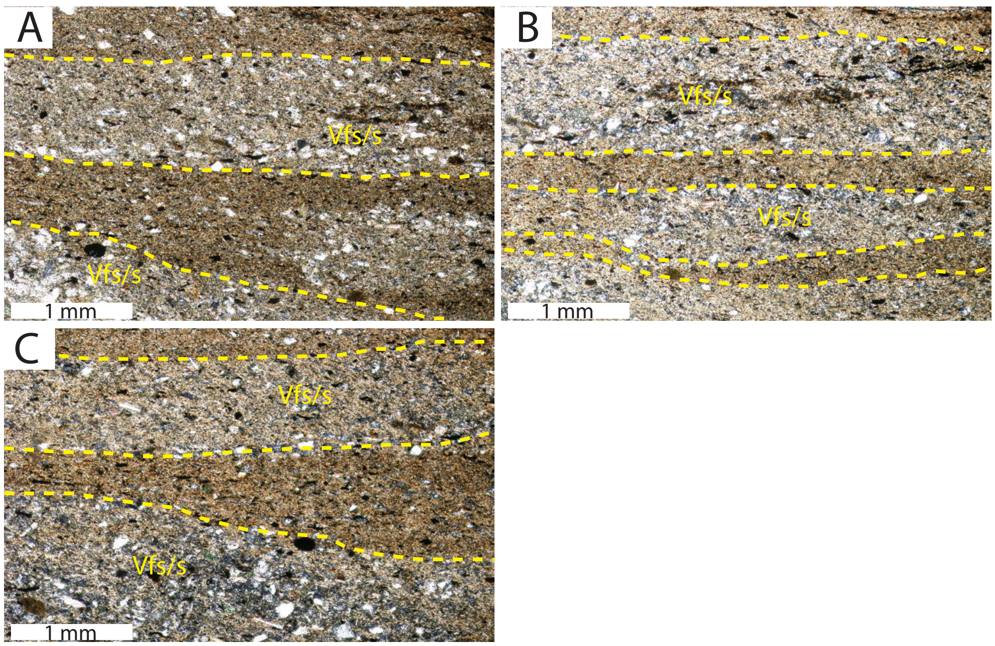

Figure 3.19. Thin sections photomicrographs of the Nise Formation Facies F3-Laminated mudstone; plug 331, 2860 m, well 6405/7-1 T2, Ellida. All the pictures were taken under cross-polarized light XPL. **A**) Planar-parallel lamination that typifies F3. Note the recurrency of thin laminae (1 mm in average) of very fine sand/silt (Vfs/s) and dark mudstone that provides the pinstripe lamination in this facies. **B**) Thinner laminae (1 mm in average) of very fine sand/silt (Vfs/s) and dark mudstone, more likely indicative of an overall quiet depositional environment that deprived of major lithological contrast. **C**) Coarser-grained laminae alternating with a mudstone laminae and finer grained laminae of very fine sand/silt (Vfs/s). This a peculiar case that provides a relatively major lithological contrast allowing a better recognition due to increased density contrast.

The identified trace fossils in Facies-4 are dominated by horizontal burrows. Burrows are sharp-walled and can be found inclined and horizontal (Figure 3.20), rarely branching. Locally, the branching is dendritic, but generally indeterminable. Burrow length ranges from less than 1 cm to 2 cm and the diameters range from 1 mm to 5 mm (Figure 3.20). Despite the higher mud content of Facies-4, that provides major lithological contrast, it is of particular interest that the identified burrows (Figure 3.20) share roughly the same size and characteristics of the ones described for Facies 1 and 2 of the Nise Formation (Figure 3.14 and 3.16).

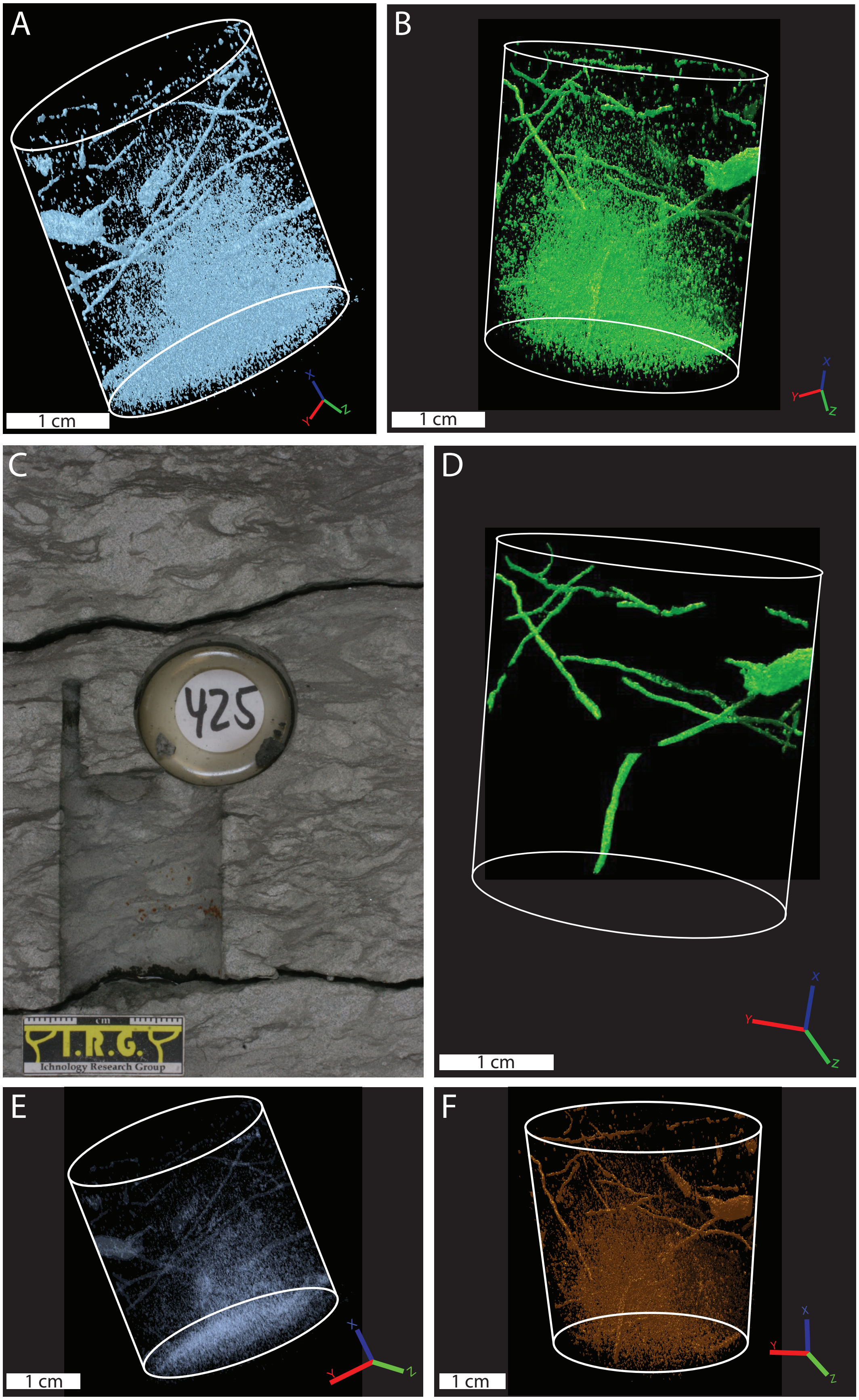
A
1 cm
B
1 cm
C
425
cm
I.R.G.
Ichnology Research Group
D
1 cm
E
1 cm
F
1 cm

Figure 3.20. X-ray computed tomography scan images and micro-CT rendered 3D volumes and models of the Lysing Formation Facies F4 Plug 425, 3768.7 m, well 6405/7-1 T2, Ellida Field. (**A**, **B**) and (**F**) false colour 3D rendered volumes of the plug allowing the identification of a highly contrasting density field interpreted as burrows and low contrasting density fields interpreted as the surrounding matrix. **C**) core plug location on the suface of the slabbed core. Note the completely disrupted fabric (BI = 6) in the interval that surrounds the location of plug 103. **D**) inclined view of the plug rendered 3D model modified in Adobe Illustrator® to isolate the burrows (i.e., high density contrast) and the surrounding particles (i.e., low density contrast) interpreted as the surrounding matrix. Thus proffering a better display of the heterogeneity and interconnectivity of the burrow system. **E**) false colour high-resolution X-ray computed tomography scan 3D volume of plug 42.

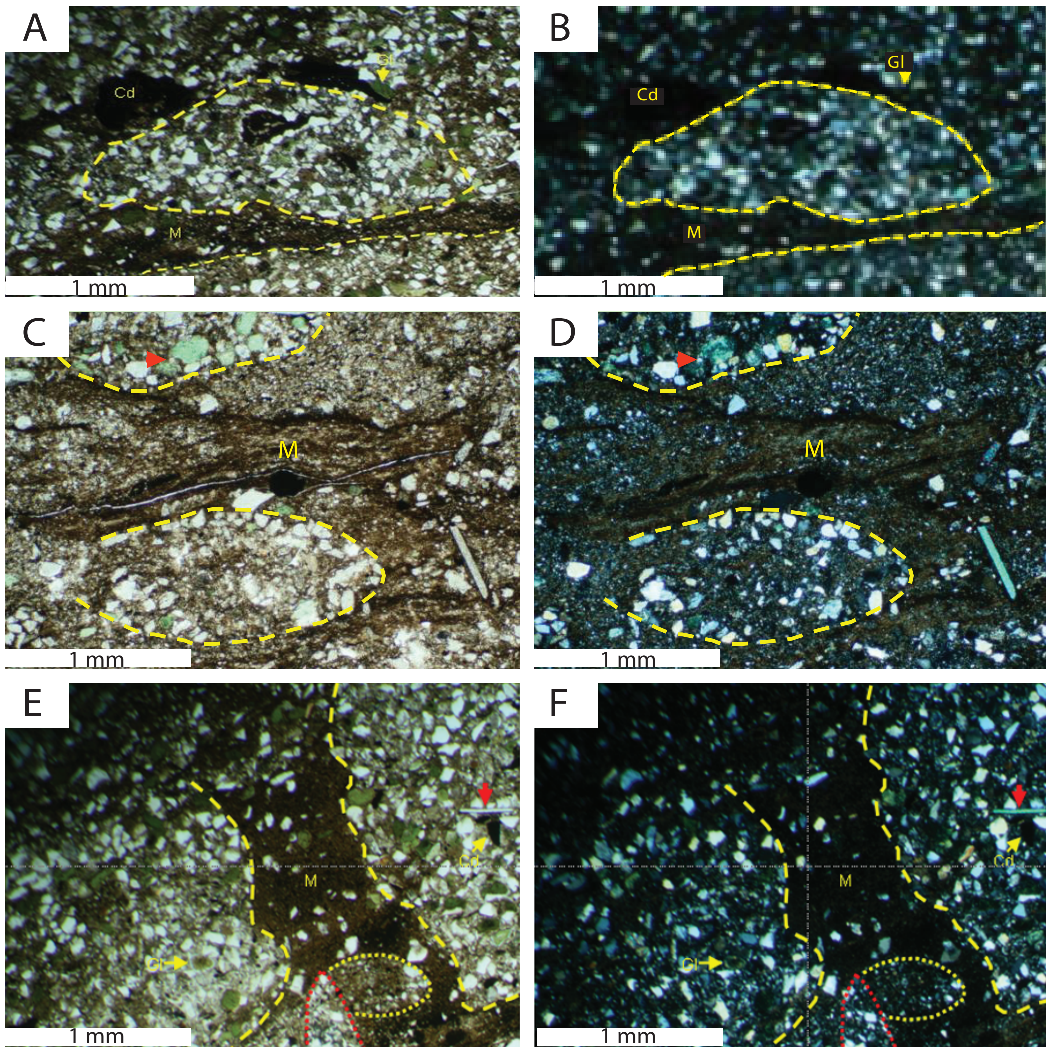

Figure 3.21. Thin section photomicrographs of the plugs samples of the Lysing Formation Facies F4. Plane-polarized light PPL and its correspondent cross-polarized light XPL photomicrographs are displayed in the left and right side of the photo mosaic respectively. All the thin sections are impregnated with blue epoxy. (**A**, **B**) coal detritus (Cd) characteristics of the Facies 1 segments, greenish sub-rounded features represent glaucony, off-white colours are quartz grains, and dark colours are organic matter, clay minerals, or siderite. (**C**, **D**) reveals a well differentiated burrow from the surrounding matrix (M) most likely attributable to *Planolites* with overprinting of a smaller burrow in the center. (**E**, **F**) Dashed yellow lines differentiate clean sand *Planolites* close up view of burrows most likely attributable to *Planolites* and *Thalassinoides*. Dashed red line also denotes interactions between two burrows probably as the result of deep-tiering. The sizes of the burrows are roughly the same as those found in the X-ray computed tomography scan images and micro-CT rendered 3D volumes displayed in figure 3.20.

DISCUSSION

Spot-permeametry

Graphs and statistical relationships between textural heterogeneity and resulting permeability anisotropy

Within the Lysing and Nise formations, fabric selective spot permeability shows that higher values are associated with the burrows as opposed to the matrix. Overall, the reservoir can be classified as a tight reservoir with higher permeability values associated to burrow-fills. These reservoirs commonly express themselves as dual-permeability systems in which the magnitude of difference between trace-fossils and matrix permeability is greater than 2 (figures 3.2 to 3.5 and 3.8 to 3.12) (Gingras et al., 2012). A recent research body documents similar fluid flow behavior in biogenically enhanced reservoirs (*e.g.*, Tonkin et al., 2010; Baniak et al., 2011; Lacroix et al., 2012). Tonkin et al., (2010) found that bioturbation can either reduce permeability and porosity by as much as approximately 33% or enhance it by up to 600%, dependent on burrow type and behavior of the trace-making organism.

Bulk assessments of permeability based on core-plug data indicate that the harmonic mean of matrix versus burrow permeabilities provides the most accurate estimate of bulk permeability in the studied samples of the Lysing Formation as well as the Facies 2 of the Nise Formation, whereas Facies 1 is better represented by the arithmetic mean. The harmonic relationship suggests that flow is largely directed across lower permeability matrix via the a not very well connected burrow network (*i.e.*, burrow to burrow) (Lacroix et al., 2012; Gingras et al., 2012). This is mostly driven by a trace fossil suite in which *Thalassinoides* and *Planolites* are very common and are interpreted herein to contribute significantly to reservoir quality. The arithmetic relationship of Facies 1 suggest a well-connected horizontal flow network for delivery of fluid similarly to the documented by Lacroix et al., (2010) and Gingras et al., (2012). By simulation experiments, La Croix et al., (2012), demonstrated that that burrow connections begin to form a 3D system at bioturbation intensities as low as 10% (BI-2). Also, their study showed that connectivity is enhanced with increasing burrowing intensity as seen in the Facies 1 samples.

Biogenic enhancement of permeability in bioturbated media has also been documented from muddy sandstone facies with clean sand-filled burrows (*e.g.*, *Thalassinoides*, *Planolites*) and clean sandstones with burrow-mottled or diffuse to massive textures (*e.g.*, Tonkin et al., 2010; Baniak et al., 2011; Gordon et al., 2011; Lemiski, 2011; Lacroix et al., 2012; Gingras et al., 2012). Biogenic reworking (*i.e.*, mixing, packing and sorting) of quartz grains has been documented to alter reservoir petrophysics through removal of silt-clay-size material from pore spaces creating macro-pore fluid networks (Spila et al., 2005; Pemberton et al., 2005; Tonkin et al., 2010; Gingras et al., 2012).

Anisotropy - variability of horizontal (k_h) vs. vertical permeability (k_v)

Within the Lysing and Nise formations, biogenic textural modifications induce differential permeability. Statoil's permeability measurements demonstrate that k_h is higher than k_v (Figure 3.2 to 3.5 and 3.8 to 3.12) and that permeability is anisotropic. Spot permeability measurements suggest that variability between k_h and k_v is controlled by the interconnectivity of a preponderant horizontal burrow network (Figure 3.6, 3. 7 and 3.13). As with most other biogenic flow media the resulting flow network is an overall intricate, locally interconnected horizontal and vertical burrow system where major interconnectivity in horizontal burrows results in higher k_h values. Alternatively, variation between k_h and k_v may be related to the small (2.54 cm = 1 inch) scale of permeability measurement on the core plug. This suggest that in order to characterize anisotropic flow media such the one presented in this thesis, core plugs may not provide a representative elemental volume (REV) (Freeze and Cherry, 1979; Gingras et al., 2012).

For both, the Lysing and Nise formations, horizontal permeability shows higher values than vertical permeability (Figure 3.6; 3.7 and 3.13), suggesting connectivity across a dominat horizontal trace-fossil suite (*e.g.*, *Thalassionoides*, *Planolites*) rather than vertical traces (*e.g.*, *Skolithos*, *Arenicolites* or vertical *Ophiomorpha*). Due to the complex, 3D nature of trace fossils (Häntzschel 1975), as seen in 3D volumes of the Lysing and Nise formations (Figure 3.14, 3.16 and 3.20), burrows systems possess at least a minimum vertical component. Therefore, changes in burrow abundance have an effect on both the bulk k_h and k_v in the Lysing and Nise Formation case.

Within the Nise Formation, higher permeability values are associated to highly bioturbated intervals (BI = 5 – 6) (Figure 3.6 and 3.7). In contrast, the Lysing Formation shows a more uniform (BI = 5 – 6) bioturbated fabric making difficult to establish any relationship between segments with low and high bioturbation index (BI) (Figure 3.13). Permeability modifications seem to be higher than porosity modifications in both formations. This is seen as permeability values that differ up to two orders of magnitude between k_h and k_v, whereas porosity values show just a slightly variation (Figures 3.6, 3.7 and 3.13). Consequently, no conclusive evidence of the relationship between porosity variation and bioturbation can be discerned from the studied dataset.

Thin sections reveal that the main pore type is intergranular porosity mostly influenced by grain-size sorting associated with biogenic reworking (Figure 3.15; 3.17 and 3.21). Petrography also shows that the *Thalassinoides* burrow-fill is commonly of a larger grain size compared to the surrounding matrix (Figure 3.15; 3.17 and 3.21). Sand-filled *Thalassinoides* create mostly horizontal and oblique networks able to deliver hydrocarbons within the Lysing and Nise formations reservoir. Burrows most likely attributable to *Paleophycus* (Figure 3.15G and 3.15H) and *Ophiomorpha* (Figure 3.17D and 3.17E) show a distinctive lining that provides lithological differences thus proffering contrasting density. Overall, the microphotographs show well differentiated burrows from the surrounding medium. The burrow-fill is texturally and mineralogy different from the hosted sediment. Consequently, petrophysical properties between trace-fossils and matrix vary significantly (Figure 3.2 to 3.5 and 3.8 to 3.12). This provides the bioturbated strata of the Lysing and Nise formation with highly contrasting permeability fields. This is more evident in sediments pertaining to Facies 2 bioturbated muddy to silty sandstone (Figure 3.17). Therein, major lithological variation provides higher textural and mineral contrast between matrix and trace-fossils (Figure 3.17). Although Facies 1 does not possess the same lithological variation of Facies 2 due to lower mud content, burrow can be well differentiated from the matrix due to textural variations (Figure 3.15).

Petrographic assessments also show that porosity is strongly influenced by the location and nature of bioturbation (Figure 3.15, 3.17 and 3.21). This occurs in two ways: 1) as re-oriented and homogenized fabrics in highly bioturbated media and, 2) through the imposition of coarser grained sediment in tunnels and shafts in otherwise fine-grained strata (Figure 3.16). Petrographic evidence of similar type of modifications has been reported for the Cretaceous Bluesky Formation. Gordon et al., (2010), documented biogenic alterations of reservoir flow and storage as a result of a local increment of the petrophysical properties (*i.e.*, porosity and permeability) in samples heavily bioturbated with *Macaronichnus* segregatus.

X-ray computed microtomography (micro-CT)

The two dimensional (2D) X-ray computed tomography scan images and three dimensional (3D) rendered models show evidence of high bioturbation levels (BI = 3 – 6) that are common throughout the studied interval of the Lysing and Nise formations. They also clearly show the internal heterogeneity present in these formations (Figure 3.14, 3.16 and 3.20). Bright spots in the images and models that are related to higher porosity as identified in thin sections are consistently associated with trace-fossils. However, diagenetic cements that also induce textural heterogeneities may be present in and around ichnofossils.

Burrow geometry and contrasting density allowed 3D visualization and the differentiation between the burrow complex and the surrounding matrix. In modern settings, grazing and dwelling structures including shafts, tunnels and galleries can be found forming complex 3D subaerial and subaqueous burrow-systems (Gingras et al., 1999) like the ones seen in the rendered 3D models. Traces of many modern species of bioturbating infauna (*e.g.*, crustaceans producers of *Ophiomorpha* and *Thalassinoides*) result in highly connected burrow networks (Pryor, 1975). These burrows networks can be infilled actively or passively with sediment of contrasting composition and/or grain size than the hosting medium. Bioturbating infauna is also responsible for the reorganization of the sediment fabric associated with animal burrowing that induces density contrast (Lacroix et al., 2012; Gingras et al., 2012). Additionally, trace fossils induce diagenetic modifications (*i.e.*, cementation, mineral replacement) introducing density heterogeneity within the bioturbated rock fabric (Keswany, 1999; Pak and Pemberton, 2003; Gingras et al., 2004a, 2004b; Keswany and Pemberton, 2010; Petrash et al., 2011; Gingras et al., in press). Consequently, trace fossils not only provide textural heterogeneity but also provide the bioturbated rock-fabric with contrasting density fields (Gingras et al., 2002).

Within the Lysing and Nise formations small burrows (1 to 2 mm) can be seen in the X-ray computed tomography scan images and three dimensional (3D) rendered models (Figure 3.14, 3.16 and 3.20). Petrographic assessments reveal well differentiated burrows from the surrounding matrix (Figure 3.15, 3.17 and 3.21). The size of the burrows is consistent with the thin section observations. Some of the burrows show a distinctive lining that isolate the burrow-fill from the matrix and can be attributable to *Paleophycus* (Figure 3.15G and 3.15H). Contrarily, traces lacking of lining can be attributable to *Planolites* (Figure 3.15C and 3.15D). The burrow system of *Planolites* and *Paleophycus* are more likely responsible of the density contrast that is seen in the X-ray computed tomography scan images and three dimensional models (Figure 3.14, 3.16 and 3.20). *Planolites* is an unlined burrow infilled with sediments having textural and fabricational characteristics that differ from those of the host rock, whereas *Paleophycus* is a lined burrow filled with sediments typically identical to those of the surrounding matrix (Pemberton and Frey, 1982). Alternatively, *Chondrites* may also contribute with the contrasting density responses in the Micro-CT analyses (Figure 3.14, 3.16 and 3.20). Of particular interest is the fact that bigger traces (*e.g., Thalassinoides, Ophiomorpha*) are not resolved in these images and models. This is even more interesting due to fact that bigger burrows can also be differentiated in the thin sections of Facies 1 and 2 (*e.g,* Figure 3.17A). This could be explained by the fact that likely non cementation could be related to bigger burrows. The lack of lithological contrast as selective fecal pellets lining (*i.e.*, *Ophiomorpha*) or a distinctive mud lining (*e.g.*, *Paleophycos*) may also be responsible for texturally selective cements that provide higher X-ray attenuation, thus better imaging. Alternatively, consistent burrow diameter and morphology throughout the X-ray images and micro-CT models of both the Lysing and Nise formations suggests that all the tiers of these burrows were created by the same or similar organisms (Figure 3.14, 3.16 and 3.20). Consequently, although diverse behavioural patterns are preserved (chapter II within this thesis), burrows that provided better images may have been produced by a single or small group of organisms (*e.g., Chondrites*).

SUMMARY

Within the Upper Cretaceous Lysing and Nise formations (Møre Basin, Offshore-mid Norway) a biogenic rock fabric contributes substantially to reservoir storativity and permeability. Core and core-plugs were studied in order to assess the relationship between bioturbation and permeability distribution. Micro-CT imaging, spot permeability measurements and petrographic assessments show that permeability distributions are strongly influenced by the location and nature of bioturbation.

Spot permeability data taken from core-plugs indicates that the burrow permeability can be up to two orders of magnitude greater than the matrix. Therefore, it proffers a biogenically induced dual-permeability flow media. Bulk assessments of permeability based on core-plug data indicate that the harmonic mean of matrix versus burrow permeabilities provides the most accurate estimate of bulk permeability in the majority of the studied samples (Facies 4 and 2), whereas Facies 1 is better represented by the arithmetic mean. Bulk permeability measurements also show that k_h is higher than k_v and that permeability distributions are anisotropic.

Micro-CT scanning reveals complex spatial distributions resulting in a mostly horizontal, intricate, highly connected burrow-system. Petrographic assessments and three-dimensional (3D) volumes and models allowed the identification of highly contrasting density fields interpreted likely to reflect burrow-fills of *Planolites* and *Chondrites* or burrow-linings of *Ophiomorpha* and *Paleophycus* responsible for the density contrast found in the micro-CT scan images. These modifications constitute selective fluid flow networks that occur through the imposition of coarser grained sediment in tunnels and shafts in otherwise fine-grained strata, as well as result in better resource quality and control the biogenically enhanced permeability distributions. Thus both the Lysing and Nise Formation reservoir constitute a case of non-constrained discrete textural heterogeneities within the biogenic permeability enhancement classification proposed by Pemberton and Gingras, (2005).

REFERENCES

ATTARD, J.J., MCDONALD, P.J., ROBERTS, S.P., AND TAYLOR, T. 1994, Solid state NMR imaging of irreducible water in reservoir cores for spatially resolved pore surface relaxation estimation: Magnetic Resonance Imaging, v. 12, p. 355 – 359.

BANIAK, G.M., BURNS, B.A., GINGRAS, M.K., PEMBERTON, S.G., 2011, Petrophysical Characterization of Bioturbated Reservoir Facies: Upper Jurassic Ula Formation, Norwegian North Sea, Europe. American Association of Petroleum Geologist (AAPG) annual conference and exhibition (ACE) Posters, Houston.

BENCSIK, M. AND RAMANATHAN, C., 2001, Direct measurement of porous media local hydrodynamical permeability using gas MRI: Magnetic Resonance Imaging, v. 19, p. 379 – 383.

CORE LABORATORIES INSTRUMENTS, 1996, Profile Permeameter PDPK – 400 Operations Manual, 40 p.

CORLETT, H.J. AND JONES, B.J., In review, "Petrographic and geochemical contrasts between calcite- and dolomite-filled burrows in the Middle Devonian Lonely Bay Formation, Northwest Territories, Canada", Journal of Sedimentary Research.

CUNNINGHAM, K.J., SUKOP, M.C., HUANG, H., ALVAREZ, P.F., CURRAN, H.A., RENKEN, R.A., AND DIXON, J.F., 2009, Prominence of ichnologically influenced macroporosity in the karst Biscayne aquifer: stratiform "super-K" zones, Geological Society of America Bulletin, v. 121, p. 164 –180.

CUNNINGHAM, K.J., AND SUKOP, M.C., 2012, Megaporosity and permeability of *Thalassinoides*-dominated ichnofabrics in the Cretaceous karst-carbonate Edwards-Trinity aquifer system, Texas: United States Geological Survey Open-File Report 2012 – 1021, 4 p.

DAWSON, W.C., 1978, Improvement of sandstone porosity during bioturbation, American Association of Petroleum Geologists, Bulletin, v. 62, p. 508 – 509.

EKDALE, A.A., EKDALE, E.G., AND COLBERT, M.W., 2006, invertebrate trace fossils inside vertebrate skulls: the worms crawl in, and the worms crawl out (abstract): Geological Society of America, Abstracts with Programs, v. 38, 476 p.

FREEZE, R.A., AND CHERRY, J.A., 1979, Groundwater, eds., Prentice-Hall, New Jersey, USA, 604 p.

FU, S., WERNER, F., AND BROSSMANN, J., 1994, Computed tomography: application in studying biogenic structures in sediment cores: Palaios, v. 9, p. 116 – 119.

GATESY, S.M., MIDDLETON, K.M., JENKINS, F.A., JR., AND SHUBIN, N.H., 1999, Threedimensional preservation of foot movements in Triassic theropod dinosaurs: Nature, v. 399, p. 141 – 144.

GINGRAS, M.K., PEMBERTON, S.G., MENDOZA, C.A., HENK, F., 1999, Assessing the anisotropic permeability of *Glossifungites* surfaces. Petroleum Geoscience 5, 349 – 357.

GINGRAS, M.K., PEMBERTON, S.G., SAUNDERS, T., 2001, Bathymetry, sediment texture, and substrate cohesiveness; their impact on modern Glossifungites trace assemblages at Willapa Bay, Washington. Palaeogeography, Palaeoclimatology, Palaeoecology. 169, 1 – 21.

GINGRAS, M.K., PEMBERTON, S.G., HENK, F., MACEACHERN, J.A., MENDOZA, C., ROSTRON, B., O'HARE, R., SPILA, M., AND KONHAUSER, K, 2005, Applications of ichnology to fluid and gas production in hydrocarbon reservoirs, *in* MacEachern, J.A., Bann, K.L., Gingras, M.K., and Pemberton, S.G., eds., Applied Ichnology, SEPM Short Course Notes 52, p. 129 –143.

GINGRAS, M.K., MENDOZA, C., AND PEMBERTON, S.G., 2004a, Fossilized worm-burrows influence the resource quality of porous media, AAPG Bulletin, v. 88, p. 875 – 883.

GINGRAS, M.K., PEMBERTON, S.G., MUEHLENBACHS, K., AND MACHEL, H., 2004b, Conceptual models for burrow-related, selective dolomitization with textural and isotopic evidence from the Tyndall Limestone, Geobiology, v. 2, p. 21 – 30.

GINGRAS, M.K., MACMILLAN, B., BALCOM, B.J., SAUNDERS, T., AND PEMBERTON, S.G., 2002, Using magnetic resonance imaging and petrographic techniques to understand the textural attributes and porosity distribution in *Macaronichnus*-burrowed sandstone, Journal of Sedimentary Research, v. 72, p. 552 – 558.

GINGRAS, M.K., BANIAK, G.,GORDON, J., HOVIKOSKI, J., KONHAUSER K.O., LA CROIX, A., LEMISKI, R., MENDOZA, C., PEMBERTON, S.G., POLO, C., AND ZONNEVELD, J., P., 2012, Permeability and Porosity in bioturbated media, *in*: D. Knaust and R.G. Bromley (eds). Trace Fossils as Indicators of Sedimentary Environments: Developments in Sedimentology. Elsevier, Amsterdam, v. 63.

GOMEZ-HERNANDEZ, J. J., AND GORELICK, S. M. (1989), Effective groundwater model parameter values: Influence of spatial variability of hydraulic conductivity, leakance, and recharge. Water Resources Research. 25(3), p. 405 – 419.

GORDON, J.B., PEMBERTON, S.G., GINGRAS, M.K., KONHAUSER, K.O., 2010, Biogenically enhanced permeability; a petrographic analysis of *Macaronichnus segregatus* in the Lower Cretaceous Bluesky Formation, Alberta, Canada. American Association of Petroleum Geologists (AAPG) Bulletin 94, p. 1779 – 1795.

GROENEWALD, G.H., WELMAN, J., AND MACEACHERN, J.A., 2001, Vertebrate burrow complexes from the Early Triassic Cynognathus Zone (Driekoppen Formation, Beaufort Group) of the Karoo Basin, South Africa: Palaios, v. 16, p. 148 – 160.

GUNATILAKA, A., AL-ZAMEL, A., SHERMAN, A.J., AND REDA, A., 1987, A spherulitic fabric in selectively dolomitized siliciclastic crustacean burrows, northern Kuwait, Journal of Sedimentary Petrology, v. 57, p. 927 – 992.

HÄNTZSCHEL W., 1975, *in* Teichert, C., ed., Treatise on Invertebrate Paleontology, Part W Miscellanea, Supplement 1, Trace Fossils and Problematica, Second Edition: University of Kansas Press and the Geological Society of America, p. W1–W269.

HASIOTIS, S.T., 2002, Continental Trace Fossils: SEPM, Short Course 51, 134 p.

HASIOTIS, S.T., 2004, Reconnaissance of Upper Jurassic Morrison Formation ichnofossils, Rocky Mountain region, USA: environmental, stratigraphic, and climatic significance of terrestrial and freshwater ichnocoenoses: Sedimentary Geology, v. 167, p. 277 – 369.

KEIGHLEY, D.G., AND PICKERILL, R.K., 1995, "Commentary", The ichnotaxa *Palaeophycus* and *Planolites*: Historical perspectives and recommendations; Ichnos, v3, p 301 – 309.

KESWANI, A. D., 1999, An integrated ichnological perspective for carbonate diagenesis; [Unpublished M.Sc. thesis], Earth and Atmospheric Sciences Department, University of Alberta, Edmonton, Alberta, Canada.

KESWANI, A. D., PEMBERTON, S. G., 2006, Applications of Ichnology in exploration and exploitation of Mississippian carbonate reservoirs, Midale Beds, Weyburn oilfield, Saskatchewan.

KESWANI, A. D., PEMBERTON, S. G., 2010, Why Are Mudstones Dolomitized in Mississippian Midale Beds, Weyburn Oilfield, Saskatchewan?, American Association of Petroleum Geologists (AAPG) Annual Convention and Exhibition (ACE), Abstracts, New Orleans, Louisiana

KNAUST D. 2009a, Ichnology as a tool in carbonate reservoir characterization: A case study from the Permian-Triassic Khuff Formation in the Middle East. *GeoArabia*, v. 14, 3, 2009, p. 17-38 Gulf Petro Link, Bahrain.

KNAUST, D. 2009b. Characterisation of a Campanian deep-sea fan system in the Norwegian Sea by means of ichnofabrics. Marine and Petroleum Geology, v. 26, p. 1199 – 1211.

LA CROIX, A., D., GINGRAS, M. K., DASHTGARD, S. E., PEMBERTON, S. G., in press, Computer modeling bioturbation: the creation of porous and permeable fluid flow pathways. American Association of Petroleum Geologists (AAPG), Bulletin, v. 96, p. 545 – 556 Bulletin.

LEMISKI, R.T., HOVIKOSKI, J., GINGRAS, M.K., AND PEMBERTON, S.G., 2011, Sedimentological, ichnological, and resource characteristics of the low-permeability, gas-charged Alderson Member (Hatton Gas Pool, southwest Saskatchewan): Implications on resource development, Canadian Bulletin of Petroleum Geology.

LIMBRUNNER, J. F., VOGEL, R. M., AND BROWN, L. C., 2000, Estimation of harmonic mean of a lognormal variable. Journal of Hydrologic Engineering, Vol. 5, No. 1, p. 59 – 66.

LUCIA, F.J., 1995, Rock fabric/petrophysical classification of carbonate pore space for reservoir characterization: The American Association of Petroleum Geologists Bulletin, v. 79, p. 1275 – 1300.

MAARTEN, G. K., JEUKENS, C., R.L.P.N. BAKKER C., J.,G., FRINGS , R, M., 2008, Magnetic Resonance Imaging of coarse sediment, Sedimentary Geology, 208 p. 69 – 78.

MARTIN, A.J., CLOSE, J. C., and SIMONES, G. C., 1994, Theoretical and practical considerations of integrating subsurface ichnologic and geophysical data in Late Cretaceous strata, southeastern Atlantic Coastal Plain, USA: 14th International Sedimentological Congress, Recife, Brazil, p. S52 – 3.

MEHRTENS, C., SELLECK, B., 2002. Middle Ordovician section at Crown Point Peninsula, in McLelland, J., Karabinos, P. (Eds.), Guidebook for Fieldtrips in New York and Vermont. University of Maine, Orono, ME, United States (USA), United States (USA).

MCKINLEY, J.M., LLOYD, C.D., AND RUFFELL, A.H., 2004, Use of variography in permeability characterization of visually homogeneous sandstone reservoirs with examples from outcrop studies, Mathematical Geology, v. 36, p. 761 – 779.

MEADOWS, P., AND TAIT, J., 1989, Modification of sediment permeability and shear strength by two burrowing invertebrates. Marine Biology. Berlin, Heidelberg 101, p. 75 – 82.

MILAN, J., CLEMMENSEN, L.B., AND BONDE, N., 2004, Vertical sections through dinosaur tracks (Late Triassic lake deposits, East Greenland)-undertracks and other subsurface deformation structures revealed: Lethaia, v. 37, p. 285 – 296.

NARUSE, H., AND NIFUKU, K., 2008, Three-dimensional morphology of the ichnofossil Phycosiphon incertum and its implication for paleoslope inclination: Palaios, v. 23, p. 270 – 279.

PAK, R., PEMBERTON, S.G., AND GINGRAS, M.K., 2001, Reservoir characterization of burrow-mottled carbonates: The Yeoman Formation of southern Saskatchewan – preliminary report; *in* Summary of Investigations 2001,Volume 1, Saskatchewan Geological Survey, Sask. Energy Mines, Misc. Rep. 2001–4.1, p.10 – 13.

PAK, R., AND PEMBERTON, S.G., 2003, Ichnology of the Yeoman Formation; *in* Summary of Investigations 2003, Volume 1, Saskatchewan Geological Survey, Sask. Industry Resources, Misc. Rep. 2003-4.1, CD-ROM, Paper A-3, 16 p.

PEMBERTON, S.G., AND FREY, R.W., 1982, Trace fossil nomenclature and the *Planolites-Palaeophycus* dilemma; Journal of Paleontology., v 56, p 843 – 881.

PEMBERTON, S.G., GINGRAS, M.K., 2005, Classification and characterizations of biogenically enhanced permeability. AAPG Bull. 89, 1493 – 1517.

PEMBERTON, S.G., SPILA, M., PULHAM, A.J., SAUNDERS, T., MACEACHERN, J.A., ROBBINS, D., SINCLAIR, I.K., 2001. Ichnology & sedimentology of shallow to marginal marine systems; Ben Nevis & Avalon reservoirs, Jeanne d'Arc Basin. Short Course Notes - Geological Association of Canada 15, 343.

PETRASH, D. A., LALONDE, S. V., GINGRAS, M. K., & KONHAUSER, K. O. 2011, A surrogate approach to studying the chemical reactivity of burrow mucus linings", Palaios.

PHILLIPS, C., AND MCILROY, D., 2010, Ichnofabrics and biologically mediated changes in clay mineral assemblages from a deep-water, fine-grained, calcareous sedimentary succession: an example from the Upper Cretaceous Wyandot Formation, offshore Nova Scotia. Bulletin of Canadian Petroleum Geology v. 58, NO. 3P. 203 – 218.

PLATT, B, F., HASIOTIS, S, T., AND HIRMAS, D, R., 2010, Use of low-cost multistripe laser triangulation (MLT) scanning technology for three-dimensional, quantitative paleoichnological and neoichnological studies. Journal of Sedimentary Research. v. 80, p. 590 – 610.

PEREZ, K.T., DAVEY, E.W., MOORE, R.H., BURN, P.R., ROSOL, M.S., CARDIN, J.A., JOHNSON, R.L., AND KOPANS, D.N., 1999, Application of computer-aided tomography (CT) to the study of estuarine benthic communities: Ecological Applications, v. 9, p.1050 – 1058.

POLO, C., BANIAK, G., GINGRAS, M.K., 2010, Biogenic influences on resource quality within the Upper Cretaceous Nise Formation, Møre basin, Norwegian Sea, American Association of Petroleum Geologist (AAPG) Annual Convention and Exhibition (ACE) Abstracts, New Orleans, Louisiana.

POLO, C., BANIAK, G.M., GINGRAS, M.K., AND PEMBERTON, S.G., 2012, Using X-ray microtomography (micro-CT) in characterizing biogenically-enhanced, low-permeability reservoirs: a case study from the Upper Cretaceous Nise Formation, Møre Basin, Norwegian Sea: American Association of Petroleum Geologists (AAPG), Annual Convention and Exhibition (ACE), Long Beach, Technical Program.

PRYOR, W. A., 1975, Biogenic sedimentation and alteration of argillaceous sediments in shallow marine environments: Geological Society of America Bulletin, v. 86, p. 1244 – 1254.

SKYSCAN N.V., 2005, SkyScan 1172 Desktop X-ray Microtomograph Instruction Manual, 53 p.

SPILA M. V., PEMBERTON S. G., ROSTRON B., GINGRAS M. K., 2005, Biogenic textural heterogeneity, fluid flow and hydrocarbon production: bioturbated facies Ben Nevis Formation, Hibernia Field, offshore Newfoundland , *in* Applied Ichnology. Society of Economic Paleontologist and Mineralogist short courses notes, p. 354 – 371.

SUTTON, S.J., ETHERIDGE, F.G., ALMON, W.R., DAWSON, W.C., AND EDWARDS, K.K., 2004, Textural and sequence-stratigraphic controls on sealing capacity of Lower and Upper Cretaceous shales, Denver Basin, Colorado, American Association of Petroleum Geologists, Bulletin, v. 88, p. 1185-1206.

TONKIN, N.S., MCILROY, D., MEYER, R., MOORE-TURPIN, A., 2010. Bioturbation influence on reservoir quality; a case study from the Cretaceous Ben Nevis Formation, Jeanne d'Arc Basin, offshore Newfoundland, Canada. AAPG Bull. 94, 1059 – 1078.

UCHMAN, A., 1995, Tiering patterns of trace fossils in the Palaeogene flysch deposits of the Carpathians, Poland: Geobios Memoire Special, v. 18, p. 389 – 394.

VAN GEET, M., LAGROU, D., SWENNEN, R., 2003, Porosity measurements of sedimentary rocks by means of microfocus X-ray computed tomography (μCT), *in* Mees, F., Swennen, R., Van Geet, M., and Jacobs, P., eds., Applications of X-ray Computed Tomography in the Geosciences, Geological Society of London, Special Publications, v. 215, p. 51 – 60.

WARREN, J.E. AND PRICE, H.S.,1961, Flow in Heterogeneous Porous Media, Society of Petroleum Engineers Journal. v. 1, p. 153 – 169

WETZEL, A., AND UCHMAN, A., 2001, Sequential colonization of muddy turbidites in the Eocene Beloveza Formation, Carpathians, Poland: Palaeogeography, Palaeoclimatology, Palaeoecology, v. 168, p. 178 – 202.

CHAPTER IV – SUMMARY AND CONCLUSIONS

This thesis provides insights into the depositional environment and distribution of the Lysing and Nise formations in the Norwegian continental shelf. This is done by describing the ichnological and sedimentological characteristics of these formations in the Ellida and Midnatsoll fields area. The study also shows applications of ichnology, not only as a paleoenvironmental indicator, but also its application in understanding porosity and permeability distributions in oil and gas reservoirs. Overall, this research contributes to the understanding on the distribution, sedimentology and ichnology as well as reservoir quality of Upper Cretaceous strata in the Møre Basin.

A significant contribution outlined in Chapter II is an alternative paleoenvironmental and depositional interpretation of the Nise Formation (Facies 1) compared to those previously recognized in the literature (*e.g.,* Kittilsen et al., 1999; Kjennerud and Vergara, 2005; Martinsen et al., 2005; Fugelli and Olsen, 2005a, 2005b; Knaust, 2009). The second contribution concerns the application of ichnology to reservoir characterization and is developed in Chapter III. The data and interpretations from both aspects of the study constitute valuable tools to be incorporated in future multidisciplinary exploration and production projects involving the studied intervals.

DEPOSITIONAL ENVIRONMENTS AND STRATIGRAPHY

Chapter II proposes a facies classification scheme pairing ichnology and sedimentology and provides insights into the depositional processes at the time of deposition of the Lysing and Nise formations. A depositional model is proposed for these formations which complements the ones available in the literature. From the observations developed in Chapter-II the following conclusions can be drawn for these two formations:

Nise Formation:

• The Nise Formation consists of recurrent intervals of alternating fine- and coarse-grained sedimentation within paleoenvironments with stable hydraulic energy and paleoecological conditions. Overall, the trace fossil is dominated by infaunal, dwelling and grazing structures that reflect predominantly deposit-, suspension-feeding and grazing behaviours. This ichnofossil assemblage contains elements of the proximal through distal *Cruziana* ichnofacies (Pemberton and MacEachern, 1995; MacEachern et al., 2007; MacEachern et al., 2010).

• The bioturbation intensity in the sandy intervals of the Nise Formation is high (BI = 4 – 6) whereas the mudstone intervals display very low levels of bioturbation (BI = 1 – 2) throughout the examined core. Recurrent overprinting of trace-fossils reveals low sedimentation rates with favourable conditions for bioturbation infauna to develop.

• A diverse and abundant trace fossil-suite (*i.e.*, Facies 1 and Facies 2) reveals that endobenthic organisms flourished under very low or none physico-chemical and environmental stresses. This is probably the result of stable, favourable ecological-conditions such as oxygenation, food availability, salinity and temperature. The lithological contrast allowed the differentiation of tiering and overprinting of burrows.

• From the interpretation of the sedimentological and ichnological datasets, the Nise Formation deposits in the Ellida and Midnatsoll Fields area are interpreted to record deposition in a siliciclastic tectonically active setting, mostly above storm wave-base (Pemberton et al., 2001; Pemberton and MacEachern, 1995; MacEachern et al., 2007).

Lysing Formation:

• The studied core interval of the Lysing Formation shows alternating fine- and coarse-grained sedimentation in a depositional environment with stable ecological and hydraulic energy conditions. The ichnofossil assemblage is dominated by infaunal dwelling and grazing structures that reflect predominantly deposit- and less common suspension-feeding and grazing behaviours. The trace fossil suite is consistent with elements of the distal *Cruziana* ichnofacies (Pemberton and MacEachern, 1995; MacEachern et al., 2007; MacEachern et al., 2010).

• The Lysing Formation shows intense bioturbation (BI = 4 – 6) throughout the studied core interval. These robust and abundant trace-fossil suites suggest favourable paleoecological conditions prevailed at the time bioturbation took place.

• Small changes in trace fossil diversity and abundance are related to continuous favourable environmental conditions with minimal fluctuations promoting colonization and continuous overprinting of trace fossils. The abundance of mud provided lithological contrast allowing the differentiation of deep tiering and recurrent overprinting of burrows.

• Based in the sedimentological and ichnological interpretations, the Lysing Formation in the Ellida field area is interpreted to record deposition in tectonically active setting, mostly below storm wave-base (Pemberton and MacEachern, 1995; Pemberton et al., 2001; MacEachern et al., 2007a).

ICHNOLOGY AND RESOURCE QUALITY

The Lysing and Nise formations as case studies in non-constrained textural heterogeneities

Chapter III explores the relationship between biogenic rock fabrics, its spatial visualization and the resulting permeability distribution. This is carried out using spot-minipermeametry, thin sections and X-ray microtomography (Micro-CT) on the main reservoir units of the Lysing (F4) and Nise (F1, F2) formations. This analysis contributes to the understanding of the relationship between bioturbate textures and the resulting heterogeneity responsible for the permeability enhancement. From the observations developed in Chapter-III the following conclusions can be outlined for these two formations:

• Within the Upper Cretaceous Lysing and Nise formations a biogenic rock fabric contributes substantially to reservoir storativity and permeability. Commonly, the bioturbated intervals have highly contrasting and well-defined permeability fields. Spot permeability data taken from core-plugs indicates that the burrow permeability can be up to two orders of magnitude greater than the matrix. Thus proffering a biogenically influenced dual-permeability flow media in which fluid flow is preferentially conducted from burrow to burrow.

• In order to evaluate the effectivity of the burrow-associated fluid flow pathways, volume-weighted averaging of the burrow- and matrix-associated permeability was employed on the data from spot-minipermeametry to approximate the bulk permeability of facies 1, 2 and 4. The arithmetic mean of permeability is a good estimate of the bulk permeability occurring through well connected burrow networks; the harmonic mean is an estimator of the bulk permeability in less well-connected burrow networks where significant short circuiting of flow conduits occur; and the geometric mean provides an equivalent bulk permeability in homogeneous, isotropic flow media (Gingras et al., 1999; Lacroix, 2010, Gingras et al, 2012). Spot permeability measurements (provided by Statoil) were plotted on graphs of the three respective means for the full range of bioturbation intensity (*i.e.*, 0-100%). In the Lysing and Nise Formation case, the majority of data fell in the vicinity of the harmonic mean (Facies 2 and Facies 4) that point towards a poorly connected flow network and flow path isolation. Alternatively, within Facies 1 of the Nise Formation, bulk permeability is better represented by the arithmetic mean of trace fossils and matrix permeabilities. Thus suggesting that burrows form interconnected planiform networks that induce preferential fluid flow conduits (Gingras et al., 2012).

• The planiform burrow networks are dominated by *Thalassinoides* and *Planolites*. However, in some instances, rare traces with vertical components (*e.g., Skolithos, Arenicolites*, and *Rhyzocorallium*) locally provide hydraulic communication between discontinuous horizontal burrow systems. The harmonic relationship aforementioned suggests that flow is largely directed across lower permeability matrix from burrow to burrow. Biogenic enhancement classified as non-constrained discrete heterogeneities dominated by sparse bioturbation exhibit this characteristics (Pemberton and Gingras, 2005; Gingras et al., 2012). As with most other biogenically-enhanced flow media the resulting flow network is an overall intricate, well-connected horizontal and vertical burrow system consistent with the observation in the Lysing and Nise formations case.

• In the Lysing and Nise formations reservoir units, bulk permeability measurements also show that k_h is higher than k_v. This is likely the result of increased horizontal burrowing associated with trace-fossil assemblages exhibiting elements of the proximal through distal *Cruziana* ichnofacies, or may be related to the small (2.54 cm) scale of the probe used in the permeability measurements.

• Spatial visualization of the Lysing and Nise formations bioturbated fabrics reveals complex distributions resulting in a mostly horizontal, intricate, highly connected burrow-system. Petrographic assessments and spatial imaging via X-ray microtomography (Micro-CT) scanning show that porosity is strongly influenced by the location and nature of bioturbation. This occurs in two ways: (1) as reoriented and homogenized fabrics in highly bioturbated media; and, (2) through the imposition of coarser grained sediment in galleries and tunnels in otherwise fine-grained, impermeable strata. These modifications constitute selective fluid flow pathways within the studied interval, resulting in reservoir quality enhancement.

Future work

Future research should attempt to assess the effectivity of the bioturbate flow networks identified in the Lysing and Nise formations case studies. This can be done through numerical modeling based on determining the pore distribution of selected samples and its interconnectivity (*e.g.*, Gingras et al., 1999: Spila et al., 2005; Lacroix et al., 2012). Many variables need to be considered: amount of bioturbation, permeability contrast between burrow and matrix, and the degree of connectivity account as the most important (Gingras et al, 2012). The modeling of fluid flow within bioturbated intervals may aid in the optimization of secondary recovery methods and the selection of future drilling targets in similar burrow-modified flow media in the area.

REFERENCES

FUGELLI, E. M. G., AND T. R. OLSEN, 2005a, Screening for deep-marine reservoirs in frontier basins: Part 1–Examples from offshore mid-Norway: AAPG Bulletin, v. 89, p. 853 – 882.

FUGELLI, E. M. G., AND T. R. OLSEN, 2005b, Risk assessment and play fairway analysis in frontier basins: Part 2–Examples from offshore mid-Norway: AAPG Bulletin, v. 89, p. 883 – 896.

GINGRAS, M.K., PEMBERTON, S.G., MENDOZA, C.A., HENK, F., 1999, Assessing the anisotropic permeability of *Glossifungites* surfaces. Petroleum Geoscience 5, p. 349 – 357.

GINGRAS, M.K., BANIAK, G.,GORDON, J., HOVIKOSKI, J., KONHAUSER K.O., LA CROIX, A., LEMISKI, R., MENDOZA, C., PEMBERTON, S.G., POLO, C., AND ZONNEVELD, J., P., 2012, Permeability and Porosity in bioturbated media, *in*: D. Knaust and R.G. Bromley (eds). Trace Fossils as Indicators of Sedimentary Environments: Developments in Sedimentology. Elsevier, Amsterdam, v. 63.

KITTILSEN, J. E., OLSEN, R. R., MARTEN, R. F., HANSEN, E. K. AND HOLLINGSWORTH, R. R., 1999, The first deepwater well in Norway and its implications for the Upper Cretaceous Play, Vøring Basin. *in* Fleet, A. J. and Boldy, S. A. R., eds., Petroleum Geology of North–west Europe: Proceedings of the 5th Conference. Geological Society, London, p. 275 – 280.

KJENNERUD, T. AND VERGARA, L., 2005, Cretaceous to Palaeogene 3D palaeobathymetry and sedimentation in the Vøring Basin, Norwegian Sea. *in* Dore, A. G. and Vining, B. A., eds., Petroleum Geology: North-West Europe and Global Perspectives–Proceedings of the 6th Petroleum Geology Conference, p. 815 – 831.

KNAUST, D., 2009, Characterisation of a Campanian deep-sea fan system in the Norwegian Sea by means of ichnofabrics. Marine and Petroleum Geology. v. 26, p. 1199 – 1211.

LACROIX, A., 2010, Ichnology, sedimentology, stratigraphy and trace fossil-permeability relationships in the Upper Cretaceous Medicine Hat Member, Medicine Hat gas field, southeast Alberta, Canada. Unpublished M.Sc. thesis, Earth and Atmospheric Sciences Department, University of Alberta, Edmonton, Alberta, Canada.

LA CROIX, A., D., GINGRAS, M. K., DASHTGARD, S. E., PEMBERTON, S. G., in press, Computer modeling bioturbation: the creation of porous and permeable fluid flow pathways. American association of Petroleum Geologist (AAPG) Bulletin.

MACEACHERN, J.A., PEMBERTON, S.G., BANN, K.L., AND M.K. GINGRAS, 2007a, Departures from the archetypal ichnofacies: effective recognition of environmental stress in the rock record, *in* MacEachern, J.A., Bann, K.L., Gingras, M.K., and Pemberton, S.G., eds., Applied Ichnology: Tulsa, Oklahoma, SEPM (Society for Sedimentary Geology) Short Course Notes 11.

MACEACHERN, J.A., PEMBERTON, S.G., M.K. GINGRAS, AND BANN, K.L., 2010. Ichnology and facies models, *in* Facies Models 4, eds., by James, N. P., and Dalrympe, R. W., Geological Association of Canada IV, Series: GEOtext 6, p. 19 – 58.

MARTINSEN, O. J., LIEN, T., AND JACKSON, C., 2005, Cretaceous and Palaeogene turbidite systems in the North Sea and Norwegian Sea Basins: source, staging area and basin physiography controls on reservoir development. Geological Society, London, Petroleum Geology Conference series 2005, v. 6, p. 1147 – 1164.

PEMBERTON, S.G., SPILA, M., PULHAM, A.J., SAUNDERS, T., MACEACHERN, J.A., ROBBINS, D., AND I.K. SINCLAIR, 2001, Ichnology and sedimentology of shallow to marginal marine systems: Ben Nevis and Avalon reservoirs, Jeanne d'Arc Basin: Geological Association of Canada, Short Course Notes v. 15.

PEMBERTON, S.G., AND MACEACHERN, J.A., 1995, The sequence stratigraphic significance of trace fossils: Examples from the Cretaceous foreland basin of Alberta, Canada, *in* Van Wagoner, J.C., and Bertram, G.T., eds., Sequence Stratigraphy of Foreland Basin Deposits: American Association of Petroleum Geologists, Memoir 64, p. 429 – 475.

PEMBERTON, S.G., GINGRAS, M.K., 2005, Classification and characterizations of biogenically enhanced permeability. American association of Petroleum Geologist (AAPG) Bulletin. 89, p. 1493-1517.

SPILA M. V., PEMBERTON S. G., ROSTRON B., GINGRAS M. K., 2005, Biogenic textural heterogeneity, fluid flow and hydrocarbon production: bioturbated facies Ben Nevis Formation, Hibernia Field, offshore Newfoundland, *in* Applied Ichnology. Society of Economic Paleontologist and Mineralogist short courses notes, p. 354-371.

APPENDIX I - ICHNOLOGICAL COMPOSITE LOG

Statoil Sponsored Joint Industry Project

University of Alberta, Ichnology Research Group - Statoil

6405/7-1 T2 ELLIDA, COMPOSITE ICHNOLOGICAL LOG

Date logged: June 23th, 2009.
Logged by: Camilo Polo.
Assistant: Greg Baniak.
Supervised and approved by: Dr. Murray Gingras.

Well preserved core
Observations and logging made in Cut-A
Slabbed core, 10 cm wide-1 m long.
Core stored at Weatherford Resevoir Labs.
Stavanger, Norway.

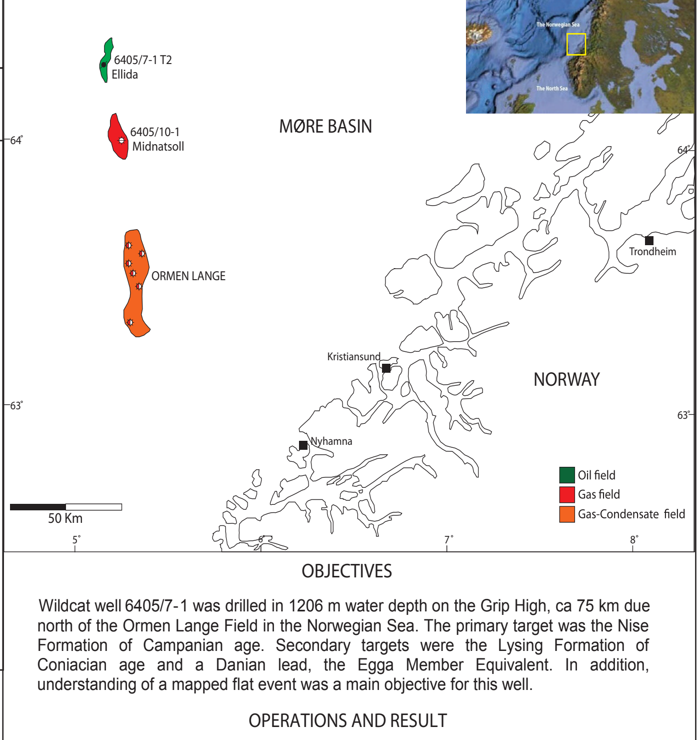

EXPLORATION WELLBORE: 6405/7-1 T2
GENERAL INFORMATION FOUND AT THE NPD'S FACT-PAGES

Wellbore name	7/1/6405
NPDID wellbore	4749
Main area	NORWEGIAN SEA
Discovery	6405/7-1 ELLIDA
Well name	7/1/6405
Seismic location	GH0103 -Inline 1268 &
Geodetic datum	ED50
NS degrees	64° 17' 16.42'' N
EW degrees	5° 7' 58.6'' E
NS UTM [m]	7131004
EW UTM [m]	603242.59
UTM zone	31
Drilled in production licence	281
Drilling operator	Statoil ASA (old)
Drill permit	1060-L
Drilling facility	WEST NAVIGATOR
Drilling days	113
Entry date	20.06.2003
Completion date	10.10.2003
Release date	10.10.2005
Publication date	07.11.2005
Type	EXPLORATION
Purpose - planned	WILDCAT
Purpose	WILDCAT
Status	P&A
Reentry	NO
Content	OIL
Discovery wellbore	YES
1st level with HC, age	LATE CRETACEOUS
1st level with HC, formation	NISE FM
Kelly bushing elevation [m]	36
Water depth [m]	1206
Total depth (MD) [m RKB]	4300
Final vertical depth (TVD) [m	4299
Maximum inclination [°]	7.2
Bottom hole temperature [°C]	129
Oldest penetrated age	LATE CRETACEOUS
Oldest penetrated formation	LYSING FM

The primary target, the Nise Formation, 2757 m to 2816 m in well 6405/7 1and 2760.6 m to 2960 m in 6405/7-1T2, consists of layered/laminated and bioturbated claystones, siltstones and sandstones with poor reservoir quality. The Nise formation proved to be oil-bearing from the top at 2760.5 m and down to 2823 m. However, good oil shows are also described below this depth, to the base of the deepest core at 2881 m and on SWCs down to 2892 m. Oil samples were collected from wire line testing tool at 2763 m, 2770.5 m and 2828 m. Water samples were taken with wire line testing tool at 2828 m and 2850 m. The secondary target, the Lysing Formation, was encountered at 3665 m. The base of the Lysing Formation was not seen. The reservoir properties were poor. It consisted of highly bioturbated, very fine to fine grained sandstones, siltstones and claystones. Quartz cementation is common. The Lysing sands were water wet. No samples were taken due to tight formation. Five cores were cut in the interval 2754 m - 2881 m and two cores were cut in the interval 3751 m to 3784 m. All cores were cut in the T2 track. The well was permanently abandoned on 15 October 2003 as an oil discovery.

Cores at the NPD

Core sample number	Core sample top depth [m]	Core sample bottom depth [m]
1	2754	2764
2	2781	2806.6
3	2808	2831.6
4	2835	2861.5
5	2862	2869.4
6	3751	3756
7	3757	3783.1

Total core sample length [m]	124.2
Core samples available	YES

OBJECTIVES

Wildcat well 6405/7-1 was drilled in 1206 m water depth on the Grip High, ca 75 km due north of the Ormen Lange Field in the Norwegian Sea. The primary target was the Nise Formation of Campanian age. Secondary targets were the Lysing Formation of Coniacian age and a Danian lead, the Egga Member Equivalent. In addition, understanding of a mapped flat event was a main objective for this well.

OPERATIONS AND RESULT

Well 6405/7-1 was spudded with the dynamically positioned drill ship West Navigator on 21 June 2003 and drilled to TD at 4300 m in the Late Cretaceous Lysing Formation. In the 12 1/4" several incidents with high gas levels and also gain in the active system were recorded and responded to. In the end the mud weight had been increased from initially 1,33 g/cm3 when drilling to core point at 2816 m, to 1,42 g/cm3 prior to pulling out of the hole. The decision was made to plug back the 12 1/4" hole and initiate a technical side track (T2) with an 11 3/4" liner set above top of the reservoir. When the well was at TD and the discovery confirmed quality MWD data from the 26" section interval had to be collected. To obtain this a new 8 1/2" hole was drilled 15 m from the original hole from seafloor to 1920 m using LWD in one derrick, while performing wire line logging in the other. The well was drilled with seawater and hi-vis pills down to 1910 m and with Glydril DW (water based KCl/NaCl/Glycol/MEG/polymer) from 1910 m to TD. The post-TD 8 1/2" hole for MWD logging was drilled with seawater and hi-vis sweeps.

SEDIMENTOLOGICAL AND ICHNOLOGICAL LEGEND

TRACE FOSSILS

Rhizocorallium
Planolites
Arenicolites
Thalassinoides
Zoophycos
Arenicolites
Helminthopsis
Phycosiphon
Scolicia
Chondrites
Paleophycus
Skolithos
Cosmorhaphe
Schaubcylindrichnus
Teichichnus
Ophiomorpha
Diplocraterium
Nereites
Asterosoma

SEDIMENTARY STRUCTURES

Planar lamination
Soft-sediment deformation
Low-angle cross lamination
Convolute lamination
Wavy-parallel lamination
Mud laminae
Sand laminae

LITHOLOGY & FACIES

Muddy Sandstone
Muddy to Silty Sandstone
Laminated Mudstone
F1a *Facies 1: Burrowed Muddy Sandstone*
F1b *Facies 2: Burrowed Muddy to Silty Sandstone*
F1c *Facies 3: Laminated Mudstone*
F4 *Facies 4: Burrowed Sandy Mudstone*

ACCESSORY ELEMENTS

Glauconite
Coal Detritus
Siderite

LYSING FORMATION

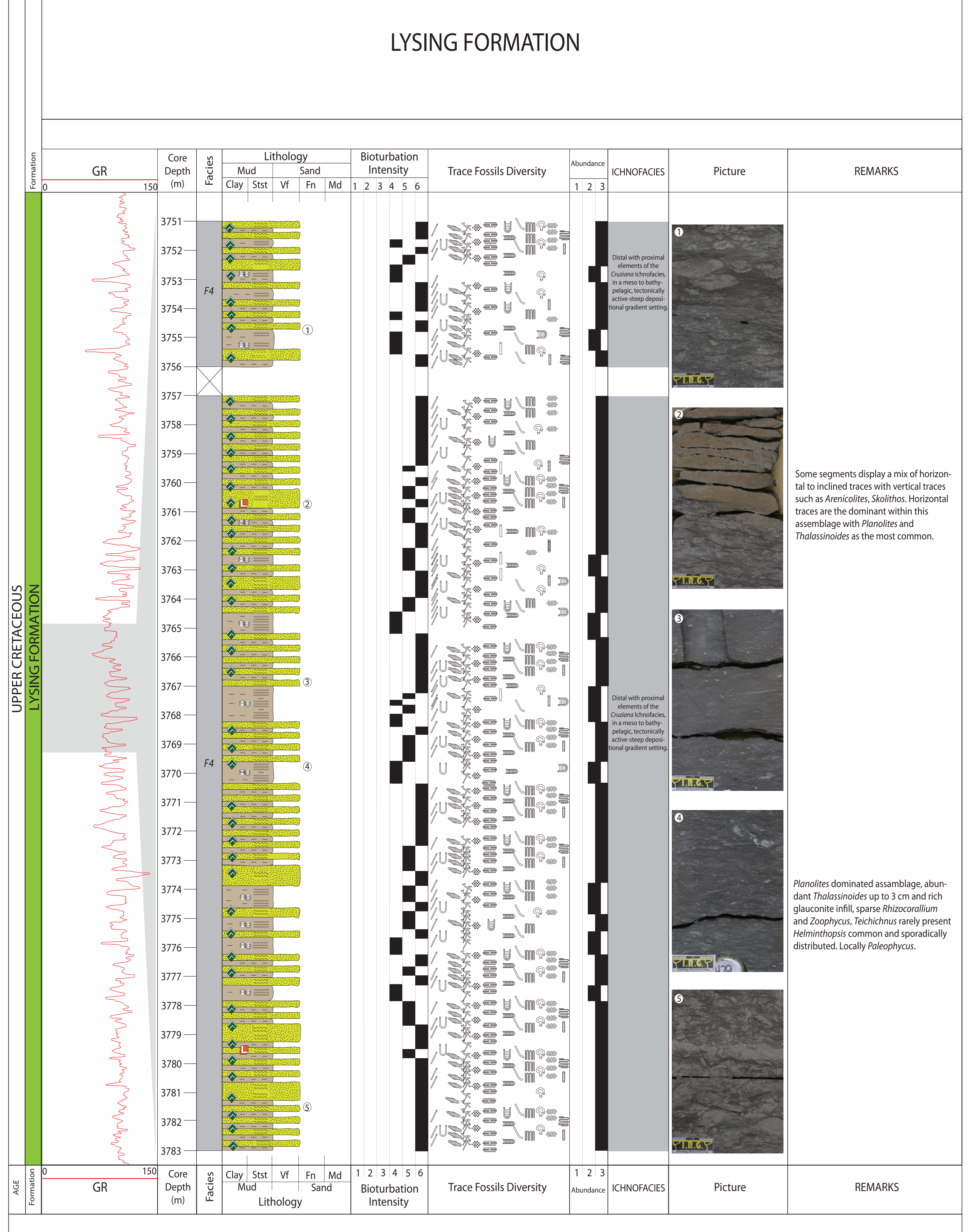

SEDIMENTOLOGICAL AND ICHNOLOGICAL LEGEND

TRACE FOSSILS

Rhizocorallium
Planolites
Arenicolites
Thalassinoides
Zoophycos
Arenicolites
Helminthopsis
Phycosiphon
Scolicia
Chondrites
Paleophycus
Skolithos
Cosmorhaphe
Schaubcylindrichnus
Teichichnus
Ophiomorpha
Diplocraterium
Nereites
Asterosoma

SEDIMENTARY STRUCTURES

Planar lamination
Soft-sediment deformation
Low-angle cross lamination
Convolute lamination
Wavy-parallel lamination
Mud laminae
Sand laminae

LITHOLOGY & FACIES

Muddy Sandstone
Muddy to Silty Sandstone
Laminated Mudstone
F1 *Facies 1: Burrowed Muddy Sandstone*
F2 *Facies 2: Burrowed Muddy to Silty Sandstone*
F3 *Facies 3: Laminated Mudstone*
F4 *Facies 4: Burrowed Sandy Mudstone*

ACCESSORY ELEMENTS

Glauconite
Coal Detritus
Siderite

APPENDIX II: Bioturbation Index

BIOTURBATION INDEX (BI)

The bioturbation index (BI) was originally formalized by Reineck (1963). Then modified by Droser and Bottjer (1986), and later refined by Taylor and Goldring (1993). A summary of the meaning and extents of each scale is summarized in the following table:

Grade	Percent Bioturbated (%)	Classification
0	0	• No bioturbation.
1	1 – 4	• Sparse bioturbation. • Bedding distinct. • Few discrete traces and/or escape structures.
2	5 – 30	• Low bioturbation. • Bedding distinct. • Low trace density. • Escape structures often common.
3	31 – 60	• Moderate bioturbation. • Bedding boundaries sharp. • Traces discrete. • Overlap rare.
4	61 – 90	• High bioturbation. • Bedding boundaries indistinct. • High trace density. • Overlap common.
5	91 – 99	• Intense bioturbation. • Bedding completely disturbed (just visible). • Limited reworking, later burrows discrete.
6	100	• Complete bioturbation. • Sediment reworking due to repeated Overprinting.

Adapted from Lemisky, 2010 and MacEachern et al., 2010.

APPENDIX III:
Cored intervals in wells involved in this thesis and corresponding pictures taken from:

http://factpages.npd.no/ReportServer?/FactPages/PageView/wellbore_exploration&rs:Command=Render&rc:Toolbar=false&rc:Parameters=f&NpdId=4749&IpAddress=70.72.214.123&CultureCode=en

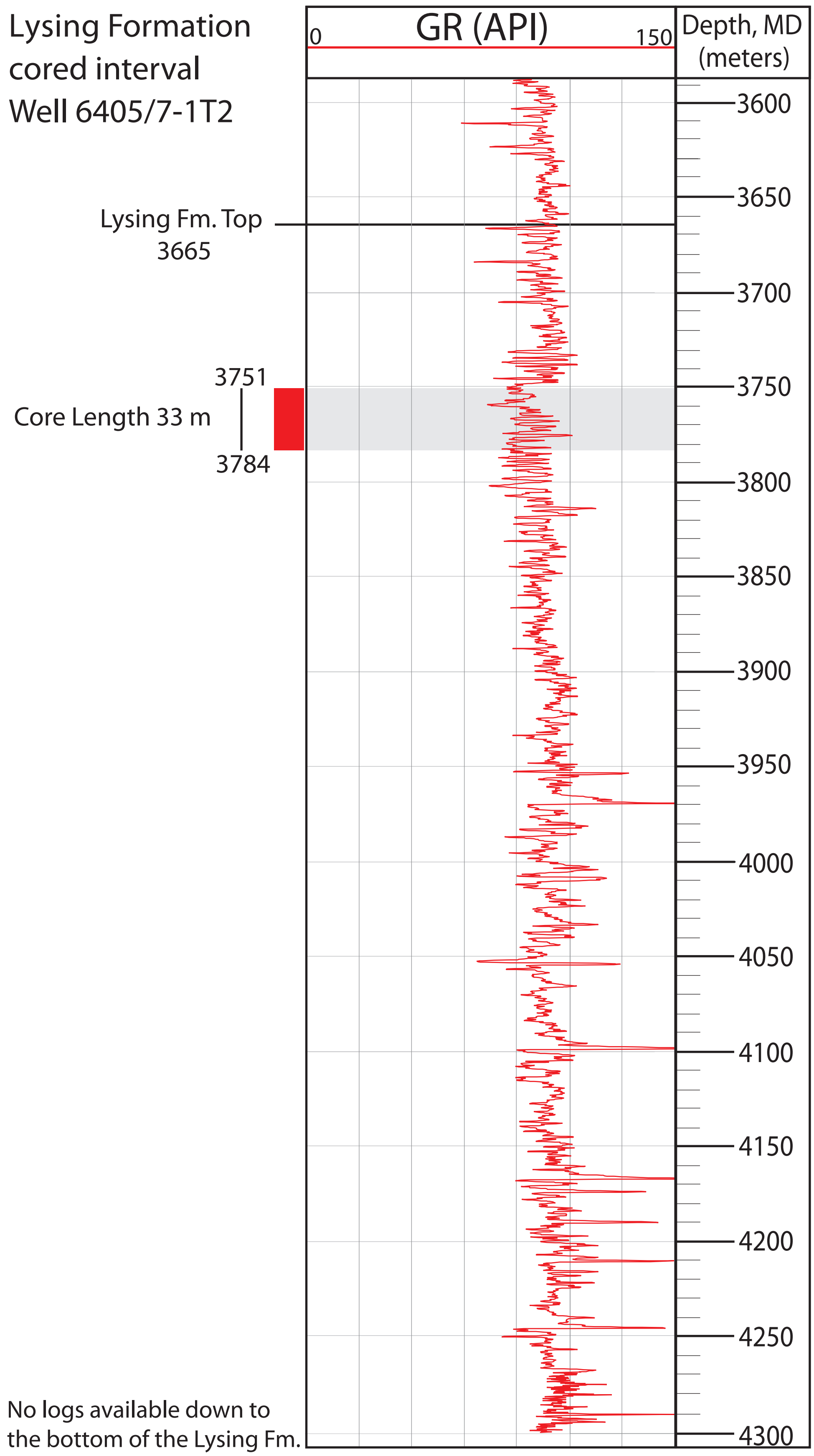
Lysing Formation
cored interval
Well 6405/7-1T2
GR (API)
0
150
Depth, MD
(meters)
Lysing Fm. Top
3665
3751
Core Length 33 m
3784
3600
3650
3700
3750
3800
3850
3900
3950
4000
4050
4100
4150
4200
4250
4300
No logs available down to
the bottom of the Lysing Fm.

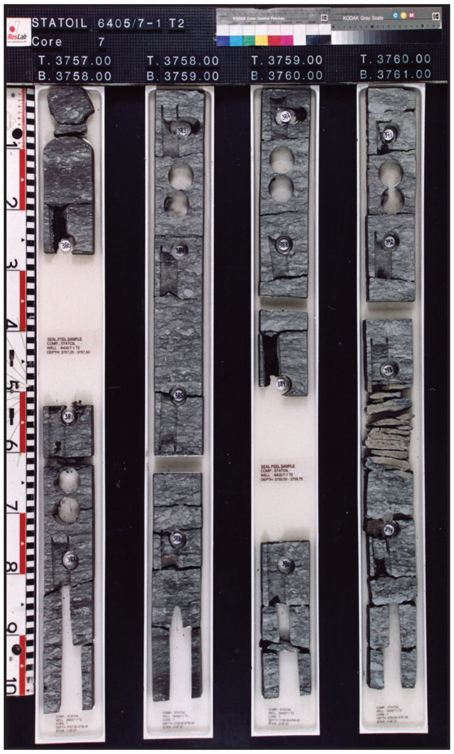
STATOIL 6405/7-1 T2
Core 7
T. 3757.00
B. 3758.00
T. 3758.00
B. 3759.00
T. 3759.00
B. 3760.00
T. 3760.00
B. 3761.00

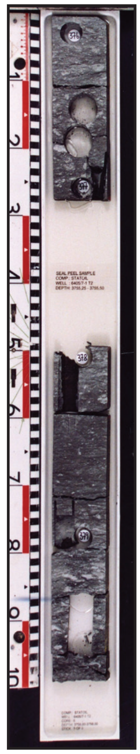

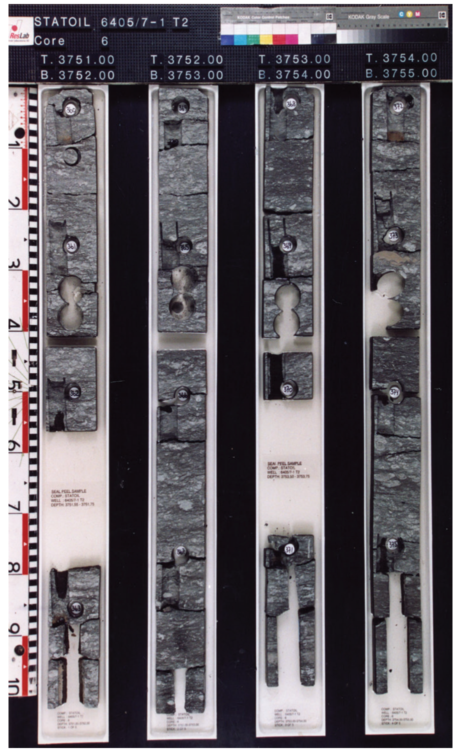
STATOIL 6405/7-1 T2
Core 6
T. 3751.00
B. 3752.00
T. 3752.00
B. 3753.00
T. 3753.00
B. 3754.00
T. 3754.00
B. 3755.00

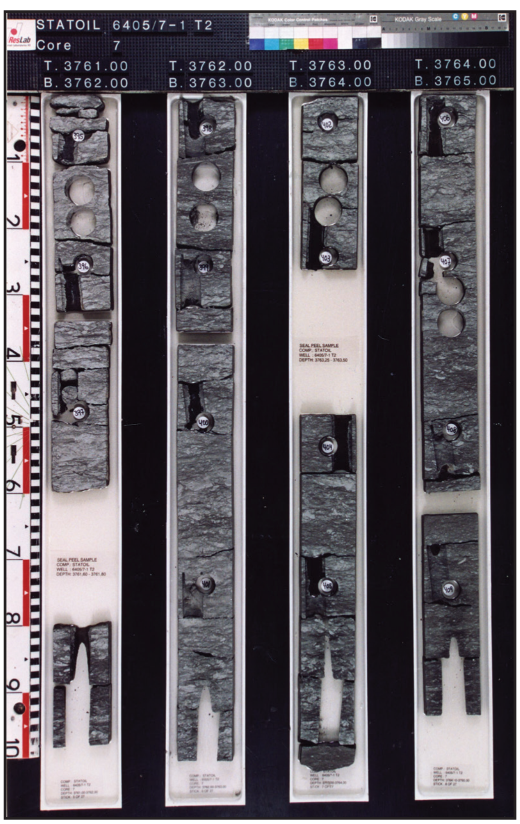
STATOIL 6405/7-1 T2
Core 7
T. 3761.00
B. 3762.00
T. 3762.00
B. 3763.00
T. 3763.00
B. 3764.00
T. 3764.00
B. 3765.00

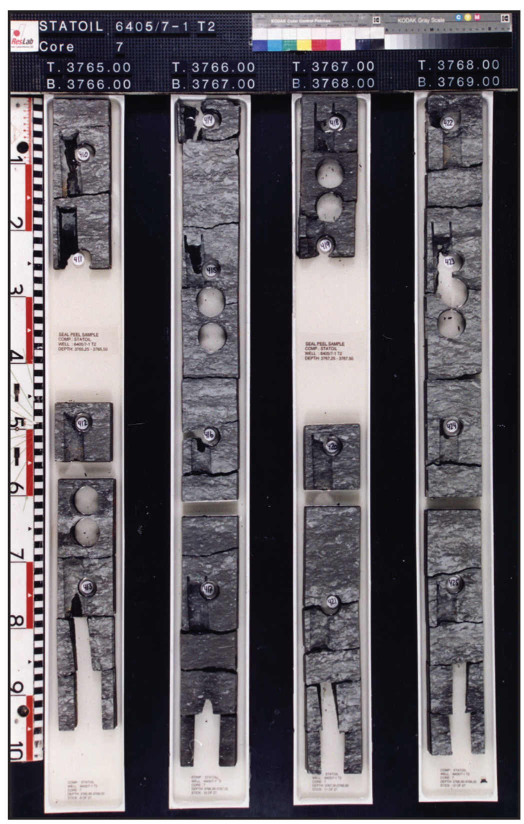
STATOIL 6405/7-1 T2
Core 7
T. 3765.00
B. 3766.00
T. 3766.00
B. 3767.00
T. 3767.00
B. 3768.00
T. 3768.00
B. 3769.00

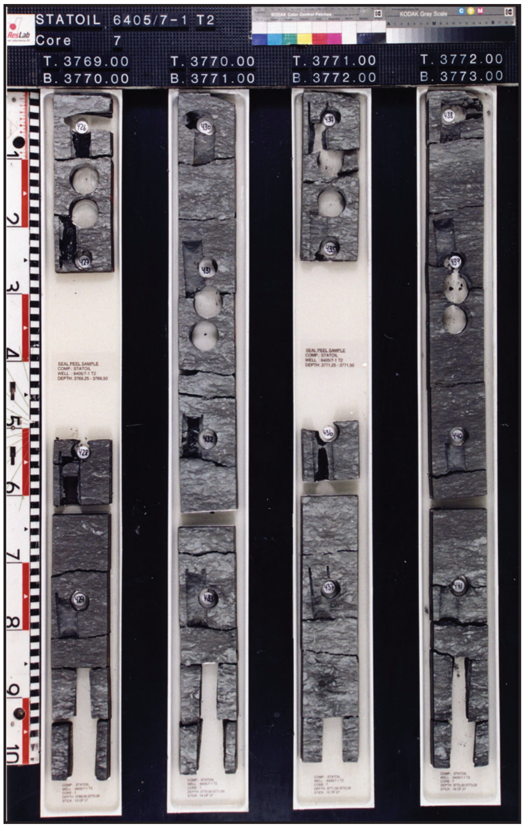
STATOIL 6405/7-1 T2
Core 7
T. 3769.00
B. 3770.00
T. 3770.00
B. 3771.00
T. 3771.00
B. 3772.00
T. 3772.00
B. 3773.00


STATOIL 6405/7-1 T2
Core 7
T. 3773.00
B. 3774.00
T. 3774.00
B. 3775.00
T. 3775.00
B. 3776.00
T. 3776.00
B. 3777.00

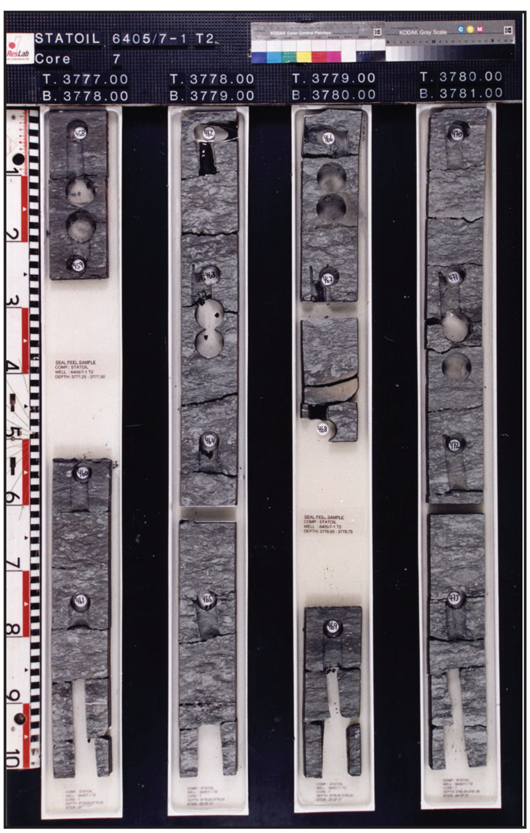
STATOIL 6405/7-1 T2
Core 7
T. 3777.00
B. 3778.00
T. 3778.00
B. 3779.00
T. 3779.00
B. 3780.00
T. 3780.00
B. 3781.00

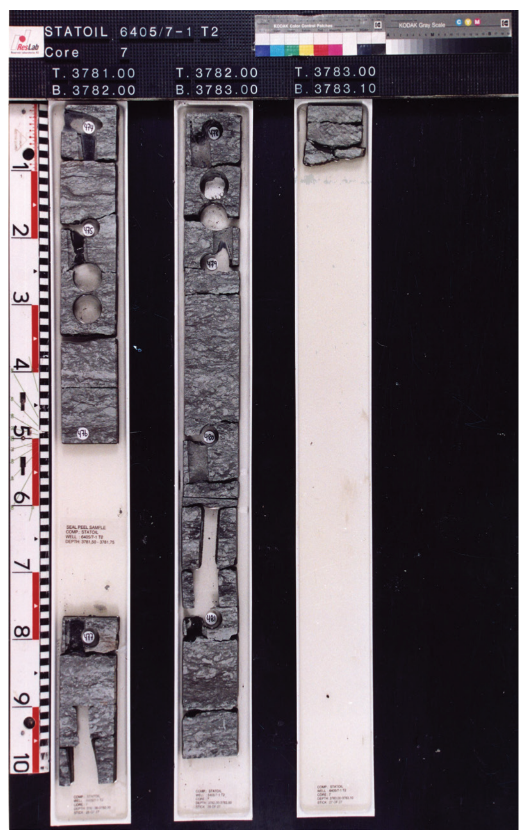
STATOIL 6405/7-1 T2
Core 7
T. 3781.00
B. 3782.00
T. 3782.00
B. 3783.00
T. 3783.00
B. 3783.10

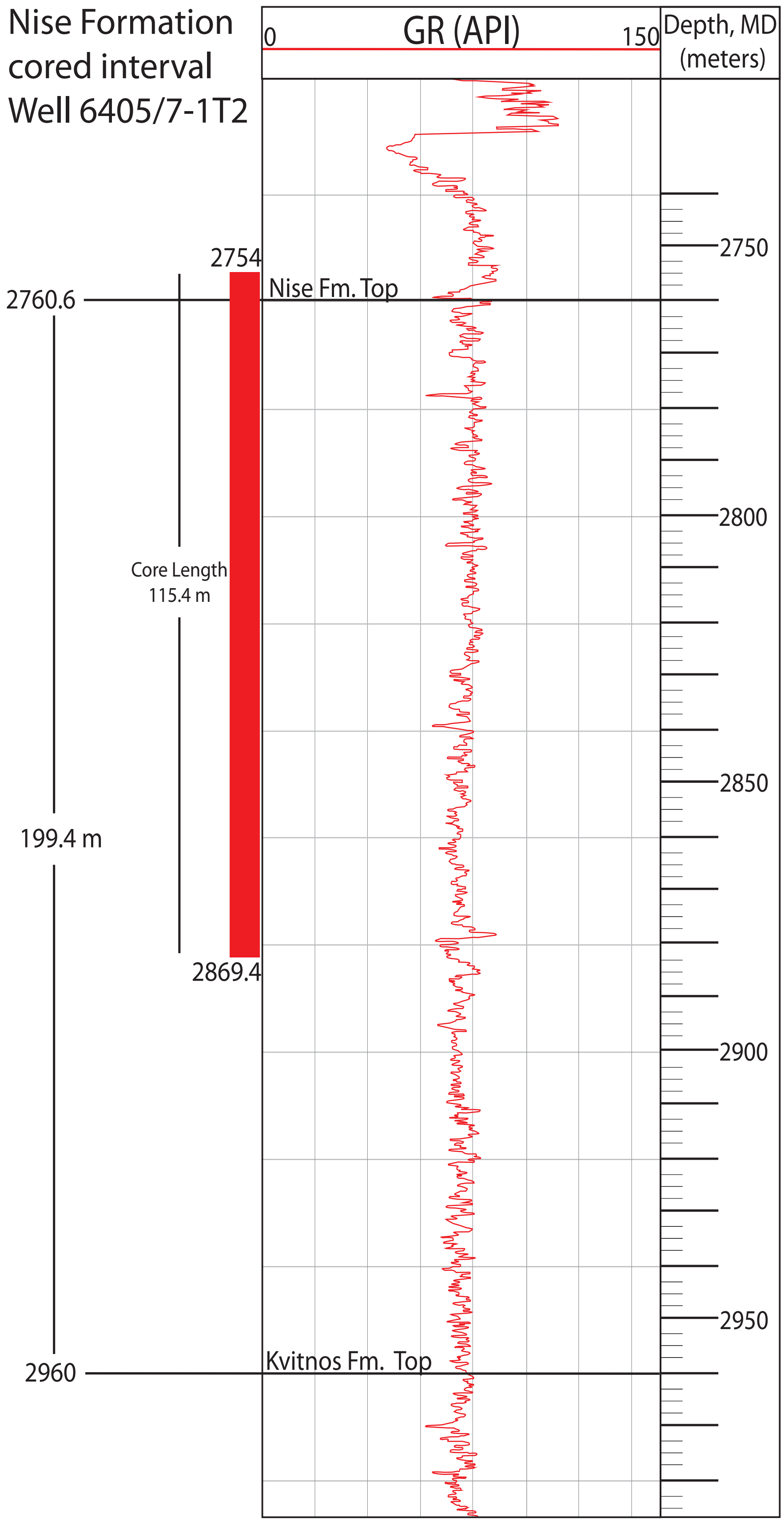
Nise Formation
cored interval
Well 6405/7-1T2
0
GR (API)
150
Depth, MD
(meters)
2754
2760.6
Nise Fm. Top
Core Length
115.4 m
199.4 m
2869.4
2960
Kvitnos Fm. Top
2750
2800
2850
2900
2950

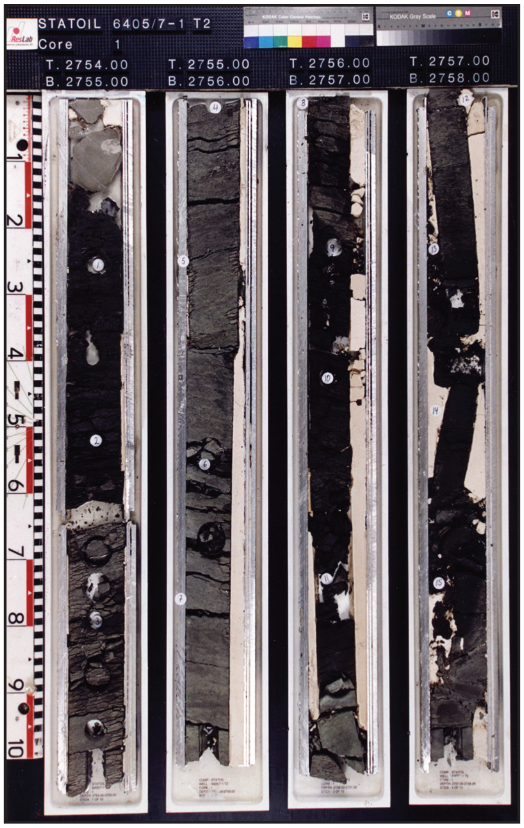
STATOIL 6405/7-1 T2
Core 1
T. 2754.00
B. 2755.00
T. 2755.00
B. 2756.00
T. 2756.00
B. 2757.00
T. 2757.00
B. 2758.00

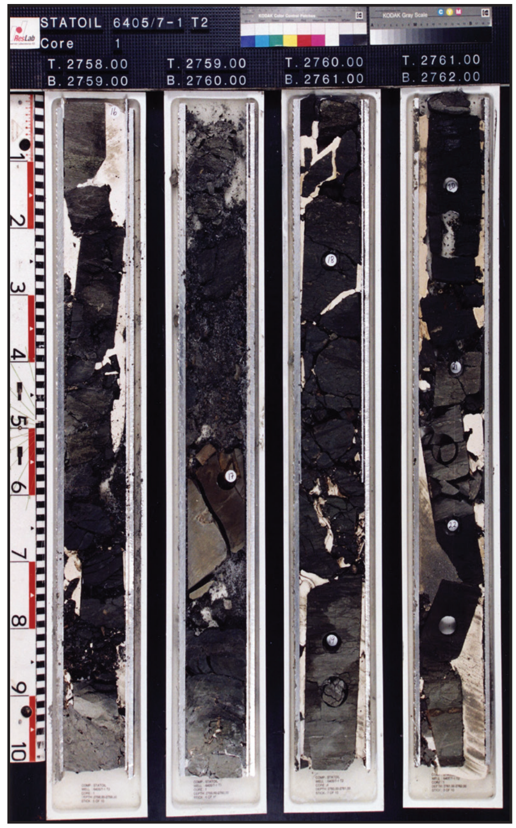
STATOIL 6405/7-1 T2
Core 1
T. 2758.00
B. 2759.00
T. 2759.00
B. 2760.00
T. 2760.00
B. 2761.00
T. 2761.00
B. 2762.00

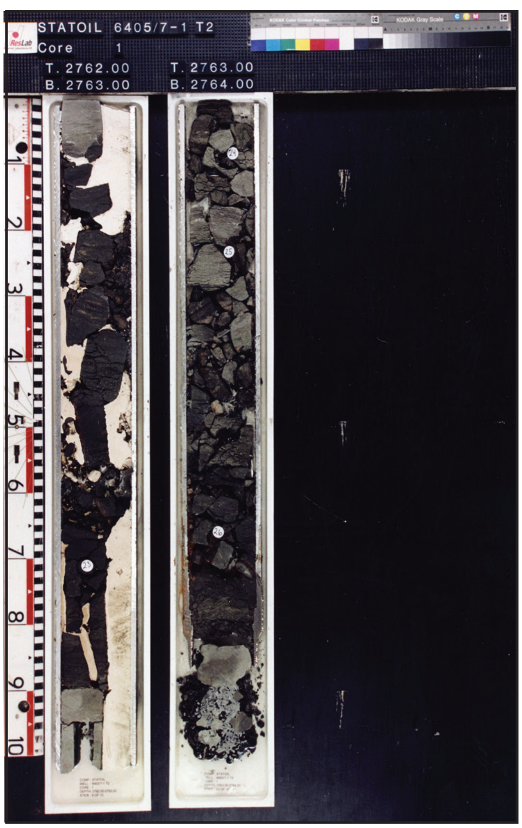
STATOIL 6405/7-1 T2
Core 1
T. 2762.00
B. 2763.00
T. 2763.00
B. 2764.00

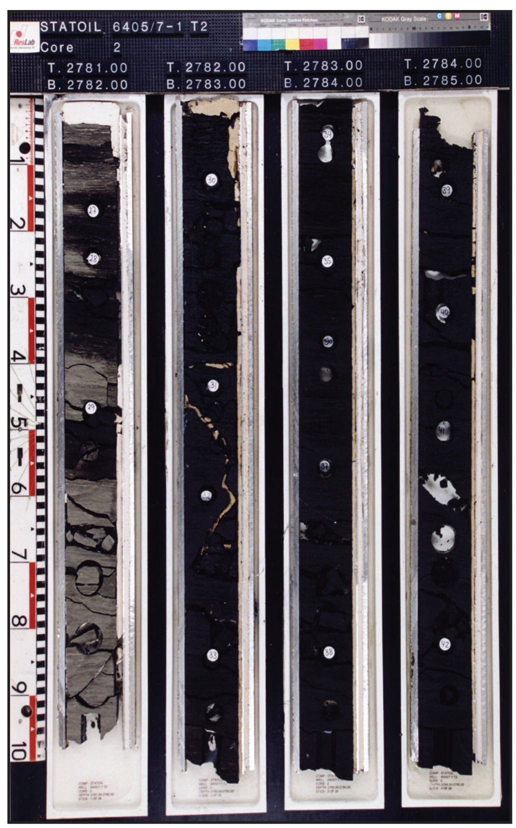
STATOIL 6405/7-1 T2
Core 2
T. 2781.00
B. 2782.00
T. 2782.00
B. 2783.00
T. 2783.00
B. 2784.00
T. 2784.00
B. 2785.00

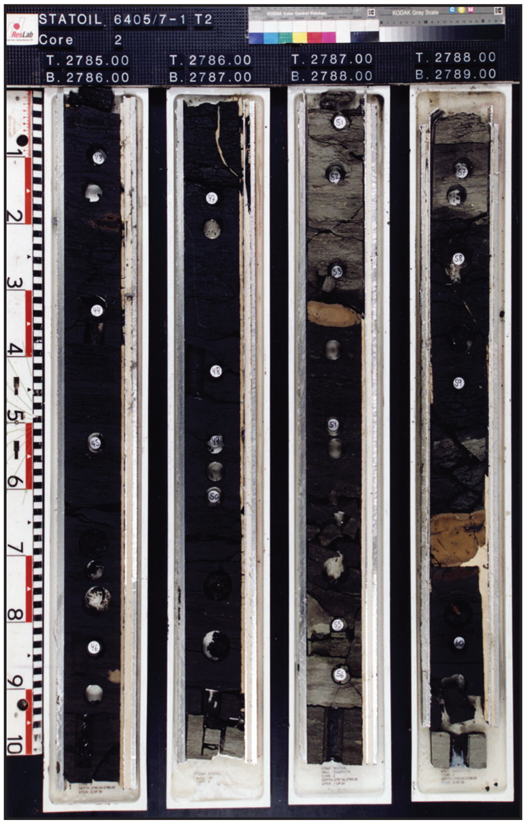
STATOIL 6405/7-1 T2
Core 2
T. 2785.00
B. 2786.00
T. 2786.00
B. 2787.00
T. 2787.00
B. 2788.00
T. 2788.00
B. 2789.00


STATOIL 6405/7-1 T2
Core 2
T. 2789.00
B. 2790.00
T. 2790.00
B. 2791.00
T. 2791.00
B. 2792.00
T. 2792.00
B. 2793.00

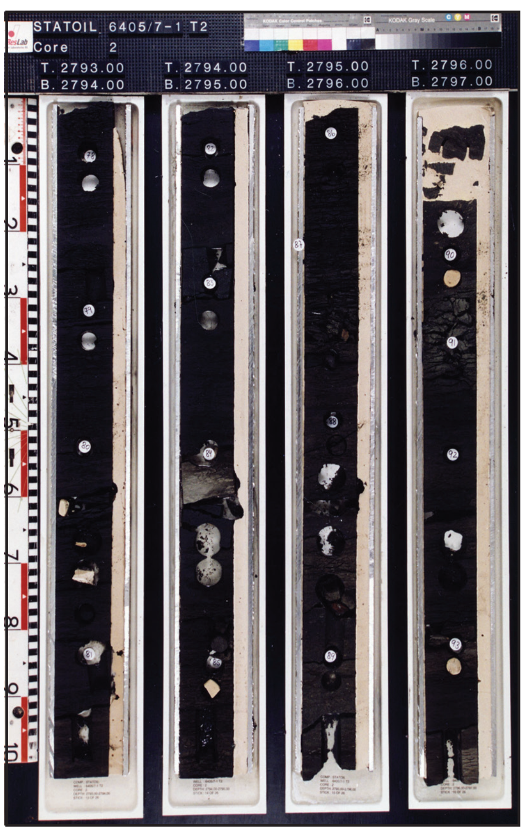
STATOIL 6405/7-1 T2
Core 2
T. 2793.00
B. 2794.00
T. 2794.00
B. 2795.00
T. 2795.00
B. 2796.00
T. 2796.00
B. 2797.00

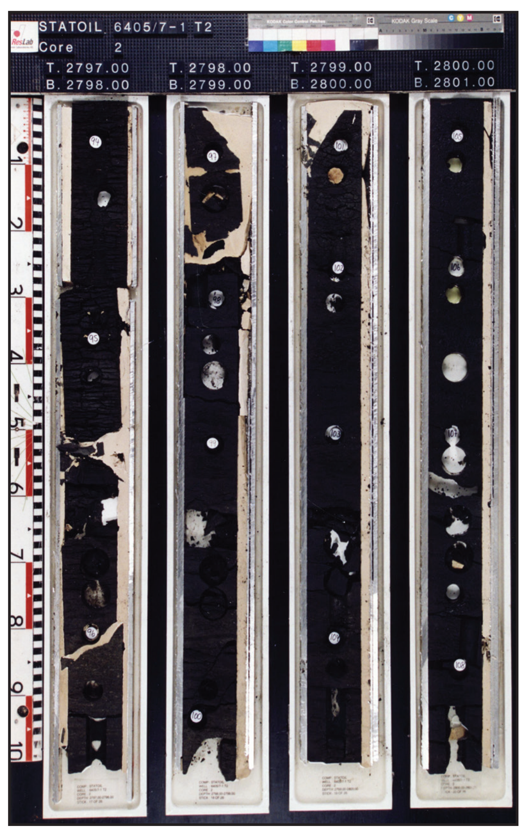
STATOIL 6405/7-1 T2
Core 2
T. 2797.00
B. 2798.00
T. 2798.00
B. 2799.00
T. 2799.00
B. 2800.00
T. 2800.00
B. 2801.00

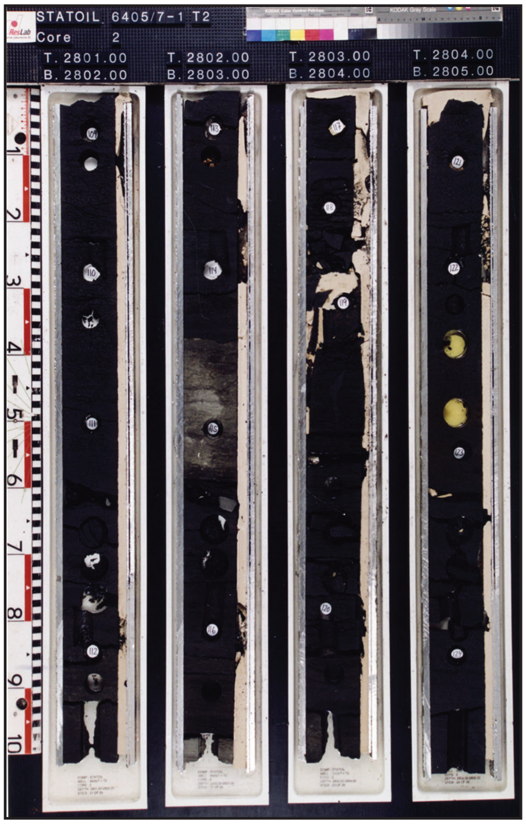
STATOIL 6405/7-1 T2
Core 2
T. 2801.00 B. 2802.00
T. 2802.00 B. 2803.00
T. 2803.00 B. 2804.00
T. 2804.00 B. 2805.00

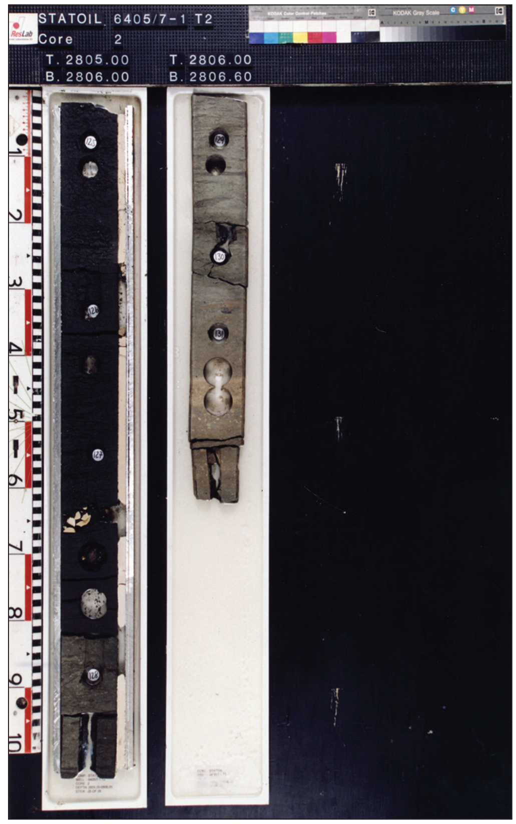
STATOIL 6405/7-1 T2
Core 2
T. 2805.00 B. 2806.00
T. 2806.00 B. 2806.60

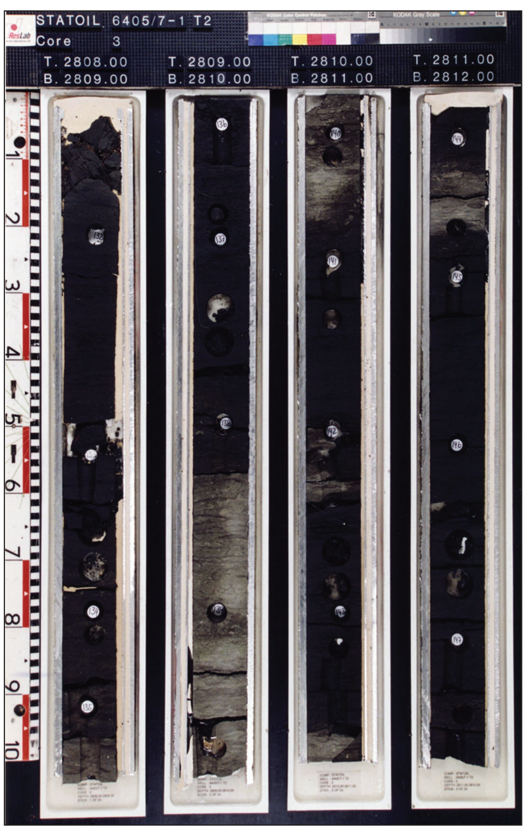
STATOIL 6405/7-1 T2
Core 3
T. 2808.00 B. 2809.00
T. 2809.00 B. 2810.00
T. 2810.00 B. 2811.00
T. 2811.00 B. 2812.00

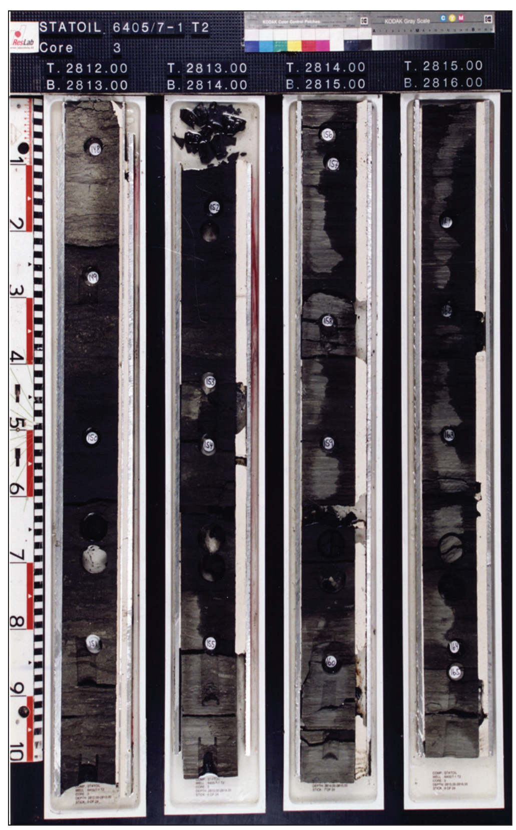
STATOIL 6405/7-1 T2
Core 3
T. 2812.00 B. 2813.00
T. 2813.00 B. 2814.00
T. 2814.00 B. 2815.00
T. 2815.00 B. 2816.00

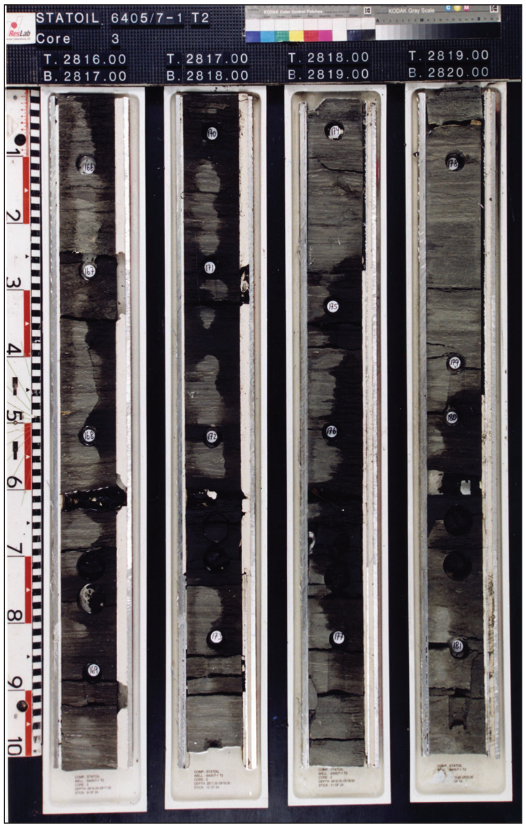
STATOIL 6405/7-1 T2
Core 3
T. 2816.00
B. 2817.00
T. 2817.00
B. 2818.00
T. 2818.00
B. 2819.00
T. 2819.00
B. 2820.00

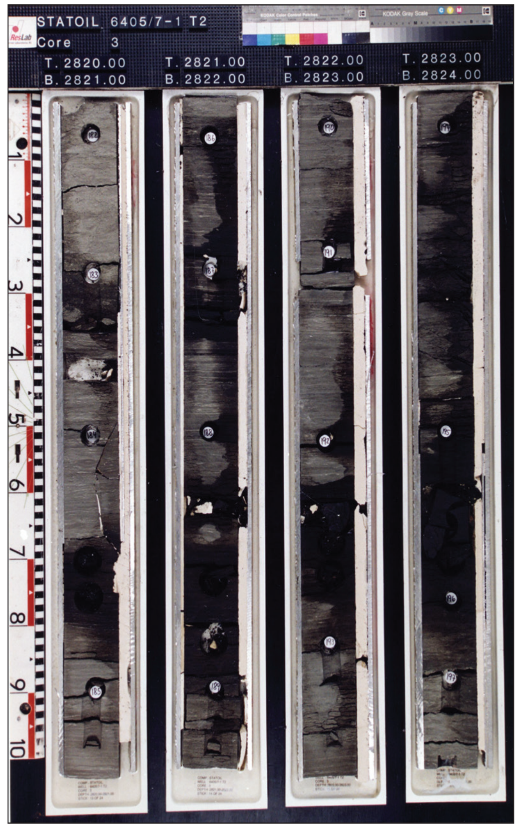
STATOIL 6405/7-1 T2
Core 3
T. 2820.00
B. 2821.00
T. 2821.00
B. 2822.00
T. 2822.00
B. 2823.00
T. 2823.00
B. 2824.00

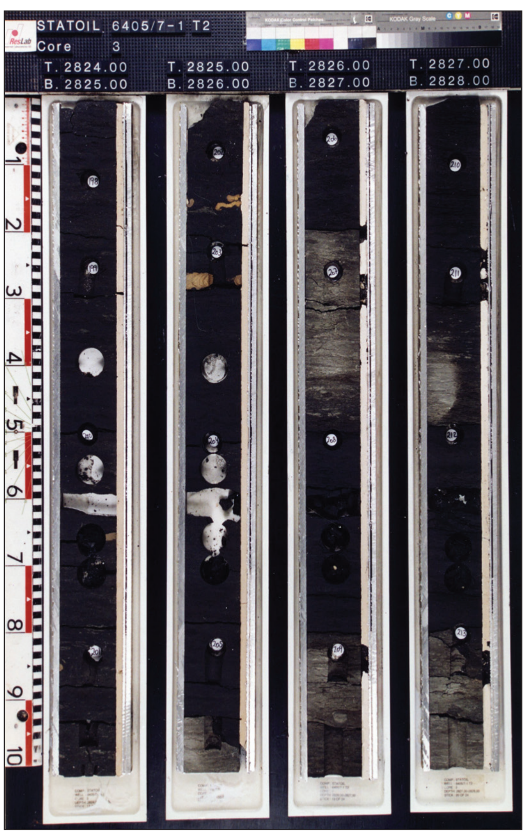
STATOIL 6405/7-1 T2
Core 3
T. 2824.00
B. 2825.00
T. 2825.00
B. 2826.00
T. 2826.00
B. 2827.00
T. 2827.00
B. 2828.00

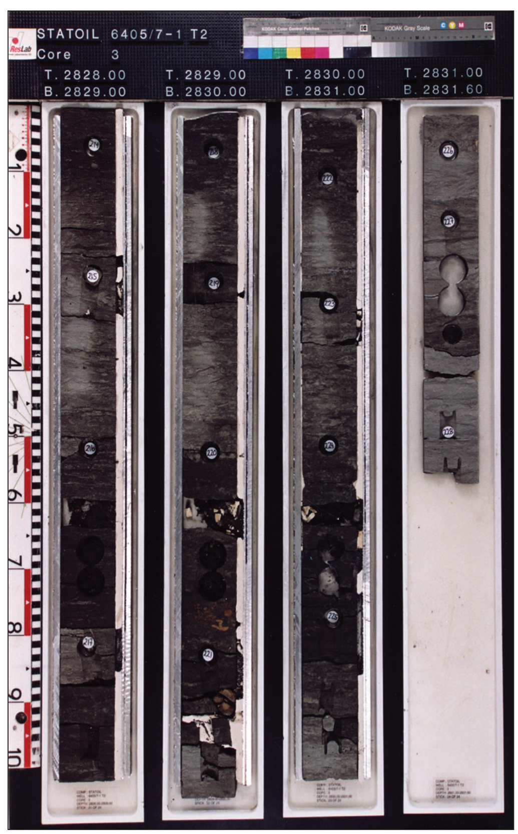
STATOIL 6405/7-1 T2
Core 3
T. 2828.00
B. 2829.00
T. 2829.00
B. 2830.00
T. 2830.00
B. 2831.00
T. 2831.00
B. 2831.60

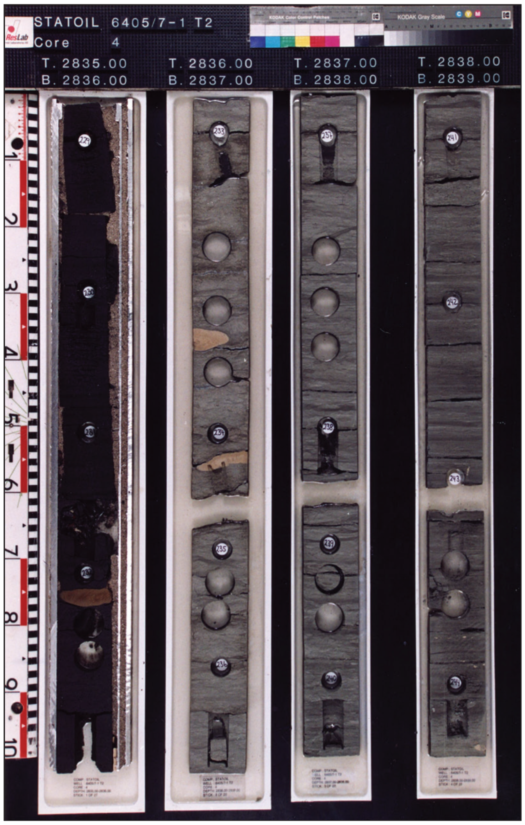
STATOIL 6405/7-1 T2
Core 4
T. 2835.00
B. 2836.00
T. 2836.00
B. 2837.00
T. 2837.00
B. 2838.00
T. 2838.00
B. 2839.00

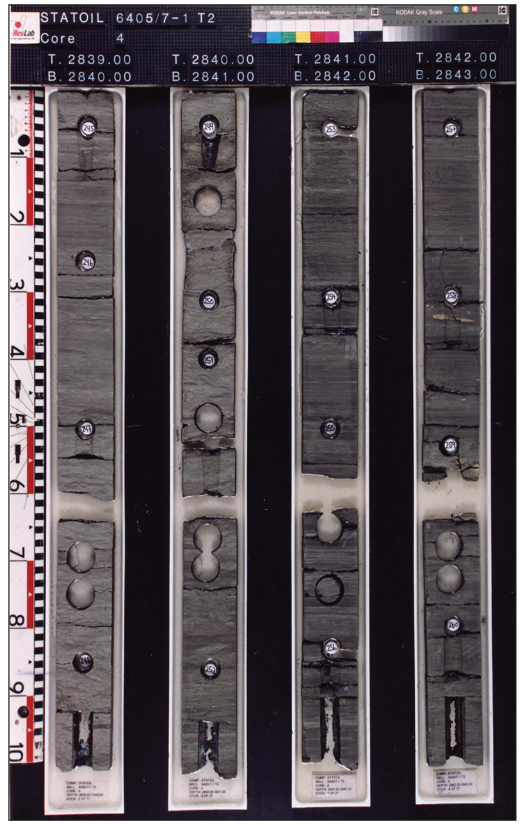
STATOIL 6405/7-1 T2
Core 4
T. 2839.00
B. 2840.00
T. 2840.00
B. 2841.00
T. 2841.00
B. 2842.00
T. 2842.00
B. 2843.00

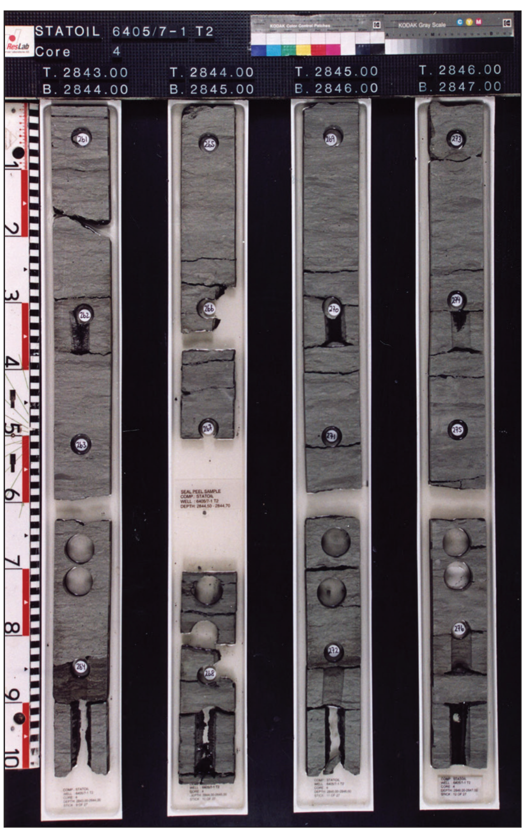
STATOIL 6405/7-1 T2
Core 4
T. 2843.00
B. 2844.00
T. 2844.00
B. 2845.00
T. 2845.00
B. 2846.00
T. 2846.00
B. 2847.00

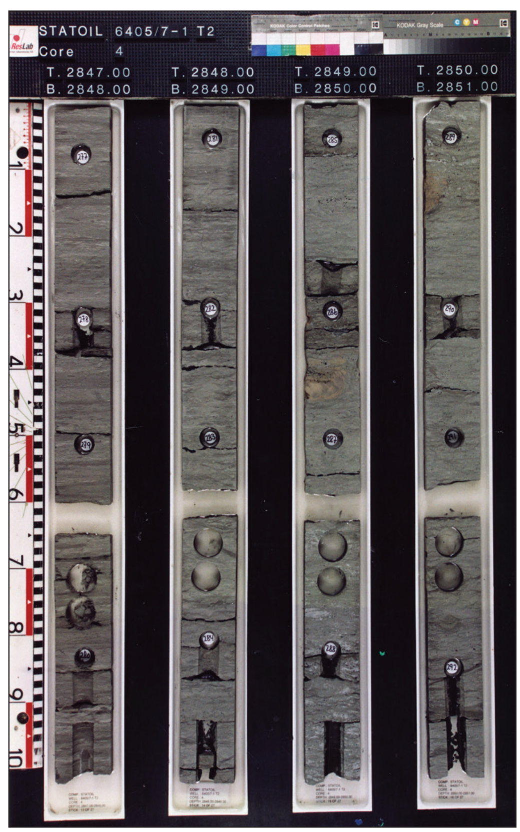
STATOIL 6405/7-1 T2
Core 4
T. 2847.00
B. 2848.00
T. 2848.00
B. 2849.00
T. 2849.00
B. 2850.00
T. 2850.00
B. 2851.00

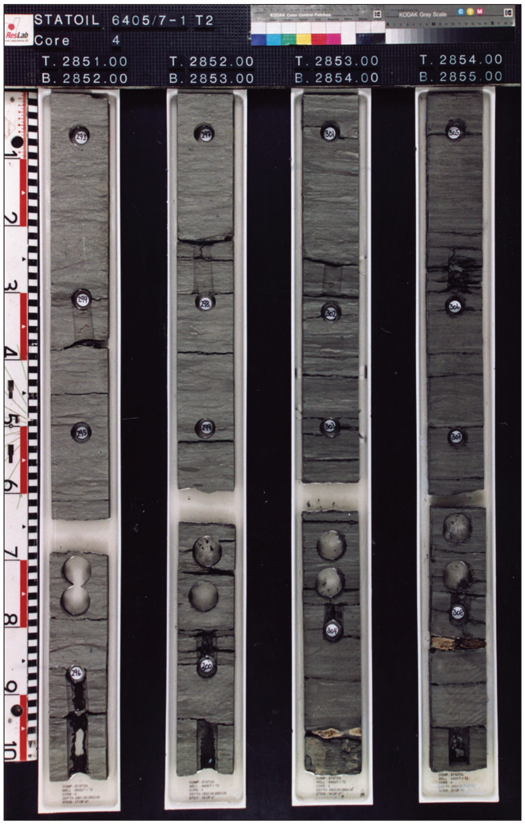
STATOIL 6405/7-1 T2
Core 4
T. 2851.00
B. 2852.00
T. 2852.00
B. 2853.00
T. 2853.00
B. 2854.00
T. 2854.00
B. 2855.00

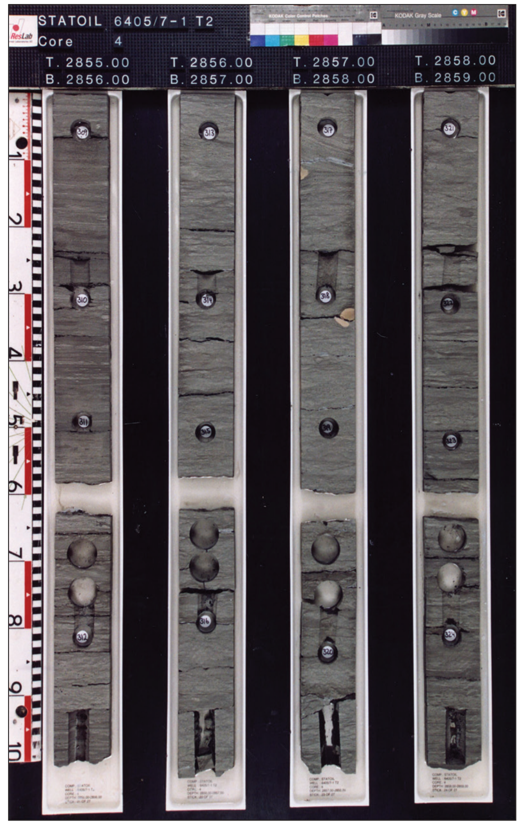
STATOIL 6405/7-1 T2
Core 4
T. 2855.00
B. 2856.00
T. 2856.00
B. 2857.00
T. 2857.00
B. 2858.00
T. 2858.00
B. 2859.00

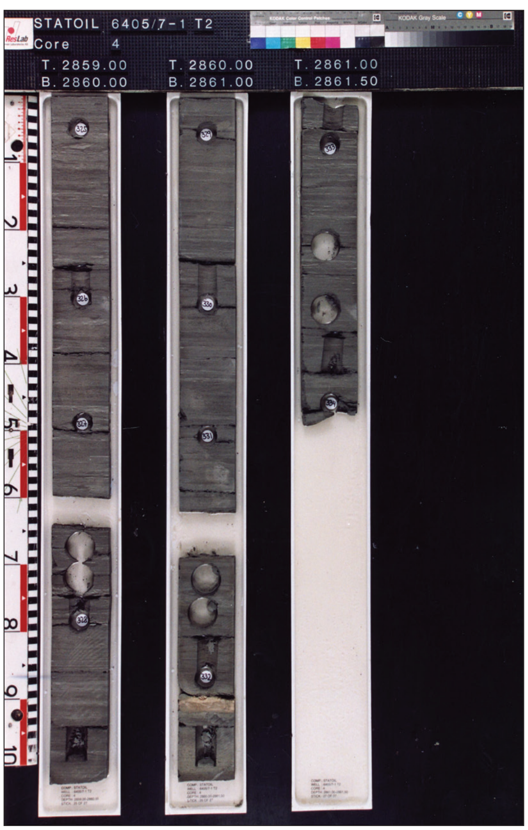
STATOIL 6405/7-1 T2
Core 4
T. 2859.00
B. 2860.00
T. 2860.00
B. 2861.00
T. 2861.00
B. 2861.50

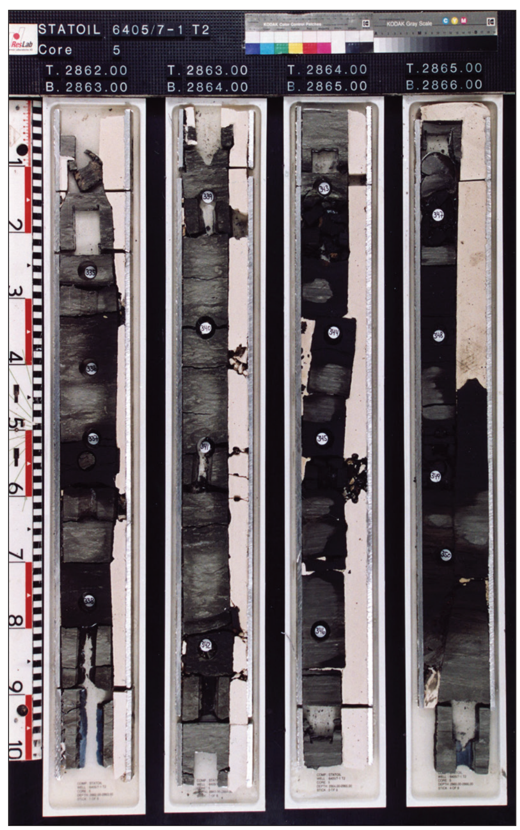
STATOIL 6405/7-1 T2
Core 5
T. 2862.00
B. 2863.00
T. 2863.00
B. 2864.00
T. 2864.00
B. 2865.00
T. 2865.00
B. 2866.00

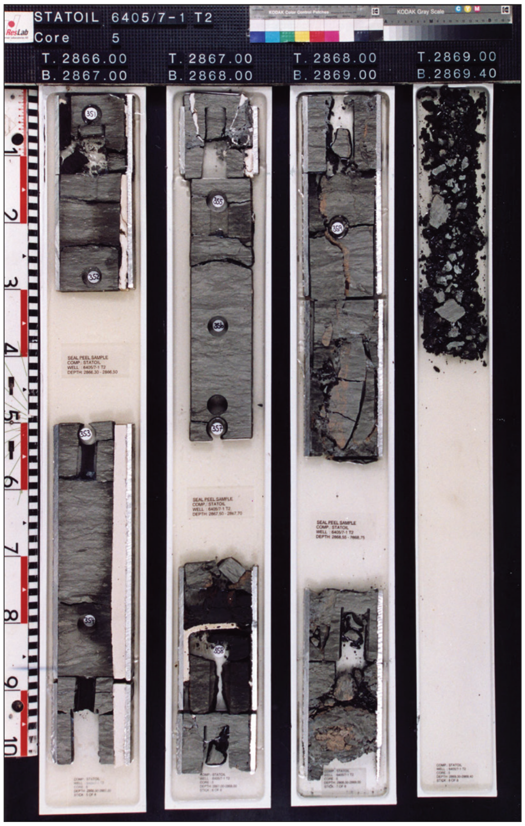
STATOIL 6405/7-1 T2
Core 5
T. 2866.00
B. 2867.00
T. 2867.00
B. 2868.00
T. 2868.00
B. 2869.00
T. 2869.00
B. 2869.40